

CHLAMYDIA PNEUMONIAE TYPE III SECRETION

**STRUCTURAL AND BIOCHEMICAL CHARACTERIZATION OF THE
CHLAMYDIA PNEUMONIAE TYPE III SECRETION SYSTEM**

By CHRISTOPHER BLAIR STONE, B.Sc.H.

A Thesis Submitted to the School of Graduate Studies in Partial Fulfilment of the
Requirements for the Degree Doctor of Philosophy

Descriptive Note

Doctor of Philosophy (2012) McMaster University (Medical Sciences) Hamilton,
Ontario

TITLE: Structural and biochemical characterization of the *Chlamydia pneumoniae* type
III secretion system

AUTHOR: Christopher Stone, B.Sc.H. (McMaster University)

SUPERVISOR: Dr. J.B. Mahony

NUMBER OF PAGES: xvii, 272

To Mom and Dad
with all my love

ABSTRACT

Chlamydia pneumoniae is a Gram-negative intracellular pathogen that uses type III secretion to invade and survive within eukaryotic cells. The T3SS secretes specific effector proteins during the infection process to facilitate immune evasion and nutrient acquisition. Unfortunately, the genetic intractability and difficult culturing conditions of Chlamydiae has inhibited progress in the chlamydial T3S field. This thesis characterizes fundamental aspects of the *C. pneumoniae* injectisome such as the ATPase, the inner-membrane export apparatus, and a specific effector protein Cpn0803.

Initially, we explored whether *C. pneumoniae* encodes a functional T3S ATPase and if it associates with other T3S components. We found that CdsN has enzymatic activity consistent with other Gram-negative T3S ATPases, and that CdsN associates with inner-membrane and soluble components such as CdsD, CdsQ, CopN and CdsL. We also found that CdsN has binding surfaces for either structural or putative effector / chaperone T3S proteins. Next, we explored the putative flagellar genes, which were of interest since *Chlamydia* is a non-motile bacteria that lacks flagellum. We found that the flagellar proteins associate with the T3S apparatus, suggesting that they play a role in T3S during the life-cycle. We extended this observation to show that CdsL, a T3S component, down-regulates both CdsN and FliI enzymatic activity, suggesting that the flagellar proteins are involved in T3S. Furthermore, we characterized Cpn0803 as an exemplary effector, which associates with both CdsN and FliI. We found that Cpn0803 is secreted into host cells upon *Chlamydia* infection. Cpn0803 was thought to be the T3S needle-tip protein; however, the crystal structure does not support this hypothesis.

Presently, the actual role of Cpn0803 in the T3S apparatus remains unknown. Overall, our data suggests that CdsN and FliI both function during the chlamydial life-cycle in the T3S process, possibly coordinating effector proteins (such as Cpn0803) for secretion into host cells.

ACKNOWLEDGEMENTS

First and foremost, I would like to thank Dr. James Mahony. It has been over seven years since he first hired me as a summer student, which in turn led to an undergraduate thesis project, and ultimately to this graduate work. His scientific enthusiasm is contagious, and it pushed me to always think of the next project. His mentoring and guidance have been the most valuable education I will receive over the course of my life. The lessons he taught me I will apply to every endeavor I undertake. With sincere gratitude, thank you for everything you have taught me and let me experience. I could not have asked for a better mentor or friend over the last seven years. Thanks to our lunch hour driving range excursions and your guidance, my golf game has finally reached an acceptable competence level. I have no doubt that our work together is not over and that more exciting times are to come.

The time I spent as a graduate student has felt more like play than work. Dave, you are (begrudgingly) one of the smartest people I've ever met and I have no doubt you will do great things. Thank you for all the good times. Rob and Tiff, you came into the lab just in time to become close friends. Tiff, you never cease to make me laugh. Rob, thank you for all the golf and conversations. Jodi, your enthusiasm makes me smile and I have no doubt our friendship will only grow. Sylvia, you've trained me from the start and made me the scientist I am today. I will always look up to your ability to fix my problems. Dustin, you made science look easy. I will never forget the lessons you taught me and the friendship we have. I would also like to thank Dan Jang, Dr. Max Chernesky, Kathy Lunestra, Raman Toor, Alex Ruyter, and Andrea Granados for their help over the

years. Also, a special thanks to my committee members Dr. Brian Coombes and Dr. Justin Nodwell, whose advice and guidance has pushed me to become a better scientist.

This thesis does not provide enough length to properly thank my family. Thank you for celebrating my achievements, supporting me during my disappointments, and always listening when I rambled on about my work. Laura, thank you for all our talks and all the advice you have given me over the years. I will always cherish the time we spent together in Hamilton and all the time we have spent bonding over the Sword of Truth. Kayleigh, thank you for always being there for me and listening to my problems. You always make me laugh and the speed at which you respond to Facebook posts is unparalleled. I look forward to being in Toronto where we can do lunch... everyday. Robert, as a brother and my best friend I couldn't have asked for more. I will never forget our trip to Europe since it was one of the best times of my life. I look forward to many more adventures with you to come. You three will do great things and I am proud to be your brother. To my Aunt Pat, thank you for being an amazing Aunt. Your ability to string together words into something beautiful never ceases to amaze me. Mom, your constant support and love has made me who I am today. I strive to be half as kind, generous, and loving as you are. You are the kind of mother that one could write a story about since you have no flaws. Dad, thank you for everything. You motivate me to be better and keep me moving when I feel stuck. Your ability to effortlessly solve the most complex problems both humbles and inspires me. I hope that one day I can be the kind of father you have been to me. If only I had time to thank all my family out east. Let me just

say that every year I feel as though I know you better, and I know that in the future we will only grow closer.

Janna, you've been with me through my most difficult and challenging times. I never thought I would meet someone that could both challenge me and make me feel at peace. You are everything I could ask for and more. Your ability to make me laugh and smile never ceases to amaze me. You are the most unique, strong, and impressive person I've ever met. Thank you for always supporting me.

TABLE OF CONTENTS

ABSTRACT.....	iv - v
ACKNOWLEDGEMENTS.....	vi-viii
TABLE OF CONTENTS.....	ix - xii
LIST OF TABLES.....	xiii
LIST OF FIGURES.....	xiv - xv
LIST OF ABBREVIATIONS AND TERMS.....	xvi - xvii
CHAPTER ONE.....	
INTRODUCTION.....	
1.1 The Chlamydiae phylum.....	2
1.2 Taxonomy.....	2-3
1.3 <i>Chlamydia pneumoniae</i> life cycle.....	3-5
1.4 <i>Chlamydia pneumoniae</i> pathogenesis.....	6
1.5 <i>Chlamydia</i> genetics.....	6-7
1.6 Bacterial secretion systems.....	8-10
1.7 Type III secretion.....	11-19
1.8 Type III secretion ATPases.....	19-20
1.9 Needle-tip proteins.....	21-22
1.10 Type III secretion inhibitors.....	22-25
1.11 <i>Chlamydia</i> type III secretion.....	25-28
1.12 <i>Chlamydia</i> type III secretion effectors.....	28-29
1.13 <i>Chlamydia</i> flagellar genes.....	29-30

Foreword.....	30-32
CHAPTER TWO.....	33
AUTHORS PREFACE TO CHAPTER 2.....	34
CHARACTERIZATION OF THE PUTATIVE TYPE III SECRETION ATPASE CDSN (CPN0707) OF <i>CHLAMYDOPHILA PNEUMONIAE</i>	
Abstract.....	36
Introduction.....	37-40
Methods.....	41-46
Results.....	47-51
Discussion.....	52-55
Acknowledgements.....	56
References.....	57-62
CHAPTER THREE.....	76
AUTHORS PREFACE TO CHAPTER THREE.....	77
INTERACTIONS BETWEEN FLAGELLAR AND TYPE III SECRETION PROTEINS IN <i>CHLAMYDIA PNEUMONIAE</i>	
Abstract.....	79
Introduction.....	80-83
Methods.....	84-89
Results.....	90-95
Discussion.....	96-100
Acknowledgements	101
References.....	102-107
CHAPTER FOUR.....	118
AUTHORS PREFACE TO CHAPTER FOUR.....	119

***CHLAMYDIA PNEUMONIAE* CDSL REGULATES CDSN ATPASE ACTIVITY AND DISRUPTION WITH A PEPTIDE MIMETIC PREVENTS BACTERIAL REPLICATION**

Abstract.....	121
Introduction.....	122-125
Methods.....	126-134
Results.....	135-139
Discussion.....	140-144
Acknowledgments.....	145
References.....	146-152
CHAPTER FIVE.....	163

AUTHORS PREFACE TO CHAPTER FIVE..... 164

UNIQUE STRUCTURAL FEATURES OF THE *CHLAMYDIA PNEUMONIAE* TYPE III SECRETION PROTEIN CPN0803

Abstract.....	166
Introduction.....	167-169
Results.....	170-175
Discussion.....	176-180
Methods.....	181-186
Acknowledgements.....	187
References.....	188-192
CHAPTER SIX.....	205

DISCUSSION.....

***CHLAMYDIA* TYPE III SECRETION GENETIC REDUNDANCY-POSSIBLE ROLES..... 207-214**

CdsN and FliI: the two type III secretion ATPases.....

FliA and FliF: possible role for duplication of inner-membrane component

Other examples of genetic redundancy in Chlamydia.....	
POSSIBLE ROLES OF THE <i>CHLAMYDIA</i> TYPE III SECRETION ATPASES.....	214-219
Coordination of effector – chaperone complexes at the inner membrane	
Co-regulation of the type III secretion ATPases.....	
CPN0803: FUNCTION UNKNOWN.....	219-224
Cpn0803 may be secreted by both EBs and RBs.....	
Evidence supporting the role of Cpn0803 as the needle-tip protein.....	
Evidence refuting the role of Cpn0803 as the needle-tip protein.....	
MAKING SENSE OF THE INNER MEMBRANE COMPLEX.	224-227
The export apparatus of Chlamydia pneumoniae.....	
SECRETION PATHWAY OF CPN0803- POSSIBLE MECHANISM	227-229
EB secretion pathway.....	
RB secretion pathway.....	
FUTURE EXPERIMENTS AND SUGGESTION	230-231
CLOSING REMARKS.....	231-232
REFERENCES.....	233-263
APPENDICES.....	
Supplemental Figures.....	264-270
Supplemental Materials and Methods.....	271-272

LIST OF TABLES

Table 2.1- Plasmids used in this study

Table 2.2- Bacterial-2-hybrid analysis of CdsN oligomerization

Table 2.3- Interactions between CdsN and other T3S components using the bacterial-2-hybrid system

Table 2.4- Interaction of CdsN with the hypothetical protein Cpn0706

Table 3.1- Interaction between the flagellar proteins of *C. pneumoniae* using the bacterial-2-hybrid system

Table 5.1- Data collection and model refinement statistics

LIST OF FIGURES

Figure 1.1- Chlamydial life cycle

Figure 1.2- Structure of the *Yersinia* type III secretion needle-complex (NC)

Figure 1.3- Genetic organization and operon prediction for *Chlamydia trachomatis* T3S genes

Figure 2.1- Sequence conservation of CdsN with other T3S ATPases

Figure 2.2- Purification of soluble GST-CdsN₁₋₄₀₅ and CdsL analyzed by Coomassie blue stain and Western blot

Figure 2.3- Oligomerization of CdsN and CdsL by Western blot analysis

Figure 2.4- Time course and dose response of CdsN ATPase activity

Figure 2.5- Interaction between CdsN and other T3SS proteins

Figure 2.6- Interaction of CdsN with a putative chaperone, Cpn0706

Figure 3.1- Sequence conservation of FliI from *C. pneumoniae* with *C. trachomatis* and *Salmonella*

Figure 3.2- Expression, purification, and optimal conditions for the time- and dose-dependant ATPase FliI

Figure 3.3- Interaction between the flagellar components using GST pull-down assays

Figure 3.4- Interaction of His-Cpn0859 and GST-Cpn0859, and dimerization of His-Cpn0859

Figure 3.5- Interaction of FliI and FlhA with T3S components

Figure 3.6- Interacting regions between FliI and FlhA, FliF, and Cpn0859

Figure 4.1- CdsL down-regulations CdsN enzymatic activity in a dose-dependent fashion

Figure 4.2- PepScan Analysis of the CdsL binding domain on CdsN

Figure 4.3- The CdsN₂₂₁₋₂₇₀ peptide, containing both the predicted CdsN - CdsL binding domains, co-purifies with CdsL

Figure 4.4- CdsL binding domains mapped onto the predicted three dimensional structure of CdsN reveals two distinct domains

Figure 4.5- Uptake of a GST-Membrane transport signal (MTS) fusion protein into EBs

Figure 4.6- CdsN peptide containing the CdsL binding sequence TRFARA inhibits the infection of HeLa cells in a dose-dependent fashion and shows low toxicity at 50 μ M

Figure 4.7- CdsN peptide reduces chlamydial infectivity of HeLa cells by IF staining and EM

Figure 5.1- Cpn0803 interacts with type III secretion components *in vitro*

Figure 5.2- Cpn0803 interacts with type III secretion components *in vivo*

Figure 5.3- Stereo image of Cpn0803 monomer and dimer

Figure 5.4- Stereo image of Cpn0803 oligomer colored by chain

Figure 5.5- Stereo image of the hydrophobic pocket in Cpn0803

Figure 5.6- Cpn0803 interacts with phosphatidylinositol and phosphatidic acid

Figure 5.7- Cpn0803 exists in a hexameric and dimeric state in solution

Figure 5.8- PepScan mapping of the Cpn0803 binding regions shown in stereo

Figure 6.1.1- Secretion of Cpn0803 into HeLa cells

Figure 6.1.2- Ring-like structure of Cpn0803 in solution

Figure 6.1.3- CdsN binding domain for Cpn0803

Figure 6.1.4- CdsL down-regulates the flagellar ATPase FliI

Figure 6.1.5- Cpn0803 tetramer based on RosettaDock and PepScan mapping

Figure 6.1.6- CdsN has two distinct binding domains for effectors and structural components

Figure 6.1.7- His-Cpn0803 copurifies with GST-FliI

LIST OF ABBREVIATIONS

ATP	Adenosine triphosphate
C-terminus	Carboxy terminus
Cds	Contact dependent secretion
C-ring	Cytoplasmic ring
DNA	Deoxyribonucleic acid
EB	Elementary body
EDTA	Ethylenediaminetetraacetic acid
EM	Electron microscopy
FHA	Fork-head associated
GST	Glutathione-S-transferase
His	6 x histidine tag
IB	Intermediate body
IM	Inner membrane
IF	Immunofluorescence
IFN- γ	Interferon-gamma
IPTG	Isopropyl β -D-1-thiogalactopyranoside
kDa	kilo Daltons
Msc	Multi cargo secretion chaperone
N-terminus	Amino terminus
OD	Optical Density
NC	Needle-complex
OM	Outer membrane
PAGE	Polyacrylamide Gel Electrophoresis
PBS	Phosphate buffered saline
PepScan	Peptide scanning epitope mapping
PMF	Proton motive force
RB	Reticulate body
RNA	Ribonucleic acid
rRNA	Ribosomal Ribonucleic acid
SDS	Sodium Dodecyl Sulfate
SPI 1/2	<i>Salmonella</i> Pathogenicity Island 1/2
T2S	Type II secretion
T3S	Type III secretion
T4S	Type IV secretion
T5S	Type V secretion
T6S	Type VI secretion
T3SS	Type III secretion system
TEM	Transmission electron microscopy
TARP	Translocated Actin Recruitment Protein

WB

Western blot

CHAPTER ONE

INTRODUCTION

1.1 The Chlamydiae phylum

Chlamydiae have been enigmatic since their discovery in 1907. Halberstaedter and von Prowazek were the first to isolate *Chlamydia* from diseased human conjunctiva. They proceeded to infect conjunctiva epithelial cells of orangutans with this novel pathogen and observed intracellular inclusions by light microscopy. Initially, the organism (*Chlamydia trachomatis*) was incorrectly classified as protozoa. In 1929, *Chlamydia psittaci* was discovered and classified as a virus after an outbreak of psittacosis, a zoonotic respiratory disease (Schacter 1980). In the 1960s, when electron microscopy studies identified ribosomes and cell envelopes in *Chlamydia*, they were correctly categorized as bacterial pathogens (Moulder 1965; 1966).

The Chlamydiae are Gram-negative, obligate, intracellular organisms with a unique biphasic lifecycle. They are found in a wide range of organisms including single-celled protozoa such as acanthamoeba (Corsara 2006; Essig 1997), amphibians such as frogs (Berger 1999), fish (Meijer 2006), avian species such as turkeys, pigeons (Vanrompay 1997), and poultry (Schachter 1980), and mammals such as rodents, rabbits, koalas, and humans.

1.2 Taxonomy

Species in the order *Chlamydiales* have more than 80% sequence identity at the 16S rRNA level. Based on 16S rRNA sequence identity, the *Chlamydiales* can be divided into six *Chlamydia*-like families (Waddliaceae, Parachlamydiaceae, Simkaniaceae,

Rhabdochlamydiaceae, Piscichlamydia and Criblamydia), and one *Chlamydia* family Chlamydiaceae. The Chlamydiaceae family is divided into two genera; *Chlamydia* and *Chlamydophila* based on differences in the 16S rRNA genes, glycogen levels, and differences in the developmental cycle (Everett 1999). However, these two genera are often used interchangeably since some debate exists regarding the classifications. The *Chlamydia* and *Chlamydophila* genera contain nine species; *C. caviae*, *C. abortus*, *C. psittaci*, *C. felis*, *C. pecorum*, *C. suis*, *C. muridarum*, *C. trachomatis*, and *C. pneumoniae*.

1.3 *Chlamydia pneumoniae* life cycle

Chlamydia pneumoniae is an obligate, intracellular Gram-negative bacterium with a biphasic lifecycle (Figure 1.1). Infectious chlamydial particles (elementary bodies, EBs) attach to the host cells through both electrostatic interactions and interactions between *Chlamydia*-specific ligands and host-cell receptors. The role of electrostatic interactions during chlamydial attachment was confirmed by treating host cells with positively charged polycations or negatively charged polysaccharides and observing changes in the ability of *Chlamydia* to attach and enter host cells (Kuo 1972; Kuo 1973). Regarding the *Chlamydia*-specific host-cell ligands, heparin sulfate (a glycosaminoglycan) has been implicated in attachment and entry of *Chlamydia* (Zhang 1992). Zhang et al. found that treatment of host cells with heparitinase, which specifically degrades heparin, reduced *Chlamydia* infectivity. This decrease in infectivity could be reversed by adding heparin sulfate during the infection.

Once attached, *Chlamydia* enters the host cell through receptor-mediated endocytosis into clathrin-coated pits (Wyrick 1989). It has also been proposed that

Chlamydia can enter host cells via particular lipid microdomains in the host cell plasma membrane, known as detergent-insoluble glycolipid-rich domains (lipid rafts) (Stuart 2003). The host MEK-ERK and PI-3 kinase pathways are also involved in chlamydial uptake, possibly modulated through secreted *Chlamydia* proteins. Once inside the host cell, the bacteria reside within a host-membrane derived vacuole known as an inclusion. The single EB (which is metabolically reduced) transforms into the larger, non-infectious but metabolically active Reticulate body (RB), which then divides by binary fission while associated with the inclusion membrane. This interaction of the RB with the inclusion membrane allows the RB to communicate with the host cell cytosol, commandeering host cell pathways and scavenging lipids, cholesterol, and other nutrients required for its survival. During the RB stage, specific T3S effector proteins cleave golgin-84, which facilitates bacterial propagation (Heuer 2009). The developmental cycle is temporally regulated and may occur over the span of 30-84 hours, depending on the *Chlamydia* species (Hackstadt 1999). As the RBs replicate, the inclusion expands in size, and following an unknown stimulus the RBs detach from the inclusion membrane and transform back into infectious EBs. This transformation involves a transitive form, the intermediate body (IB), which can be observed as an RB with a condensed nucleoid (Saka 2011). One hypothesis for the mechanism by which RBs are signaled to reassemble back to EBs is the “contact-dependant hypothesis” (Hoare 2008). This hypothesis predicts that the replicating RBs are attached to the inclusion membrane through the type III secretion (T3S) injectisome needle. As the inclusion expands to accommodate

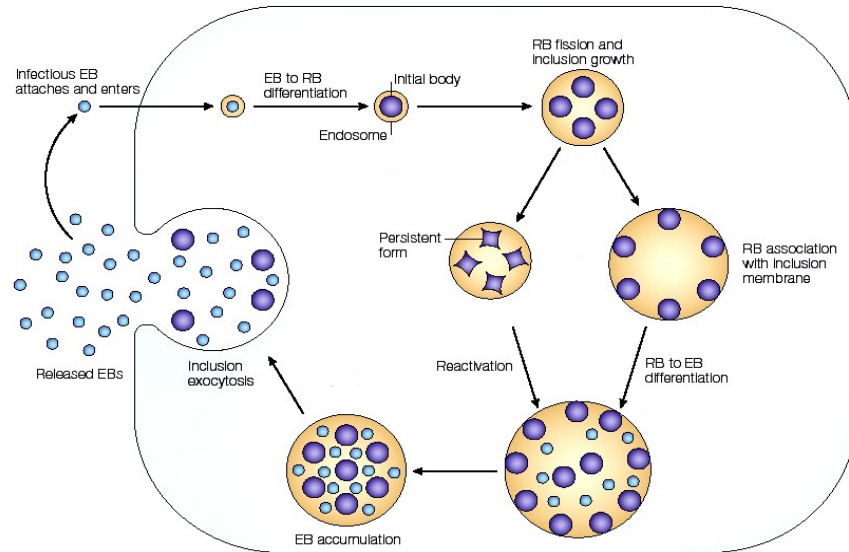


Figure 1.1 Chlamydial life cycle. Depiction of the chlamydial life-cycle from EB attachment to cell lysis.

the replicating RBs, the T3S injectisome anchor is weakened, and eventually released.

This release from the inclusion membrane signals reassembly from RBs to EBs (Hoare 2008). The EBs then exit the host cell either by cell lysis or a packaged released mechanism termed extrusion (Hybiske 2007).

Under specific circumstances, *Chlamydia* is able to enter a persistent state, which is described as the ability of the organism to reside in cells in a viable but non-cultivable state. Studies have identified aberrant inclusion morphology in response to IFN- γ , amino acid (tryptophan) deprivation, antibiotic treatment, iron depletion, or in response to a phage (Beatty 1994, Coles 1993). IFN- γ functions to deplete tryptophan through induction of indoleamine dioxygenase (IDO), which degrades tryptophan. In this state, the RBs continue to replicate but cease to divide, forming enlarged persistent bodies or

“maxiRBs.” Once the stressor is removed, the RB will divide and continue through the replication cycle.

1.4 *Chlamydia pneumoniae* pathogenesis

C. pneumoniae primarily causes respiratory infections such as pharyngitis, laryngitis, and bronchitis, and was first characterized in 1989 by Grayston et al. (Grayston 1989). *C. pneumoniae* is the causative agent of approximately 10% of community acquired pneumonia in the United States (Kuo 1995) and Canada (Marrie 2003). It has also been associated with atherosclerosis (Grayston 2005), arthritis (Villareal 2002), multiple sclerosis (Stratton 2006), and Alzheimer’s disease (Dress-Werringloer 2009). *C. pneumoniae* infections become more prominent with age, and it is estimated that 40-60% of adults are immunopositive for *C. pneumoniae* IgG antibodies (Paldonius 2005). A single dose of azithromycin is known to treat chlamydial infections in adults, but mutations in the 23S rRNA gene can lead to macrolide resistance (Hammerschlag 1993, Misyurina 2004). Also, sub-optimal concentrations of antibiotics can force *Chlamydia* into a persistent state in which they become refractory to further antibiotic therapy (Gieffers 2004). Based on the emergence of resistant strains, and the ability of *Chlamydia* to circumvent antibiotic therapy through persistence, novel therapies are required.

1.5 *Chlamydia* genetics

The historical genetic intractability of Chlamydiae has severely limited molecular dissection of their unique intracellular lifestyle and of the virulence factors involved with

infection and intracellular survival. However, there has been recent progress towards a genetic system for *Chlamydia*. Binet et al. elegantly demonstrated that genetic recombination could be used to target specific point mutations in *Chlamydia psittaci* (Binet 2009). Initially, they identified specific point mutations in the *Chlamydia psittaci* genome over a 398 bp region associated with resistance to kasugamycin. Elementary bodies were then electroporated with linearized rRNA homologous to the chromosome (except for the nucleotide substitutions). Resistant plaques were isolated and sequenced, confirming that the linearized rRNA was incorporated into the genome through homologous recombination. However, this approach can only be used under unique circumstances in which the recombination event itself results in activation of a selectable trait (in this case, kasugamycin resistance). Generally, this method cannot be used to target specific mutations in genes of interest. More recently, Kari et al. developed a method to selectively mutate specific chlamydial genes using a reverse-genetics approach (Kari 2011). Low-level mutagenesis induced by ethyl methanesulfonate and subsequent selection and identification of mutations allowed for reproducible isolation of targeted mutants. The only disadvantage of this technique is that it is labor-intensive, but can be applied to any *Chlamydia* gene. However, the most exciting advancement in *Chlamydia* genetics was by Wang et al., who developed a simple, plasmid-based genetic transformation system using penicillin selection and calcium chloride treatment of EBs to render them competent (Wang 2011). This was accomplished by clearing the plasmid from a *Chlamydia trachomatis* strain and re-introducing the plasmid with the desired genes. Using this method, they successfully created a *C. trachomatis* strain that expresses

GFP. These recent advances will ultimately allow for facile genetic manipulation of the *Chlamydia* genome.

1.6 Bacterial secretion systems

Substrate secretion from the bacterial cytoplasm into either the periplasmic space or the extracellular environment is crucial for bacterial survival, as well as establishing active infections in host cells. Proteins, small molecules, or DNA are all potential substrates of bacterial secretion systems and can play a role in bacterial adhesion, motility, survival, invasion, communication, or nutrient acquisition. In Gram-negative bacteria, type I – VI secretion systems have been identified. The following section describes the function of each secretion system (except type III secretion, which has a dedicated section).

Type I secretion (T1S) systems are used for the transport of unfolded proteins (20 – 900 kDa) from the bacterial cytoplasm to the extracellular environment in a single step. This system consists of three proteins, all of which are required for secretion. First, in the cytoplasmic membrane, an ATP-binding cassette protein (comprised of a nucleotide-binding domain and a transmembrane domain) recognizes substrates based on a conserved secretion signal in the C-terminal end. This protein is important for specificity and selection of secretion substrates. Next, spanning the inner and outer membrane is a membrane fusion protein or adaptor which consists of a short N-terminal cytoplasmic domain, a membrane anchor domain, and a large periplasmic domain. The outer membrane component (outer membrane protein) functions as a trimer and forms a long,

solvated channel between the periplasm and the extracellular environment. *E. coli* uses the T1S system to secrete alpha-hemolysin (Delepelaire 2004).

The type II secretion (T2S) pathway is encoded by at least 12-15 genes and supports the secretion of specific proteins across the outer membrane. This secretion complex functions in the export of enzymes such as proteases, cellulases, pectinases, phospholipases, lipases, and toxins (Filloux 2004; Sandkvist 2001). T2S secreted proteins function in degrading the host milieu to enhance virulence and invasion of the bacterial pathogen. Although T2S spans both the inner and outer membranes, export occurs in a two-step process (Filloux 2004; Sandkvist 2001). First, sec or tat machinery is used to transport proteins across the inner membrane (Filloux 2004). This process requires attachment of the sec translocator, SecB, to the N-terminal signal sequence of the unfolded export protein (Filloux, 2004). After crossing the inner membrane, the sec signal is cleaved and the export protein is released into the periplasm (Filloux 2004, Sandkvist 2001). The second step involves transport of a fully or nearly fully folded protein across the outer membrane (OM). This process is species specific and the proteins associated with this function are not conserved across different bacterial species, even those that are closely related (Gerard-Vincent 2002). Since extrusion of proteins occurs after folding, it has been proposed that the method of substrate recognition is via a structural motif (Gerard-Vincent 2004). *Vibrio cholera* uses type II secretion to release cholera toxin during infection.

Type IV secretion systems are used for the transport of proteins or DNA across the inner and outer membrane of Gram-negative bacteria. This system is the most

versatile of all the bacterial secretion systems and can be found in Gram-positive and Gram-negative bacteria, as well as some archaea. Generally, there are 3 functional classes of type IV secretion systems. The first is used to transfer DNA from one cell to another in an event called conjugation, which is an important mechanism behind the exchange of antibiotic resistance genes among pathogenic bacteria. The second class is involved in DNA uptake and release within the extracellular environment. The third class is to secrete effector proteins into the extracellular milieu or into the host cell. Type IV secretion systems are composed of multiple proteins, forming a complex that spans the inner and outer membrane. Secretion can occur by one or two steps (it can also secrete periplasmic proteins) (Ayers 2010).

The type V secretion (T5S) systems are considered to be the simplest of secretion systems. Three classes of type V transporters have been discovered; the autotransporter system (V_a), the two-partner secretion pathway (V_b), and the V_c system. T5S systems are Sec-dependant systems that recognize an N-terminal secretion signal (leader sequence). The type V cargo also contains a passenger domain (α -domain) and a translocation unit (β -domain). Once the cargo is transported through the inner membrane, the N-terminal sequence is cleaved and the β -domain inserts into the outer membrane, forming a pore. After formation of the pore, the passenger domain is translocated to the bacterial cell surface (Henderson 2004).

Type VI secretion was first identified in *Vibrio cholerae* and *Pseudomonas aeruginosa* in 2006. It has many similarities with the type III and IV secretion systems, such as consisting of 15-25 proteins spanning the inner and outer membranes. Effector

proteins are translocated to either the extracellular medium or the cytosol of a eukaryotic cell upon host-cell contact (Mekalanos 2006).

1.7 Type III secretion

T3S is a common virulence mechanism used by a more than 25 Gram-negative bacterial pathogens such as *Salmonella*, *Pseudomonas*, *Burkholderia*, *Chlamydia* and *Yersinia* (Cornelis 2006; Cornelis 2010; Galan 1999; Hueck 1998; Peters 2007). T3SS are complex multi-protein organelles that assemble in the bacterial membrane and consist of approximately 25 proteins. The T3S machinery, or injectisome, spans the inner and outer bacterial membranes allowing for direct delivery of toxic effector proteins into the host cell cytoplasm through a pore in the host cell membrane (Cornelis 2006, Cornelis 2010; Hueck 1998). The assembly of the T3S system is dependent on hierarchical delivery of the individual components to the assembly site. For this section, the *Yersinia* T3SS is primarily referenced since it is the best characterized of the Gram-negative bacteria.

Electron microscopy has allowed the details of the T3S machinery to be deciphered, emphasizing the morphological similarity across various T3S-utilizing species (Figure 1.2) (Diepold 2010; Edqvist 2007; Galan 2006; Moraes 2008). The structure, called the needle complex, consists of two rings that span the inner membrane (IM) and outer membrane (OM), joined together by a narrow cylinder and terminated by a needle (Diepold 2010; Enninga 2009; Moraes 2008). The needle is a hollow tube assembled through helical polymerization of approximately 150 copies of YscF (the

filament protein) with an inner diameter of 25 Å and a length of 40 – 60 nm (Sun 2008). The length of this needle is controlled by YscP, the ruler protein, possibly by anchoring to both the basal body and the tip of the extending needle (Journet 2003). Complete extension of the YscP protein is believed to signal a switch from secretion of YscF to later T3S components.

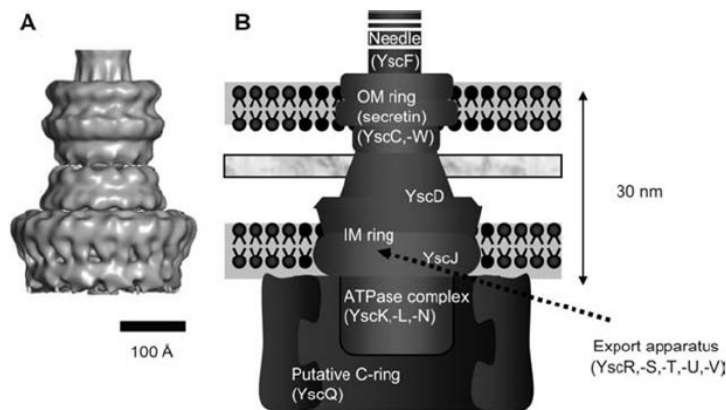


Figure 1.2. Structure of the *Yersinia* type III secretion needle complex (NC). **A.** The NC is modeled by cryo-EM based on single particle analysis (Hodgkinson 2009). **B.** A cartoon is shown to display the individual components of the *Yersinia* injectisome based on similarity with the flagellar basal body. Adapted from Cornelis *et al.*, 2010 (Cornelis 1999).

(Journet 2003). Some debate still exists as to whether YscP controls needle length through its amino acid length or helical content. The needle complex is capped by a tip structure consisting of LcrV, which is used to sense host cell contact and transmit a signal through the injectisome to initiate T3S (Fields 1999; Mueller 2005; Pettersson 1999). The ring spanning the OM and protruding into the periplasm consists of 12-14 copies of the

YscC (secretin) protein (Burghout 2004). Secretins exist in the outer membrane as stable oligomeric complexes that have been visualized by electron microscopy. This revealed that they form large ring-like structures with an internal cavity that may function as an export channel (Burghout 2004). The lower ring, spanning the inner membrane (IM), is referred to as the membrane supramembrane (MS) ring. The lipoprotein YscJ forms a 170 Å, 24 subunit ring and is thought to be anchored to the inner membrane by N-terminal lipidation, and possibly also by a C-terminal transmembrane domain (Silva-Herzog 2008). The less conserved protein YscD is thought to take part in MS ring formation, possibly functioning as a connector of the inner and outer membrane rings. This is supported by the fact that YscJ and YscC only copurify in the presence of YscD (Diepold 2010). The partial structure of a YscD ortholog, PrgH, has been crystallized and found to have a distinctive boot shape with a N-terminal transmembrane domain (Spreter 2009). The injectisome contains five essential integral membrane proteins (YscR, S, T, U, V), which are believed to recognize secretion substrates and form an export channel across the inner membrane (Hodgkinson 2009; Hueck 1998). These proteins are referred to as the 'export apparatus' of the injectisome. Since there is no clear hierarchy in the synthesis of T3S components, the export apparatus must switch its substrate specificity over time from early to late effectors. YscU is known to play an important role in substrate switching, in part by a specific cleavage event at the conserved NPTH domain in its C terminal region (Riordan 2008; Sorg 2007; Wiesand 2009). A recent study demonstrated that injectisome assembly is initiated by the YscC, which acts as a nucleator for distal ring assembly. After the distal ring is in place, assembly proceeds inwards with

attachment of YscD and YscJ. A separate pathway initiated from the inner membrane involves YscV which forms multimers in the presence of YscR, S and T. Once the inner-membrane proteins are in place, the cytoplasmic components can dock (Diepold 2011).

Peripherally associated with the bacterial inner membrane is the ATPase, YscN, which plays an important role as an inner membrane recognition gate for effectors, as well as to dissociate effectors from their cognate chaperones (Akeda 2005; Sorg 2006; Thomas 2004; Woestyn 1994). These ATPases have significant sequence orthology to the β subunit of the F_0F_1 ATPase (Woestyn 1994; Zarivach 2007). They are discussed in detail below. Prior to secretion, effector proteins are maintained in a secretion-incompetent state by a specific chaperone protein, which prevents unfolding of the effector and subsequent translocation through the needle (Akeda 2005; Thomas 2004). The needle is not large enough to support a native protein, so at least partial unfolding is required prior to secretion. The ATPase functions to dissociate the chaperone / effector complexes, allowing the effector protein to unfold and enter the needle (Akeda 2005). Some data suggests that a T3S unfoldase may assist in effector unfolding prior to secretion (Wilharm 2004). Once the effector protein is primed for secretion, the proton motive force (PMF) is used for translocation through the injectisome (Minamino 2011). In *Yersinia*, the ATPase tethering protein YscL localizes the ATPase to the inner membrane, potentially by performing a function similar to that of the gamma-stalk of the F_0F_1 ATPase (Pallen 2006). YscL also plays a role in regulation of ATPase activity by down-regulating enzymatic function (Blaylock 2006). The quaternary structure of the ATPase, *viz.* the hexamer, has been associated with enhanced enzymatic activity and

most likely reflects the native conformation of the protein (Pozidis 2003). Another protein that exists in both the soluble and insoluble fractions of the T3S system is YscQ, which may function as a platform to recognize effector / chaperone complexes, subsequently shuttling them to the inner membrane (Spaeth 2009). In *Salmonella*, it has been shown that SpaO (YscQ ortholog), OrgA and OrgB form a sorting-platform at the inner membrane to regulate the secretion hierarchy of the T3S effectors (Lara-Tejero 2011).

Secretion of effectors across the eukaryotic cell membrane requires three early effector proteins, specifically YopB, YopD, and LcrV. YopB and YopD are known as the hydrophobic translocators, while LcrV is the hydrophilic translocator (Broms 2003; Edqvist 2007; Roehrich 2010; Shen 2010). The hydrophobic translocators form pores in erythrocyte membranes, while LcrV is believed to coordinate their controlled insertion into the eukaryotic cell, acting as an extracellular chaperone (Hakansson 1996; Roehrich 2010). LcrV is exposed extracellularly and involved in host cell-sensing since polyclonal LcrV antibodies neutralize *Yersinia* infection (Weeks 2002). Evidence also suggests that LcrV may play an additional role inside the host cell inhibiting LPS-induced polymerization of actin and cytoskeleton rearrangement (Henderson-Begg 2006). Crystallographic analyses of LcrV have revealed a dumbbell-like structure with two globular domains on either end of a “grip” formed by a conserved coiled-coil motif (Hiroyuki 2009; Hodgkinson 2005). Recently, CT584 in *C. trachomatis* has been proposed as the needle tip protein based on comparisons of biophysical properties to other tip proteins, however, nothing is known about the structure or function of

chlamydial needle tip proteins (Hu 2009). One hypothesis is that a pre-formed tip complex consisting of both LcrV (pentameric or hexameric) and YopB (single copy) act in concert to sense the host cell. A single copy of YopB is inserted into the host cell membrane, acting as a primer for the remainder of the YopB proteins to form a membrane ring, followed by YopD to complete the conduit for protein translocation (Roehrich 2010). Recently, Montagner et al. demonstrated that host-cell membranes contained integrated, and not simply adherent, YopB and YopD translocators (Montagner 2011). However, there are some discrepancies as to whether YopB is present on the tip with LcrV, and this requires further investigation. In some species, such as *Shigella*, the YopB orthologs also have host-effector functions involved in actin polymerization during invasion (Mounier 2009).

T3S effector proteins are crucial during the invasion process, as well as for bacterial survival in the intracellular environment. In *Yersinia*, the effector proteins are known as the Yops. Seven common Yop effectors (YopE, N, H, O, M, J/P, and T) are found in most strains of *Yersinia* (Hiroyuki 2009; Shao 2008). Studies probing the function of these effector proteins have revealed that many targets are cellular components that influence the host innate immune response. Yop J/P functions to inhibit multiple MAPK and NF- κ B signaling pathways, which are known to play a role in the earliest stages of the immune response (Mittal 2006; Orth 2002; Pandey 2011). Based on recent studies, YopJ/P acetylates specific residues in the activation loop of MKKs and IKKs which inhibits subsequent phosphorylation and cellular function (Mittal 2006; Orth 2002; Pandey 2011). YopO interferes with the Rho family of proteins by mimicking

RhoGD1 and interacting with RhoA and Rac1, preventing nucleotide exchange and activation (Matsumoto 2009; Prehna 2006). Recognition and engulfment of the bacteria through a process called phagocytosis is regulated by Rho family GTPases. YopE, one of the earliest effectors, is a Rho GTPase-activating protein (RhoGAP) which interferes with actin depolymerization mediated by the Rho family of proteins (Bartra 2001; Viboud 2006). This functions to inhibit bacterial phagocytosis and destruction. This process is also inhibited by YopH, a protein tyrosine phosphatase, by interacting with proteins such as FAK, Cas and paxillin (Barta 2001; Mueller 2005). YopM, the least characterized of the *Yersinia* effectors, is known to enter the nucleus upon secretion (Kerschen 2004). YopN is thought to function as a negative regulator of T3S that functions from within the bacterial cell as a molecular 'plug' (Marenne 2003). In *Shigella*, the YopN ortholog (MxiC) is thought to have multiple conformational states, allowing for secretion of early effectors (such as the translocator proteins), middle effectors, and late effectors (Martinez-Argudo 2010). Upon host-cell contact, YopN is secreted into the host cell where it has effector functions (Marenne 2003). The genetic signal leading to substrate recognition has been proposed to be encoded in either the N-terminal peptide or in the underlying mRNA, and evidence exists for both theories (Anderson 1998; Arnold 2010). Recently, Amer et al. demonstrated that the first five codons of YopD are sufficient for secretion (Amer 2011). Evidence supporting a peptide-based signal is that the N-terminal amino acids are sufficient to signal secretion of effector proteins. It has also been found that frame-shift mutations in the N-terminus does not abolish secretion, whereas silent mutations on the underlying mRNA does have an influence on protein transport,

supporting the mRNA based signal hypothesis (Anderson 1998; Arnold 2010). The crystal structures of effector proteins are very diverse and show no typical folds or domains, although the N-termini share a unique amino acid composition (Arnold 2010). The first 50 amino acids of *Pseudomonas* effector proteins are enriched in Serine and Proline, and have an aliphatic amino acid present at position 3 or 4. In addition, no acidic amino acids are found within the first 12 residues (Arnold 2010).

Secretion of the majority of effector proteins requires the assistance of specific T3S chaperones. Multiple classes of T3S chaperones exist, all with dedicated functions. Class I chaperones are typically low molecular weight (~ 15 kDa), acidic proteins that assemble as homodimers and are required for secretion of their cognate effector protein (Boyd 2000; Burghout 2004; Hu 2009; Spaeth 2009). These chaperones have been further classified as to whether they interact with one (Class Ia) or several (Class Ib) effectors. Class II chaperones specifically interact with translocator proteins, masking the hydrophobic domains and neutralizing their potential toxicity (Spaeth 2009; Sun 2008). Class III chaperones prevent the premature polymerization of the needle filament protein, YscF, in the bacterial cytoplasm (Sun 2008). The best characterized chaperone / effector pair in *Yersinia* is the YopE / SycE pair (Boyd 2000; Birtalan 2001; Hu 2009; Rodgers 2008; Rodgers 2010). SycE is a compact, globular dimer with a novel fold and two large hydrophobic patches that may form binding sites for YopE or other T3S components (Rodgers 2008; Rodgers 2010). The interaction between YopE and SycE is necessary for YopE secretion. SycE binding to YopE promotes a pronounced disorder – order transition in the chaperone binding domain region, but has no effect on other areas of

YopE (Rodgers 2008). This interaction may play an ancillary role in targeting YopE to the inner membrane for secretion, or it may purely be involved in maintaining YopE in a secretion incompetent state (Cheng 1999).

Recently, a novel T3S mechanism has been proposed that occurs from the surface of bacterial cells (Akopyan 2011). Akopyan et al. found that the effectors YopH, YopE, YopB and YopD are found primarily on the surface of the bacterium prior to host-cell contact. Also, they found that a YopH-bla fusion coated on the surface of *Salmonella* was secreted into host cells. Based on these observations, they proposed a two-step model of T3S translocation in which the N-terminal secretion signal allows for extracellular secretion, but a second translocation domain (common in T3S effectors) is required for secretion into the host-cell.

1.8 Type III secretion ATPases

T3S ATPases play a key role in the secretion process by acting as an inner membrane recognition gate and preparing effectors for secretion. In 1994, Woestyn et al. identified the putative energizer of the of the *Yersinia* Yop machinery, YscN, which was similar to the F₀F₁ related ATPases (Woestyn 1994). YscN contained two consensus binding motifs (Walker boxes A and B) in the catalytic domain. These domains play a role in nucleotide binding and coordinating the phosphate group of ATP. Walker A domains have a consensus sequence of GX₄GKT, and are also known as the phosphate binding loop (P-loop). Walker B domains have the consensus sequence RX_nh₄D and are involved in binding co-factors such as Magnesium (Pedersen 1993). Upon discovery of

YscN, it was believed to energize the translocation of effectors through the injectisome channel and into the host cell and injectisome construction itself (Woestyn 1994).

Recently, it has been shown that the PMF energizes the actual secretion event, and not the ATPase (Minamino 2011). Since the initial discovery of YscN, several T3S ATPases have been characterized such as EscN from *E. coli*, InvC from *Salmonella*, and HrcN from *Pseudomonas* (Strynadka 2007, Akeda 2004, Pozidis 2003). The ATPase tethering protein (YscL orthologs) play two roles: 1) they down-regulate enzymatic function and control ATPase-associated effector secretion, and 2) function as the gamma stalk of the F₀F₁ ATPase and tether the enzyme to the inner membrane (Pallen 2006, Blaylock 2006). T3S ATPases are also known to oligomerize at the inner membrane and form a hexamer with enhanced enzymatic activity (Pozidis 2003). In 2007, Zarivach et al. was the first to crystallize a T3S ATPase, EscN. They found that oligomerization allowed for enhanced ATP binding to the active site by cooperating with a neighbouring Arginine residue. They also proposed that the C-terminal domain of EscN could bind T3S chaperone proteins based on structural modeling (Zarivach 2007). This hypothesis corroborates the observation that T3S ATPases dissociate effector proteins from their cognate chaperones (Akeda 2005). Thus, T3S ATPases function at the inner membrane as a hexamer, associating with T3S effector / chaperone complexes. The ATPase associates with both the effector and chaperone prior to effector secretion through the injectisome. For example, Gauthier et al. demonstrated that the intimin receptor (an *E. coli* effector protein) and its cognate chaperone associate with the T3S ATPase EscN (Gauthier 2003). CdsN of *C. pneumoniae* has also recently been characterized and shown to associate with

several inner membrane T3S components (Stone 2008), as well as effectors and chaperones (Toor 2011).

1.9 Needle-tip proteins

Needle-tip proteins are positioned at the tip of the injectisome and function in sensing host-cell contact and initiating T3S (Sato 2011). In animal pathogens, there are three major classes of needle-tip proteins: the Ysc family that includes the V-tip proteins (such as LcrV), the Inv-Mxi-Spa family of needle-tip proteins (such as IpaD), and the Esc family (such as EspA) (Sato 2011). CT584 of *C. trachomatis* has also been proposed as a needle-tip protein in the Inv-Mxi-Spa family based on biophysical comparison to other tip proteins (Markham 2009). Generally, the three families of needle-tip proteins have similar structures, particularly a long, central coiled-coil of two α -helices (Mueller 2005). The Inv-Mxi-Spa family has a similar structure, but also contains an N-terminal chaperone-like domain, suggesting that these proteins have a self-chaperoning function (Johnson 2007). Deletion of needle-tip proteins results in non-specific release of effectors into culture medium and the inability to translocate effectors into host cells (Sato 2011). However, needle-tip proteins neither insert in nor interact with membranes (Goure 2005). Instead, they chaperone the translocator proteins and ensure correct pore-formation in the host cell membrane. The exact mechanism by which the needle-tip proteins sense the host cell is unknown. However, needle-tip proteins are known to associate with specific small-molecules such as deoxycholate or other bile salts (Chatterjee 2011). For example, the *Shigella* needle-tip protein IpaD is known to bind deoxycholate and chenodeoxycholate,

which induces a conformational change and subsequent secretion of IpaB to the tip (Dickenson 2010). *Salmonella* SipD is also known to associate with bile salts (Wang 2010). On the injectisome tip, needle-tip proteins are thought to form a ring-like structure with a central pore to allow for passage of translocator proteins (Caroline 2008). It is believed that the unfolding / refolding process that occurs during passage through the injectisome promotes the formation of this oligomeric state. The oligomeric state of the tip complexes are believed to be either tetrameric or pentameric (Broz 2007, Johnson 2007). It is also possible that the complex is hetero-pentameric, consisting of four needle-tip proteins and one translocator protein (Johnson 2007). Recently, it was proposed that the needle-tip complex may form a large cavity to facilitate effector refolding after secretion and prior to translocation into the host cell (Lunelli 2011).

1.10 Type III secretion inhibitors

The development of classical antibiotics such as β -lactams and aminoglycosides were crucial during the 20th century, but bacterial resistance appeared shortly after the introduction of these new drugs and similar patterns followed the development of new antimicrobial agents. Horizontal gene transfer between cells led to the rapid spread of resistance augmented by the strong selective pressure imposed by bactericidal and bacteriostatic antibiotics (Alksne 2000; Hender-Begg 2006; Keyser 2008; Lee 2003). Bacterial secretion systems, as discussed above, are crucial for invasion of and survival within a host cell by facilitating evasion of the immune system. Hypothetically, antivirulence drugs targeting these secretion systems would not kill the bacteria, but

rather inhibit their ability to evade immune detection (Alksne 2000; Baron 2010; Keyser 2008). By using antivirulence agents that do not kill the bacteria, it is believed that the development of resistance will be much slower than with classical antibiotics (Baron 2010; Gauthier 2005). Several studies have been undertaken in search of specific T3S system inhibitors of Gram-negative bacteria (Dahlgren 2007; Felise 2008; Gauthier 2005; Kauppi 2007).

The first study on a specific T3S inhibitor of *Yersinia* was published in 2003 by Kauppi et al. (Kauppi 2003). They applied a whole-cell bacterial reporter gene assay, based on *Yersinia pseudotuberculosis*, to screen a 9400 compound library in search of inhibitors. T3S protein expression was monitored by cloning the luciferase-encoding gene *luxAB* under the control of the YopE promoter. By taking this approach, it was possible to monitor processes regulating T3S-specific transcription. Using a high throughput screening (HTS) approach, they searched for molecules that inhibited promoter activity without impacting *Yersinia* growth. They found three molecules in particular with a potent effect against the T3S system. One of these molecules functioned to inhibit bacterial motility, and thus is not a virulence inhibitor, while the other two are specific to virulence-associated T3S but the bacterial targets are unknown (Kauppi 2003). The majority of the hits were acylated salicylaldehyde hydrazones, and this was the first line of evidence demonstrating the potential of this class of molecules. Shortly thereafter, in 2005, Gauthier et al. published a study in which a small molecule library of 20000 compounds was screened in search of direct inhibitors of *E. coli* secretion (Gauthier 2005). They found 30 molecules, most of which were similar in structure to the

salicylaldehyde hydrazones, which specifically inhibited protein secretion but not bacterial growth. These compounds did not appear to act directly on T3S but rather on the expression of T3S associated genes, reducing the concentration of effector proteins. Despite having an unidentified target, this study provided further evidence for the potency of this class of molecules as T3S system inhibitors. In an attempt to identify the exact target of these compounds, specific effects of 23 salicylidene acylhydrazides were evaluated on *Yersinia* T3S (Dahlgren 2007; Kauppi 2007). The authors evaluated T3S gene expression, protein stability and substrate translocation, concluding that the most highly active compound seemed to function on the T3S system itself, not gene transcription. To expand on this, the compounds have now been shown to inhibit the T3S systems of *Pseudomonas*, *Salmonella*, *Shigella* and *Chlamydia* (Baron 2010; Nodfelth 2005). Most recently, Pan et al. used a unique HTS assay based on relieving growth inhibition associated with T3S in *Yersinia* (Pan 2009). They identified four compounds that inhibited secretion of T3S effectors. Despite the numerous studies surrounding these broad spectrum antimicrobials, the target is not unambiguously identified.

A second class of T3S inhibitors were characterized in 2008 by Felise et al. the thiazolidinones, and were found to inhibit T3S dependent functions (Felise 2008). They constructed a strain of *Salmonella typhimurium* that secreted a phospholipase A2 reporter construct (YplA) in a T3S dependent manner. Phospholipase is a well-known reporter for HTS because of the availability of phospholipase substrates with fluorescent cleavage products. Using this assay, they screened a library of 92,000 small molecules for compounds that produced a decrease in fluorescence. To confirm that this compound was

having an effect on T3S they monitored protein translation, Sec-dependent secretion, disulfide-bond isomerization, and gene transcription of T3S operons (Felise 2008). They proposed that this compound directly targeted the secretin, the outer membrane component, and therefore is a true type III secretion inhibitor. Interestingly, this compound also reduced the number of assembled NCs on the bacterial membrane, stressing the fact that this compound requires further investigation.

1.11 *Chlamydia* type III secretion

Initial evidence suggesting that *Chlamydia* express a T3SS was presented by Matsumoto using freeze-deep-etching, visualizing surface projections on both *Chlamydia* elementary and reticulate bodies (Matsumoto 1982). Hsia et al. in 1997 first recognized a locus within the *C. psittaci* genome containing four genes with orthology to T3S genes in other bacteria. Further studies have identified that *C. trachomatis* (Stephens 1998), *C. caviae* (Read 2003), *C. pneumoniae* (Read 2000) and *C. muridarum* (Read 2000) contain a complete repertoire of T3S genes. Unlike other bacterial species, where the genes encoding T3S proteins are organized into one or two distinct operons, or on virulence plasmids, the T3S genes of *Chlamydia* are scattered throughout the genome in several fragmented operons (Hefty 2007) (Figure 1.3). Also, the T3S genes of typical Gram-negative bacterial pathogens have lower G + C content than the remainder of their genomes. *Chlamydia* spp., however, show no significant differences in the G + C content of their T3S genes. These observations do not support horizontal acquisition of T3S genes, and some have speculated that the chlamydial T3SS may have preceded the T3SS

of other pathogens. Reports on the initial characterization of some T3SS proteins in *C. pneumoniae* have recently appeared. Johnson et al. have shown that CdsD, a unique protein homologous to YscD that contains two fork-head associated domains, interacts with the predicted *C. pneumoniae* ATPase tethering protein, CdsL, and CdsQ, a cytosolic component of the inner membrane that presumably forms the bulk of the T3S C-ring (Johnson 2008). Betts et al. have also recently characterized CdsF, the needle filament protein of the *C. pneumoniae* T3SS (Betts 2008). *C. trachomatis* CopN, a homolog of the negative-regulator of T3S in other species (that blocks the injectisome channel and is a known effector protein) has been shown to be translocated through heterologous T3S

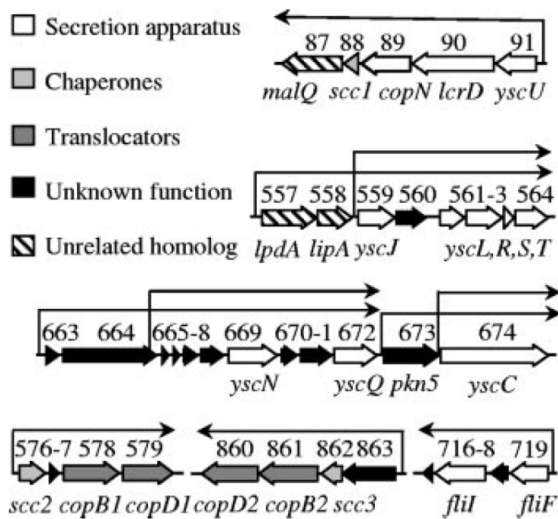


Figure 1.3. Genetic organization and operon prediction for *Chlamydia trachomatis* T3S genes. Gene orientations and locations are shown by block arrows (Hefty 2007).

systems and may be an effector protein in *C. pneumoniae* (Fields 2000; Herrmann 2006). CopN is further discussed in the next section. Also, Scc1 and Scc4 have recently been characterized as the CopN specific chaperones and promote effective secretion of CopN in a heterologous system. Scc3 (Lcrh-2), which binds to the C-terminus of CopN, reduced

CopN secretion (Silva-Herzog 2011). Chellas-Gery et al. have recently characterized the putative *C. trachomatis* translocator proteins, CopB and CopB2. They found that CopB is detected early in infection, while CopB2 was detected throughout development. Also, CopB and CopB2 were associated with the inclusion membrane (Chellas-Gery 2011). Lorenzini et al. have structurally characterized the Cpn0706 ortholog (CT670) in *C. trachomatis* and found that it associated with type III secretion components and forms a single coiled-coil containing two long helices (Lorenzini 2010). CT584 in *C. trachomatis* has been proposed as the needle tip protein based on comparisons of biophysical properties to other tip proteins, however, nothing is known about the structure or function of chlamydial needle tip proteins (Markham 2009). Spaeth et al. characterized CdsQ in *C. trachomatis*, hypothesizing that it binds a multi cargo secretion chaperone (mcsc) and organizes effector / chaperone complexes at the inner membrane (Spaeth 2010). Our lab extended these observations by showing that CdsQ and CdsN have similar protein interaction patterns, suggesting that CdsQ delivers these chaperone/effector complexes to CdsN. We have also shown that CdsN interacts with CopN, the putative T3S negative regulator, CdsD and CdsL. Furthermore, we have shown that CdsL down-regulates CdsN enzymatic activity, possibly by blocking access of ATP to the P-loop.

Saka et al. have recently shown that specific T3S components are enriched in EBs but absent from RBs. For example, the T3S ATPase CdsN and the C-ring protein CdsQ are absent from RBs but abundant in EBs (Saka 2011). CdsD, however, is abundant in both EBs and RBs. It is intriguing to speculate that these T3S components that are absent from RBs are replaced by other components, such as the putative flagellar proteins. Also,

Betts-Hampikian observed that *Chlamydia* T3S components have an abnormally high level of cysteine residues (Betts-Hampikian 2011). They found the redox state of specific T3S structural proteins is closely associated with the developmental cycle.

1.12 *Chlamydia* type III secretion effectors

Despite the genetic limitations of working with *Chlamydia*, several type III secretion effectors have been characterized. The best characterized effector, the translocated actin recruitment protein (TARP), is spatially and temporally associated with recruitment of actin to the site of EB attachment and is present in all chlamydial species examined to date. It is known to interact directly with actin and stimulate nucleation of new actin filaments by forming a large homogenous multimeric protein complex (Jewett 2006). TARP is believed to participate in the parasite-specified phagocytosis by promoting rapid polymerization of actin and subsequent EB uptake. TARP is also known to be tyrosine-phosphorylated upon *C. trachomatis* infection and translocation into the host cell (Clifton 2004).

CPAF is another important *Chlamydia* effector protein that is secreted from the RB into the host-cell mid-cycle. Several CPAF proteolytic targets have been identified, but their importance remains unknown (Zhong 2009). Recently, CPAF has been shown to cleave golgin-84 to facilitate chlamydial reproduction. CT847 is a *C. trachomatis* effector protein identified in RBs that decreases human GCIP concentrations. CopN was one of the first identified effector proteins and can be secreted using a heterologous system (Fields 2000). It is also known to sequester tubulin and prevent microtubule assembly in

the host cell (Archuleta 2011). CopN is essential for *Chlamydia* development and infection (Huang 2008).

An important class of RB T3S effectors are the inclusion proteins (Inc proteins). All Inc proteins share a common feature that is now a hallmark of the family; a large, hydrophobic domain (40 to 60 residues) with hydrophilic residues in the middle. This results in a bilobal pattern on hydrophobicity plots. Numerous Inc proteins have been identified in *Chlamydia* (IncA, IncB, IncC, Cpn0585), and recent advances in T3S effector prediction have identified several more (Dehoux 2011).

1.13 *Chlamydia* flagellar genes

Flagellar motility is an ancient, conserved mechanism that may have evolved from the same ancestor as T3S (Aizawa 2011). This motility facilitates bacterial migration towards less hostile environments. In non-motile bacteria, however, the presence of flagella would be evolutionarily redundant and energetically expensive, unless the proteins played a role in another mechanism involving bacterial replication or survival. Although *C. pneumoniae* is thought to be a non-motile bacterium, it is known to contain at least three orthologs of flagellar genes, namely *flhA*, *fliF*, and *fliI* (Kalman 1999). Microarray and proteomic experiments have suggested that these genes are expressed at mid-cycle (Kalman 1999). The proteins encoded by these genes are paralogs of the T3S proteins CdsV, CdsJ and CdsN, respectively. In motile bacteria, FlhA orthologs are integral membrane proteins required for flagellin export and swarming differentiation which interact with soluble components of the flagellar system (McMurry

2004). FliF orthologs are integral membrane components that form the membrane and supramembrane (MS) ring (Kihara 2001). FliF forms a base for the other membrane components to form a molecular pore, through which components of the flagella that exist outside the cell membrane are exported. The flagellar ATPase, FliI orthologs, provides energy for construction of the flagellum by aiding in export of flagellar proteins outside the bacterial cell where the proteins form molecular complexes (Imada 2007). The presence of FliI, FlhA and FliF in *C. pneumoniae* is not sufficient to form a fully functional flagellar apparatus but they could potentially form a rudimentary base for a flagellum structure (Kubori 1992). In Chlamydiae, the identity of other proteins (if they exist) that play important roles in the flagellar apparatus is currently pending, but it is possible that the flagellar apparatus, if it exists, is a hybrid structure of *C. pneumoniae* T3S and flagellar proteins. Another possibility is that flagellar proteins are involved in T3S, aiding in secretion of effector proteins or structural components. This is supported by the observation that the flagellar proteins associate with T3S components (Stone 2010, Spaeth 2009). In *Pseudomonas*, there is evidence to support that flagellar assembly actually antagonizes the T3SS, suggesting a negative cross-regulation of the two systems (Soscia 2007).

FOREWORD

T3S is crucial for both bacterial invasion of host cells and replication. Molecular understanding of the system can lead to development of powerful antimicrobial compounds applicable to a wide-range of Gram-negative bacteria. Characterizing the

protein-interactions in the T3S network is the first step to truly understanding the function and mechanism of T3S.

The goal of my work was to advance the *Chlamydia* T3S field by characterizing protein-interactions and studying specific components of the system. During this project, genetic manipulation of the *Chlamydia* genome was not possible, which forced me to apply cutting-edge techniques, some of which have never been applied to bacteriology.

This thesis is organized into five major chapters, each of which contributes to the thesis story. Chapter Two discusses the identification and characterization of Cpn0707, the *C. pneumoniae* T3S ATPase. Cpn0707 associates with numerous T3S components of the basal body. This work has been published in the *Journal of Bacteriology*. Chapter Three shifts focus to the flagellar genes, demonstrating that they likely associate with T3S components and may play a role in the T3S process. This work has been published in *BMC Microbiology*. Chapter Four demonstrates that CdsL, a T3S component, can regulate CdsN enzymatic activity and applies PepScan epitope mapping to identify the CdsN binding domain for CdsL. This work has been published in *Frontiers Microbiology*. Chapter Five discusses the characterization of a specific effector protein, Cpn0803, using x-ray crystallography and basic biochemistry techniques. This work has been published in PLoS One. During my thesis, I have accumulated other pieces of data that effectively link and apply to these four chapters. These figures are presented in the appendices. Much of my data is the result of collaboration with experts at McMaster University: Dr. Murray Junop was invaluable with his crystallography knowledge regarding the Cpn0803 crystallography story. Dr. Joaquin Ortega is an expert in electron

microscopy and was instrumental in identifying a ring-like Cpn0803 structure in solution.

Dr. Jerry Sloatstra at PepScan Presto in The Netherlands was also invaluable and performed the PepScan epitope mapping. Dr. James Mahony guided my experiments throughout the entire duration of my studies, and edited my manuscripts and thesis, resulting in the final product presented here.

CHAPTER TWO

AUTHOR'S PREFACE TO CHAPTER 2

In this chapter, I describe the characterization of Cpn0707, which is predicted to be the *Chlamydia pneumoniae* T3S ATPase based on sequence similarity to other T3S ATPases. This work is the first to demonstrate enzymatic activity of Cpn0707, and identifies novel interactions with other T3S components. The implications of this work are (i) Cpn0707 has enzymatic activity consistent with other T3S ATPases, (ii) Cpn0707 interacts with structural and cytoplasmic components of the T3S system, and (iii) Cpn0707 interacts with the hypothetical protein Cpn0706, whose function is currently unknown. These observations support the role of Cpn0707 in *Chlamydia pneumoniae* T3S.

The material presented in Chapter 2 has been published in the peer-reviewed journal, *Journal of Bacteriology*. The experiments described in this section are presented as the final version of the published manuscript. I performed all experimental procedures in this study. David Bulir and Dustin Johnson helped with the bacterial-2-hybrid cloning and screening for Cpn0707 interactions. Jodi Gilchrist cloned and prepared Cpn0322. Dr. James Mahony provided comments and helped with experimental design.

Full citation:

Stone C, Johnson D, Bulir D, Gilchrist J, Mahony J (2008) Characterization of the putative type III secretion ATPase CdsN (Cpn0707) of *Chlamydomphila pneumoniae*. J. Bacteriol. 190: 6590-8

Characterization of the Putative Type III Secretion ATPase CdsN (Cpn0707) of

Chlamydophila pneumoniae

Chris B. Stone, Dustin L. Johnson, David C. Bulir, Jodi D. Gilchrist, and James B.

Mahony*

M.G. DeGroote Institute for Infectious Disease Research, Faculty of Health Sciences and
the Department of Pathology and Molecular Medicine, McMaster University, and the
Father Sean O'Sullivan Research Centre, St. Joseph's Healthcare, Hamilton, Ontario,
CANADA

*** Address correspondence to:**

Dr. J.B. Mahony
Regional Virology and Chlamydiology Laboratory, St. Joseph's Hospital

50 Charlton Avenue East, Hamilton, Ontario, CANADA

L8N 4A6

Phone: 905-521-6021

Fax: 905-521-6083

Email: mahonyj@mcmaster.ca

Running title: Characterization of CdsN in *C. pneumoniae*

ABSTRACT

Type III secretion is utilized by a wide range of gram-negative bacterial pathogens to allow for the efficient delivery of effector proteins into the host cell cytoplasm through the use of a syringe-like injectisome. *Chlamydomphila pneumoniae* is a gram-negative, obligate intracellular pathogen that has the structural genes coding for a T3S system, but functionality of the system has not yet been demonstrated. T3S is dependent on ATPase activity which catalyzes the unfolding of proteins and secretion of effector proteins through the injectisome. CdsN (Cpn0707) is predicted to be the T3S ATPase of *C. pneumoniae* based on sequence similarity to other T3S ATPases. Full length CdsN and a C-terminal truncation of CdsN were cloned as GST-tagged constructs and expressed in *E. coli*. The GST-tagged C-terminal truncation of CdsN possessed ATPase activity, catalyzing the release of ADP and P_i from ATP, at a rate of 0.55 ± 0.07 $\mu\text{mol min}^{-1} \text{mg}^{-1}$ in a time- and dose-dependant manner. CdsN formed oligomers and high molecular weight multimers, as assessed by formaldehyde fixation and non-denaturing polyacrylamide gel electrophoresis. Using bacterial-2-hybrid and GST pull-down assays, CdsN was shown to interact with CdsD, CdsL, CdsQ and CopN, four putative structural components of the *C. pneumoniae* T3S system. CdsN also interacted with an unannotated protein, Cpn0706, a putative CdsN chaperone. Interactions between CdsN, CdsD and CopN represent novel interactions not previously reported for other bacterial T3S systems and may be important in localization and/or function of the ATPase at the inner membrane of *C. pneumoniae*.

INTRODUCTION

Type III secretion systems (T3SS) are essential virulence factors utilized by a variety of gram-negative bacterial pathogens such as *Salmonella*, *Pseudomonas*, *Yersinia*, and *Escherichia coli* to facilitate invasion of host cells (12,13,15). The T3SS facilitates the injection of effector proteins from the cytoplasm of the bacteria directly into the host cell cytoplasm across the inner membrane, periplasmic space, and the outer membrane of the bacteria. Bacterial effector proteins exert a number of effects on the host cell, facilitating bacterial uptake by manipulating the actin cytoskeleton, and subsequently growth by providing an environmentally friendly niche (20). The distinguishing feature of the T3SS is a needle-like nanomachine, or injectisome, which protrudes from the bacterial outer membrane and interacts with lipid rafts in the host cell membrane, through which effector proteins are transported (8).

C. pneumoniae is an obligate intracellular pathogen that has been associated with pneumonia, bronchitis, and atherosclerosis. The developmental cycle of *C. pneumoniae* begins when an elementary body (EB), a metabolically attenuated developmental form, attaches to the host cell cytoplasmic membrane (21). Bacterial uptake is induced by an as yet unknown mechanism that involves activation of the host MEK-ERK and PI 3-kinase pathways (6,9,37) possibly mediated by T3S effector proteins. The injection of one effector, translocated actin-recruiting protein or TARP, is believed to play a key role in the activation of a signaling cascade that recruits and remodels actin at the site of EB attachment, facilitating chlamydial entry into the cell (7,26). Once inside the cell, EBs exist in a parasitophorous membrane-bound vesicle known as an inclusion, where they

differentiate into the metabolically active, non-infectious reticulate bodies (RBs). Inside the inclusion RBs are associated with the inclusion membrane injecting Inc proteins into the membrane and other proteins into the host cell cytoplasm, possibly using the T3S injectisome, although this has not yet been shown. RBs divide by binary fission until an unknown signal triggers asynchronous differentiation into infectious EBs that exit the host cell either by lysis of the inclusion and host cell or by a packaged release mechanism known as extrusion which leaves the host cell intact (21,29). Differentiation of RBs into EBs may be triggered by chlamydial T3S (18,34,36).

Although *C. pneumoniae* contains all the genes coding for a functional T3SS, a systematic study of the injectisome proteins has not been undertaken and little is known about individual proteins (11,19,32,38). Unlike other bacterial species, where the genes encoding T3S proteins are organized into one or two distinct operons, or on virulence plasmids, the T3S genes of *C. pneumoniae* are scattered throughout the genome in several fragmented operons (16). Reports on the initial characterization of some T3SS proteins in *C. pneumoniae* have recently appeared. Johnson et al have shown that CdsD, a unique protein homologous to YscD that contains two fork-head associated domains, interacts with the predicted *C. pneumoniae* ATPase tethering protein, CdsL, and CdsQ, a cytosolic component of the inner membrane that presumably forms the bulk of the T3S C-ring (23). Betts et al have also recently characterized CdsF, the needle filament protein of the *C. pneumoniae* T3SS (4). *C. trachomatis* CopN, a homolog of the negative-regulator of T3S in other species (that blocks the injectisome channel and is a known effector protein) has recently been shown to be translocated through heterologous T3S

systems and may be an effector protein in *C. pneumoniae* (10,17). Two important T3S genes, however, have not yet been identified in *Chlamydia*. These include the needle sensor protein, an LcrV homolog, which is important for sensing the host cell and initiating pore formation in the host cell membrane. The gene encoding the ruler protein, a YscP homolog, that is thought to act as a molecular ruler controlling the length of the needle, also has not been identified in *C. pneumoniae* (24). Cpn0705 in *C. pneumoniae* is the putative ruler protein based on sequence homology and its location in the genome, but no further studies have been completed with this protein.

T3S ATPase proteins are assembled as a dodecameric ring at the basal body of the injectisome in the bacterial cytosol and are believed to play a role in delivery of effector proteins through the injectisome. Several T3S ATPases have been characterized, including EscN from *E. coli* (3,41), YscN from *Yersinia* (5,40) and InvC from *Salmonella* (2). These proteins have been shown to have significant sequence homology to the β subunit of the F_0F_1 ATPase, and have been shown to hydrolyze ATP. Not only are these ATPases important for providing energy for protein transport, but they are believed to play a role in unfolding the effector proteins before translocation, which may be accomplished by removing the chaperone from its cognate effector protein (1). In *Yersinia*, the ATPase tethering protein YscL localizes the ATPase to the inner membrane (5,31). YscL has recently been shown to play a role in regulation of ATPase activity by down-regulating enzymatic function (5,28). T3S ATPases oligomerize as a dodecamer at the inner membrane, and this oligomeric state has been associated with enhanced enzymatic activity (30,33). The predicted *C. pneumoniae* T3S ATPase, CdsN (Cpn0707),

has significant sequence similarity to other T3S ATPases such as InvC, YscN and EscN. The *C. trachomatis* homolog of CdsN has been shown to localize to the inner membrane by immunofluorescent staining (27). Here we report an initial characterization of *C. pneumoniae* CdsN and show that it possesses ATPase activity and interacts with CdsD, CdsQ, and CdsL, three putative components of the *C. pneumoniae* T3S apparatus, but not Cpn0705, the putative ruler protein. We also show that CdsN interacts with the effector and negative regulator of T3S, CopN, implying a role for CdsN in effector selection before secretion through the injectisome. The importance of these protein interactions is discussed in the context of T3S injectisome assembly and function in *C. pneumoniae*.

METHODS

Expression Plasmids

C. pneumoniae CWL029 (VR1310:ATCC) (GenBank accession # AE001363) was the strain used to isolate genomic DNA for cloning and protein expression. Full length CdsN, CdsL, CdsD, CopN, CdsQ, Cpn0705 and Cpn0706 were amplified from CWL029 using AttB-containing primers (Gateway; Invitrogen). The amplified products were cloned into pDONR₂₀₁ (Gateway; Invitrogen) to generate pENT vectors. The pENT vectors were then used in LR reactions (Gateway; Invitrogen) to produce pEX vectors containing the genes of interest. A C-terminal truncation of CdsN (amino acids 1-405) was amplified in the same manner. We used either pEX₁₇ (His-tagged) or pEX₁₅ (GST-tagged) vectors for our protein expression. Table 1 outlines the final constructs used for protein expression. All constructs were confirmed by sequencing at MOBIX Labs (McMaster University).

The bacterial-2-hybrid system was used to identify protein-protein interactions (25). Genes of interest were cloned into pT18 and pT25, each vector expressing a different fragment of adenylate cyclase. If the proteins of interest interact, the two subunits of adenylate cyclase will be brought together and produce cAMP. Increases in cAMP results in increased transcription of the β -galactosidase gene that can be monitored using β -galactosidase activity assays. pT18 and pT25 were digested with KpnI (New England Biolabs) as well as genes amplified from CWL029 (CopN, CdsD, CdsQ, CdsL, Cpn0706, Cpn0705, and PknD) that had a KpnI site designed into the primers. For a

positive control, the FHA-2 domain of CdsD (CdsD-FHA-2) was also cloned to interact with PknD. Ligation was performed overnight at 16°C using T4 Ligase (Invitrogen) and the resulting mixture was used to transform *E. coli* XL-1 cells and transformants were selected on 100 µg/µL ampicillin and 34 µg/µL chloramphenicol LB plates. Plasmids were prepared using the GenElute Plasmid Miniprep Kit (Sigma). Table 1 summarizes the final constructs used in the bacterial-2-hybrid system.

Protein Expression

All constructs were expressed in *E. coli* BL21 (*DE3*) with the exception of CdsL, which was expressed in *E. coli* BL21 (*DE3*) pLysS to reduce basal expression of the protein. Expression plasmids were used to transform *E. coli* BL21 (*DE3*) and plated on Luria Bertani (LB) plates containing 100 µg/mL ampicillin. LB broth (750mL), containing antibiotics, was then inoculated with 5mL of an overnight culture and grown at 37 °C until they reached an optical density (OD)₆₀₀ of approximately 0.8. Cultures were then cooled on ice to 20 °C and induced with 0.2 mM of isopropyl β-D galactosidase (IPTG). Cultures were then incubated at 23 °C for 3 hours and bacteria were harvested by centrifugation at 6500 x g for 20 minutes in a Sorvall RC-5B centrifuge and washed with ice-cold phosphate buffered saline (PBS). Bacteria containing His-tagged protein were resuspended in Binding Buffer (50 mM potassium phosphate pH 7.2, 150 mM KCl, 1 mM MgCl₂) while the bacteria containing GST-tagged protein were resuspended in PBS and stored at -20°C until further use.

Purification of Recombinant Proteins

E. coli pellets containing over-expressed proteins were thawed on ice and sonicated using a Fischer Scientific Sonic Dismembrator Model 100, followed by centrifugation at 20,000 x g for 30 minutes to remove insoluble material. Supernatants containing His-tagged protein were stored at 4 °C for use in GST pull-down assays while the GST-tagged protein supernatants were filtered through 0.2 µm acrodisc filters (Pall Corporation) and incubated overnight at 4 °C with 300 µL of Glutathione-agarose beads (Sigma). For GST pull-down assays, beads were blocked overnight in Tris Buffered Saline with 0.1% Tween and 4% BSA and stored at 4°C until use. For ATPase activity measurements, glutathione beads were washed on a column with PBS + 0.1% Tween until the flow-through had an OD₂₈₀ of less than 0.005. GST-tagged protein was then eluted off the column using 1.5 µg/µL reduced glutathione (Sigma) and dialyzed into activity buffer (50 mM Tris-HCL pH 7.0, 5 mM MgCl₂, 10 mM KCl). Purity was confirmed using SDS-PAGE gel electrophoresis.

ATPase Activity

ATP hydrolysis by GST-CdsN₁₋₄₀₅ purified from glutathione-agarose beads was measured using a malachite green assay (R & D Systems). For all experiments, the specific activity was determined using the equation of a standard line generated from a phosphate standard (R & D Systems). Reaction mixtures contained 600 ng of GST-CdsN₁₋₄₀₅, 4 mM ATP, 50 mM Tris-HCL pH 7.0, 5 mM MgCl₂, and 10 mM KCl. The reaction mixture (1 mL) was incubated at 37 °C for 1 hour and 50 µL of the mixture was

taken for inorganic phosphate determination at various time points. The reaction was stopped by the addition of 10 μL of Malachite Green Reagent A followed by 10 μL of Malachite Green Reagent B and incubated at room temperature for one minute before an OD_{610} reading was taken, according to the manufacturer's instructions. For the negative control, purified CdsN was digested for 10 minutes at 37 $^{\circ}\text{C}$ using Proteinase K (Invitrogen). ATPase activity was expressed as μmol phosphate released $\text{min}^{-1} \text{mg}^{-1}$ of protein, and all experiments were performed in triplicate.

Oligomerization Assay

In order to determine whether CdsN and CdsL form oligomers, formaldehyde fixation and non-denaturing PAGE gel electrophoresis were used. GST-CdsN₁₋₄₀₅ was purified from glutathione-agarose beads, dialyzed against PBS and concentrated using Amicon 10 kDa (Millipore) concentrators to a final concentration of 5 ng/ μL . Formaldehyde was added to purified GST-CdsN₁₋₄₀₅ to a final concentration of 10% and fixation was allowed to continue for 10 minutes. Samples containing 100 ng of GST-CdsN₁₋₄₀₅ were electrophoresed on an 8% non-denaturing PAGE gel and visualized by Western blot using anti-GST antibody (Sigma). His-CdsL was purified from Ni-NTA beads and utilized in the same manner with the following difference; formaldehyde was not necessary to visualize dimerization of CdsL and anti-His antibody (Sigma) was used. As a control for the presence of the GST and His tag, GST-CopN and His-CopN, a protein not known to form oligomers, was also formaldehyde fixed and run on a non-denaturing PAGE gel to test for oligomerization.

GST Pull-down Assays

To examine the interaction of CdsN with other T3S components, GST pull-down assays were performed as described previously by Johnson et al, 2008, with the following modifications (23). Briefly, glutathione agarose beads (30 μ L) bound to fifty nanograms of GST tagged CdsN or CdsN₁₋₄₀₅ protein was used in the assay. The beads were incubated overnight at 4 °C with the *E. coli* lysate expressing the His-tagged proteins. The beads were collected by centrifugation and washed with 0.1% Triton X-100 and increasing concentrations of NaCl to eliminate spurious protein interactions. All proteins were eluted from the Glutathione beads and electrophoresed on an 11% SDS-PAGE gel before being probed for His-tagged protein.

Bacterial-2-Hybrid Assay

The bacterial-2-hybrid assay uses protein-protein interactions to bring two fragments of adenylate cyclase catalytic domain together to produce cAMP, stimulating β -galactosidase activity. β -galactosidase activity is therefore a representation of protein interaction. This protocol was performed as described by Karimova et al, 2005 (25). Briefly, *E. coli* DHP-1 cells (an adenylate cyclase deficient cell line) were transformed using pT18-CdsN/pT25-CdsN and either pT25-CopN, pT25-CdsD, pT25-CdsQ, pT25-CdsL, pT25-Cpn0706, pT25-Cpn0705 (putative ruler protein) or pT25-CdsN and selected with 100 μ g/ μ L ampicillin and 34 μ g/ μ L chloramphenicol. Three individual colonies

were selected from each plate and grown overnight in 3.0 mL of LB at 30°C in the presence of 0.5 mM IPTG plus appropriate antibiotics. Overnight culture (200 µL) was diluted 1 in 5 into 70 mM Na₂HPO₄-H₂O, 30 mM NaHPO₄-H₂O, 1 mM MgSO₄, and 0.2 mM MnSO₄ (PM2 buffer) and the optical density at 600 nm was recorded. The cells were permeabilized using 0.01% Toluene and 0.01% SDS. For the reaction, 50 µL of the permeabilized cells were diluted into 450 µL of LB broth. The diluted cells were then added to 500 µL of PM2 buffer containing 100 mM β-mercaptoethanol. The reaction was initiated by adding 250 µL of 12 mg/mL *ortho*-nitrophenyl-β-galactoside and allowed to continue for 15 seconds at 28°C. The reaction was stopped by the addition of 500 µL of 1.0 M Na₂CO₃. The absorbance was measured at 420 nm and the β-galactosidase activity was expressed as units of β-galactosidase activity per milligram of bacteria. Empty pT18 and pT25 vectors were transformed into *E. coli* DHP1 cells as a negative control and pT18-PknD and pT25-CdsD-FHA-2, which is the FHA-2 domain of CdsD, were used as a positive control (22). The cutoff for a positive interaction (677 units activity / mg bacteria) was determined as the mean plus two standard deviations of the negative control values obtained from 20 assays.

RESULTS

CdsN shares significant similarity with other T3S ATPases

CdsN (Cpn0707) is 443 amino acids in length with a predicted molecular weight of 48.1 kDa and an acidic pI of 6.10. CdsN has significant sequence similarity with the β subunit of the F_0F_1 -ATPase as well as with other T3S ATPases including EscN from *E. coli* and YscN from *Yersinia* (Fig. 1A). CdsN has a non-conserved N-terminal region which is possibly important for oligomerization (amino acids 1 to 155), a catalytic domain with Walker A and B domains (amino acids 155-403) and a C-terminal domain of unknown function (amino acids 403-443). Based on the similarity of CdsN to EscN, the structure of the catalytic domain is most likely a mixed α / β Rossmann fold, typical of the catalytic domain of EscN (41). Using NCBI-BLAST, the expect values of the CdsN catalytic domain with the YscN catalytic domain is $9e^{-95}$, and with the EscN catalytic domain is $2e^{-81}$, demonstrating a highly conserved catalytic domain. The catalytic domain of CdsN is 54% identical to the catalytic domains of EscN and YscN.

CdsN₁₋₄₀₅ and CdsL Oligomerize in Solution

The GST-tagged C-terminal truncation of CdsN, GST-CdsN₁₋₄₀₅, was over-expressed in *E. coli* BL21 (DE3) and purified using glutathione-agarose beads. Figure 2A, left, shows that GST-CdsN₁₋₄₀₅ was essentially free of contaminating proteins by SDS-PAGE gel electrophoresis followed by Coomassie blue stain. To determine whether CdsN was capable of forming oligomers we first used a bacterial-2-hybrid system to assess the

interactions between CdsN monomers. CdsN monomers exhibited levels of interaction that were significantly above that seen with background (empty vectors) (Table 2). To confirm this observation and analyze for the presence of higher molecular weight oligomers we allowed CdsN to form oligomers in solution, then fixed the protein with formaldehyde and ran the sample on a non-denaturing PAGE gel. Due to the insolubility of full length GST-CdsN, we utilized the C-terminal truncation GST-CdsN₁₋₄₀₅. The predicted molecular weight of GST-CdsN₁₋₄₀₅ is 64 kDa and CdsN monomers migrated in the gel at a position corresponding to the 64 kDa molecular weight marker (Fig. 3A). Multiple high molecular weight bands corresponding to 120 kDa and 180 kDa complexes were also seen, demonstrating oligomer formation of CdsN (Fig 3A). Smaller bands were also seen on the gel, possibly representing N-terminal fragments oligomerizing in solution. N-terminal fragments were visible when purified GST-CdsN₁₋₄₀₅ was analyzed by Western blot (Fig 2A, right). This suggests that the oligomerization domain of CdsN is near the N-terminal region since the GST tag is also present on the N-terminus of CdsN. Some GST-tagged protein was also seen at the top of the gel, possibly representing high molecular weight oligomers. The high molecular weight bands could be consistent with the formation of dodecamers which have been described for other T3S ATPases (30,33). Since YscL homologs have been shown to dimerize in other bacteria, CdsL was assessed for its ability to form dimers (31). His-tagged CdsL was over-expressed in *E. coli* BL21 (DE3) pLysS, analyzed by SDS-PAGE gel electrophoresis and Coomassie blue staining (Fig 2B, left), and anti-His western blot analysis (Fig 2B, right), then purified on Ni-NTA beads and analyzed for its ability to form oligomers using non-denaturing PAGE gels and

Western blot. Purified His-CdsL monomers migrated with a molecular weight of 25.9 kDa, as seen in Figure 2B, right. The presence of CdsL dimers is indicated by a band migrating with a molecular weight of approximately 50 kDa (Fig. 3B). To demonstrate that GST and His tags alone had no effect on the oligomerization of these proteins GST-CopN and His-CopN were run as controls and neither tagged protein formed oligomers (Figure 3C).

ATPase Activity of CdsN

Purified GST-CdsN₁₋₄₀₅ was assessed for its ability to hydrolyze ATP using the malachite green binding assay. GST-CdsN₁₋₄₀₅ hydrolyzed ATP in a linear, time- dependent manner (Fig 4A, triangles), with phosphate release occurring at a rate of $0.55 \pm 0.07 \mu\text{mol min}^{-1} \text{mg}^{-1}$. This activity is comparable with other T3S ATPases such as InvC, HrcN, and EscN (3,5). Also, ATPase activity seemed to decrease at higher protein concentrations (Fig. 4B, triangles), and may be indicative of positive cooperativity which is characteristic of other T3S ATPases (3,5). The Proteinase K treated CdsN₁₋₄₀₅ (squares) displayed no ATPase activity as well as purified GST-CopN as a negative control.

CdsN interacts with CdsD, CdsL, CdsQ and CopN

We have used the bacterial-2-hybrid system described by Karimova et al, 2005, to screen for interactions between CdsN and other chlamydial T3SS proteins (25). CdsN showed significant interaction with CdsD, CdsL, CdsQ and CopN (Table 3). CdsN was also

screened against Cpn0705, the YscP ‘ruler protein’ homolog, but no interaction was detected. Following screening with the bacterial-2-hybrid assay, protein interactions were further evaluated using a GST pull-down assay. GST pull-down assays were used to confirm the interactions of CdsN with other chlamydial T3S proteins at both low and high salt conditions in the presence of 0.1% Triton X-100 to dissociate spurious protein-protein interactions. GST-CdsN interacted with His-CdsD, His-CdsL, His-CdsQ and His-CopN (Fig. 5A) while GST alone, used as a negative control, did not pull down any of the T3S proteins under any salt concentrations (lane 1 for each sample). The interactions were very specific and there were no contaminating bands on the Western blots. GST-CdsN, however, did not interact with Cpn0705, the putative ruler protein. To determine whether the C-terminus of CdsN is important for mediating interactions with these T3S proteins, pull-down assays were performed with GST-CdsN₁₋₄₀₅ fragment. GST-CdsN₁₋₄₀₅ interacted with CdsD, CdsL, CdsQ, and CopN, suggesting that the C-terminal 38 amino acids of CdsN is not involved in these protein-protein interactions (Fig. 5B). All interactions were stable in the presence of 500 mM NaCl (Fig. 5, lane 4), suggesting that CdsN forms stable interactions with CdsD, CdsQ, CdsL and CopN. Consistent with full length CdsN, the GST-CdsN₁₋₄₀₅ protein also did not interact with Cpn0705 under any salt conditions.

Interaction of CdsN with a putative chaperone Cpn0706

Cpn0706 encodes a 169 amino acid protein with a predicted molecular weight of 19.8 kDa protein and a pI of 9.70. The *Cpn0706* ORF is located directly upstream of the T3S

ATPase CdsN (*Cpn0707*). The bacterial-2-hybrid assay and GST pull-down assays used to test for interactions between Cpn0706 and CdsN. Table 4 shows that CdsN interacts with recombinant Cpn0706 in the bacterial-2-hybrid assay. To corroborate the interaction seen in the bacterial-2-hybrid system, a GST pull-down was used. An interaction was seen when the full length GST-CdsN beads were used to interact with Cpn0706 under low salt conditions in the presence of 0.1% Triton X-100, but no interaction was detected between GST-CdsN and Cpn0706 at 200 mM or 500 mM NaCl (Fig. 6A, top). When GST-CdsN₁₋₄₀₅ was used to pull down Cpn0706, no interaction was seen suggesting that Cpn0706 interacts with the C-terminal 38 amino acids of CdsN (Fig. 6A). Since T3S effectors and their chaperones have been shown to form dimers, we tested Cpn0706 for its ability to dimerize. Purified His-Cpn0706 was electrophoresed on a non-denaturing gel and visualized using Western blot. As shown in Figure 6B, Cpn0706 monomers migrate at their predicted molecular weight of approximately 19.8 kDa, and dimers can be seen migrating with an apparent molecular weight of 40 kDa.

DISCUSSION

Although *C. pneumoniae* contains all the genes coding for a T3SS, only a fraction of these have been biochemically characterized. Here we report a preliminary characterization of CdsN, the putative T3S ATPase of *C. pneumoniae*. We have demonstrated that CdsN possesses ATPase activity, hydrolyzing ATP in a time- and dose-dependant manner. CdsN also forms oligomers in solution and interacts with other putative T3S components including CdsD, CdsQ, CdsL and CopN. We also identified an interaction with Cpn0706, a small protein located directly upstream from CdsN, which may be a CdsN chaperone. Collectively, these data suggest that CdsN is the ATPase of the *C. pneumoniae* T3SS.

CdsN hydrolyzes ATP in a linear, time-dependant manner at a rate of $0.55 \pm .06$ $\mu\text{mol phosphate min}^{-1} \text{mg}^{-1}$ which is typical of other T3S ATPases (3,5). At higher protein concentrations, ATPase activity decreased, suggesting a positive cooperativity of CdsN, which has been described for other T3S ATPases (3,5,30). We have shown that both CdsN and the tethering protein, CdsL, form dimers, and in the case of CdsN, higher molecular weight oligomers. The presence of high molecular weight forms of CdsN may correspond to dodecamers that have been reported for T3S ATPases in *E. coli*. (30).

Interactions between specific proteins of the T3SS in various bacteria have been reported but studies on chlamydial T3SS proteins are limited. We have previously shown that the putative T3S structural protein, CdsD, interacts with the putative CdsN tethering protein, CdsL, and CdsQ, a T3S structural component localized to the inner membrane (23). In the present report we extend these studies and show that CdsN interacts with

CdsL, CdsD and CdsQ. These interactions likely form a tetrameric or higher-order complex at the inner membrane of *C. pneumoniae*. The interaction between CdsN and CdsD is a novel finding not previously shown in other bacteria. This interaction appears to be specific since it is not disrupted by high salt (500 mM). It is possible that CdsD acts as a docking platform at the chlamydial inner membrane to allow the ATPase to dock and form a dodecamer during injectisome assembly. CdsQ, which has been shown to interact with the effector protein CopN, and resides in both the inner membrane and cytosol of *C. pneumoniae* (Toor et al., unpublished data) may play a role in shuttling chaperone/effector complexes to the ATPase at the basal body of the injectisome. An important observation is that the C-terminal truncated CdsN protein, lacking the C-terminal 38 amino acid residues, is capable of interacting with CdsL, CdsD and CdsQ, indicating that the binding site for these proteins is not located in the C-terminal 38 amino acid residues. It is tempting to speculate that the interactive domains of CdsN for CdsL, CdsD and CdsQ resides in the N-terminal 155 amino acids of the protein since the catalytic domain encompasses the remainder of the protein. This is presently under investigation.

We have also shown that CdsN interacts with the putative effector and plug protein, CopN, using both a bacterial-2-hybrid assay and a GST pull-down assay. CopN is known to negatively regulate T3S by physically blocking the injectisome in *Yersinia*, but its role in *C. pneumoniae* T3S has not yet been elucidated. CopN from *C. trachomatis*, has, however, been shown to be secreted by heterologous T3S systems suggesting it is an effector in *C. pneumoniae*. The fact that CopN interacts strongly with

CdsN, even in the presence of 500 mM NaCl, suggests that CdsN may be important for effector protein recognition, as has been seen in other bacteria (14, 35). CopN interacts with both full length and CdsN₁₋₄₀₅, indicating that the binding site for CopN is located within the first 405 amino acids of CdsN and likely within the first 155 amino acids preceding the catalytic domain. In other bacteria, the ATPases have been shown to interact with chaperones of effector proteins (14,39), often via the C-terminal region (41), but this has not been demonstrated for CdsN in *Chlamydia*. Since we have shown that CdsN interacts with the effector, CopN, it is likely that it interacts with other effectors or their chaperones, as has been shown for other bacteria (14).

Cpn0706, a previously unannotated ORF, encodes a small protein with a predicted molecular weight of 19.8 kDa and a PI of 9.7. *Cpn0706* lies adjacent to CdsN (*Cpn0707*) suggesting that it may be a CdsN chaperone. We have shown that Cpn0706 interacts with CdsN using both GST pull-down and bacterial-2-hybrid assays. The binding sites for effector chaperones on other characterized T3S ATPases are thought to be on the C-terminal end of the protein (41). The CdsN₁₋₄₀₅ protein did not interact with Cpn0706 (even when washed with the low salt buffer) while the full length CdsN did, suggesting that the binding site for Cpn0706 lies within the C-terminal 38 amino acids of CdsN. Since non-denatured CdsN was used for this assay, and chaperones are known to interact with both folded and unfolded proteins, it could be expected that any interaction between CdsN and its potential chaperone, Cpn0706, would be weak and transient. This may explain why the interactions seen in the GST pull-down assay were disrupted by

high salt. More corroborating experiments will be required before Cpn0706 can be designated as a CdsN chaperone.

Bacterial T3S is a virulence factor that has been shown to play a crucial role in the invasion of host cells for a number of bacteria. Although this has not yet been demonstrated for *Chlamydomphila*, the presence of T3S genes in both *C. pneumoniae* and *C. trachomatis*, as well as the secretion of chlamydial effector proteins TARP, CopN and Pkn5 through heterologous systems, is highly suggestive of a functional T3S apparatus (17,26). In this study we have shown that CdsN is a functional ATPase and interacts with other key proteins of *C. pneumoniae* T3SS. We have also shown that CdsN interacts with a putative chaperone, Cpn0706, and with CopN, the putative plug and effector protein. These observations add to the accumulating evidence that *C. pneumoniae* contains a structurally intact and functional T3SS. In the absence of a functional T3S assay or a genetic transformation system for the *chlamydiae*, direct evidence for a functional T3SS continues to elude us. Further studies on protein interactions, together with genetic complementation and injectisome reconstruction in heterologous bacteria may provide tools to investigate the role of T3S in *Chlamydia* pathogenesis.

ACKNOWLEDGEMENTS

We would like to thank Dr. Justin Nodwell for the pT18 and pT25 vectors, as well as the DHP-1 *E. coli* strain for use in the bacterial-2-hybrid assay. We would like to thank Dr. Brian Coombes for his critical review of the manuscript. CBS and DLJ are both recipients of a Father Sean O'Sullivan Research Center Studentship. This research was funded by a Canadian Institute of Health Research grant to JBM.

REFERENCES

1. **Akeda, Y., Galan, J.** 2005. Chaperone release and unfolding of substrates in type III secretion. *Nature*. **437**:911-915
2. **Akeda, Y., Galan, J.** 2004. Genetic analysis of the *Salmonella enterica* type III secretion-associated ATPase InvC defines discrete functional domains. *J. Bacteriol.* **186**:2402-2412.
3. **Andrade, A., Pardo, J., Espinosa, N., Perez-Hernandez, G., Gonzalez-Pedrajo, B.** 2007. Enzymatic characterization of the enteropathogenic *Escherichia Coli* type III Secretion ATPase EscN. *Arch. Biochem. Biophys.* **468**: 121-7
4. **Betts, H., Twiggs, L., Sal, M., Wyrick, P., Fields, K.** 2008. Bioinformatic and biochemical evidence for the identification of the type III secretion system Needle protein of *Chlamydia Trachomatis*. *J. Bacteriol.* **190**: 1680-1690.
5. **Blaylock, B., Riordan, K., Missiakas, D., Schneewind, O.** 2006. Characterization of the *Yersinia enterocolitica* type III secretion ATPase YscN and its regulator, YscL. *J. Bacteriol.* **188**:3525-3534.
6. **Carabeo, R., Grieshaber, S., Hasenkrug, A., Dooley, C., Hackstadt, T.** 2004. Requirement for the Rac GTPase in *Chlamydia trachomatis* invasion of non-phagocytic cells. *Traffic*. **5**:418-425.
7. **Clifton, D., Fields, K., Grieshaber, S., Dooley, C., Fischer, E., Mead, D., Carabeo, R., Hackstadt, T.** 2004. A chlamydial type III translocated protein is

- tyrosine-phosphorylated at the site of entry and associated with recruitment of actin. Proc. Natl. Acad. Sci. U S A. **101**: 10166-71.
8. **Cornelis, G.** 2006. The type III secretion injectisome. Nat. Rev. Microbiol. **4**:811-825.
 9. **Coombes, B., Mahony, J.** 2002. Identification of MEK- and phosphoinositide-3-kinase-dependant signaling as essential events during *Chlamydia pneumoniae* invasion of HEp2 cells. Cell Microbiol. **4**: 447-60.
 10. **Fields, K., Hackstadt, T.** 2000. Evidence for the secretion of *Chlamydia trachomatis* CopN by a type III secretion mechanism. Mol. Microbiol. **38**:1048-1060.
 11. **Fields, K., Mead, D., Dooley, C., Hackstadt, T.** 2003. *Chlamydia trachomatis* type III secretion: evidence for a functional apparatus during early-cycle development. Mol. Microbiol. **48**:671-683.
 12. **Galan, J., Collmer, A.** 1999. Type III secretion machines: bacterial devices for protein delivery into host cells. Science. **284**: 1322-1328.
 13. **Galan, J., Wolf-Watz, H.** 2006. Protein delivery into eukaryotic cells by type III secretion machines. Nature. **444**: 567-573.
 14. **Gauthier, A., Finlay, B.** 2003. Translocated intimin receptor and its chaperone interact with ATPase of the type III Secretion apparatus of Enteropathogenic *Escherichia coli*. J. Bacteriol. **185**:6747-6755.

15. **Ghosh, P.** 2004. Process of protein transport by the type III secretion system. *Microbiol. Mol. Biol. Rev.* **68**:771-795.
16. **Hefty, P., Stephens, R.** 2007. Chlamydial type III secretion system is encoded on ten operons preceded by sigma 70-like promoter elements. *J. Bacteriol.* **189**:198-206.
17. **Herrmann, M., Schuhmacher, A., Muhldorfer, I., Melchers, K., Prothmann, C., Dammeier, S.** 2006. Identification and characterization of secreted effector proteins of *Chlamydomonas reinhardtii* TW183. *Res. Microbiol.* **157**:513-524.
18. **Hoare, A., Timms, P., Bavoil, P., Wilson, D.** 2008. Spatial constraints within the chlamydial host cell inclusion predict interrupted development and persistence. *BMC Microbiol.* **8**: 5.
19. **Hsia, R., Pannekoek, Y., Ingerowski, E., Bavoil, P.** 1997. Type III secretion genes identify a putative virulence locus of *Chlamydia*. *Mol. Microbiol.* **23**: 351-9.
20. **Hueck, C.** 1998. Type III secretion systems in bacterial pathogens of animals and plants. *Microbiol Mol. Biol. Rev.* **62**: 379-433.
21. **Hybiske, K., Stephens, R.** 2007. Mechanisms of host cell exit by the intracellular bacterium *Chlamydia*. *Proc. Natl. Acad. Sci. U. S. A* **104**:11430-11435.

22. **Johnson, D., Mahony, J.** 2007. *Chlamydomphila pneumoniae* PknD exhibits dual amino acid specificity and phosphorylates Cpn0712, a putative type III secretion YscD homolog. *J. Bacteriol.* **189**: 7549-55.
23. **Johnson, D., Stone, C., Mahony, J.** 2008. Interactions between CdsD, CdsQ, and CdsL, three putative *Chlamydomphila pneumoniae* type III secretion proteins. *J. Bacteriol.* **190**: 2972-2980.
24. **Journet, L., Agrain, C., Broz, P., Cornelis, G.** 2003. The needle length of bacterial injectisomes is determined by a molecular ruler. *Science.* **302**: 1757-60.
25. **Karimova, G., Dautin, N., Ladant, D.** 2005. Interaction network among *Escherichia coli* membrane proteins involved in cell division as revealed by bacterial two-hybrid analysis. *J. Bacteriol.* **187**: 2233-2243.
26. **Lane, B., Mutchler, C., Khodor, S., Grieshaber, S., Carabeo, R.** 2008. Chlamydial entry involves TARP binding of guanine nucleotide exchange factors. *PLoS Pathog.* **4**: 1-11
27. **Lugert, R., Kuhns, M., Polch, T., Gross, U.** 2004. Expression and localization of type III secretion-related proteins of *Chlamydia pneumoniae*. *Med. Microbiol. Immunol.* **193**:163-171.
28. **Minamino, T., Macnab, M.** 2000. FliH, a soluble component of the type III flagellar export apparatus of *Salmonella*, forms a complex with FliI and inhibits ATPase activity. *Mol. Microbiol.* **37**: 1494-1503.

29. **Moulder, J.** 1991. Interaction of *chlamydiae* and host cells in vitro. Microbiol. Rev. **55**: 143-190.
30. **Muller, S., Pozidis, C., Stone, R., Meesters, C., Chami, M., Engel, A., Economou, A., Stahlberg, H.** 2006. Double hexameric ring assembly of the type III protein translocase ATPase HrcN. Mol. Microbiol. **61**: 119-125
31. **Pallen, M., Bailey, C., Beatson, S.** 2006. Evolutionary links between FliH/YscL-like proteins from bacterial type III secretion systems and second-stalk components of the F₀F₁ and vacuolar ATPases. Protein Sci. **15**:935-940.
32. **Peters, J., Wilson, J., Myers, G., Timms, P., Bavoil, P.** 2007. Type III secretion a la *Chlamydia*. Trends Microbiol. **15**:241-251.
33. **Pozidis, C., Chalkiadaki, A., Gomez-Serrano, A., Stahlberg, H., Brown, I., Tampakaki, A., et al.** 2003. Type III protein translocase: HrcN is a peripheral ATPase that is activated by oligomerization. J. Biol. Chem. **278**: 25816-25824.
34. **Scidmore, M., Hackstadt, T.** 2001. Mammalian 14-3-3beta associates with the *Chlamydia trachomatis* inclusion membrane via its interaction with IncG. Mol. Microbiol. **39**: 1638-1650.
35. **Sorg, J., Blaylock, B. Schneewind, O.** 2006. Secretion signal recognition by YscN, the *Yersinia* type III secretion ATPase. Proc. Natl. Acad. Sci. U S A. **103**: 16490-16495.

36. **Su, H., McClarty, F., Dong, G., Hatch, Z., Pan, K., Zhong, G.** 2004. Activation of Raf/Mek/Erk/cPLA2 signaling pathway is essential for chlamydial acquisition of host glycerophospholipids. *J. Biol. Chem.* **279**: 9409-9416.
37. **Subtil, A., Wyplosz, B., Balana, M., Dautry-Varsat, A.** 2004. Analysis of *Chlamydia caviae* entry sites and involvement of Cdc42 and Rac activity. *J. Cell Sci.* **117**:3923-3933.
38. **Stephens, R., Kalman, S., Lammel, C., Fan, J., Marathe, R., Aravind, L., Mitchell, W., Olinger, L., Tatusov, R., Zhao, Q., Koonin, E., Davis, R.** 1998. Genome sequencing of an obligate intracellular pathogen of humans: *Chlamydia Trachomatis*. *Science.* **282**: 754-759.
39. **Thomas, J., Stafford, G., Hughes, C.** 2004. Docking of cytosolic chaperone-substrate complexes at the membrane ATPase during flagellar type III protein export. *Proc. Natl. Acad. Sci. U. S. A.* **101**:3945-3950.
40. **Woestyn, S., Allaoui, A., Wattiau, P., Cornelis, G.** 1994. YscN, the putative energizer of the *Yersinia* Yop secretion machinery. *J. Bacteriol.* **176**: 1561-9
41. **Zarivach, R., Vuckovic, M., Deng, W., Finlay, B., Strynadka, N.** 2007. Structural analysis of a prototypical ATPase from the type III secretion system. *Nat. Struct. Mol. Biol.* **14**:131-137.

TABLE 2.1 Plasmids used in this study.

Plasmid	Description
Gateway Expression Vectors	
pEx17-CdsD	Express His tagged CdsD
pEx17-CopN	Express His tagged CdsN
pEx17-CdsQ	Express His tagged CdsQ
pEx17-CdsL	Express His tagged CdsL
pEx17-Cpn0706	Express His tagged Cpn0706
pEx17-Cpn0705	Express His tagged Cpn0705
pEx15-CdsN	Express GST tagged CdsN
pEx15-CdsN ₁₋₄₀₅	Express GST tagged C-terminal truncation of CdsN
Bacterial-2-Hybrid Constructs	
pT18-CdsN	Express CdsN with C-term AC fragment
pT18-PknD	Express PknD with C-term AC fragment
pT25-CdsN	Express CdsN with N-term AC fragment

pT25-CopN	Express CopN with N-term AC fragment
pT25-CdsD	Express CdsD with N-term AC fragment
pT25-CdsQ	Express CdsQ with N-term AC fragment
pT25-CdsL	Express CdsL with N-term AC fragment
pT25-Cpn0706	Express Cpn0706 with N-term AC fragment
pT25-Cpn0705	Express Cpn0705 with N-term AC fragment
pT25-CdsD-FHA-2	Express the FHA-2 domain of CdsD with N-term AC fragment

TABLE 2.2 Bacterial-2-hybrid Analysis of CdsN oligomerization

Plasmids	β -Galactosidase Activity in units/mg bacteria
Negative Control:	
pT18 + pT25	431.0 \pm 122.7 units of activity
Positive Control:	
pT18-PknD + pT25-CdsD-FHA-2	1019.3 \pm 52.2 units of activity
Positive interactions:	
pT18-CdsN + pT25-CdsN	799.4 \pm 45.1 units of activity

* CdsN was cloned into both pT18 and pT25 for association studies in the bacterial-2-hybrid system. Both vectors were transformed into an *E. coli* adenylate cyclase knockout (DHP1) and grown for 24 hours at 30°C. The B2H assay was performed in triplicate as described in the Materials and Methods. Empty pT18 and pT25 vectors were used as a negative control while pT18-PknD + pT25-CdsD-FHA-2 was used as a positive control. The cut off for a positive interaction (677 units of activity / mg protein), is the mean of the negative control values (empty pT18 + pT25) plus two standard deviations obtained from 20 assays.

**TABLE 2.3 Interaction between CdsN and other T3S proteins
using the Bacterial-2-hybrid System**

Plasmids	β -Galactosidase Activity in units/mg bacteria
Negative Control:	
pT18 + pT25	355.0 \pm 122.7 units of activity
Positive Control:	
pT18-PknD + pT25-CdsD-FHA-2	1019.3 \pm 52.2 units of activity
Negative Interactions:	
pT18-CdsN + pT25-Cpn0705	405.2 \pm 45.1 units of activity
Positive Interactions:	
pT18-CdsN + pT25-CdsD	937.2 \pm 22.4 units of activity
pT18-CdsN + pT25-CdsL	716.3 \pm 51.2 units of activity
pT18-CdsN + pT25-CdsQ	714.2 \pm 38.4 units of activity
pT18-CdsN + pT25-CopN	1046.4 \pm 157 units of activity

* CdsN was cloned into the pT18 vector and CdsD, CdsL, CdsQ, Cpn0705 and CopN were cloned into the pT25 vector. The bacterial-2-hybrid was performed in triplicate as described in the Materials and Methods section. Empty pT18 and pT25 vectors were used as a negative control while pT18-PknD + pT25-CdsD-FHA-2 was used as a positive control. The cut off for a positive interaction (677 units of activity / mg protein), is the mean of the negative control values (empty pT18 + pT25) plus two standard deviations obtained from 20 assays.

TABLE 2.4 Interaction of CdsN with the hypothetical protein Cpn0706

Plasmids	β -Galactosidase Activity in units/mg bacteria
Negative Control:	
pT18 + pT25	203.0 \pm 75.7 units of activity
Positive Control:	
pT18-PknD + pT25-CdsD-FHA-2	1019.3 \pm 52.2 units of activity
Positive interactions:	
pT18-CdsN + pT25-0706	683.2 \pm 36.2 units of activity

* CdsN was cloned into the pT18 vector while Cpn0706 was cloned into the pT25 vector. The bacterial-2-hybrid system was performed as described in the Materials and Methods. Empty pT18 and pT25 vectors were used as a negative control while pT18-PknD + pT25-CdsD-FHA-2 was used as a positive control. The cut off for a positive interaction (677 units of activity / mg protein), is the mean of the negative control values (empty pT18 + pT25) plus two standard deviations obtained from 20 assays.

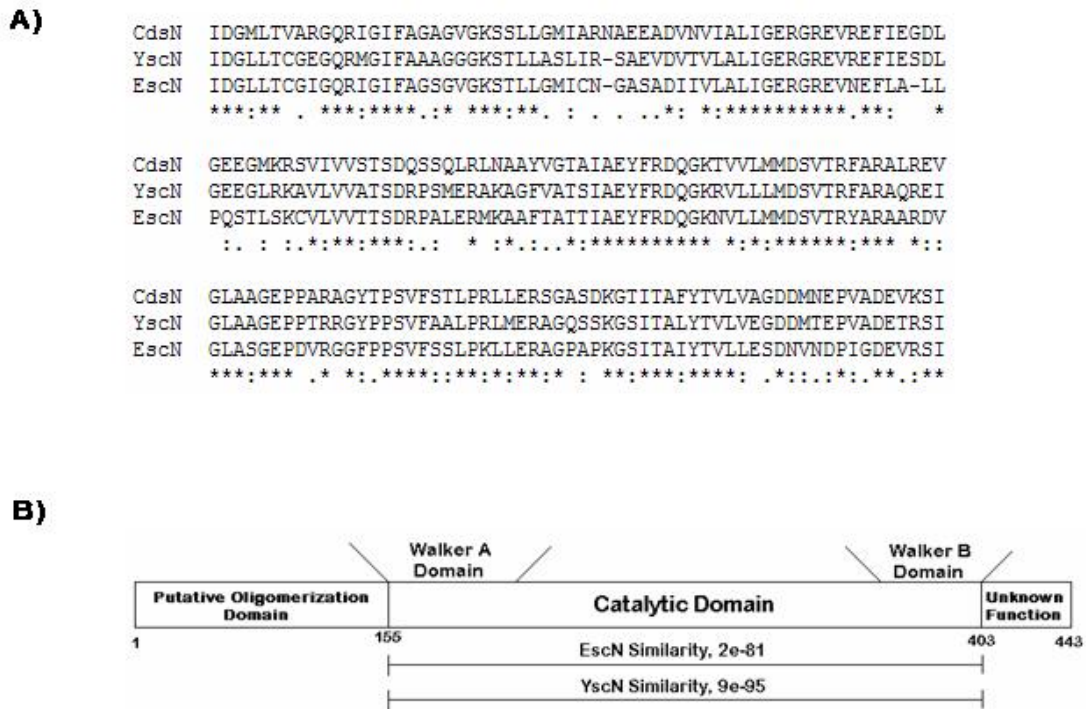


Figure 2.1. Sequence conservation of CdsN with other T3S ATPases. A: Sequence alignment of the putative catalytic domain of CdsN (amino acids 155-403) with the active domains of YscN from *Yersinia* and EscN from *E. coli*. Asterisk refers to identical amino acids, a double dot refers to a conserved substitution and a single dot refers to a semi-conserved substitution. **B:** Domain organization of CdsN based on structural similarity to EscN and YscN. CdsN contains Walker A and B domains, and a highly conserved catalytic domain most likely as an α/β Rossmann fold. The expected value is shown for similarity between the CdsN catalytic subunit and the catalytic subunit of EscN and YscN representing the similarity between the species.

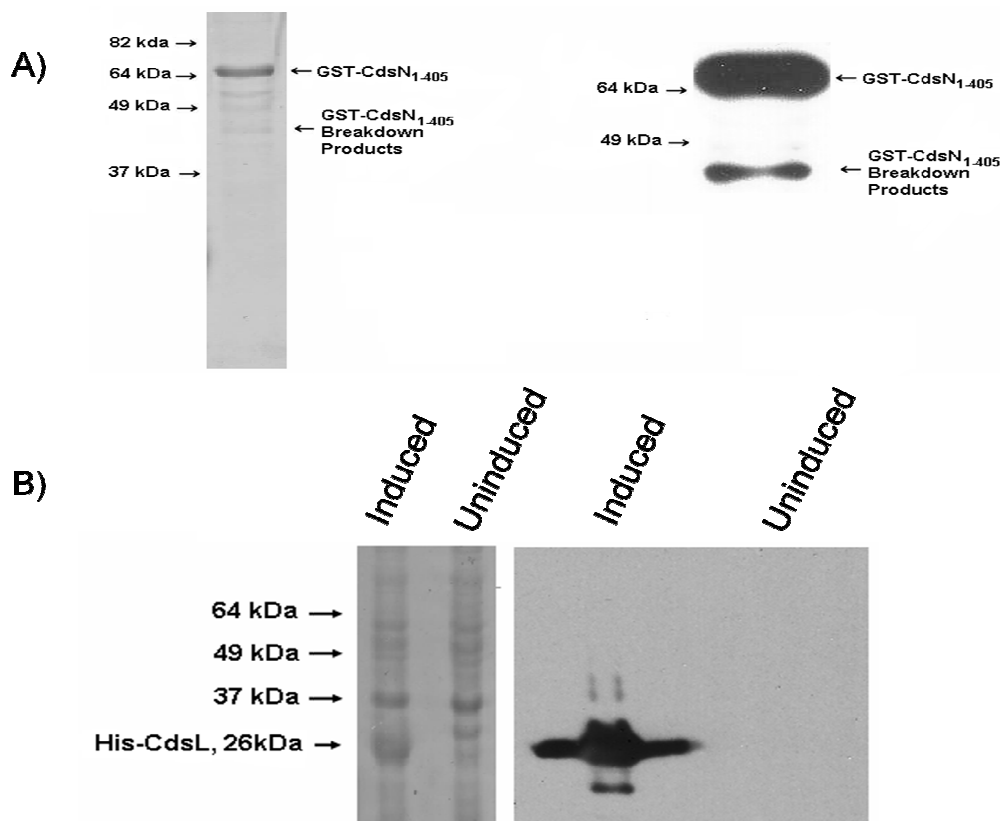


Figure 2.2. Purification of soluble GST-CdsN₁₋₄₀₅ and CdsL analyzed by Coomassie blue stain and Western blot. A. GST-CdsN₁₋₄₀₅ (0.1 μ g) electrophoresed on an 11% SDS-PAGE gel and stained with Coomassie blue migrating at slightly slower than the 64 kDa molecular marker (left). GST-CdsN₁₋₄₀₅ (0.05 μ g) electrophoresed on an 11% SDS-PAGE gel and analyzed by anti-GST Western blot. The presence of C-terminal breakdown products is visible migrating at smaller sizes (right). Ladder markers are shown on the left of each figure. **B:** *E. coli* BL21 (*DE3*) pLysS, either induced with IPTG or not induced, over-expressing His-CdsL, stained with Coomassie blue (left). CdsL, in the induced sample, can be seen migrating at approximately 26 kDa (left). The induced

and uninduced samples were also probed by anti-His Western blot. His-CdsL is seen migrating at 26 kDa in the induced sample (right). Ladder markers are shown on the left.

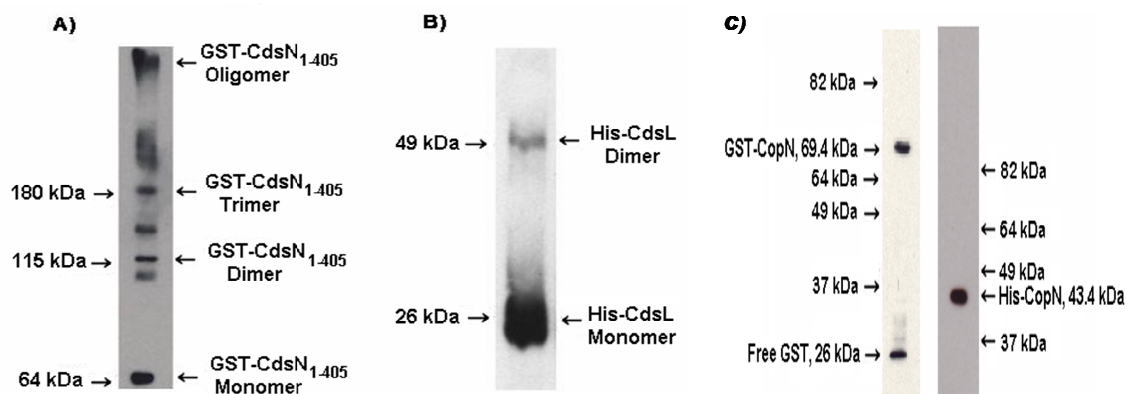


Figure 2.3. Oligomerization of CdsN and CdsL by Western Blot Analysis. **A:** GST-CdsN₁₋₄₀₅ monomers can be seen on a non-denaturing PAGE gel probed by anti-GST Western blot with a molecular weight of 64 kDa, and the formation of dimers and trimers can be seen at 120 and 180 kDa, respectively. Smaller GST-tagged bands are also seen migrating faster than the 115 kDa and 180 kDa marker, possibly corresponding to N-terminal fragments of CdsN oligomerizing. **B:** His-CdsL monomers can be seen on a non-denaturing PAGE gel probed by anti-His Western blot migrating with a molecular weight of 25.9 kDa, and the formation of a dimer can be seen at approximately 50 kDa. **C:** GST-CopN, after formaldehyde fixation and being run on a non-denaturing PAGE gel, probed by anti-GST western blot. GST-CopN monomers can be seen migrating at approximately 70 kDa as a monomer and free GST can be seen at approximately 26 kDa (left). His-CopN, after formaldehyde fixation, being run on a non-denaturing PAGE gel, and probed by anti-His western blot can be seen running in its monomeric form at approximately 45 kDa (right).

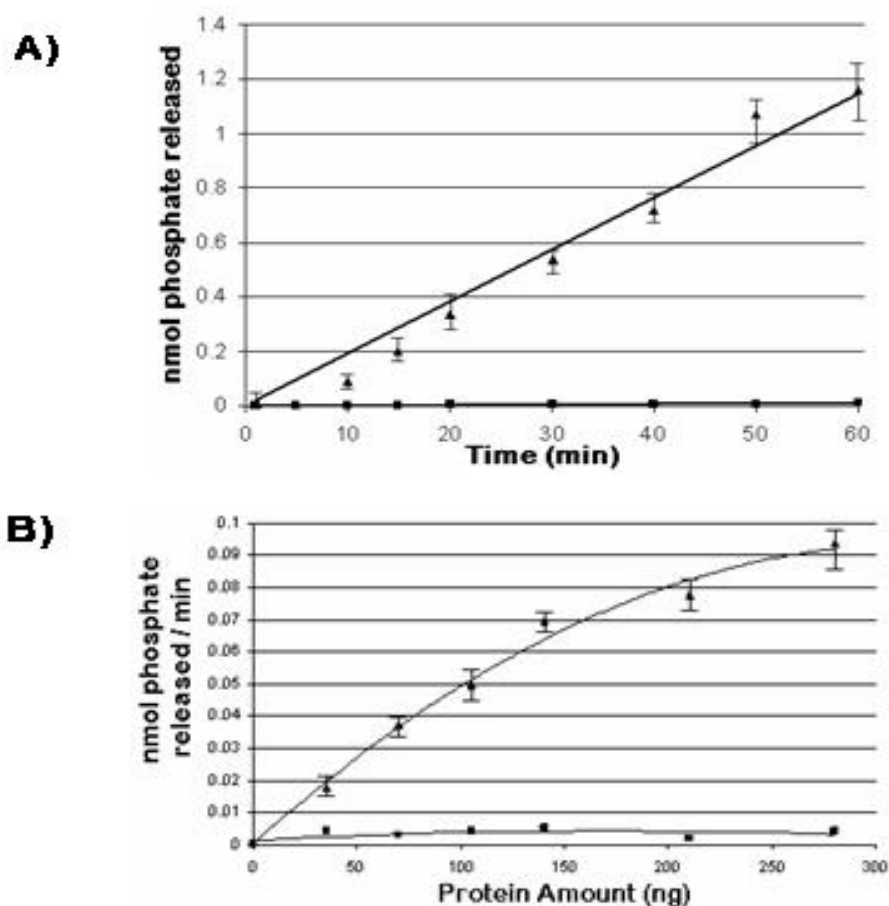


Figure 2.4. Time course and dose response of CdsN ATPase activity. A: Time course of GST-CdsN₁₋₄₀₅ ATP hydrolysis (triangles) and Proteinase K digested GST-CdsN₁₋₄₀₅ ATP hydrolysis (squares). All experiments were performed in triplicate. **B:** Inorganic phosphate released at different concentrations of GST-CdsN₁₋₄₀₅ (triangles) or Proteinase K digested GST-CdsN₁₋₄₀₅ concentrations (squares). All experiments were performed in triplicate.

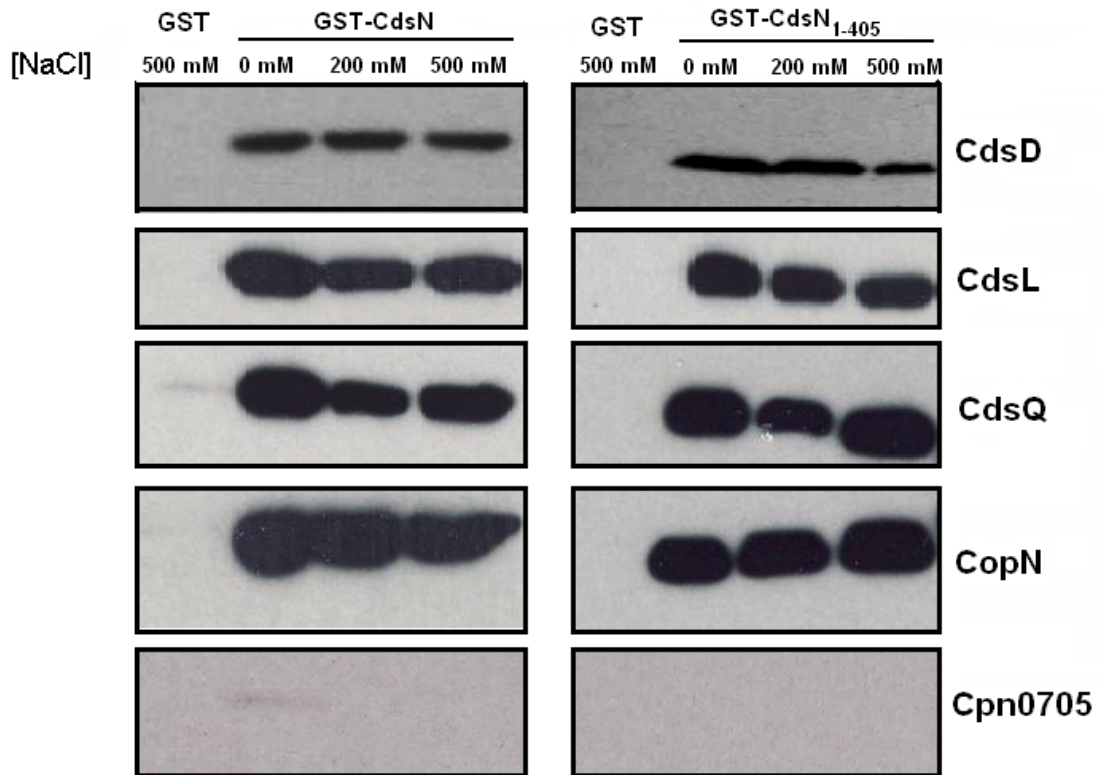


Figure 2.5. Interaction between CdsN and other T3SS proteins. A: Full length GST-CdsN was bound to glutathione beads and was used to pull down His-tagged protein from *E. coli* lysates. Beads were harvested by centrifugation, washed with 0 mM (lane 2), 200 mM (lane 3) and 500 mM (lane 4) NaCl and probed for His-tagged protein by Western blot using anti-His antibody. GST-CdsN pulled down CdsD, CdsL, CdsQ and CopN while GST alone did not pull down any of these proteins (lane 1). GST-CdsN also could not pull-down Cpn0705. **B:** GST-CdsN₁₋₄₀₅ bound to glutathione beads and used to pull down CdsD, CdsL, CdsQ, and CopN from *E. coli* lysates. As a negative control Cpn0705 was used, which GST-CdsN₁₋₄₀₅ could not pull-down.

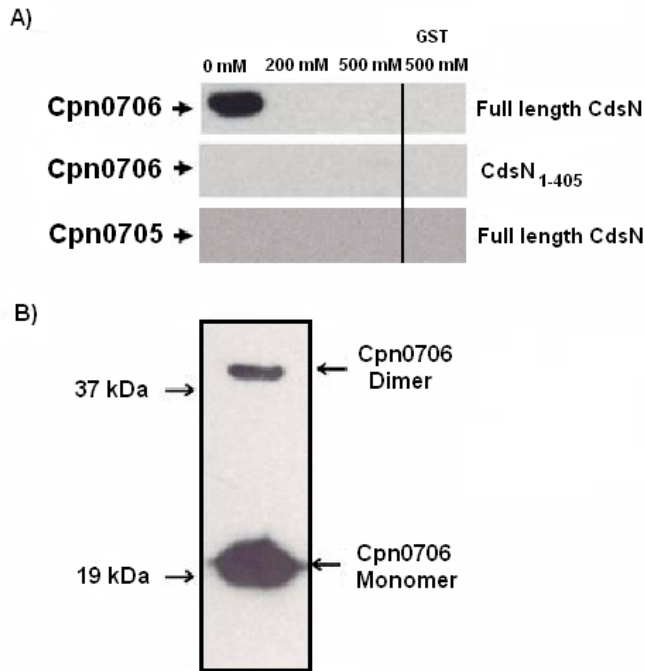


Figure 2.6. Interaction of CdsN with a putative chaperone, Cpn0706. A. Full length GST-CdsN was bound to glutathione beads and used to pull-down His-tagged Cpn0706. The beads were washed with 0.1% Triton X-100 alone (lane 1) or 0.1% Triton X-100 plus 200mM NaCl (lane 2) or 500mM NaCl (lane 3) and probed by anti-His western blot. GST alone did not interact with Cpn0706 (lane 4). Full length CdsN interacted with Cpn0706 under the low salt condition. C-terminal truncated GST-CdsN₁₋₄₀₅ was not able to interact with Cpn0706 under any salt conditions. As a negative control, full length CdsN can not pull down Cpn0705. **B.** Cpn0706 monomers, which have a predicted molecular weight of 19.8 kDa, migrate slightly slower than the 19 kDa molecular marker. Cpn0706 forms dimers which migrate at an apparent molecular weight of 40 kDa as shown by anti-His western blot of soluble Cpn0706 run on a non-denaturing SDS-PAGE gel.

CHAPTER THREE

Authors Preface to Chapter 3

In this chapter, I discuss the characterization of a set of genes present in all *Chlamydia* characterized to date, known as the ‘flagellar’ genes. Using GST pull-down assays, I demonstrate that the flagellar ATPase, FliI, associates with T3S components. I also show that FliI has enzymatic activity similar to CdsN. This work is the first to characterize these putative ‘flagellar’ genes and demonstrate that they in fact associate with T3S components. The overall implications of this work are (i) the flagellar ATPase has enzymatic activity, (ii) the flagellar proteins may be involved in the T3S process, and (iii) Cpn0859 is a novel protein that interacts with flagellar and T3S components.

The material presented in Chapter 3 has been accepted for publication in the peer-reviewed journal, *BMC Microbiology*. I performed the pull-down experiments and enzymatic activity assays. David Bulir assisted with the bacterial-2-hybrid experiments. Jodi Gilchrist and Raman Toor assisted with protein purification. Dr. James Mahony assisted with experimental design and editing of the manuscript.

Full citation:

Stone C, Bulir D, Gilchrist J, Toor R, Mahony J (2010) Interactions between flagellar and type III secretion proteins in *Chlamydia pneumoniae*. *BMC Microbiol.* 10: 18.

Interactions between flagellar and type III secretion proteins in *Chlamydia pneumoniae*

Chris B. Stone, David C. Bulir, Jodi D. Gilchrist, Raman K. Toor, and James B. Mahony*

M.G. DeGroote Institute for Infectious Disease Research, Faculty of Health Sciences and the Department of Pathology and Molecular Medicine, McMaster University, and the Father Sean O'Sullivan Research Centre, St. Joseph's Healthcare, Hamilton, Ontario, CANADA

* **Address correspondence to:**

Dr. J.B. Mahony
Regional Virology and Chlamydiology Laboratory, St. Joseph's Hospital

50 Charlton Avenue East, Hamilton, Ontario, CANADA

L8N 4A6

Phone: 905-521-6021

Fax: 905-521-6083

Email: mahonyj@mcmaster.ca

Running title: Characterization of the flagellar proteins of *C. pneumoniae*

Abstract

Flagellar secretion systems are utilized by a wide variety of bacteria to construct the flagellum, a conserved apparatus that allows for migration towards non-hostile, nutrient rich environments. *Chlamydia pneumoniae* is an obligate, intracellular pathogen whose genome contains at least three orthologs of flagellar proteins, namely FliI, FlhA and FliF, but the role of these proteins remains unknown. Full length FliI, and fragments of FlhA, FliF, and FliI, were cloned and expressed as either GST or His tagged proteins in *E. coli*. The GST-tagged full length FliI protein was shown to possess ATPase activity, hydrolyzing ATP at a rate of $0.15 \pm .02 \mu\text{mol min}^{-1} \text{mg}^{-1}$ in a time- and dose-dependant manner. Using bacterial-2-hybrid and GST pull-down assays, the N-terminal domain of FliI was shown to interact with the cytoplasmic domain of FlhA, but not with FliF, and the cytoplasmic domain of FlhA was shown to interact with the C-terminus of FliF. Another unannotated protein, Cpn0859, also interacted with FliI and FlhA, and could be another flagellar component. The lack of other flagellar orthologs led us to explore cross-reaction of flagellar proteins with type III secretion proteins, and we found that FliI interacted with CdsL and CopN, while FlhA interacted with CdsL and Cpn0322 (YscU ortholog). The specific interaction of the four orthologous flagellar proteins in *C. pneumoniae* suggests that they interact *in vivo* and, taken together with their conservation across members of the chlamydiae *sps.*, and their interaction with T3S components, suggests a role in bacterial replication and/or intracellular survival.

Introduction

Chlamydia pneumoniae is a gram negative, obligate intracellular pathogen that has been associated with community-acquired pneumonia (14), atherosclerosis (13), arthritis (4), and Alzheimer's disease (5). *C. pneumoniae* is characterized by a unique, biphasic life cycle beginning with an infectious, metabolically attenuated elementary body (EB). Chlamydial invasion is initiated by attachment of the EB to the host eukaryotic cell membrane and recruitment of actin to the site of attachment. This remodeling of the actin cytoskeleton is thought to be mediated by the type III secretion (T3S) effector protein, the translocated actin recruitment protein (TARP), which facilitates chlamydial entry into the host cell (8, 25). Bacterial uptake involves modulation of the host MEK-ERK pathway and PI 3-kinase, possibly through the action of T3S effectors (9, 29). Once internalized, the remainder of the chlamydial life cycle takes place within a parasitophorous membrane-bound vesicle known as an inclusion, where EBs differentiate into the non-infectious, metabolically active form, termed a reticulate body (RB). Within the inclusion, RBs acquire amino acids, nucleotides, lipids and cholesterol from the host cell, events possibly orchestrated via T3S across the inclusion membrane, while at the same time inhibiting apoptosis to ensure survival (15, 30, 39). Golgi fragmentation appears to be a crucial step in intercepting host pathways to obtain these nutrients and compounds, as well as in the maturation of the chlamydiae *sps.* within the inclusion (16). The RB interacts with the inclusion membrane until such time as inclusion membrane RB docking sites are no longer available and an unknown signal triggers detachment of RB from the inclusion membrane followed by asynchronous

differentiation into EBs (17, 36). The newly formed EBs then exit the cell by either cellular lysis or a packaged release mechanism termed extrusion (18).

Flagellar motility is an ancient, conserved mechanism that may have evolved from the same ancestor as T3S (1). This motility facilitates bacterial migration towards less hostile environments. In non-motile bacteria, however, the presence of flagella would be evolutionarily redundant and energetically expensive, unless the proteins played a role in another mechanism involving bacterial replication or survival. Although *C. pneumoniae* is thought to be a non-motile bacteria, it has been shown to contain at least three orthologs of flagellar genes, namely *flhA*, *fliF*, and *fliI* (21, 35). The proteins encoded by these genes are paralogs of the T3S proteins CdsV, CdsJ and CdsN, respectively. In motile bacteria, FlhA orthologs are integral membrane proteins required for flagellin export and swarming differentiation which interact with soluble components of the flagellar system (12, 27). FliF orthologs are integral membrane components that form the membrane and supramembrane (MS) ring (7). FliF forms a base for the other membrane components to form a molecular pore, through which components of the flagella that exist outside the cell membrane are exported. The flagellar ATPase, FliI orthologs, provide energy for construction of the flagellum by aiding in export of flagellar proteins outside the bacterial cell where the proteins form molecular complexes (2, 34). The presence of FliI, FlhA and FliF in *C. pneumoniae* is not sufficient to form a fully functional flagellar apparatus but they could potentially form a rudimentary base for a flagellum structure (24). In chlamydiae, the identity of other proteins (if they exist) that play other important roles in the flagellar apparatus is currently pending, but it is possible

that the flagellar apparatus, if it exists, is a hybrid structure of *C. pneumoniae* T3S proteins and the flagellar proteins. Another possibility is that flagellar proteins are involved in T3S, aiding in secretion of effector proteins or structural components. In *Pseudomonas*, there is evidence to suggest that flagellar assembly actually antagonizes the T3SS, suggesting a negative cross-regulation of the two systems (37). No interaction between chlamydial T3S and flagellar components, however, has been reported to our knowledge.

The protein interactions that occur within the bacterial flagellar system have been characterized previously (6, 24, 26). Genetic evidence, followed by direct biochemical assays, suggests an interaction of FlhA and FliF (23, 27). The C-terminal end of FlhA, which is predicted to be cytoplasmic, is known to interact with the soluble components of the flagellar system such as FliI, FliH and FliJ (27). FliH acts as a negative regulator of the flagellar ATPase, FliI, and binds FliI as a homodimer, forming a trimeric (FliI)(FliH)₂ complex (28, 32, 33). FliJ, a second soluble component which interacts with FlhA, acts as a general chaperone for the flagellar system to prevent premature aggregation of export substrates in the cytoplasm, and also interacts with the FliH/FliI complex (11). This complex of FliI/FliH/FliJ is believed to be crucial for selection of export substrates and construction of the flagellar apparatus, although the proton motive force could play a role in the actual secretion of flagellar proteins (34). In *C. pneumoniae*, FliH and FliJ have not been annotated in the genome.

FliI, the putative *C. pneumoniae* flagellar ATPase ortholog, has significant amino acid similarity with both CdsN, the *C. pneumoniae* T3S ATPase, and FliI, the *Salmonella*

flagellar ATPase, suggesting that it possesses enzymatic activity. Here we report an initial characterization of FliI, the flagellar ATPase, and show that it hydrolyzes ATP at a rate similar to that of its T3S ATPase paralog CdsN as well as orthologs in other bacteria (3, 10, 38). We have also characterized the protein-interactions occurring between FliI, FliF and FlhA, demonstrating a direct interaction of FliI and FlhA, and FlhA and FliF. As well as interactions between the flagellar proteins, we have also characterized four novel interactions between the flagellar and T3S components. The role of these interactions in the chlamydial replication cycle is discussed.

Methods

Expression Plasmids

C. pneumoniae CWL029 (VR1310:ATCC) (GenBank accession # AE001363) was the strain used to isolate genomic DNA for cloning and protein expression. Full length *fliI*, *Cpn0859*, *cdsL*, *copN*, *Cpn0322*, and fragments of *flhA*, *fliF*, and *fliI* were amplified from CWL029 using AttB-containing primers (Gateway; Invitrogen). The amplified products were cloned into pDONR₂₀₁ (Gateway; Invitrogen) to generate pENT vectors. The pENT vectors were then used in LR reactions (Gateway; Invitrogen) to produce pEX vectors containing the genes of interest. We used either pEX₁₇ (His-tagged) or pEX₁₅ (GST-tagged) vectors for our protein expression. All constructs were confirmed by sequencing at the Molecular Biology Facility at McMaster University.

To identify protein interactions we utilized the bacterial-2-hybrid system (22). Genes of interest were cloned into either pT18 or pT25 plasmids, each of which expresses a different fragment of adenylate cyclase. When these two plasmids are co-expressed, expressing the protein of interest fused to the adenylate cyclase fragment, any interaction between the two proteins results in expression of cAMP. Increases in cAMP results in an increase in the β -galactosidase gene that can be monitored using β -galactosidase activity assays. pT18 and pT25 were digested with KpnI (New England Biolabs) as well as genes amplified from CWL029 (*fliI*, *flhA*, *fliF*, *cdsL*, *Cpn0322*, *copN*) that had a KpnI site designed into the primers. Ligation was performed overnight at 16°C using T4 Ligase (Invitrogen) and the resulting mixture was used to transform *E. coli* XL-1 cells and transformants were selected on 100 μ g/ μ L ampicillin and 34 μ g/ μ L

chloramphenicol (Luria Bertani) LB plates. Plasmids were prepared using the GenElute Plasmid Miniprep Kit (Sigma).

Protein Expression

All constructs were expressed in *E. coli* Rosetta pLysS. Expression plasmids were used to transform *E. coli* Rosetta pLysS and plated on LB plates containing 100 µg/mL ampicillin. LB broth (750mL), containing antibiotics, was then inoculated with 12 mL of an overnight culture and grown at 37 °C until they reached an optical density (OD)₆₀₀ of approximately 0.8. Cultures were then cooled on ice to 20 °C and induced with 0.2 mM of isopropyl β-D galactosidase (IPTG). Cultures were then incubated at 23 °C for 2 hours and bacteria were harvested by centrifugation at 6500 x g for 10 minutes in a Sorvall RC-5B centrifuge and washed with ice-cold phosphate buffered saline (PBS). Bacteria containing His-tagged protein were resuspended in Binding Buffer (50 mM potassium phosphate pH 7.2, 150 mM KCl, 1 mM MgCl₂) while the bacteria containing GST-tagged protein were resuspended in PBS and stored at -20°C until further use.

Purification of Recombinant Proteins

E. coli pellets containing over-expressed proteins were thawed on ice and sonicated using a Fischer Scientific Sonic Dismembrator Model 100, followed by centrifugation at 20,000 x g for 40 minutes to remove insoluble material. Supernatants containing His-tagged protein were stored at 4 °C for use in GST pull-down assays while the GST-tagged protein supernatants were filtered through 0.45 µm acrodisc filters (Pall

Corporation) and incubated overnight at 4 °C with 300 µL of Glutathione-agarose beads (Sigma). For GST pull-down assays, beads were blocked overnight in Tris Buffered Saline with 0.1% Tween-20 and 4% BSA and stored at 4°C until use. For ATPase activity measurements, glutathione beads were washed on a column with PBS + 0.1% Tween until the flow-through had an OD₂₈₀ of less than 0.005. GST-tagged protein was then eluted off the beads using 1.5 µg/µL reduced glutathione (Sigma) and dialyzed against activity buffer (50 mM Tris-HCL pH 7.0, 5 mM MgCl₂, 10 mM KCl). Purity was confirmed using SDS-PAGE and Coomassie blue staining.

Dimerization Assay

In order to determine whether Cpn0859 formed dimers, formaldehyde fixation and non-denaturing PAGE were used. His-Cpn0859 was purified from Ni-NTA beads, dialyzed against PBS and concentrated using Amicon 10 kDa (Millipore) concentrators to a final concentration of 1 µg/µl. Formaldehyde was added to purified His-FliH to a final concentration of 10% and fixation was allowed to continue for 10 minutes. Samples containing 1 µg of FliH were electrophoresed on an 8% non-denaturing PAGE gel and visualized by Western blot using anti-His antibody (Sigma).

ATPase Activity

ATP hydrolysis by GST-FliI purified from glutathione-agarose beads was measured using a malachite green assay (R & D Systems). For all experiments, the specific activity was determined using the equation of a standard line generated using

phosphate standard (R & D Systems). Reaction mixtures contained 150 ng of GST-FliI, 4 mM ATP, 50 mM Tris-HCL pH 7.0, 5 mM MgCl₂, and 10 mM KCl. The reaction mixture (1 mL) was incubated at 37 °C for 1 hour and 50 µL of the mixture was taken for inorganic phosphate determination at various time points. The reaction was stopped by the addition of 10 µL of Malachite Green Reagent A followed by 10 µL of Malachite Green Reagent B and incubated at room temperature for one minute before an OD₆₁₀ reading was taken, according to the manufacturer's instructions. For the negative control, purified FliI was digested for 10 minutes at 37 °C using Proteinase K (Invitrogen). Also, as a negative control, another GST-tagged protein (CopN) known not to have ATPase activity was purified in the same manner and tested for activity. ATPase activity was expressed as µmol phosphate released min⁻¹ mg⁻¹ of protein, and all experiments were performed in triplicate.

GST Pull-down Assays

To examine the interaction of the flagellar proteins, GST pull-down assays were performed as described previously with the following modifications (20). Briefly, glutathione agarose beads (30 µL) bound to fifty nanograms of GST tagged FliI, Cpn0859, or FlhA was used in the assay. The beads were incubated overnight at 4 °C with the *E. coli* lysate expressing the His-tagged proteins. The beads were collected by centrifugation and washed with increasing concentrations of NaCl to eliminate spurious protein interactions. All proteins were eluted from the Glutathione beads and

electrophoresed on an 11% SDS-PAGE gel before being probed for His-tagged protein. As a negative control, GST alone was incubated on beads with the *E. coli* lysates.

Bacterial-2-Hybrid Assay

The bacterial-2-hybrid assay uses protein-protein interactions to bring two fragments of adenylate cyclase catalytic domain together to produce cAMP, stimulating β -galactosidase activity. β -galactosidase activity is therefore a representation of protein interaction. This protocol was performed as described by Karimova et al, 2005 (22). Briefly, *E. coli* DHP-1 cells (an adenylate cyclase deficient cell line) were transformed using pT18-FliI / pT18-FlhA / pT18-FliF and either pT25-FlhA or pT25-FliF and selected with 100 $\mu\text{g}/\mu\text{L}$ ampicillin and 34 $\mu\text{g}/\mu\text{L}$ chloramphenicol. Three individual colonies were selected from each plate and grown overnight in 3.0 mL of LB at 30°C in the presence of 0.5 mM IPTG plus appropriate antibiotics. Overnight culture (200 μL) was diluted 1 in 5 into M63 buffer (75 mM $(\text{NH}_4)_2\text{SO}_4$, 110 mM KH_2PO_4 , 200 mM K_2HPO_4 , 5 mM $\text{FeSO}_4\cdot 7\text{H}_2\text{O}$) and the optical density at 600 nm was recorded. The cells were permeabilized using 0.01% Toluene and 0.01% SDS. For the reaction, 50 μL of the permeabilized cells were diluted into 450 μL of LB broth. The diluted cells were then added to 500 μL of PM2 (70 mM $\text{Na}_2\text{HPO}_4\cdot\text{H}_2\text{O}$, 30 mM $\text{NaHPO}_4\cdot\text{H}_2\text{O}$, 1 mM MgSO_4 , and 0.2 mM MnSO_4) buffer containing 100 mM β -mercaptoethanol. The reaction was initiated by adding 250 μL of 12 mg/mL *ortho*-nitrophenyl- β -galactoside and allowed to continue for 15 seconds at 28°C. The reaction was stopped by the addition of 500 μL of

1.0 M Na_2CO_3 . The absorbance was measured at 420 nm and the β -galactosidase activity was expressed as units of β -galactosidase activity per milligram of bacteria. Empty pT18 and pT25 vectors were transformed into *E. coli* DHP1 cells as a negative control and pT18-CopN and pT25-CdsN were used as a positive control (38). The cutoff for a positive interaction (677 units activity / mg bacteria) was determined as the mean plus two standard deviations of the negative control values obtained from 20 assays.

Results

Sequence analysis of FliI, FlhA and FliF

FliI (Cpn0858) is 434 amino acids in length with a predicted molecular mass of 47.5 kDa and a pI of 8.00. FliI has significant sequence similarity with the β subunit of the F₀F₁-ATPase and both its type III secretion paralog, CdsN, and other flagellar ATPases. FliI has a non-conserved N-terminal region (amino acids 1-150) which may be important for mediating protein-protein interactions, a catalytic domain (amino acids 150-329), containing a conserved P loop, Walker A and B domains, and a C-terminal non-conserved domain (amino acids 329-434) of unknown function. FliI has a 34 percent sequence similarity to CdsN, the *C. pneumoniae* T3S ATPase, and 36 percent similarity with FliI from *Salmonella*. The active domain of FliI has the most similarity to its paralogs and orthologs, while the N- and C-terminal regions have the lowest amount of similarity (Figure 1).

FlhA (Cpn0363) is 583 amino acids in length with a predicted molecular mass of 65.6 kDa and a pI of 5.60. The FlhA paralog in *C. pneumoniae* is the T3S protein CdsV. FlhA has seven predicted transmembrane regions in the N-terminal half of the protein (FlhA₁₋₃₀₈), while the C-terminal half of the protein is predicted to be cytoplasmic (TMpred). FlhA from *C. pneumoniae* is 30 percent similar to CdsV from *C. pneumoniae*, and 23 percent similar to FlhA from *Salmonella*.

FliF (Cpn0860) is 342 amino acids in length with a predicted molecular mass of 38.2 kDa and a pI of 9.5. The FliF paralog in *C. pneumoniae* is the T3S protein CdsJ. FliF has two predicted TM regions, one located near the N-terminus and one located near

the C-terminus. FliF is only 7 percent similar to its paralog, CdsJ, and 15 percent similar to FliF from *Salmonella*.

Expression and ATPase activity of FliI

FliI has significant similarity with many characterized ATPases, and this led us to explore the ATPase activity of this protein. Purified GST tagged FliI was tested for its ability to hydrolyze ATP using the malachite green binding assay. Figure 2A shows that GST-FliI was essentially free of contaminating proteins by SDS-PAGE and anti-GST Western blot (left) or Coomassie blue stain (right). GST-FliI hydrolyzed ATP in a dose- and time-dependant manner at a rate of $0.15 \pm .02 \mu\text{mol min}^{-1} \text{mg}^{-1}$ (Figure 2B i and ii, diamonds). This level of activity is comparable to other flagellar ATPases as well as the T3S paralog, CdsN (10, 28, 38). ATPase activity of GST-FliI peaked at 37°C, and at a pH of 8.0 (Figure 2 iii and iv). Another GST-tagged protein, GST-CopN, purified in the same manner as GST-FliI had negligible ATPase activity (Fig 2B i and ii, squares).

FlhA interacts with FliF

FlhA is known to interact with the MS ring protein, FliF, in other flagellar systems (23, 27). We explored the interactions of these two proteins in *C. pneumoniae*. Two fragments of FliF were cloned and expressed as His-tagged proteins. His-FliF₁₋₂₇₁ lacked the distal C-terminal 70 amino acids while His-FliF₃₅₋₃₄₁ lacked the N-terminal 35 amino acids. Each fragment contained only one of the two predicted TM regions. FliF₁₋₂₇₁ migrated with an apparent molecular weight of 30 kDa, while His-FliF₃₅₋₃₄₁ migrated at

34 kDa. FlhA was cloned and expressed as a soluble fragment with either a GST or His tag. FlhA₃₀₈₋₅₈₃ encoded the C-terminal half of the protein, lacking the stretch of seven TM domains. Expression and detection of His-FlhA₃₀₈₋₅₈₃ used as the bait protein in GST pull-down assays migrated at the expected molecular weight of 30 kDa. We used the bacterial-2-hybrid assay to test for interactions between FliF and FlhA. Full length FlhA interacted significantly with full length FliF, with a β -galactosidase activity of 847.2 ± 21.2 units of activity, as compared with a negative control value of 412.0 ± 82.4 units of activity (Table 1). We next used GST pull-downs to confirm the interactions found by the bacterial-2-hybrid system and to determine the exact regions of the proteins mediating these interactions (Figure 3A). All protein complexes were washed with either low or high salt buffers containing 0.1% Triton X-100 to dissociate spurious protein-protein interactions. GST-FlhA₃₀₈₋₅₈₃ co-purified with His-FliF₃₅₋₃₄₁ but not His-FliF₁₋₂₇₁, suggesting that the C-terminus of FliF (amino acids 271-341) is required for interactions with the cytoplasmic portion of FlhA.

FliI interacts with FlhA

In orthologous systems, it has been shown that FlhA interacts with several soluble components of the flagellar machinery, including the ATPase, FliI (27). Therefore, we investigated the possibility of whether FlhA interacts with FliI in *C. pneumoniae*. The bacterial-2-hybrid system was initially used to screen for potential protein interactions. FlhA interacted with FliI, with β -galactosidase activity of 942.9 ± 123.1 units of activity as compared to the negative control with a value of 412.0 ± 82.4 units of activity (Table

1). To confirm these protein-protein interactions we used GST pull-down assays (Figure 3B). Initially FliI was cloned as three constructs, full length FliI, a C-terminal truncation of FliI (FliI₁₋₄₀₀) and a N-terminal truncation of FliI (FliI₁₅₀₋₄₇₁). These three constructs were tested for interaction with the His-FlhA₃₀₈₋₅₈₃ construct. Full length GST-FliI co-purified with His-FlhA₃₀₈₋₅₈₃, suggesting that the cytoplasmic fragment of FlhA contains the interactive domain. To determine the region of FliI that interacts with FlhA, we reacted the two truncation constructs of FliI with the cytoplasmic domain of FlhA. Only FliI₁₋₄₀₀ was able to co-purify with FlhA, and not FliI₁₅₀₋₄₇₁, suggesting that the FlhA binding domain resides in the N-terminal 150 amino acids of FliI (Figure 3B). We next wanted to know if FliI interacts with FliF. We therefore reacted GST-FliI against the two FliF constructs and found that there was no co-purification, suggesting that any interaction between FliI and FliF, if there is an association, would seem to be indirect and mediated through the action of FlhA or other intermediate proteins (Figure 3C).

Cpn0859 interacts with FliI and FlhA

Cpn0859 is a predicted 179 amino acid protein with a PI of 6.10 and a molecular mass of 20.3 kDa. The *Cpn0859* ORF is encoded directly upstream of *fliF* and downstream of *fliI*, the flagellar ATPase. Based on its location relative to FliI and FliF, we hypothesized that it may interact with other flagellar components. We used GST pull-down assays to explore this possibility. Initial GST pull-downs indicated that full length His-Cpn0859 interacts with GST-Cpn0859, suggesting the presence of a dimerization domain (Figure 4A). To explore this observation we treated Cpn0859 with formaldehyde

prior to PAGE and observed the presence of a monomer and a dimer, migrating with apparent molecular weights of 22 kDa and 45 kDa (Figure 4B). We next explored the possible interaction of Cpn0859 with other flagellar proteins in *C. pneumoniae*. Using GST pull-downs, His-Cpn0859 co-purified with the full length GST-FliI protein as well as the GST-FliI₁₋₄₀₀ protein, but not GST-FliI₁₅₀₋₄₇₁ (Figure 4C). This suggests that Cpn0859 binds to the N-terminus of FliI. GST pull-down assays showed an interaction between Cpn0859 and the FlhA₃₀₈₋₅₈₃ protein, the cytoplasmic domain of FlhA (Figure 4D). Cpn0859 did not co-purify with either FliF₃₅₋₃₄₁ or FliF₁₋₂₇₁ (Figure 4D), suggesting that Cpn0859 does not interact with FliF.

FliI and FlhA interact with T3S components

Since *Chlamydia* have no apparent flagella, we investigated whether the flagellar proteins FliI, FlhA and FliF interact with T3S components. Using bacterial-2-hybrid screening we found that FliI and FlhA interacted with CdsL, the putative T3S ATPase regulator and tethering protein, with a β -galactosidase activity of 874.3 ± 59.3 and 832 ± 23.3 units of activity, respectively. FliI also interacted with CopN, the putative T3S plug protein, with a β -galactosidase activity of 943.2 ± 74.2 units of activity. We also found that FlhA interacted with the putative YscU ortholog, Cpn0322 (CdsU), with a β -galactosidase activity of 779.9 ± 32.7 units of activity, as well as CdsL, with a β -galactosidase activity of 832.1 ± 23.3 units of activity (Table 1). To corroborate these findings we utilized GST pull-down assays and showed that GST-FliI interacted with CdsL and CopN, but not Cpn0706 (Figure 5A), and GST-FlhA co-purified with both

CdsL and Cpn0322 (Figure 5B). Control GST coated beads did not co-purify with CdsL, CopN or Cpn0322.

Discussion

Sequencing of several chlamydial genomes revealed a conserved set of flagellar orthologs, despite the fact that *C. pneumoniae* lack a flagellum and are considered non-motile bacteria (21, 35). Here we report an initial characterization of three annotated flagellar proteins of *C. pneumoniae*, FliI, FlhA and FliF, demonstrating ATPase activity of FliI and interactions between these flagellar orthologs. We have demonstrated that FliI hydrolyzes ATP in a linear, time- and dose-dependent manner, with optimal activity at a pH of 8.0 and a temperature of 37°C. FliI also interacts with the cytoplasmic domain of FlhA, while FlhA interacts with the C-terminal region of the FliF protein. No direct interaction of FliI and FliF was detected. Also, we have characterized an interaction of both FlhA and FliI with Cpn0859, a fourth unannotated protein. We also show that FliI interacts with CdsL and CopN, two T3S components, while FlhA interacts with CdsL and a third T3S component, Cpn0322. Collectively, this data suggests that the flagellar proteins of *C. pneumoniae* interact in a specific way with T3S proteins and may play an important, as yet unidentified role in the chlamydial replication cycle.

FliI hydrolyzes ATP in a linear, time- and dose-dependent manner at a rate of $0.15 \pm .02 \mu\text{mol min}^{-1} \text{mg}^{-1}$. This rate is typical of other secretion ATPases such as CdsN, EscN, or FliI from other bacterial species (3, 10, 28, 38). The optimal pH for FliI ATPase activity is 8.0, which is the same as that for other flagellar ATPases (10). Extreme low or high pH greatly reduced the activity, possibly due to protein denaturation. Also, the enzyme activity peaked at a temperature of 37°C and declined substantially beyond that. Although the formation of higher-order complexes was not explored here, other flagellar

ATPases are thought to form a hexameric complex, and this is currently being investigated (19).

The presence of three flagellar genes in *chlamydiae* is intriguing since *chlamydiae* are thought to be non-motile and not to possess flagella. FliF, FlhA and FliI alone do not contain all the necessary components for a functional flagella or secretion apparatus, however, a rudimentary basal body or pore complex could be formed by these three components. It is known that the most rudimentary flagellar structure that can be assembled is the MS ring, which consists of only the FliF protein (24). We have shown that these proteins interact with one another (FliI, FlhA and FliF), most likely at the inner membrane of *C. pneumoniae*. The interaction between FliI and FlhA is mediated by the N-terminal 150 amino acids of FliI and appears to be specific since it is not disrupted by high salt (500 mM). Only the cytoplasmic domain of FlhA (amino acids 308-583) was utilized in the GST pull-down, suggesting that any protein interactions that occur are within this region. Protein interaction studies with the full length FlhA protein are difficult due to the presence of seven transmembrane domains rendering full length FlhA insoluble and making this portion of the protein unable to bind with soluble flagellar components. Since FlhA is known to interact with soluble components of the flagellar apparatus in other bacteria, it is expected that the cytoplasmic domain mediates an interaction with FliI (27). FliF is known to form the MS ring in flagellated bacteria, and is one of the first components of the flagellar basal body to be incorporated into the membrane (6, 7). We detected an interaction of the C-terminal 70 amino acids of FliF with the cytoplasmic domain of FlhA. These interactions were also stable in 500 mM

NaCl, suggesting that the interaction is specific. We did not, however, detect any interaction between FliI and FliF, suggesting that any interaction between those two components may be mediated through the action of another protein, possibly FlhA

In *C. pneumoniae*, *Cpn0859* is encoded directly downstream of the ATPase, which led us to explore any interactions *Cpn0859* may have with other flagellar proteins in *C. pneumoniae*. We initially found that *Cpn0859* was able to interact with itself using a GST pull-down assay, suggesting that it could form dimers in solution. To confirm this observation we utilized formaldehyde fixation followed by PAGE analysis to visualize the formation of dimers. Using this method we saw that *Cpn0859* migrated in two molecular forms, with sizes corresponding to both monomers and dimers. We then explored possible interactions between *Cpn0859* and the other flagellar proteins and detected interactions of *Cpn0859* with both FliI and FlhA, but not FliF. *Cpn0859* bound to the N-terminal 150 amino acids of FliI and the cytoplasmic region of FlhA. The interaction of *Cpn0859* with the cytoplasmic domain of FlhA was expected as FlhA is known to interact with soluble components of other flagellar systems (27). Figure 6 summarizes the interactions between FliI, FlhA and FliF (Figure 6A) and interactions between *Cpn0859*, FlhA and FliI (Figure 6B).

Bacterial type III secretion (T3S) and flagellar secretion systems are structurally similar, and may have a common ancestry (1). Although *C. pneumoniae* does not contain a full repertoire of flagellar genes, it does encode a complete T3S system which consists of specific protein complexes located in the inner membrane (20, 35, 38). We have characterized an interaction of FliI with CdsL, the T3S ATPase tethering protein. The *C.*

pneumoniae FliH ortholog has not yet been identified, and in the absence of FliH, CdsL may play a regulatory role for both FliI and CdsN. FliI also interacts with the CopN, the T3S plug protein, suggesting that FliI may be involved in either the secretion of effector proteins or regulation of the T3S system. YscU orthologs have a flagellar paralog, FlhB, and Cpn0322 is believed to be the *C. pneumoniae* YscU orthologs (CdsU). FlhB is known to interact with FlhA, but in *C. pneumoniae* no FlhB ortholog has been annotated. We found that FlhA interacts with Cpn0322 (CdsU), suggesting integration of FlhA into the inner membrane, associating with T3S components.

Based on all of our observations, it is possible that the flagellar proteins may interact with components of the T3S injectisome, forming a hybrid structure, thereby playing an ancillary or accessory role in secretion of type III effectors across either the cytoplasmic or inclusion membrane. Another possibility is that there are other, as yet unannotated proteins that play a role in a putative flagellar system in *C. pneumoniae*. For example, along with the FliH/FliI complex that is formed in other bacteria, another protein, FliJ, which is a general chaperone, is believed to be involved in this complex (11); FliJ has not been identified in *C. pneumoniae*. In the absence of a genetic manipulation system for the *chlamydiae*, direct evidence for the role of these flagellar proteins remains elusive. The fact that FliI is enzymatically active and forms complexes *in vitro* with other flagellar proteins, all of which are present in all other *chlamydiae* *sps.* studied to date, suggests that these proteins play an important role in chlamydial replication or survival. Further studies using heterologous systems and genetic

complementation could help to decipher the exact role of these flagellar proteins in chlamydiae.

Acknowledgments

We would like to thank Dr. Patrik Bavoil for scientific discussion involving the flagellar proteins. CBS is a recipient of a Father Sean O'Sullivan Research Center Studentship.

This research was funded in part by a Canadian Institute of Health Research grant to JBM.

References

1. **Aizawa, S.** 2001. Bacterial flagella and type III secretion systems. *FEMS Microbiol. Lett.* **202**: 157-164.
2. **Akeda, Y., Galan, J.** 2005. Chaperone release and unfolding of substrates in type III secretion. *Nature.* **437**:911-915
3. **Andrade, A., Pardo, J., Espinosa, N., Perez-Hernandez, G., Gonzalez-Pedrajo, B.** 2007. Enzymatic characterization of the enteropathogenic *Escherichia coli* type III Secretion ATPase EscN. *Arch. Biochem. Biophys.* **468**: 121-127
4. **Ardeniz O, Gulbahar O, Mete N, Cicek C, Basoglu OK, Sin A et al.** 2005. *Chlamydia pneumoniae* arthritis in a patient with common variable immunodeficiency. *Ann. Allergy Asthma Immunol.* **94**: 504-508.
5. **Balin, B., Little, C., Hammond, C., Appelt, D., Whittum-Hudson J., Gerard, H., et al.** 2008. *Chlamydia pneumoniae* and the etiology of late-onset Alzheimer's disease. *J. Alzheimers Dis.* **13**: 371-380.
6. **Berg, H.** 2003. The rotary motor of bacterial flagella. *Annu. Rev. Biochem.* **72**:19-54.
7. **Bigot, A., Pagniez, H., Botton, E., Frehel, C., Dubail, I., Jacquet, C., Charbit, A., Raynaud, C.** 2005. Role of FliF and FliI of *Listeria monocytogenes* in flagellar assembly and pathogenicity. **73**: 5530-5539.
8. **Clifton, D., Fields, K., Grieshaber, S., Dooley, C., Fischer, E., Mead, D., Carabeo, R., Hackstadt, T.** 2004. A chlamydial type III translocated protein is

tyrosine-phosphorylated at the site of entry and associated with recruitment of actin.
Proc. Natl. Acad. Sci. U S A. **101**: 10166-10171

9. **Coombes, B., Mahony, J.** 2002. Identification of MEK- and phosphoinositide-3-kinase-dependant signaling as essential events during *Chlamydia pneumoniae* invasion of HEp2 cells. Cell Microbiol. **4**: 447-460.
10. **Fan, F., Macnab, R.** 1996. Enzymatic characterization of FliI. J. Biol. Chem. **271**: 31981-31988.
11. **Fraser, G., Gonzalez-Pedrajo, B., Tame, J., Macnab, R.** 2003. Interactions of FliJ with the *Salmonella* type III flagellar export apparatus. J. Bacteriol. **185**: 5546-5554.
12. **Ghelardi, E., Celandroni, F., Salvetti, S., Beecher, D., Gominet, M., Lereclus, D., Wong, A., Senesi, S.** 2002. Requirement of flhA for swarming differentiation, flagellin export, and secretion of virulence-associated proteins in *Bacillus thuringiensis*. J. Bacteriol. **184**: 6424-6433.
13. **Grayston, J.** 2000. Background and current knowledge of *Chlamydia pneumoniae* and atherosclerosis. J. Infect. Dis. **181**: S402-S410.
14. **Hahn D, Azenabor A, Beatty W, Byrne G.** 2002. *Chlamydia pneumoniae* as a respiratory pathogen. Front Biosci. **7**: e66-e76.
15. **Hatch, T.** 1975. Utilization of L-cell nucleoside triphosphates by *Chlamydia psittaci* for ribonucleic acid synthesis. J. Bacteriol. **122**: 393-400.

16. **Heuer, D., Lipinski, A., Machuy, N., Karlas, A., Wehrens, A., Siedler, F., Brinkmann, V., Meyer, T.** 2009. Chlamydia causes fragmentation of the Golgi compartment to ensure reproduction. *Nature*. **457**: 731-735.
17. **Hoare, A., Timms, P., Bavoil, P., Wilson, D.** 2008. Spatial constraints within the chlamydial host cell inclusion predict interrupted development and persistence. *BMC Microbiol.* **8**: 5.
18. **Hybiske, K., Stephens, R.** 2007. Mechanisms of host cell exit by the intracellular bacterium *Chlamydia*. *Proc. Natl. Acad. Sci. U. S. A* **104**:11430-11435.
19. **Imada, K., Minamino, T., Tahara, A., Namba, K.** 2007. Structural similarity between the flagellar type III ATPase FliI and F1-ATPase subunits. *Proc. Natl. Acad. Sci. U. S. A* **104**: 485-490.
20. **Johnson, D., Stone, C., Mahony, J.** 2008. Interactions between CdsD, CdsQ, and CdsL, three putative *Chlamydomydia pneumoniae* type III secretion proteins. *J. Bacteriol.* **190**: 2972-2980.
21. **Kalman, S., Michell, W., Marathe, R., Lammel, C., Fan, J., Hyman, R., Olinger, L., Grimwood, J., Davis, R., Stephens, R.** 1999. Comparative genomes of *Chlamydia pneumoniae* and *C. trachomatis*. *Nat Genet.* **21**: 385-389.
22. **Karimova, G., Dautin, N., Ladant, D.** 2005. Interaction network among *Escherichia coli* membrane proteins involved in cell division as revealed by bacterial two-hybrid analysis. *J. Bacteriol.* **187**: 2233-2243.

23. **Kihara, M., Minamino, T., Yamaguchi, S., Macnab, R.** 2001. Intergenic suppression between the flagellar MS ring protein FliF of *Salmonella* and FlhA, a membrane component of its export apparatus. *J. Bacteriol.* **183**: 1655-1662.
24. **Kubori, T., Shimamoto, N., Yamaguchi, A., Namba, K., Aizawa, S.** 1992. Morphological pathway of flagellar assembly in *Salmonella typhimurium*. *J. Mol. Biol.* **226**: 433-446.
25. **Lane, B., Mutchler, C., Khodor, S., Grieshaber, S., Carabeo, R.** 2008. Chlamydial entry involves TARP binding of guanine nucleotide exchange factors. *PLoS Pathog.* **4**: 1-11
26. **Marykwas, D., Schmidt, S., Berg, H.** 1996. Interacting components of the Flagellar Motor of *Escherichia coli* revealed by the two-hybrid system in Yeast. *J. Mol. Bio* **256**: 564-576.
27. **McMurry, J., Arnam, J., Kihara, M., Macnab, R.** 2004. Analysis of the cytoplasmic domains of *Salmonella* FlhA and interactions with components of the flagellar export machinery. *J. Bacteriol.* **186**: 7586-7592.
28. **Minamino, T., Macnab, M.** 2000. FliH, a soluble component of the type III flagellar export apparatus of *Salmonella*, forms a complex with FliI and inhibits ATPase activity. *Mol. Microbiol.* **37**: 1494-1503.
29. **Moulder, J.** 1991. Interaction of *chlamydiae* and host cells in vitro. *Microbiol. Rev.* **55**: 143-190.

30. **Moore, E., Fischer, E., Mead, D., Hackstadt, T.** 2008. The Chlamydial inclusion preferentially intercepts basolaterally directed sphingomyelin-containing exocytic vacuoles. *Traffic*. **9**: 2130-2140,
31. **Muller, S., Pozidis, C., Stone, R., Meesters, C., Chami, M., Engel, A., Economou, A., Stahlberg, H.** 2006. Double hexameric ring assembly of the type III protein translocase ATPase HrcN. *Mol. Microbiol.* **61**: 119-125
32. **Okabe, M., Minamino, T., Imada, K., Namba, K., Kihara, M.** 2009. Role of the N-terminal domain of FliI ATPase in bacterial flagellar protein export. *FEBS lett.* **583**: 743-748.
33. **Pallen, M., Bailey, C., Beatson, S.** 2006. Evolutionary links between FliH/YscL-like proteins from bacterial type III secretion systems and second-stalk components of the F₀F₁ and vacuolar ATPases. *Protein Sci.* **15**:935-940.
34. **Paul, K., Erhardt, M., Hirano, T., Blair, D., Hughes, K.** 2008. Energy source of flagellar type III secretion. *Nature*. **451**: 489-492.
35. **Peters, J., Wilson, J., Myers, G., Timms, P., Bavoil, P.** 2007. Type III secretion in *Chlamydia*. *Trends Microbiol.* **15**:241-251.
36. **Scidmore, M., Hackstadt, T.** 2001. Mammalian 14-3-3beta associates with the *Chlamydia trachomatis* inclusion membrane via its interaction with IncG. *Mol. Microbiol.* **39**: 1638-1650.

37. **Soscia, C., Hachani, A., Bernadac, A., Filloux, A., Bleves, S.** 2007. Cross talk between type III secretion and flagellar assembly systems in *Pseudomonas aeruginosa*. *J. Bacteriol.* **189**: 3124-3132.
38. **Stone, C., Johnson, D., Bulir, D., Mahony, J.** 2008. Characterization of the putative type III secretion ATPase CdsN (Cpn0707) of *Chlamydophila pneumoniae*. *J. Bacteriol.* **190**: 6580-6588.
39. **Wylie, J., Hatch, G., McClarty, G.** 1997. Host cell phospholipids are trafficked to and then modified by *Chlamydia trachomatis*. *J. Bacteriol.* **179**: 7233-7242

TABLE 3.1 Interaction between the flagellar proteins of *C. pneumoniae* using the Bacterial-2-hybrid System

Plasmids	β -Galactosidase Activity in units/mg bacteria
Negative Control:	
pT18 + pT25	412.0 \pm 82.4 units of activity
Positive Control:	
pT18-PknD + pT25-CdsD-FHA-2	996.3 \pm 50.0 units of activity
Negative Interactions:	
pT18-FliI + pT25-FliF	396.4 \pm 32.1 units of activity
pT18-FliF + pT25-Cpn0859	421.1 \pm 25.9 units of activity
pT18-FliI + pT25-Cpn0706	404.4 \pm 19.5 units of activity
pT18-Cpn0706 + pT25-FlhA	443.0 \pm 32.3 units of activity
Positive Interactions:	
pT18-FliF + pT25-FlhA	847.2 \pm 21.2 units of activity
pT18-FliI + pT25-FlhA	942.9 \pm 123.1 units of activity
pT18-FliI + pT25-CdsL	874.3 \pm 59.3 units of activity

pT18-FliI + pT25-CopN	943.2 ± 74.2 units of activity
pT18-Cpn0322 + pT25-FlhA	779.9 ± 32.7 units of activity
pT18-CdsL + pT25-FlhA	832.1 ± 23.3 units of activity

* FliI, FliF, FlhA, CdsL, CopN, Cpn0706 and Cpn0322 were cloned into both the pT18 and pT25 vectors. The bacterial-2-hybrid was performed in triplicate as described in the Materials and Methods section. Empty pT18 and pT25 vectors were used as a negative control while pT18-PknD + pT25-CdsD-FHA-2 was used as a positive control. The cut off for a positive interaction (577 units of activity / mg protein), is the mean of the negative control values (empty pT18 + pT25) plus two standard deviations obtained from 20 assays.

<i>C.pneumoniae</i>	-----MNHLNKEKLIHINWQPYRACGLLSKVSGNLIIEVDGLSACLGELCKISSTKDP	52
<i>C.trachomatis</i>	-----MTHLQEETLLIHQWRPYRECGILSRISGSLLLEAQGLSACLGELCQISLSRSD	52
<i>Salmonella</i>	MTTRLTRWLTALDNEAKMALLPAVRRYGRLTRATGLVLEATGLQLPLGATCIIERQDGP	60
	:. *: : : : . * * *: : * :*: ** . ** * * . .	
<i>C.pneumoniae</i>	---NLLAEVIGFHNHTLLMSLSPLHSVALGTEVLP-----LRRPSSLHLSHDHLLGRV	102
<i>C.trachomatis</i>	---PILAEVIGIHNRTTLLALTPIYYLAIGAEVVP-----LRRPASLPLSNHLLGRV	102
<i>Salmonella</i>	ETKEVESEVVGFNQQLFLMPLLEEVGILPGARVYARNGHDGLQSGKQLPLGPALLGRV	120
	:*:*:*:*: :*: * : : *:* . *: . * * . *****	
<i>C.pneumoniae</i>	LDAFGNPIDKKEDLPKTHRKPLLSLPPSPMMRQPIDQIFPTGIKAI DAFLTLGKQGRIGV	162
<i>C.trachomatis</i>	LDGFGNPLDGGPQLPKTNLSPLFSSPPSPMSRTPIQEVFPTGIRAIDALLTIGEGQRVGI	162
<i>Salmonella</i>	LDGGGKPLDGLPAPDLETGALITPPFNPLQRTPIEHVLDTGVRAINALLTVGRGQRMGL	180
	** . *:*: * . . .*: : * *: * * *: : : * *: * *: * *: * *: * *: *	
<i>C.pneumoniae</i>	<u>FSEPGSGKSSLLSAIALGSKSTINVIALLIGERGREVREYIEKHSNALKQQRITIIAAPAH</u>	222
<i>C.trachomatis</i>	<u>FSEPGGGKSSLLSTIAKGSQQTINVIALLIGERGREVVDYVNHKEGLAAQRTVIIASTAY</u>	222
<i>Salmonella</i>	<u>FAGSGVGKSVLLGMMARYTRADVIVVGLIGERGREVKDFIENILGPDGRARSVVIAAPAD</u>	240
	*: . * ** ** . : * : : *: .*****: : : : : : * *: * *: *	
<i>C.pneumoniae</i>	ETAPTKVIAGRAAMTIAEYFREQGHEVLFIMDSLRSRWIAALQEVALARGETLSAHQYAAS	282
<i>C.trachomatis</i>	ETAASKVIAGRAAITIAEYFRDQGARVLFIMDSLRSRWIESLQEVAIARGETLSTHHYAAS	282
<i>Salmonella</i>	VSPLLRMQGAAYATRIAEDFRDRGQHVLLIMDSLTRYAMAQREIALAIGEPATKGYPPS	300
	: . : : . . * ** * *: * *: * *: * *: : : * *: * ** . : : * ..*	
<i>C.pneumoniae</i>	VFHHVSEFTERAGN--NDKGSITALYAILLYPK-HPDIFTDYLKSLLDGHHFLTS-QGKA	338
<i>C.trachomatis</i>	VFHHVAEFLERAGN--NDKGSITSFYAILHYAN-HPDIFTDYVKSLLDGHHFLSP-QEKS	338
<i>Salmonella</i>	VFAKL PALVERAGNGIHGGGSITAFYTVLTEGDDQQDPIADSARAILDGHI VLSRRLAEA	360
	** : : : ***** : . *****: : * . : * : * : : *****: : :	
<i>C.pneumoniae</i>	LASPPIDILSSLSRSAQALALPHHYAAAERLRSLLKVYNEALDI IHLGAYTPGQDEELDK	398
<i>C.trachomatis</i>	FSSPPINVLTSLSRSSRQLALPHHYAAQELLSLLKAYHEAIDIIQLGAYVSGQDAHLDR	398
<i>Salmonella</i>	GHYPAIDIEASISRAMTALITEQHYARVRLFKQLLSFQRNRDLVSVGAYAKGSDPMLDK	420
	*. *: : : * : * : * * * .. : . * . : : : * : : * * * * * :	
<i>C.pneumoniae</i>	AVKLLPSIKAFLAQPLSSYCYLDNTLKQLEALADS-	433
<i>C.trachomatis</i>	AIRLLPSVKQFLSQPYSHYSALHETIEQLCQLLKHE	434
<i>Salmonella</i>	AITLWPQLEAFLLQGGIFERADWEDSLQALDLIFPTV	456
	*: * * *: : * * . . : : : * :	

Figure 3.1. Sequence conservation of FliI from *C. pneumoniae* with *C. trachomatis* and *Salmonella*. Sequence alignment (ClustalW) of the full length FliI protein from *C. pneumoniae*, *C. trachomatis*, and *Salmonella*. Asterisk refers to identical amino acids, a double dot refers to a conserved substitution and a single dot refers to a semi-conserved substitution. Outlined is the conserved P loop region in the Walker A domain.

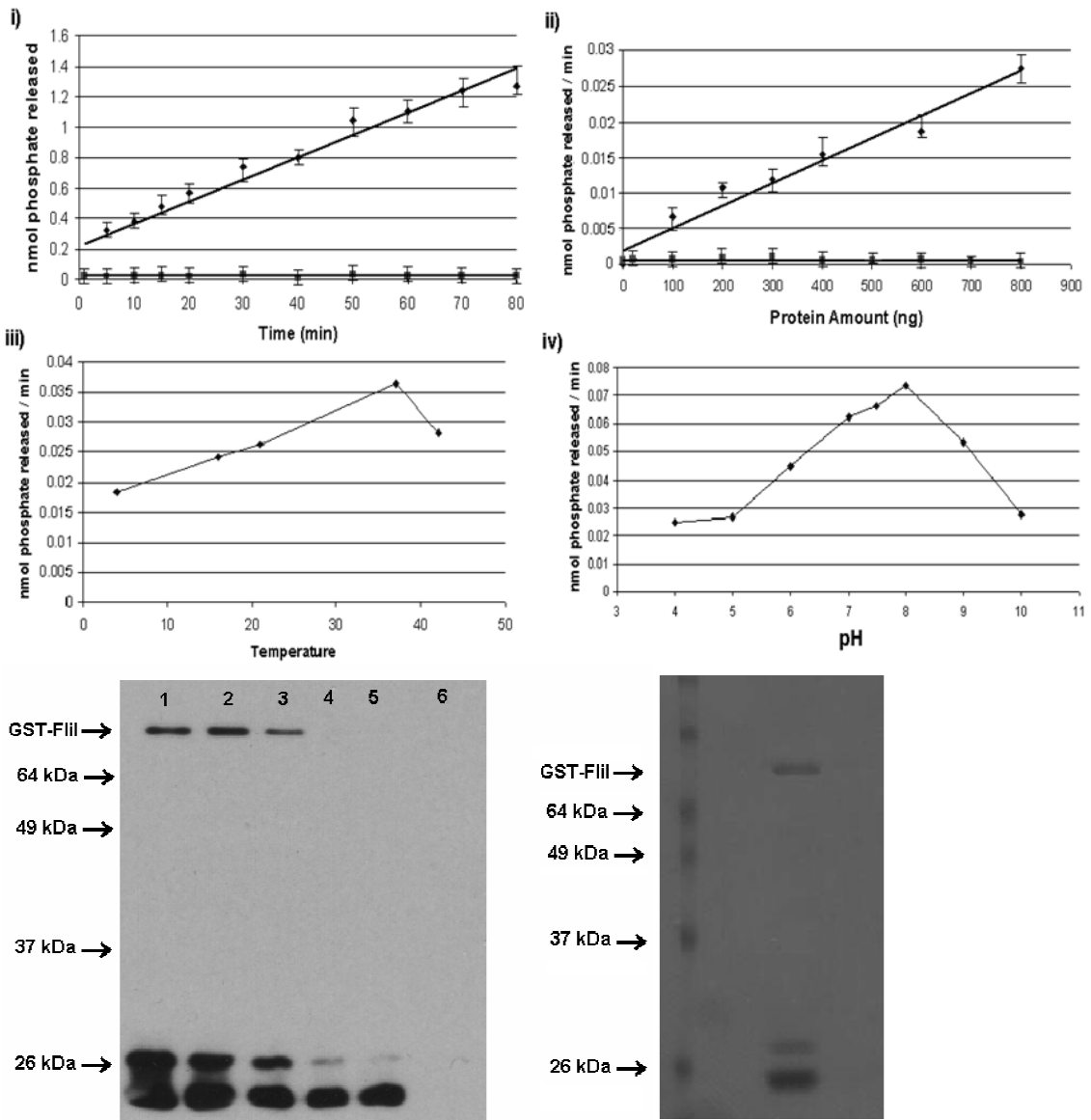


Figure 3.2. Expression, purification, and optimal conditions for the time- and dose-dependant ATPase FliI. A: GST-FliI eluted off a glutathione column (1 mL aliquots) and electrophoresed on an 11% SDS-PAGE gel and either probed for by anti-GST Western blot (left) or stained by Coomassie blue (right). GST-FliI migrated at approximately 73 kDa, its predicated molecular mass. Numbers refer to the eluted

fraction. **B:** i) Time course of purified GST-FliI ATP hydrolysis (diamonds) and GST-CopN ATP hydrolysis as a negative control (squares). ii) Inorganic phosphate released at different concentrations of GST-FliI (diamonds) and GST-CopN as a negative control (squares) iii) GST-FliI ATPase activity at either 4°C, 16 °C, 23 °C, 37 °C or 42 °C. iv) GST-FliI ATPase activity at varying pH.

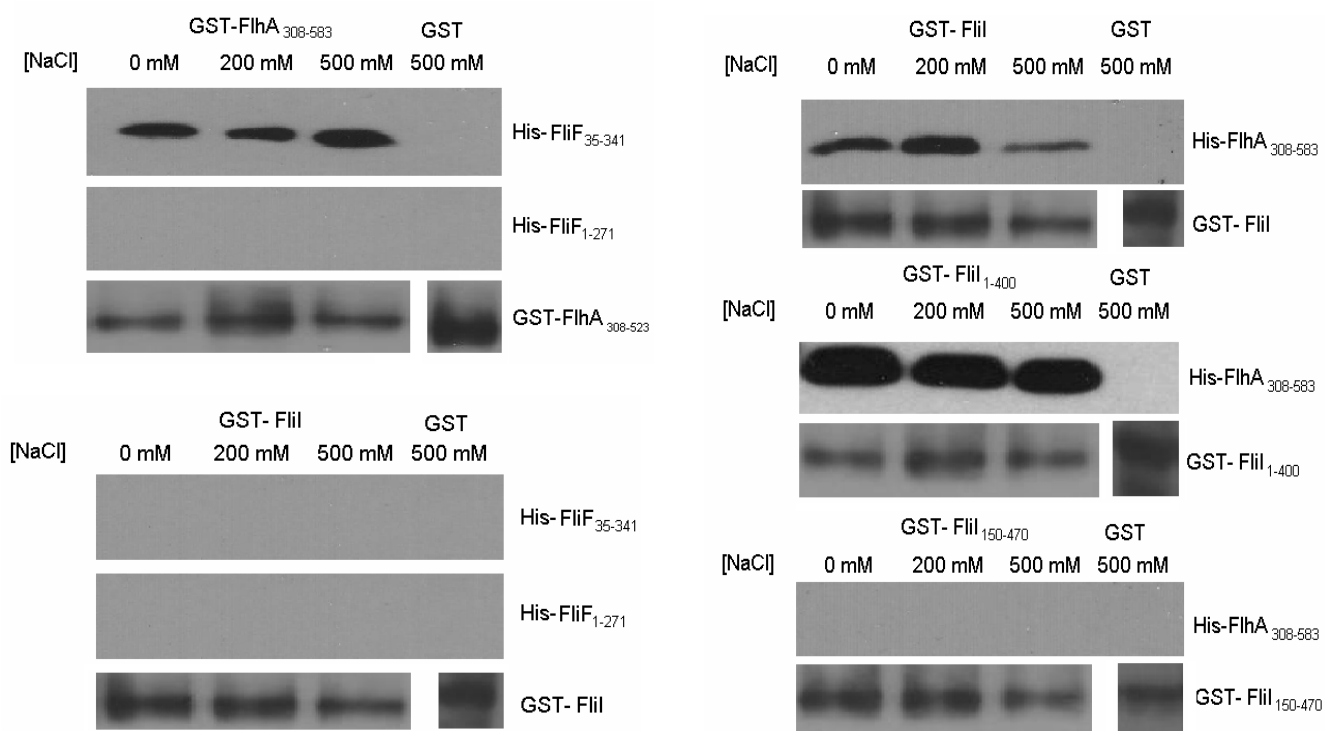


Figure 3.3. Interaction between the flagellar components using GST pull-down

assays. A: GST- FlhA₃₀₈₋₅₈₃ was bound to glutathione beads and was used to pull down either His-FliF₃₅₋₃₄₁ or His-FliF₁₋₂₇₁ from an *E. coli* lysate. Beads were harvested by centrifugation and washed with either 0mM, 200mM or 500mM NaCl and probed for His-tagged protein by Western blot using anti-his antibody. GST- FlhA₃₀₈₋₅₈₃ co-purified with His-FliF₃₅₋₃₄₁ but not His-FliF₁₋₂₇₁ while GST alone did not co-purify with either. GST-FlhA₃₀₈₋₅₈₃ is shown as a loading control. **B:** Full length GST-FliI, GST-FliI₁₋₄₀₀, or GST-FliI₁₅₀₋₄₇₀ were bound to glutathione beads and were used to pull down His-FlhA₃₀₈₋₅₈₃ from an *E. coli* lysate. Full length GST-FliI and GST-FliI₁₋₄₀₀ were able to co-purify with FlhA₃₀₈₋₅₈₃ while GST-FliI₁₅₀₋₄₇₀ was not. GST alone was not able to co-purify with His-FlhA₃₀₅₋₅₈₃. **C:** Full length GST-FliI was bound to glutathione beads and used to pull

down His-FliF₃₅₋₃₄₁ and His-FliF₁₋₂₇₁. GST-FliI did not co-purify with either FliF fragment. **D:** Full length GST-FliI, GST-FliI₁₋₄₀₀, or GST-FliI₁₅₀₋₄₇₀ were bound to glutathione beads and were used to pull down His-Cpn0859 from an *E. coli* lysate. They were washed in the same manner as above, and only full length GST-FliI and GST-FliI₁₋₄₀₀ were able to co-purify with His-Cpn0859. **E:** Full length GST-Cpn0859 was bound to glutathione beads and was used to pull down either His-FlhA₃₀₈₋₅₈₃, His-FliF₃₅₋₃₄₁ or His-FliF₁₋₂₇₁ from an *E. coli* lysate. GST-Cpn0859 co-purified with His- FlhA₃₀₈₋₅₈₃, but not His-FliF₃₅₋₃₄₁ or His-FliF₁₋₂₇₁ while GST alone did no co-purify with either.

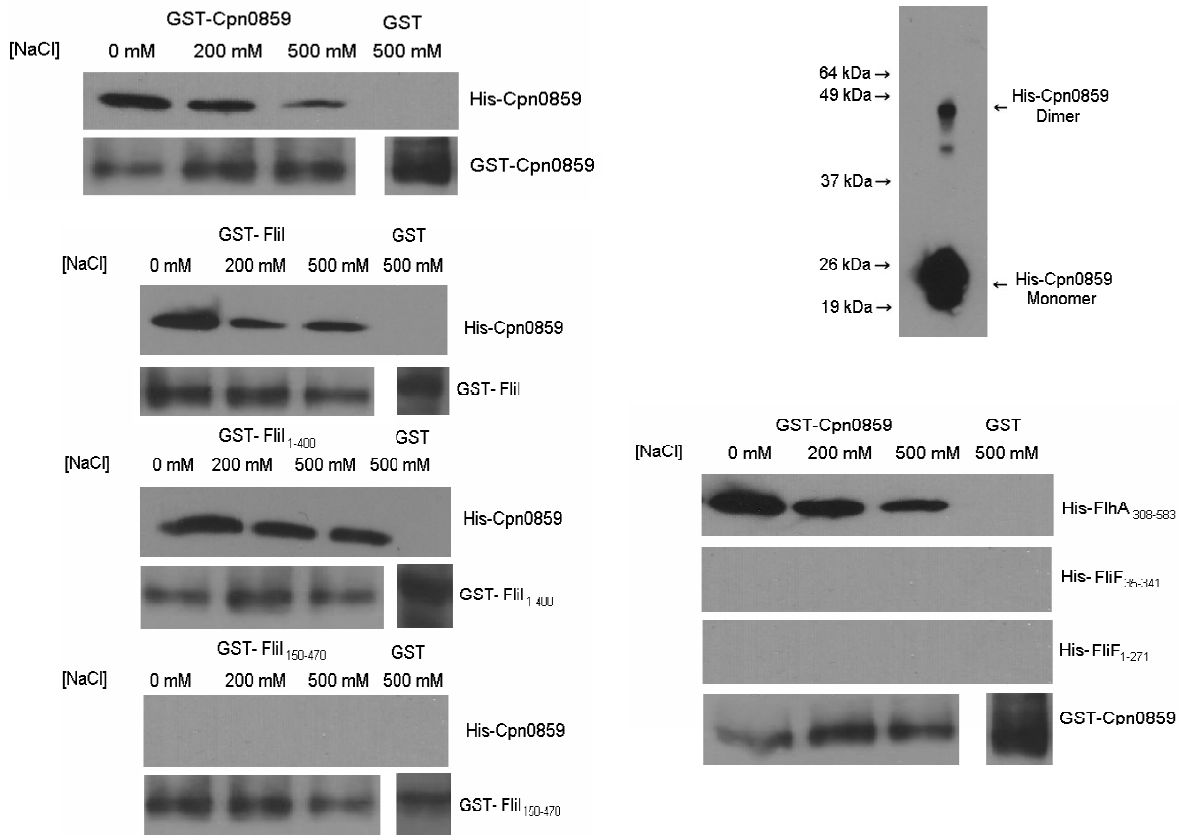


Figure 3.4. Interaction of His-Cpn0859 and GST-Cpn0859, and dimerization of His-Cpn0859. **A:** Full length GST-Cpn0859 was bound to glutathione beads and was used to pull down full length His-Cpn0859 from an *E. coli* lysate, as seen in Figure 3. GST-Cpn0859 co-purified with His-Cpn0859. GST alone did not co-purify with His-Cpn0859, and GST-Cpn0859 is shown as a loading control. **B:** Full length His-Cpn0859 was fixed with formaldehyde for 10 minutes prior to being electrophoresed on an 11% PAGE gel and probed for by anti-His Western blot. Cpn0859 monomers can be seen migrating at approximately 22 kDa while the formation of a dimer can be seen migrating at approximately 44 kDa.

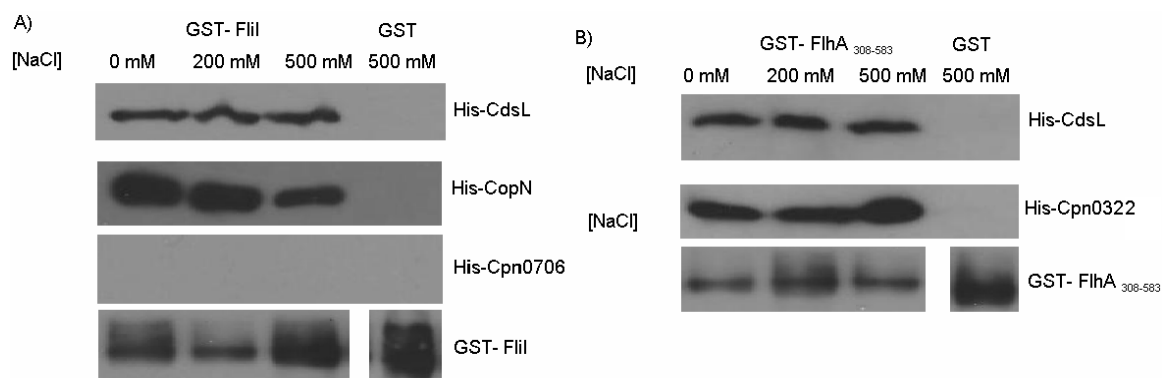


Figure 3.5. Interaction of FliI and FlhA with T3S components. A: Full length GST-FliI was bound to glutathione beads and were used to pull down His-CdsL, His-CopN and His-Cpn0706. GST-FliI co-purified with both His-CdsL and His-CopN, but not His-Cpn0706. GST alone was not able to co-purify with any of the proteins. GST-FliI is shown as a loading control. **B:** GST-FlhA₃₀₈₋₅₈₃ was bound to glutathione beads and used to pull down His-CdsL and His-Cpn0322. GST-FlhA₃₀₈₋₅₈₃ co-purified with both CdsL and Cpn0322. GST alone did not co-purify with either protein. GST-FlhA₃₀₈₋₅₈₃ is shown as a loading control.

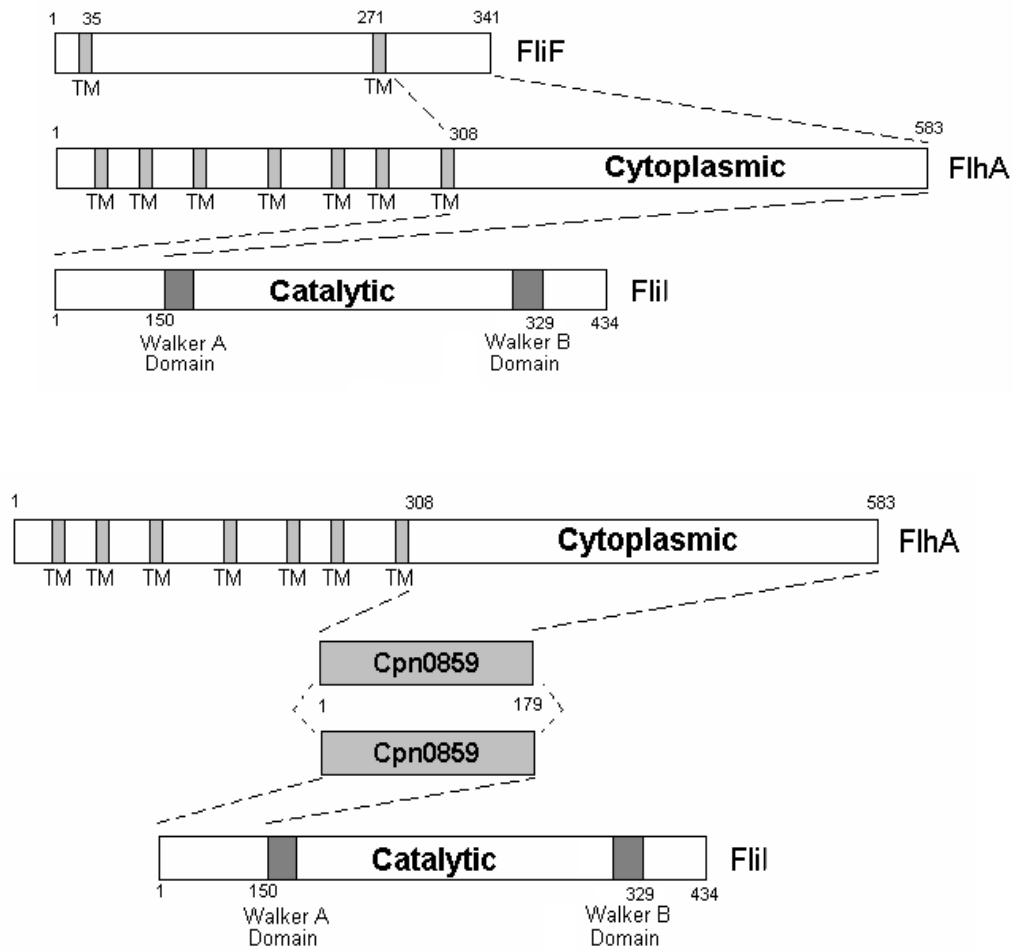


Figure 3.6. Interacting regions between FliI and FlhA, FliF, and Cpn0859. A: FliF contains two transmembrane regions and interacts with the cytosolic domain of FlhA by its extreme C-terminal end. FlhA contains seven transmembrane regions and interacts with the N-terminal region of FliI by its cytoplasmic domain. FliI contains a Walker A and B domain and mediates protein interactions by its N-terminus. **B:** Cpn0859 appears to dimerize, and interacts with the cytosolic domain of FlhA and the N-terminal 150 amino acids of FliI.

CHAPTER FOUR

Authors preface to Chapter 4

In this chapter, I identify and characterize a specific down-regulator of CdsN enzymatic activity (CdsL). Using Pepscan epitope mapping, I identify the amino acid domains in CdsN responsible for the CdsL interaction. This work is the first to apply Pepscan epitope mapping to the T3S field. Also, based on the Pepscan epitope mapping, a specific CdsN cognate peptide was used to target the CdsN / CdsL interaction. We found that this peptide prevents bacterial replication. The overall implications of this work are (i) CdsL down-regulates CdsN enzymatic activity, (ii) CdsL may sterically block ATP access to the p-loop, and (iii) a cognate CdsN peptide can prevent *Chlamydia* replication, although the exact mechanism for this inhibition remains unknown.

The material presented in Chapter 4 has been accepted for publication in the peer-reviewed journal, *Frontiers in Microbiology*. I performed and designed the majority of the experiments in this study. Dr. Jerry Slootstra at PepScan Presto in The Netherlands performed the PepScan epitope mapping. David Bulir, Connor Emdin, and Elisa Porfilio helped with cloning. Ryan Pirie performed the peptide toxicity experiment. Dr. James Mahony provided comments on the manuscript and helped with experimental design.

Full Citation:

Stone C, Bulir D, Emdin C, Pirie R, Porfilio E, Slootstra J, Mahony J (2011) *Chlamydia pneumoniae* CdsL regulates CdsN ATPase activity, and disruption with a peptide mimetic prevents bacterial invasion. *Front Microbiol* 2:21.

***C. pneumoniae* CdsL regulates CdsN ATPase activity, and disruption with a peptide
mimetic prevents bacterial invasion**

Chris B. Stone, David C. Bulir, Connor A. Emdin, Ryan M. Pirie, Elisa A. Porfilio, Jerry
W. Slootstra² and James B. Mahony*

M.G. DeGrootte Institute for Infectious Disease Research, Faculty of Health Sciences and
the Department of Pathology and Molecular Medicine, McMaster University, and the
Father Sean O’Sullivan Research Centre, St. Joseph’s Healthcare, Hamilton, Ontario,
CANADA

² PepScan Presto, Zuiderluisweg 2, 8243 RC Lelystad, The Netherlands

*** Address correspondence to:**

Dr. J.B. Mahony
Regional Virology and Chlamydiology Laboratory, St. Joseph’s Hospital
50 Charlton Avenue East, Hamilton, Ontario, CANADA
L8N 4A6
Phone: 905-521-6021
Fax: 905-521-6083
Email: mahonyj@mcmaster.ca

Running title: CdsN possesses discreet binding domains for CdsL

Abstract

Chlamydiae are obligate intracellular pathogens that likely require type III secretion (T3S) to invade cells and replicate intracellularly within a cytoplasmic vacuole called an inclusion body. *C. pneumoniae* possess a YscL ortholog, CdsL, that has been shown to interact with the T3S ATPase (CdsN). In this report we demonstrate that CdsL down-regulates CdsN enzymatic activity in a dose-dependent manner. Using PepScan epitope mapping we identified two separate binding domains to which CdsL binds *viz.* CdsN₂₂₁₋₂₂₉ and CdsN₂₆₅₋₂₇₀. We confirmed the binding domains using a pull-down assay and showed that GST-CdsN₂₂₁₋₂₇₀, which encompasses these peptides, co-purified with His-CdsL. Next, we used orthology modeling based on the crystal structure of a T3S ATPase ortholog from *E. coli*, EscN, to map the binding domains on the predicted three dimensional structure of CdsN. The CdsL binding domains mapped to the catalytic domain of the ATPase, one in the central channel of the ATPase hexamer and one on the outer face. Since peptide mimetics have been used to disrupt essential protein interactions of the chlamydial T3S system and inhibit T3S-mediated invasion of HeLa cells, we hypothesized that if CdsL – CdsN binding is essential for regulating T3S then a CdsN peptide mimetic could be used to potentially block T3S and chlamydial invasion. Treatment of EBs with a CdsN peptide mimetic inhibited *C. pneumoniae* invasion into HeLa cells in a dose-dependent fashion. This report represents the first use of Pepscan technology to identify binding domains for specific T3S proteins *viz.* CdsL on the ATPase, CdsN, and demonstrates that peptide mimetics can be used as anti-virulence factors to block bacterial invasion.

Introduction

Chlamydia pneumoniae is an obligate, intracellular Gram-negative bacteria that has been associated with community acquired pneumonia (Clifton 2004), atherosclerosis (Grayston 2000), arthritis (Ardiniz 2005), and Alzheimer's disease (Balin 2008). The members of the genus *Chlamydia* all share a unique, biphasic life cycle that is initiated by attachment of the metabolically quiescent elementary body (EB) to the host cell. The association between the EB and the host cell membrane is poorly understood, but glycosaminoglycans may be involved (Chen 1997). Once attached to the host cell, type III secretion (T3S) is utilized to inject the Translocated Actin Recruitment Protein (TARP) to facilitate bacterial internalization into a plasma-membrane derived vacuole, termed an inclusion (Lane 2008, Clifton 2004). The MEK-ERK and PI 3-kinase pathways of the host cell are also involved in bacterial uptake, and are possibly targets of other T3S effectors translocated across the cytoplasmic membrane upon EB contact and binding to host cells (Coombes 2002, Carabeo 2004, Subtil 2004). Once inside the host cell the remainder of the life cycle occurs inside the inclusion body where EBs differentiate into the metabolically active, non-infectious reticulate bodies (RB). The RB remains in close association with the inclusion membrane, suggesting a need for active T3S in RBs. This interaction with the inclusion membrane allows the RB to communicate with the host cell via T3S, allowing the *Chlamydia* to commandeer host cell pathways to obtain lipids, cholesterol, and other nutrients crucial for its growth and replication, and also to prevent phagosome endosome fusion (Hoare 2008, Scidmore 2008, Wylie 1997). Following inclusion body growth to accommodate replicating RBs, an unknown signal (possibly

quorum sensing) triggers the detachment of RBs from the membrane and subsequent re-assortment into infectious EBs. The EBs then exit the host cell either by cell lysis or through extrusion, a packaged release mechanism which leaves the host cell intact (Hybiske 2007).

T3S is a virulence mechanism commonly used by Gram-negative bacteria to directly translocate effector proteins from the bacterial cytoplasm to the host cell cytoplasm in a single step, through the use of a syringe-like apparatus termed an injectisome (Galan 1999, Galan 2006, Ghosh 2004). The injectisome is constructed of 20-25 proteins spanning the inner membrane, periplasm and outer membrane, extending into the extracellular milieu to allow for host cell sensing and contact. Upon host cell contact, the T3S injectisome apparatus injects two translocator proteins into the host cell membrane to form the translocon, a molecular pore through which secreted proteins can enter the host cell (Goure 2004). Despite the fact that *Chlamydia* possesses a full repertoire of T3S genes scattered throughout the genome on at least ten distinct operons, a systematic study of the injectisome has yet to be undertaken as *Chlamydial* species are genetically intractable (Hefty 2007). Recent reports have identified a few T3S structural and effector proteins, providing some understanding of the *Chlamydia* T3SS. Our laboratory has shown that CdsD, a unique protein orthologous to YscD that contains two fork-head associated domains, interacts with the predicted *C. pneumoniae* ATPase tethering protein, CdsL, as well as CdsQ, a putative multi-cargo transport protein (Johnson 2008, Spaeth 2009). We extended these findings to show that CdsN also binds to this complex, and interacts independently with CdsD, CdsL and CdsQ (Stone 2008).

Betts *et. al.* have also recently identified the *C. trachomatis* CT666 gene encoding CdsF, the needle filament protein of the injectisome (Betts 2008). The role of a few effector proteins of *C. pneumoniae* have been recently discovered. Cpn0585 is found in the inclusion membrane and interacts with Rab 1, 10 and 11, possibly recruiting these ATPases to the inclusion membrane (Cortes 2007). Cpn0827 is a second effector protein that is detectable in the inclusion membrane at 20 hpi (Hermann 2006). The *Chlamydia* protein associating with death domains (CADD) is a conserved effector known to interact with TNF family receptors (Stenner-Liewen 2002). Recent biophysical evidence has also been presented by Markham *et al.*, suggesting that the *C. trachomatis* protein CT584 could function as the needle tip protein, which is imperative for host cell sensing and translocator insertion into the host cell membrane (Markham 2009).

T3S ATPases are believed to be assembled as a hexameric ring at the basal body of the injectisome and play a role in delivery of effector proteins through the injectisome (Zarivach 2007). Several T3S ATPases have been partially characterized, including EscN from *E. coli* (Andrade 2007), YscN from *Yersinia* (Blaylock 2006) and InvC from *Salmonella* (Akeda 2004), although the ability of the T3S ATPase to coordinate numerous protein interactions has not been explored. These ATPases have been shown to have significant sequence orthology to the β subunit of the F_0F_1 ATPase, and to hydrolyze ATP. Not only are these ATPases important for providing energy for protein transport, but they are believed to play a role in unfolding the effector proteins before translocation, which may be accomplished by releasing the chaperone from its cognate effector protein (Akeda 2005). In *Yersinia*, the ATPase tethering protein YscL localizes

the ATPase to the inner membrane, potentially by performing a function similar to that of the gamma-stalk of the F_0F_1 ATPase (Pallen 2006). YscL has also been shown to play a role in regulation of the ATPase activity by down-regulating enzymatic activity (Blaylock 2006). The quaternary structure of ATPase, *viz.* the hexamer, has been associated with enhanced enzymatic activity and most likely reflects the native conformation of this protein.

In this report we show that CdsL down-regulates the enzymatic activity of CdsN. We utilized PepScan epitope mapping to determine where CdsL binds to CdsN, and used an orthology modeling approach to map this domain onto the predicted three dimensional structure of CdsN (Bernard 2004, Teeling 2006, Timmerman 2007). We found that CdsN possesses two distinct binding domains for CdsL, one to potentially mediate the tethering function and the other to mediate the down-regulation function. We also show that a CdsN peptide acts as a peptide mimetic preventing bacterial invasion. This is the first report to identify binding domains for a T3S ATPase regulating protein and the use of a peptide mimetic as a novel antimicrobial agent to potentially target T3S.

Methods

Expression Plasmids

C. pneumoniae CWL029 (VR1310:ATCC) (GenBank accession # AE001363) was the strain used to isolate genomic DNA for cloning and protein expression. Full length *cdsL* and *cdsN* were amplified from CWL029 using AttB-containing primers (Gateway; Invitrogen). The amplified products were cloned into pDONR₂₀₁ (Gateway; Invitrogen) to generate pENT vectors. The pENT vectors were then used in LR reactions (Gateway; Invitrogen) to produce pEX vectors containing the genes of interest. We used either pEX₁₇ (N terminal His-tag) or pEX₁₅ (N terminal GST-tag) vectors for our protein expression. All constructs were confirmed by sequencing at the Molecular Biology Facility at McMaster University.

Protein Expression

All constructs were expressed in *E. coli* Rosetta pLysS. Expression plasmids were used to transform *E. coli* Rosetta pLysS and plated on LB plates containing 100 µg/mL ampicillin. LB broth (750mL), containing antibiotics, was then inoculated with 12 mL of an overnight culture and grown at 37 °C until they reached an optical density (OD)₆₀₀ of approximately 0.8. Cultures were then cooled on ice to 20 °C and induced with 0.2 mM of isopropyl β-D thiogalactopyranoside (IPTG). Cultures were then incubated at 23 °C for 2 hours and bacteria were harvested by centrifugation at 6500 x g for 10 minutes in a Sorvall RC-5B centrifuge and washed with ice-cold phosphate-buffered saline (PBS).

Bacteria containing His-tagged protein were resuspended in either Binding Buffer (50 mM potassium phosphate pH 7.2, 150 mM KCl, 1 mM MgCl₂) when used in GST pull-downs, or Nickel A buffer (20 mM Tris pH 7.0, 0.02% β-mercaptoethanol, 400 mM KCl, 1% Triton X-100) when used in ATPase activity assays, while the bacteria containing GST-tagged protein were resuspended in PBS and stored at -20°C until further use.

Purification of Recombinant Proteins

E. coli pellets containing over-expressed His- or GST-tagged proteins were thawed on ice and sonicated using a Fischer Scientific Sonic Dismembrator Model 100, followed by centrifugation at 20,000 x g for 40 minutes to remove insoluble material. Supernatants containing His-tagged protein for use in GST pull-down assays were stored at 4 °C. GST tagged protein for use in GST pull-down assays were bound to 300 µL of glutathione beads overnight at 4°C, then blocked overnight in Tris Buffered Saline with 0.1% Tween-20 and 4% BSA and stored at 4°C until use. His- and GST-tagged protein supernatants for use in ATPase activity assays were filtered through 0.45 µm acrodisc filters (Pall Corporation) and purified on either a 1 mL GStTrap FF column (GE Healthcare) or a 1 mL HisTrap HP column (GE Healthcare). For GST-tagged protein, columns were washed with PBS + 0.1% Tween until the flow-through had an OD₂₈₀ of less than 0.005. GST-tagged protein was then eluted off the beads using 1.5 µg/µL reduced glutathione (Sigma) and dialyzed against activity buffer (50 mM Tris-HCL pH 7.0, 5 mM MgCl₂, 10 mM KCl). Purity was confirmed using SDS-PAGE and Coomassie blue staining. For His-tagged proteins, columns were washed with increasing imidazole

concentrations and eluted with 300 mM imidazole then dialyzed into activity buffer.

Purity was confirmed using SDS-PAGE and Coomassie blue staining.

CdsN enzymatic activity down-regulation experiments

ATP hydrolysis by GST-CdsN purified from GSTrap columns was measured using a malachite green assay (R & D Systems) which measures released inorganic phosphate from ATP. For all experiments, the specific activity was determined using the equation of a standard line generated using phosphate standard (R & D Systems).

Reaction mixtures contained 150 ng of GST-CdsN, 40 μ M ATP, 50 mM Tris-HCL pH 7.0, 5 mM $MgCl_2$, and 10 mM KCl. The reaction mixture (1 mL) was incubated at 37 °C for 1 hour and 50 μ L of the mixture was taken for inorganic phosphate determination at various time points. The reaction was stopped by the addition of 10 μ L of Malachite Green Reagent A followed by 10 μ L of Malachite Green Reagent B and incubated at room temperature for one minute before an OD_{610} reading was taken, according to the manufacturer's instructions. For the negative control, purified CdsN was digested for 10 minutes at 37 °C using Proteinase K (Invitrogen). Also, as a negative control, another GST-tagged protein (CopN) that lacks ATPase activity was purified in the same manner and tested for activity. ATPase activity was expressed as nmol phosphate released min^{-1} , and all experiments were performed in triplicate. His-CdsL was purified from Ni-NTA agarose beads and tested for any contaminating ATPase activity using the Malachite Green Assay. It was then added in varying amounts into the reaction mixture with CdsN

prior to addition of ATP and incubated for 20 minutes on ice. The activity assay was then performed as described above.

GST Pull-down Assays

To examine the interaction of CdsN₂₂₁₋₂₇₀ with CdsL, GST pull-down assays were performed as described previously by Johnson et al, 2008, with the following modifications (Johnson 2008). Briefly, glutathione-agarose beads (30 µL) bound to fifty nanograms of GST-tagged CdsN₂₂₁₋₂₇₀ protein was used in the assay. The beads were incubated overnight at 4 °C with the *E. coli* lysate expressing the His-tagged proteins. The beads were collected by centrifugation and washed with 0.1% Triton X-100 and increasing concentrations of NaCl to eliminate spurious protein interactions. The presence of the GST- and His-tagged proteins were confirmed by both Coomassie blue and Western blot. All proteins were eluted from the glutathione beads and electrophoresed on an 11% SDS-PAGE gel before being probed for His-tagged protein. GST alone bound to glutathione beads was used as a negative control for the pull-down.

Peptide library synthesis, screening assays and 3D modeling

The linear and/or CLIPS peptides are synthesized based on the amino acid sequence of the target protein using standard Fmoc-chemistry and de-protected using trifluoric acid with scavengers. The constrained peptides are synthesized on chemical scaffolds in order to reconstruct conformational epitopes, using Chemically Linked

Peptides on Scaffolds (CLIPS) technology (Timmerman 2007). For example, the single looped peptides are synthesized containing a dicysteine, which was cyclized by treating with alpha, alpha'-dibromoxylene and the size of the loop is varied by introducing cysteine residues at variable spacing. If other cysteines besides the newly introduced cysteines are present, they are replaced by alanine. The side-chains of the multiple cysteines in the peptides are coupled to CLIPS templates by reacting onto credit-card format polypropylene PEPSCAN cards (455 peptide formats/card) with a 0.5 mM solution of CLIPS template such as 1,3-bis (bromomethyl) benzene in ammonium bicarbonate (20 mM, pH 7.9)/acetonitrile (1:1(v/v)). The cards are gently shaken in the solution for 30 to 60 minutes while completely covered in solution. Finally, the cards are washed extensively with excess of H₂O and sonicated in disrupt-buffer containing 1 percent SDS/0.1 percent beta-mercaptoethanol in PBS (pH 7.2) at 70°C for 30 minutes, followed by sonication in H₂O for another 45 minutes. The binding of antibody or labeled protein/peptide to each peptide is tested in a PEPSCAN-based ELISA. The 455-well credit card format polypropylene cards containing the covalently linked peptides are incubated with peptide solution for example consisting of 1 micrograms/mL diluted in blocking solution, for example 4% horse serum, 5% ovalbumin (w/v) in PBS / 1% Tween. After washing, the peptides are incubated with a monoclonal mouse anti-his tag antibody (1/1000, Novagen, 70796-3) and subsequently after washing with a rabbit-anti-mouse antibody peroxidase conjugate (1/1000, Southern Biotech, 6175-05) for one hour at 25°C. After washing, the peroxidase substrate 2,2'-azino-di-3-ethylbenzthiazoline sulfonate (ABTS) and 2 microlitres of 3 percent H₂O₂ are added. After one hour, the

color development is measured. The color development is quantified with a charge coupled device (CCD) – camera and an image processing system. The raw data are optical values obtained by a CCD-camera. The values mostly range from 0 to 3000, a log scale similar to 1 to 3 of a standard 96-well plate elisa-reader. First the CCD-camera makes a picture of the card before peroxidase coloring and then again a picture after the peroxidase coloring. These two pictures are subtracted from each other which results in the data which is called raw-data. This is copied into the Peplab™ database. Then the values are copied to excel and this file is labeled as raw-data file. One follow-up manipulation is allowed. Sometimes a well contains an air-bubble resulting in a false-positive value, the cards are manually inspected and any values caused by an air-bubble are scored as zero. 3D structure prediction was performed using 3D JIGSAW (<http://www.bmm.icnet.uk/~3djigsaw/>). Modeling was then performed using PYMOL software.

Peptide design and entry into EBs

Based on the PepScan epitope mapping of CdsN, two domains were found that mediate the interaction between CdsN and CdsL. The smaller of the two domains (residues 265-279), corresponding to TRFARA, was chosen to create a peptide mimetic compound. We synthesized the TRFARA peptide with a N-terminal membrane transport sequence (MTS), YGRKKRRQRRR (Efthymiadis 1998). We also extended the CdsN sequence flanking the TRFARA peptide to ensure the entire binding domain was

included, and flanked the peptide with cysteine residues to assist with any disulfide bonding that may be required for binding. The final peptide utilized was the 28 amino acid sequence YGRKKRRQRRRCVVLMMDSVTRFARALC and was used in its linear form for inhibition experiments. Peptides were synthesized by Peptide 2.0.

GST-MTS uptake by EBs

Chlamydial EBs were purified using a discontinuous gastrografin gradient, and resuspended in PBS. Either GST or GST-MTS was incubated at varying concentrations (0, 100, 500 μ M) or for varying times (5, 30 or 60 min) with the purified EBs at 4 °C. The EBs were then pelleted and washed three times with PBS, followed by trypsinization for 30 min to ensure that no protein was bound to the outside of the EB. EBs were then boiled in loading dye and probed for the presence of GST using Western blot.

Peptide Cytotoxicity

The cytotoxicity was performed as described by Johnson et al., 2009 (Johnson 2009). The effect of the CdsN TRFARA peptide on HeLa cell viability was determined. Briefly, 50 or 100 μ M of the CdsN peptide, control peptides, or the positive control (1 percent SDS plus 0.1 percent Triton X-100) were added to sub-confluent HeLa cells in 6-well plates. At 1 hr supernatants were harvested and tested for the presence of adenylate kinase using a cytotoxicity assay (Lonza ToxiLight[®] BioAssay, Rockland). The cytotoxicity assay was performed as per the manufacturer's protocol. Briefly,

supernatants from HeLa cell cultures incubated with the CdsN TRFARA peptide (in MEM containing cycloheximide) were tested for evidence of eukaryotic cell cytotoxicity. Aliquots (5 uL) of each supernatant were mixed with 25 uL of Adenylate Kinase Detection Reagent and samples were incubated at room temperature for 5 minutes. Relative light units (RLUs) were measured using a 20/20 n Single Tube Luminometer from Turner BioSystems (Sunnyvale). Assays were conducted in triplicate for each condition. Cell monolayers were washed with warm PBS. 0.75 mL of trypsin was added to each well, and 0.75 mL of MEM was added after complete trypsinization (trypsinization was monitored by light microscopy). Each sample was thoroughly resuspended and aliquoted into a plastic cuvette and the cell number immediately quantitated by determining the optical density at 800 nM using a spectrophotometer.

Electron Microscopy and immunofluorescence

HeLa cells grown to 90% confluency in 6-well plates were infected with *C. pneumoniae*, pre-incubated with linear CdsN peptide for 30 min or with linear random peptide (MTS-MFAVNAQ) for 30 min at various concentrations, centrifuged for 45 min at room temperature, followed by incubation at 37° C for one hr. The inoculum and peptide were removed and the medium replaced with MEM containing 1 ug/ml cycloheximide to inhibit host cell protein synthesis. Cells were incubated at 37° C for 72 hr, collected by trypsinization and centrifugation at 1,000 rpm for 10 min then fixed overnight at 4°C with 2% glutaraldehyde (v/v) in cacodylate buffer, 7.2. The cell pellets were post fixed in 2% osmium tetroxide (v/v), embedded in Spurr's medium and thin

sections were cut on a Reichert Ultracut E microtome. Sections were examined in a Jeol 1200 electron microscope at 80 kV and pictures were captured with an AMT digital camera. For immunofluorescent staining of inclusions, HeLa cells were infected as above using cell monolayers on glass cover slips in shell vials, fixed in methanol and stained using the Pathfinder kit, which uses a FITC-conjugated major outer membrane protein (MOMP)-monoclonal antibody specific to Chlamydia, as per the manufacturer's instructions.

Results

Regulation of CdsN by CdsL

T3S ATPases are known to be enzymatically down-regulated by YscL orthologs (Blaylock 2006). *C. pneumoniae* encodes a YscL ortholog, CdsL (*Cpn0826*), which led us to explore whether CdsL down-regulates CdsN in *C. pneumoniae*. We have previously confirmed that CdsN interacted with CdsL using a GST pull-down assay, showing that CdsL co-purified with CdsN in 500 mM NaCl (Stone 2008). We also showed previously that a CdsN-GST fusion protein possessed enzymatic activity consistent with other T3S ATPases (Stone 2008). We found that CdsN hydrolyzed ATP at a rate of $0.0734 \pm .0053$ nmol / min at the concentration used in this assay (150 ng total). Prior to testing the ability of CdsL to regulate CdsN activity, we confirmed that CdsL lacked any ATPase activity by assaying it alone in the malachite green assay to control for possible contamination and found that CdsL possessed no ATPase activity. To test for regulation of CdsN by CdsL we added increasing amounts of CdsL to the CdsN reaction mixture. We found that addition of CdsL reduced CdsN enzymatic activity at a 0.3 CdsL : 1 CdsN molar ratio, but the effect was most dominant at a 2.1 CdsL: 1 CdsN molar ratio of CdsL : CdsN, where enzymatic activity was reduced by 82 percent (Figure 1). Further increasing the CdsL concentration only marginally reduced activity. The addition of a control His-tagged protein (His-CopN, a T3S structural component) had no effect on CdsN activity. Also as a control, His-CdsL had no effect on the enzymatic activity of a second *C. pneumoniae* ATPase, GspE (data not shown). GspE is a type II secretion ATPase which possesses enzymatic activity (Porfilio et al, unpublished data).

PepScan analysis of CdsN – CdsL interaction

We have shown that CdsN is enzymatically down-regulated by CdsL, but the mechanism by which this occurs is unknown. In an attempt to expand our understanding of how CdsL may function to down-regulate CdsN, we have utilized PepScan epitope mapping to identify the domains within CdsN responsible for the CdsL interaction. Purified His-CdsL was added to an over-lapping peptide library consisting of 4000 overlapping linear and conformational peptides of the CdsN protein in search for the peptide domain mediating protein binding (Timmerman 2007). CdsN contained two binding regions that mediated the interaction with CdsL. The two CdsL binding sequences spanned residues 221 to 229, and residues 265 to 270 corresponding to the amino acids “RSVIVVSTS” and “TRFARA”, respectively, both of which are present within the catalytic domain (Figure 2). To corroborate the PepScan data, we cloned and expressed a fragment of CdsN spanning residues 221 to 270 containing both of the CdsL predicted binding domains to test whether this CdsN fragment bound to His-CdsL. We found that the CdsN₂₂₁₋₂₇₀ co-purified with His-CdsL in the presence of 500 mM NaCl while GST alone did not co-purify with CdsL under any salt conditions (Figure 3).

3D modeling of CdsN – CdsL binding domain

The crystal structure of the *E. coli* T3S ATPase, EscN, has recently been elucidated, allowing us to use an orthology modeling approach to obtain a predicted 3D structure of CdsN and to visualize the CdsL binding domains (Zarivach 2007). CdsN and EscN possess a large amount of sequence orthology within the catalytic domain, where the

CdsL binding domains are located (Stone 2008). Using 3D-JIGSAW, a 3D structure of CdsN was generated and used to model the binding domains for CdsL. Modeling of the binding regions of CdsL on the predicted CdsN monomer revealed that both of the binding domains for CdsL are present in the central region of CdsN (Figure 4A). A more revealing mapping of the binding domains is shown when hexameric CdsN is modeled from the EscN crystal structure (Zarivach 2007). For clarity, we have shown only one half of the predicted hexameric structure of CdsN (a CdsN trimeric complex). Residues 221-229 are exposed towards the outer face of the hexamer (Figure 4B, blue), while residues 265-270 are exposed in the central channel of the hexameric ring (Figure 4C, red). The location of the binding domains is consistent with a proposed mechanism of CdsL down- regulation of CdsN sterically hindering access of ATP to the P-loop (Figure 4B and 4C, magenta).

Inhibition of C. pneumoniae growth and replication by CdsN cognate peptide

The PepScan binding data revealed two distinct domains of CdsN that mediate the interaction between CdsN and CdsL. Using this information we sought to design and utilize a peptide mimetic targeting the interaction between CdsN and CdsL and examine its effect on chlamydial replication. As discussed above, CdsN possessed two different binding domains for CdsL; we selected the 6 amino acid sequence TRFARA to create a potential peptide mimetic. We synthesized the TRFARA peptide with a N-terminal membrane transport sequence (MTS), YGRKKRRQRRR (Efthymiadis 1998). We also extended the CdsN sequence flanking the TRFARA peptide to ensure the entire binding

domain was included, and flanked the peptide with cysteine residues to assist with any disulfide bonding that may be required for binding. The final peptide utilized was the 28 amino acid sequence YGRKKRRQRRRCVVLMMDSVTRFARALC. To examine whether the peptide-MTS was entering EBs, we first incubated either GST alone or GST-MTS at 50, 100, and 500 μ M with gastrografin purified EBs. We saw that the amount of GST-MTS entering EBs increased in a dose-dependent manner (Figure 5A). The GST control (500 μ m) was taken up poorly by Chlamydia. We then added either GST or GST-MTS for increasing time periods (5, 30, or 60 minutes) which showed increasing uptake with time, starting as early as 5 min (Figure 5B). Again, the GST control showed very poor uptake into Chlamydia, suggesting that the MTS facilitates peptide entry in a time- and dose-dependent manner. HeLa cells were then infected with *C. pneumoniae* at an MOI of 2 and stained for inclusions at 72 hr using a FITC conjugated anti-MOMP monoclonal antibody. The CdsN peptide was added to EBs at a 0, 20, 50 and 100 μ M concentrations for 30 min prior to infection and we saw that infectivity was reduced in a dose-response fashion (Figure 6A). In the absence of the peptide, inclusions are clearly visible at 72 hr (Figure 7). Pre-treatment of the cells with 50 μ M peptide resulted in a drastic reduction in the number of inclusions (>95%), while at 100 μ M there was toxicity for HeLa cells. To rule out the possibility that the inhibitory activity at 50 μ M might be due to toxicity we tested the effect of the peptide at 50 μ M on HeLa cells using an adenylate kinase release assay and found little or no toxicity (Figure 6B). We next examined infected cells with the CdsN or the random peptide by transmission electron microscopy. In infected cells exposed to the random peptide large inclusion bodies

containing a mixture of RBs and EBs were readily visible while infected cells incubated with 50 μ M CdsN peptide lacked any detectable inclusions when over 200 cells were examined and showed no evidence of cytotoxicity (Figure 7).

Discussion

Although *C. pneumoniae* contains all the genes coding for a T3SS, only a small number of these have been characterized. We have previously shown that CdsN possesses enzymatic activity and interacts with the putative type III secretion protein, CdsL (Stone 2008). We have now extended these observations to show that CdsL functions to down-regulate CdsN enzymatic activity. We have also used a novel approach to map the exact region within CdsN that mediates the CdsN - CdsL interaction, and used this information to design a peptide mimetic that disrupts the *Chlamydial* replication cycle. Combined, this data provides new insights into the regulation of the T3S system and its importance in the chlamydial life cycle.

YscL orthologs have been shown to down-regulate T3S ATPase enzymatic activity in *Yersinia*, and *C. pneumoniae* encodes a YscL ortholog (CdsL) (Blaylock 2006, Stone 2008). We found that CdsN treated with increasing concentrations of CdsL reduced enzymatic activity up to 82 percent. To show that the regulation by CdsL was specific we tested the ability of CdsL to down-regulate the type II secretion ATPase of *Chlamydia*, GspE, and found that it had no effect on its enzymatic activity. This suggests that CdsL is specific in its down-regulation of CdsN. CdsL has previously been shown to be expressed at all time points throughout the replication cycle with an apparent accumulation during the final 48 hours (Slepenkin 2003). This is consistent with a role for CdsL regulating T3S during invasion and intracellular replication phases of the life-cycle in EBs and RBs, respectively.

T3S ATPases are known to mediate numerous protein interactions between both structural components and chaperone / effector complexes, and play a critical role in construction of the injectisome and secretion of effectors (Akeda 2005, Gauthier 2003). We used PepScan Analysis to determine the CdsN domain that mediates the interaction with CdsL. We found that there were two distinct domains within CdsN that interacted with CdsL; one exposed in the central channel of the hexameric structure of CdsN and the other exposed on the outer face. Using GST pull-downs, we corroborated the PepScan data by demonstrating that a 49 amino acid fragment of CdsN containing both of the predicted CdsL binding domains was able to co-purify with full length CdsL. We have shown previously that CdsL forms dimers, and it is likely that the two CdsL molecules interact with different regions of CdsN (Stone 2008, Pallen 2006). This would be consistent with the two binding domains on CdsN. Along with regulating ATPase activity, CdsL is believed to tether the ATPase to the inner membrane, functioning in a similar manner as the gamma-stalk of the F_0F_1 ATPase which runs through the central channel of the F_0F_1 hexamer and may interact with the membrane (Pallen 2006). The location of the CdsL binding domain within the central channel of CdsN supports the concept that CdsL functions in a similar manner as the gamma-stalk domain for CdsN. Both binding domains are found in close proximity to the P-loop within the catalytic domain which coordinates ATP binding and cleavage (Stone 2008). It is possible that when CdsL is bound to either of these domains it could sterically hinder access of ATP to the P-Loop, reducing enzymatic function of CdsN. The tethering function of CdsL would be crucial for T3S function, and if this tethering is mediated by the binding domain

within the central channel of the CdsN hexamer then likely this interaction is maintained throughout the entire developmental cycle. The exposed binding domain on the outer surface of the CdsN hexamer, however, could be responsible for the down-regulation of CdsN by CdsL. CdsL could bind and dissociate from the outer CdsN – CdsL binding domain upon a conformational change in CdsN, thereby activating ATPase activity upon CdsL release by allowing ATP to access the P-loop. It is tempting to speculate that delivery of effector / chaperone complexes to CdsN, possibly by a multi-cargo transport protein such as CdsQ, could be the trigger for CdsL release and ATPase activation, allowing for the dissociation of the effector / chaperone complex and subsequent secretion of the effector (Spaeth 2009).

Using PepScan epitope mapping we have shown where CdsL binds to CdsN. Using this binding data we designed a cognate CdsN peptide containing a membrane transport signal to allow the peptide to enter *Chlamydia* and showed that this peptide blocked Chlamydial invasion of HeLa cells. Membrane transport signals are known to interact hydrophobically with eukaryotic membranes, triggering entry by endocytosis across the membrane (Efthymiadis 1998). Our working hypothesis is that this transport signal would facilitate entry of the CdsN peptide into EBs, and that this could potentially disrupt the CdsN – CdsL interaction and inhibit T3S, and thus invasion, although we have not shown inhibition of T3S per se. This could be achieved by either disrupting the regulation of the ATPase or interfering with the tethering function of the ATPase, displacing its peripheral association with the inner membrane. Either of these two scenarios could disrupt the T3SS, preventing Chlamydial infection and cellular invasion.

We first confirmed that the MTS facilitated uptake of the peptide into EBs in a time- and dose-dependent manner. Afterwards, we treated the Chlamydial EBs for 30 minutes with the CdsN peptide which reduced chlamydial infection in a dose-response fashion, and at a concentration of 50 μ M reduced *Chlamydia* infectivity by >95%, as determined by IF staining and counting of inclusions at 72 hours. An alternative explanation of this data could be that the peptide was bactericidal towards chlamydia, but we feel that this is unlikely since a random peptide failed to inhibit chlamydial replication. We have also shown that two additional peptide mimetics targeting other essential protein interactions can also inhibit Chlamydial replication (Mahony 2010). We are currently investigating whether the CdsN peptide mimetic can inhibit chlamydial replication if administered during the infection cycle, once infection has occurred, which if successful would indicate that the peptide can disrupt CdsN – CdsL complexes within RBs and block T3S across the inclusion membrane. This would suggest that ATPase activity is carefully regulated by CdsL in both EBs and RBs, and the CdsN – CdsL interaction is critical for Chlamydial replication.

The discovery of unique CdsN binding domains for CdsL coupled with structural modeling of the binding domains has allowed us to postulate how CdsL functions to down-regulate CdsN. This has allowed us to create a cognate CdsN peptide that functions as a novel antimicrobial agent, preventing *C. pneumoniae* from invading host cells. One of the major difficulties in working with Chlamydia is that they are genetically intractable. Peptide mimetics such as this CdsN peptide could effectively create chemical

knockouts by disrupting protein complexes, allowing us to mimic genetic knockouts and explore specific functions of various proteins in the T3SS.

Acknowledgements

CBS is a recipient of a Father Sean O'Sullivan Research Center Studentship. This research was funded by a Canadian Institute of Health Research grant to JBM.

References

- Akeda, Y., Galan, J. (2004). Genetic analysis of the Salmonella enterica type III secretion-associated ATPase InvC defines discrete functional domains. *J. Bacteriol* 186:2402-2412.
- Akeda, Y., Galan, J. (2005). Chaperone release and unfolding of substrates in type III secretion. *Nature* 437:911-915
- Andrade, A., Pardo, J., Espinosa, N., Perez-Hernandez, G., Gonzalez-Pedrajo, B. (2007). Enzymatic characterization of the enteropathogenic Escherichia Coli type III Secretion ATPase EscN. *Arch. Biochem. Biophys* 468: 121-7
- Ardeniz O, Gulbahar O, Mete N, Cicek C, Basoglu OK, Sin A et al. (2005). *Chlamydia pneumoniae* arthritis in a patient with common variable immunodeficiency. *Ann Allergy Asthma Immunol* 94: 504-508.
- Balin, B., Little, C., Hammond, C., Appelt, D., Whittum-Hudson J., Gerard, H., et al. (2008). *Chlamydia pneumoniae* and the etiology of late-onset Alzheimer's disease. *J Alzheimers Dis* 13: 371-380.
- Bernard J, Harb C, Mortier E, Quéméner A, Meloen RHI, Vermot-Desroches C, Wijdeness J, van Dijken P, Grötzinger J, Slootstra JW, Plet A, Jacques Y. (2004). Identification of an Interleukin-15 Receptor-binding Site on Human Interleukin-15. *J. Biol. Chem* 279: 24313-24322.

Betts, H., Twiggs, L., Sal, M., Wyrick, P., Fields, K. (2008). Bioinformatic and biochemical evidence for the identification of the type III secretion system Needle protein of *Chlamydia Trachomatis*. *J. Bacteriol* 190: 1680-1690.

Blaylock, B., Riordan, K., Missiakas, D., Schneewind, O. (2006). Characterization of the *Yersinia enterocolitica* type III secretion ATPase YscN and its regulator, YscL. *J. Bacteriol* 188:3525-3534.

Carabeo, R., Grieshaber, S., Hasenkrug, A., Dooley, C., Hackstadt, T. (2004). Requirement for the Rac GTPase in *Chlamydia trachomatis* invasion of non-phagocytic cells. *Traffic* 5:418-425.

Chen J, Stephens R. (1997). *Chlamydia Trachomatis* glycosaminoglycan-dependant and independent attachment to eukaryotic cells. *Microb Pathog* 22(1): 23-30.

Clifton, D., Fields, K., Grieshaber, S., Dooley, C., Fischer, E., Mead, D., Carabeo, R., Hackstadt, T. (2004). A chlamydial type III translocated protein is tyrosine-phosphorylated at the site of entry and associated with recruitment of actin. *Proc Natl Acad Sci U S A* 101: 10166-10171.

Coombes, B., Mahony, J. (2002). Identification of MEK- and phosphoinositide-3-kinase-dependant signaling as essential events during *Chlamydia pneumoniae* invasion of HEp2 cells. *Cell Microbiol* 4: 447-460.

Cortes C., Rzomp K., Tvinnereim A., Scidmore M., Wikel B. (2007). Chlamydia pneumoniae inclusion membrane protein Cpn0585 interacts with multiple Rab GTPases. *Infect Immun* 75(12): 5586-95

Efthymiadis, A., Briggs, L., Jans, D. (1998). The HIV-1 Tat nuclear localization sequences confers novel nuclear import properties. *J Biol Chem* 273: 1623-1628.

Galan, J., Collmer, A. (1999). Type III secretion machines: bacterial devices for protein delivery into host cells. *Science* 284: 1322-1328.

Galan, J., Wolf-Watz, H. (2006). Protein delivery into eukaryotic cells by type III secretion machines. *Nature* 444: 567-573.

Gauthier, A., Finlay, B. (2003). Translocated intimin receptor and its chaperone interact with ATPase of the type III Secretion apparatus of Enteropathogenic Escherichia coli. *J. Bacteriol* 185:6747-6755.

Ghosh, P. (2004). Process of protein transport by the type III secretion system. *Microbiol. Mol. Biol. Rev* 68: 771-795.

Goure J., Pastor A., Faudry E., Chabert J., Dessen A., Attree I. (2004). The V antigen of *Pseudomonas aeruginosa* is required for assembly of the function PopB/PopD translocation pore in host cell membranes. *Infect Immun* 72(8): 4741-50.

Grayston, J. (2000). Background and current knowledge of Chlamydia pneumoniae and atherosclerosis. *J Infect Dis* 181: S402-S410.

Hoare, A., Timms, P., Bavoil, P., Wilson, D. (2008). Spatial constraints within the chlamydial host cell inclusion predict interrupted development and persistence. *BMC Microbiol* 8: 5.

Hefty, P., Stephens, R. (2007). Chlamydial type III secretion system is encoded on ten operons preceded by sigma 70-like promoter elements. *J. Bacteriol* 189:198-206.

Hermann, M., Schuhmacher, A., Muhldorfer, I., Melchers, K., Prothmann, C., Dammeier, S. (2006). Identification and characterization of secreted effector proteins of *Chlamydomonas reinhardtii* TW183. *Res Microbiol* 157(6): 513-24.

Hybiske, K., Stephens, R. (2007). Mechanisms of host cell exit by the intracellular bacterium *Chlamydia*. *Proc Natl Acad Sci U. S. A* 104:11430-11435.

Pallen, M., Bailey, C., Beatson, S. (2006). Evolutionary links between FliH/YscL-like proteins from bacterial type III secretion systems and second-stalk components of the F_0F_1 and vacuolar ATPases. *Protein Sci* 15:935-940.

Johnson, D., Stone, C., Bulir, D., Coombes, B., Mahony, J. (2009). A novel inhibitor of *Chlamydomonas reinhardtii* protein kinase D (PknD) inhibits phosphorylation of CdsD and suppresses bacterial replication. *BMC Microbiology*. 9: 218.

Johnson, D., Stone, C., Mahony, J. (2008). Interactions between CdsD, CdsQ, and CdsL, three putative *Chlamydomonas reinhardtii* type III secretion proteins. *J. Bacteriol* 190: 2972-2980.

Lane, B., Mutchler, C., Khodor, S., Grieshaber, S., Carabeo, R. (2008). Chlamydial entry involves TARP binding of guanine nucleotide exchange factors. *PLoS Pathog* 4: 1-11

Mahony, J., Stone, C., Liu, L., Pyrie, R., Chong, S., Whittum-Hudson, J. (2010). Peptide mimetics inhibiting type III secretion decrease host cell invasion and reduce infection levels in the mouse genital tract. In: *Chlamydial Infections, Proceedings of the 12th International Symposium on Human Chlamydial Infections, Hof bei Salzburg, Austria, June 20-25, 2010*, [eds] Schachter, J., Byrne, GI., Caldwell, H., Chernesky, MA., Clarke, IN., Mabey, DC., Paavone, J., et al., pp 325-328. ISBN 0-9664383-3-7

Markham A., Jaafar, Z., Kernege, K., Middaugh, C., Hefty, P. (2009). Biophysical characterization of *Chlamydia trachomatis* CT584 supports its potential role as the type III secretion needle tip protein. *Biochemistry* 48(43): 10353-61.

Scidmore, M., Hackstadt, T. (2008). Mammalian 14-3-3beta associates with the *Chlamydia trachomatis* inclusion membrane via its interaction with IncG. *Mol Microbiol* 39: 1638-1650.

Slepenkin, A., Motin, V., de la Maza, L., Peterson, E. (2003). Temporal expression of type III secretion genes of *Chlamydia pneumoniae*. *Infect Immun* 71(5): 2555-62.

Spaeth, K., Chen, Y., Valdivia, R. (2009). The chlamydia type III secretion system c-ring engages chaperone-effector protein complexes. *PLoS pathog* 5.

Stenner-Liewen, F., Liewen, H., Zapata, J., Pawlowski, K., Godzik, A., Reed, J. (2002). CADD, a Chlamydia protein that interacts with death receptors. *J Biol Chem* 277(12): 9633-6

Stone, C., Johnson, D., Bulir, D., Mahony J. (2008). Characterization of the putative type III secretion ATPase CdsN (Cpn0707) of *Chlamydomphila pneumoniae*. *J Bacteriol* 190: 6580-6588.

Subtil, A., Wyplosz, B., Balana, M., Dautry-Varsat, A. (2004). Analysis of *Chlamydia caviae* entry sites and involvement of Cdc42 and Rac activity. *J. Cell Sci* 117:3923-3933.

Teeling JL, Mackus WJM, Wiegman LJJM, van den Brakel JHN, Beers SA, French RR, van Meerten T, Ebeling S, Vink T, Slootstra JW, Parren PWHI, Glennie MJ, and van de Winkel JGJ. (2006). The biological activity of human CD20 monoclonal antibodies is linked to unique epitopes on CD20. *J Immunol* 177(1):362-371.

Timmerman P, Puijk WC, and Meloen RH. (2007). Functional reconstruction and synthetic mimicry of a conformational epitope using CLIPS™ technology. *J. Mol. Recognit* 20: 283-299

Wylie, J., Hatch, G., McClarty, G (1997). Host cell phospholipids are trafficked to and then modified by *Chlamydia trachomatis*. *J Bacteriol* 179: 7233-7242

Zarivach, R., Vuckovic, M., Deng, W., Finlay, B., Strynadka, N. (2007). Structural analysis of a prototypical ATPase from the type III secretion system. *Nat. Struct. Mol. Biol* 14:131-137.

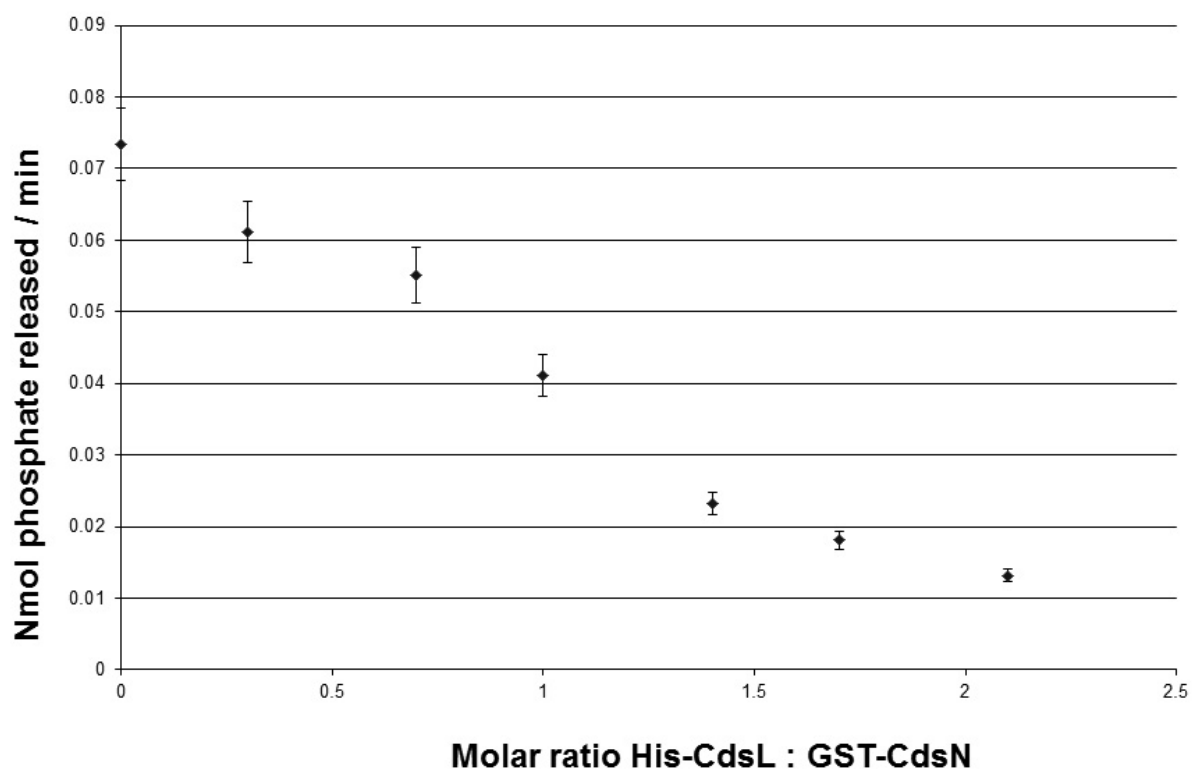


Figure 4.1. CdsL down-regulations CdsN enzymatic activity in a dose-dependent fashion. Aliquots (150 ng) of GST-CdsN were assayed for enzymatic activity using the malachite green assay to detect released inorganic phosphate from ATP. His-CdsL was added to the reaction mixture at molar ratios between 0.3 and 2.1, and ATPase activity of GST-CdsN was measured. Increasing amounts of CdsL resulted in a decrease in CdsN enzymatic activity. The maximum reduction of activity was seen at a 2.1 : 1 CdsL : CdsN molar ratio (82 percent reduction in CdsN enzymatic activity). All experiments were performed in triplicate and data is presented as the mean with error bars representing one standard deviation of the mean.

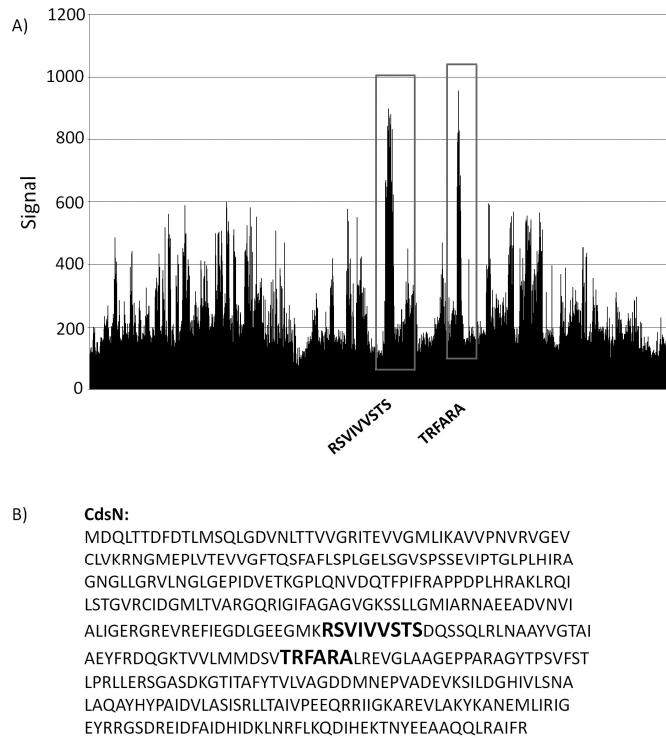


Figure 4.2. PepScan Analysis of the CdsL binding domain on CdsN. An over-lapping peptide library for full length CdsN consisting of 4000 linear and looped peptides was constructed by PepScan Presto (the Netherlands). His-CdsL was screened against the peptide library to identify CdsN peptides that interact with CdsL. **A.** Raw PepScan data obtained by screening full length His-CdsL against the overlapping peptide library of 4000 linear and looped CdsN peptides (x-axis). The two distinct CdsL binding domains are highlighted in black within the vertical boxes, and the signal strength of the interaction is visualized on the y-axis. The two peaks correspond to the sequences RSVIVVSTS and TRFARA. **B.** The two amino acid sequences to which CdsL binds (RSVIVVSTS and TRFARA) are bolded within the full length CdsN amino acid sequence.

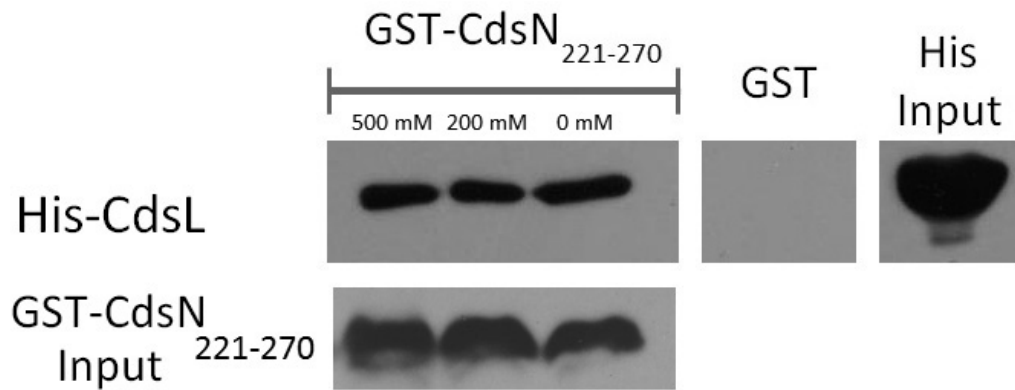


Figure 4.3. The CdsN₂₂₁₋₂₇₀ peptide, containing both the predicted CdsN - CdsL binding domains, co-purifies with CdsL. GST-CdsN₂₂₁₋₂₇₀ was bound to glutathione beads and used to pull down His-CdsL from *E. coli* lysates. Beads were collected by centrifugation, washed with 0 mM, 200 mM and 500 mM NaCl and probed for His-tagged protein by Western blot using anti-His antibody. GST-CdsN₂₂₁₋₂₇₀ co-purified with CdsL while GST alone did not.

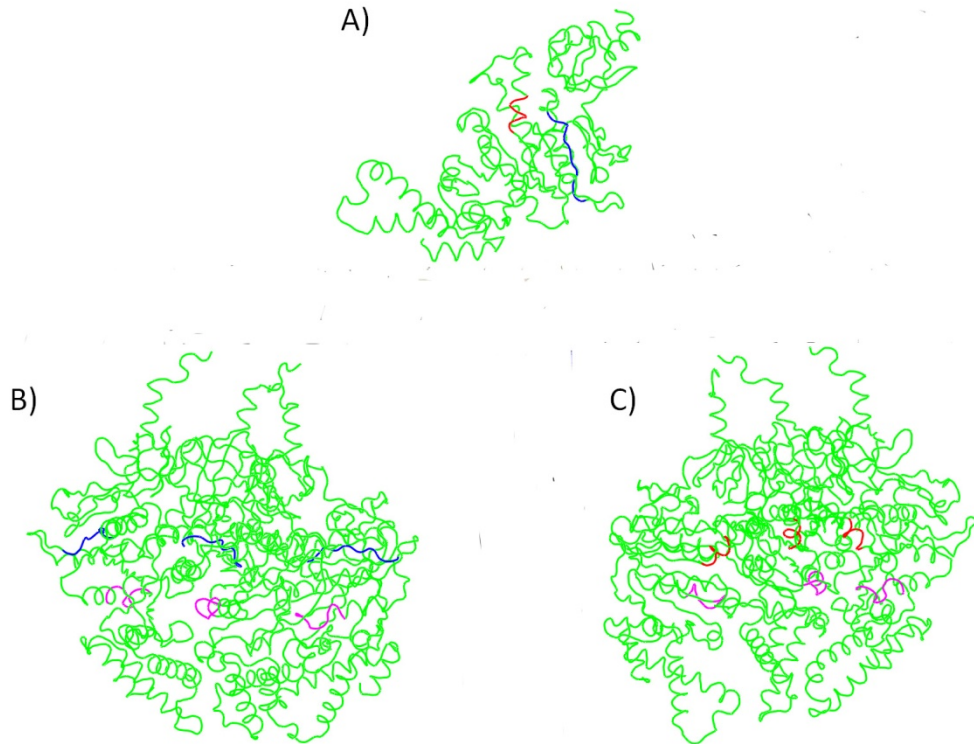


Figure 4.4. CdsL binding domains mapped onto the predicted three dimensional structure of CdsN reveals two distinct domains. A 3D structure of CdsN was generated based on orthology modeling using 3D-JIGSAW based on the structure of EscN, and used to visualize the CdsL binding domains identified from- 156 - the peptide library binding data. The two CdsL binding domains on CdsN are in blue (residues 221-229) or red (residues 265-270), and the ATP coordinating P-loop region of CdsN is highlighted in magenta. **A.** Representation of the predicted CdsN monomeric structure indicating both CdsL binding domains (RSVIVVSTS in blue, TRFARA in red). **B.** Structural model showing the

location of residues 221 – 229 (RSVIVVSTS), displayed on one half of the predicted hexameric structure and viewed from the outer face, revealing that the binding domains are exposed to the outside of the hexamer. The P-loop is represented in magenta. **C.** Structural model viewed from outside looking towards the central channel showing the location of residues 265 – 270 (TRFARA), displayed on one half of the predicted hexameric structure revealing that the domain is exposed within the central channel. The P-loop is represented in magenta.

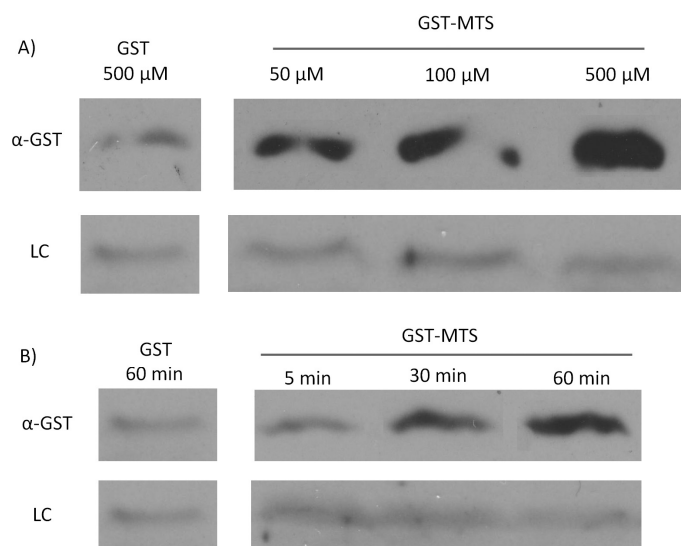


Figure 4.5. Uptake of a GST-Membrane transport signal (MTS) fusion protein into EBs. EBs were purified on a discontinuous gastrografen gradient and collected by centrifugation to ensure the use of a homogenous EB mixture. The GST alone and GST-MTS protein was expressed in *E. coli* cells and purified using glutathione beads. The EBs were then incubated with either GST or GST-MTS, trypsinized for 30 min to ensure that all extracellular GST or GST-MTS was degraded, and examined by α-GST Western blot for the presence of intracellular GST tagged protein. CdsL, an intracellular type III secretion protein, was used as a loading control (LC). **A.** Time-course for incubation of EBs with GST-MTS for 5, 30 or 60 min. GST control at 60 min displayed very little protein while GST-MTS at 5, 30 and 60 min had increasing amounts of GST-MTS present within the EBs. **B.** Dose-response of EBs incubated with GST-MTS at 50, 100, and 500 μm. GST control at 500 μm displayed very little protein while GST-MTS

accumulated within the EBs as the concentration increased. CdsL is shown as a loading control.

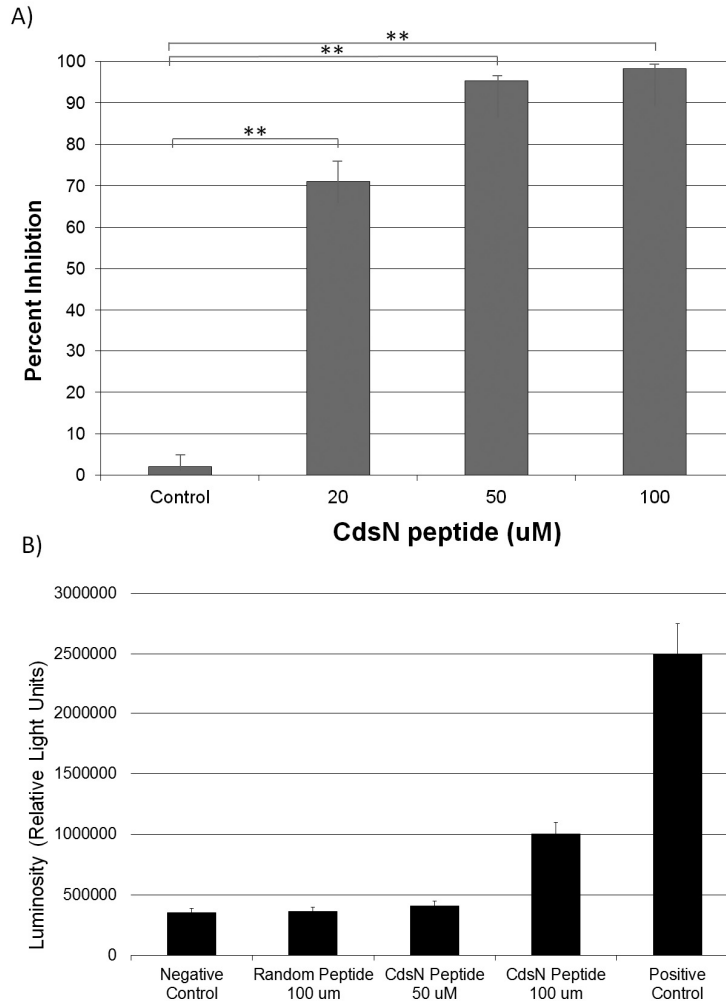


Figure 4.6. CdsN peptide containing the CdsL binding sequence TRFARA inhibits the infection of HeLa cells in a dose-dependent fashion and shows low toxicity at 50 μ M. Shell vials grown to 85 percent confluency were infected with *C. pneumoniae* at an MOI of 3 after incubation with the CdsN or control peptide. Infected cells were counted by staining with a *Chlamydia* specific major outer membrane protein (MOMP)-monoclonal antibody (Pathfinder kit). Toxicity was measured using an adenylate kinase

release assay for HeLa cells in the presence of either the CdsN or control peptide. **A.** CdsN peptide was added at increasing concentrations (20 μM , 50 μM and 100 μM) and demonstrated a dose-response in reduction of *C. pneumoniae* infectivity of HeLa cells. The control represents a random peptide with the sequence MFAVNAQ-MTS that had no effect on *C. pneumoniae* infectivity. All experiments were performed in triplicate and data is presented as the mean with error bars representing the mean plus one standard deviation with ** representing $p < .01$. **B.** Toxicity of the CdsN peptides towards HeLa cells was evaluated using the Lonza adenylate kinase release assay. The CdsN peptide was added to HeLa cells for 1 hr at 50 and 100 μM , and the random peptide was added for 1 hr at 100 μM . We saw that the CdsN peptide at 50 μM had no toxicity towards HeLa cells, and only minor toxicity at 100 μM .

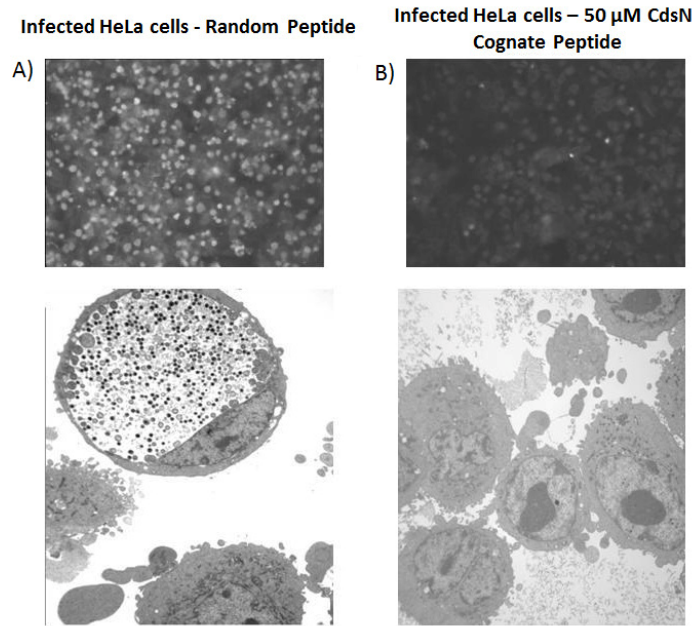


Figure 4.7. CdsN peptide reduces Chlamydial infectivity of HeLa cells by IF staining and EM. HeLa cells were pretreated with CdsN or a control peptide (MTS-MFAVNAQ), then infected with *C. pneumoniae* at an MOI of 3 and examined by either IF staining using anti-MOMP monoclonal antibody treatment with the pathfinder kit (top) or by electron microscopy (bottom). **A.** HeLa cells treated with the control peptide (100 μM) and infected with *C. pneumoniae*. Immunofluorescent staining reveals numerous infected cells (top) while electron microscopy reveals a large inclusion body with both EBs and RBs (bottom). **B.** HeLa cells treated with the CdsN peptide (50 μM) and infected with *C. pneumoniae*. Evaluation of over 200 cells treated with the CdsN peptide by IF staining and EM examination revealed a drastic reduction in *C. pneumoniae* infected cells and a complete lack of detectable inclusions by EM.

CHAPTER FIVE

Author's preface to Chapter 5

In this chapter, we further characterize a *Chlamydia pneumoniae* effector protein, Cpn0803, which we show to interact with CdsN. We also structurally analyze Cpn0803 using x-ray crystallography and identify binding domains using PepScan epitope mapping. The implications of this work are (i) Cpn0803 interacts with T3S components, including CdsN, (ii) the crystal structure of Cpn0803 does not resemble needle-tip protein orthologs, (iii) Cpn0803 has a hydrophobic pocket and interacts with lipids such as phosphatidylinositol and phosphatidic acid, and (iv) Cpn0803 contains discrete binding domains for each of the T3S proteins based on PepScan epitope mapping.

The material presented in Chapter 4 has been accepted for publication in the peer-reviewed journal, *PLoS One*. I performed and designed the majority of the experiments. Seiji Sugiman-Marangos interpreted the x-ray diffraction data of the Cpn0803 crystals and helped prepare figures. David Bulir performed the glutathione plate assays for Cpn0803 interactions with other T3S components. Rob Clayden and Tiffany Leighton helped with the GST pull-down assays. Dr. Murray Junop critically reviewed the manuscript and helped with the crystallography. Dr. James Mahony provided comments on the manuscript and experimental design.

Full citation:

Stone C, Sugiman-Marangos S, Bulir D, Clayden R, Leighton T, Slootstra J, Junop M, Mahony J (2012) Structural characterization of a novel *Chlamydia pneumoniae* type III secretion-associated protein, Cpn0803. *PLoS ONE* 7: e30220.

Structural characterization of a novel *Chlamydia pneumoniae* type III secretion-
associated protein, Cpn0803

Chris B. Stone¹, Seiji Sugiman-Marangos², David C. Bulir¹, Rob C. Clayden¹, Tiffany L.
Leighton¹, Jerry W. Slootstra³, Murray S. Junop² and James B. Mahony^{1*}

¹M.G. DeGrootte Institute for Infectious Disease Research, Faculty of Health Sciences
and the Department of Pathology and Molecular Medicine, McMaster University, and the
Father Sean O'Sullivan Research Centre, St. Joseph's Healthcare, Hamilton, Ontario,
CANADA

²Department of Biochemistry and Biomedical Sciences, McMaster University, 1200
Main Street West, Hamilton, ON, L8N 3Z5, Canada

³ Pepscan Presto, Zuidersluisweg 2, 8243 RC Lelystad, The Netherlands

*** Address correspondence to:**

Dr. J.B. Mahony
Regional Virology and Chlamydiology Laboratory, St. Joseph's Hospital
50 Charlton Avenue East, Hamilton, Ontario, CANADA

L8N 4A6

Phone: 905-521-6021

Fax: 905-521-6083

Email: mahonyj@mcmaster.ca

Running title: Characterization of *C. pneumoniae* Cpn0803

ABSTRACT

Type III secretion (T3S) is an essential virulence factor used by Gram-negative pathogenic bacteria to deliver effector proteins into the host cell to establish and maintain an intracellular infection. *Chlamydia* is known to use T3S to facilitate invasion of host cells but many proteins in the system remain uncharacterized. The *C. trachomatis* protein CT584 has previously been implicated in T3S. Thus, we analyzed the CT584 ortholog in *C. pneumoniae* (Cpn0803) and found that it associates with known T3S proteins including the needle-filament protein (CdsF), the ATPase (CdsN), and the C-ring protein (CdsQ). Using membrane lipid strips, Cpn0803 interacted with phosphatidic acid and phosphatidylinositol, suggesting that Cpn0803 may associate with host cells. Crystallographic analysis revealed a unique structure of Cpn0803 with a hydrophobic pocket buried within the dimerization interface that may be important for binding small molecules. Also, the binding domains on Cpn0803 for CdsN, CdsQ, and CdsF were identified using Pepscan epitope mapping. Collectively, these data suggest that Cpn0803 plays a role in T3S.

INTRODUCTION

Chlamydia pneumoniae is an obligate, intracellular Gram-negative bacterium associated with pneumonia and bronchitis. Members of the *Chlamydia* genus all share a unique, biphasic life cycle initiated by attachment of the metabolically quiescent elementary body (EB) to a host cell. The remaining intracellular portion of the life-cycle takes place within a plasma-membrane derived vacuole known as an inclusion. Once inside the inclusion, EBs transform into metabolically active reticulate bodies (RB) that becomes associated with the inclusion membrane. Interaction with the inclusion membrane allows RBs to communicate with the host cell via T3S, permitting *Chlamydia* to commandeer host cell pathways to acquire lipids, cholesterol, and other nutrients crucial for growth and replication [1-3]. RB replication results in expansion of the inclusion until an unknown stimulus signals non-infectious RBs to transform into infectious EBs which exit the host cell either by cell lysis or a packaged released mechanism termed extrusion, leaving the host cell intact [4].

T3S is a virulence mechanism used by several Gram-negative bacteria including *Yersinia*, *Salmonella*, *Pseudomonas* and *E. coli* to inject effector proteins from the bacterial cytosol into the host cell cytoplasm. The type III secretion system (T3SS) translocates effectors through the inner membrane, periplasmic space, and outer membrane in a single-step using a syringe-like apparatus known as an injectisome [5-7]. This apparatus is activated upon host cell-contact, possibly through interaction of the T3S injectisome with cholesterol and sphingolipid rich microdomains, termed lipid rafts, in the host cell membrane [8,9]. Insertion of hydrophobic translocator proteins into host

cell membranes is thought to be dependent on lipid-rafts since in the absence of cholesterol, translocators do not form pores and lyse artificial membranes [10]. The needle-filament protein YscF (*Yersinia*) extends from the bacterial outer-membrane and houses the needle-tip complex containing the sensor protein and possibly translocators [11]. The hierarchy of effector secretion at the inner membrane is thought to be controlled by T3S ATPases. The T3S ATPases (YscN orthologs) function at the inner membrane, interacting with T3S effector proteins to dissociate them from their cognate chaperones and allow effector passage through the injectisome [12]. Another protein that exists in both the soluble and insoluble fractions of the T3S system is the C-ring protein (YscQ orthologs), which may function as a platform to recognize effector / chaperone complexes, subsequently shuttling them to the inner membrane ATPase [13, 14]. The needle-tip complex, located at the tip of the T3S injectisome, is crucial for sensing host-cell contact and initiating secretion [15]. Needle-tip proteins first recognize cell contact and act as an extracellular chaperone facilitating translocator insertion into the host membrane [16, 17]. Crystallographic analysis of needle tip proteins revealed a dumbbell-like structure with two globular domains on either end of a “grip” formed by a conserved coiled-coil motif [18]. Based on comparisons of biophysical properties to other tip proteins, CT584 has been implicated as the needle tip protein of *C. trachomatis* [19]. At this time, nothing is known about the structure or function of Chlamydial needle tip proteins. Here, we present data demonstrating that Cpn0803 (CT584 ortholog) from *C. pneumoniae* interacts with several T3S components including the needle filament protein, the ATPase and the C-ring protein. We also mapped the regions of Cpn0803 responsible

for mediating these protein interactions. Structure determination of Cpn0803 revealed a unique overall fold with no structural similarity on the DALI server. Taken together, this data suggests that Cpn0803 plays a role in *C. pneumoniae* type III secretion.

RESULTS

Cpn0803 interacts with T3S proteins

To explore whether Cpn0803 interacts with other T3S proteins, we used ELISA and GST pull-down assays to evaluate possible protein interactions. First, GST-CdsN, GST-CdsQ and GST-CdsF were immobilized on glutathione plates, reacted against His-Cpn0803, and monitored using a colorimetric assay to evaluate possible protein interactions. Cpn0803 interacted with GST-CdsN, GST-CdsQ and GST-CdsF with absorbance values corresponding to $0.38 \pm .008$, $0.41 \pm .006$ and $0.36 \pm .01$ absorbance units, respectively, that were significantly higher than background levels (Figure 1A). As a positive control, we demonstrated that GST-Cpn0803 interacted with Cpn0803 with an absorbance of $0.45 \pm .032$. Significant interactions were considered to be two standard deviations above the negative control (GST alone), which had an absorbance value of $0.046 \pm .003$. Next, CdsN, CdsF and CdsQ immobilized on glutathione beads were mixed with *E. coli* lysates containing His-Cpn0803. The beads were harvested by centrifugation and analyzed for His-Cpn0803 protein by anti-his Western blot. In each case, His-Cpn0803 co-purified with GST-CdsN, GST-CdsF or GST-CdsQ under high (500 mM) NaCl conditions, suggesting that the interaction is specific (Figure 1B). GST alone did not co-purify with Cpn0803 under any condition. To corroborate the *in vitro* GST pull-down assays, we used recombinant GST-CdsN, GST-CdsQ and GST-CdsF to pull-down native Cpn0803 from an EB lysate (Figure 2). We found that GST-CdsN, -CdsQ and -CdsF co-purified with native Cpn0803 from an EB lysate, suggesting that

these proteins interact *in vivo*. As a positive control, GST-Cpn0803 copurified with native Cpn0803 from an EB lysate while GST alone, as a negative control, did not.

Structure of Cpn0803

The crystal structure of full-length Cpn0803 was determined by SAD phasing of an anomalous data set collected from SeMet derivatized protein (Figure 3). Cpn0803 crystallized in the hexagonal space group $P6_3$, with two monomers in the asymmetric unit. The final model was refined to R and R_{free} values of 17.58 and 20.85%, respectively. Cpn0803 is 184 amino acids in length, with the final model spanning residues 8-182 in chain A and residues 8-183 in chain B. A complete list of X-ray diffraction data and model refinement statistics can be found in Table 1.

The N-terminal 97 residues of the Cpn0803 monomer assembled into a 4-helix bundle in which the fourth helix is bent by a proline at position 87 (Figure 2). A short, five amino acid loop joins the N-terminal helical domain to a 3-stranded anti-parallel β -sheet. This β -sheet has one surface exposed to the solvent while the other is flanked by three α -helices. Helices α_6 and α_8 run anti-parallel to one another and are joined by a short, two turn helix (α_7) sitting perpendicular to both which forms a 'II' shaped motif.

PISA is a software package able to predict the oligomeric structure of a protein based on crystal contacts [20]. PISA analysis suggested the biologically active unit of Cpn0803 to be a hexamer formed by a trimer of dimers (Figure 4). In the crystal structure, Cpn0803 forms a dimer mediated primarily by the C-terminal 3-helix motif. This interface involves 68 residues from each monomer and buries 6, 430 \AA^2 ,

corresponding to approximately 35% of the total surface area of the complex. Helices $\alpha 6$ and $\alpha 8$ from either monomer associate to form a 4-helix bundle capped on either end by $\alpha 7$. This interaction is stabilized through many hydrophobic interactions, extensive hydrogen bonding and a number of salt bridges. In the N-terminal domain, a total of 21 residues from $\alpha 5$ and the loop region joining $\beta 2$ and $\beta 3$ form extensive interactions with two symmetry-mates in the crystal packing that result in the formation of a trimer, burying an additional 3,867 Å².

Dimerization of Cpn0803 forms a cone-shaped hydrophobic pocket between the two 3-stranded β -sheets and is closed off at the 'top' by $\alpha 6$ from both chains A and B (Figure 5). This pocket is lined almost entirely with hydrophobic residues and is stoppered at the 'bottom' by F129 which forms a π -stacking interaction with its counterpart from the second monomer. Five polar residues lie on either side of the pocket, however it appears that they are within close enough proximity to form a network and satisfy the hydrogen-bonding potential of their polar atoms as no ordered water molecules were observed within this hydrophobic cavity. Specifically the hydrogen-bond distances of T138--T133, T133--N119, N119--S106, and S106--H_B144 are 3.4, 2.8, 2.5, and 2.7 Å respectively. All but T128--T133 are within ideal hydrogen bonding distance, and T128--T133 can still be considered a stabilizing electrostatic interaction if not a true hydrogen-bond. The pocket is approximately 15 Å in its longest dimension and has a volume of ~211.3 Å³ as calculated by the CASTp server [21].

Cpn0803 interacts with host cell lipids

The presence of a hydrophobic pocket in Cpn0803 suggests that it may have small molecule binding partners. To explore whether Cpn0803 interacted with lipid components of the cell membrane, we incubated recombinant His-Cpn0803 with membrane lipid strips which contain small amounts of purified lipids immobilized on the surface of the strips. A positive interaction was detected by anti-His Western blot after incubation of His-Cpn0803 with the strips (Figure 6). These strips were used to analyze potential interactions with each of the following membrane components: triglycerides, diacylglycerol, phosphatidic acid, phosphatidylserine, phosphatidylethanolamine, phosphatidylcholine, phosphatidylglycerol, cardiolipin, phosphatidylinositol, PtdIns(4)P, PtdIns(4,5)P₂, PtdIns(3,4,5)P₃, cholesterol, sphingomyelin, and sulfatide. Cpn0803 interacted with two of the 15 lipid components evaluated, *viz.* phosphatidic acid (PA) and phosphatidylinositol (PI). His-CdsL (the T3S ATPase tethering protein and negative regulator) was used as a negative control and did not react with any of the lipid components.

Cpn0803 exists as a hexamer in solution

To explore whether Cpn0803 formed higher-ordered structures, we analyzed purified recombinant Cpn0803 using size-exclusion chromatography (Figure 7). Prior to performing gel chromatography, the column was standardized using the LMW and HMW gel filtration standard kit. Cpn0803 eluted as a predominant peak corresponding to a

hexamer, with a smaller peak corresponding to a dimer (Figure 7A). Both peaks were shown to contain Cpn0803 as determined by anti-His Western blot (Figure 7B).

Mapping of protein binding domains on Cpn0803

Having shown that Cpn0803 interacts with CdsN, CdsQ, and CdsF, we next mapped the Cpn0803 binding surfaces for these proteins. We used Pepscan epitope mapping for this purpose, as has been described previously [22,23]. This method can identify protein binding domains in Cpn0803 by screening binding partners against a library of 13 amino acid Cpn0803 peptides. Thus, an overlapping peptide library of Cpn0803 was synthesized and incubated with GST-CdsN, His-CdsQ, or His-CdsF (Figure 8A). Pepscan epitope mapping revealed distinct binding domains on Cpn0803 for CdsN, CdsQ, and CdsF. Specifically, CdsQ binding was localized to a surface corresponding to residues QKNPVGEKN (amino acids 153 - 161) in the C-terminal region (Figure 8A). The CdsN binding surface corresponded to residues LKRIFATPIGYTTFR (amino acids 22 - 36) (Figure 8A) at the N-terminus, and the CdsF binding surface corresponded to residues LTQQERIFLNRARVDGQE (amino acids 109 - 129). Random peptides sequences from Cpn0803, ranging from 15 - 30 amino acids in length, were used as negative controls and did not interact with CdsN, CdsQ, or CdsF in the assay. To corroborate the Pepscan epitope mapping, we cloned and expressed fragments of Cpn0803 containing the CdsQ and CdsN interacting regions fused to GST and performed GST pull-down assays against His-CdsQ and His-CdsN (Figure 8B). GST-Cpn0803₁₋₅₀, containing the CdsN binding domain, copurified with His-CdsN under

high salt conditions. GST-Cpn0803₁₂₀₋₁₇₀, containing the CdsQ binding domain, copurified with His-CdsQ under high salt conditions. GST-Cpn0803₁₋₅₀, which does not contain the CdsQ binding domains, did not copurify with CdsQ under any conditions. GST-Cpn0803₁₂₀₋₁₈₀, which does not contain the CdsN binding domain, did not copurify with CdsN under any conditions.

DISCUSSION

Although *C. pneumoniae* contains a functional T3SS, the identification and function of several key proteins of the apparatus have not been elucidated. In this report, we characterized a novel T3S-associated protein Cpn0803 in *C. pneumoniae*, demonstrating interactions with several key proteins of the T3SS. Using ELISA and co-purification assays, we show that Cpn0803 interacts with the ATPase CdsN, the needle filament protein CdsF, and the C-ring protein CdsQ, and mapped their respective binding surfaces using Pepscan mapping. We also show that Cpn0803 interacts with eukaryotic cell membrane components PA and PI, suggesting that Cpn0803 may associate with the host cell. The crystal structure of Cpn0803 revealed a relatively large, isolated, hydrophobic pocket within the dimer interface which may play a role in binding small molecules such as PA and PI. These observations suggest that Cpn0803 plays a role in T3S and may associate with host-cell components.

Chlamydial T3S genes are encoded on ten operons scattered throughout the genome [24]. The fact that Cpn0803 is not encoded on one of the ten operons does not preclude the possibility that Cpn0803 is a T3S effector or chaperone protein. For example, TARP (a known T3S effector) is encoded separately from the ten operons, not clustered with other T3S components. Thus, we evaluated binding of Cpn0803 to T3S membrane and peripheral-membrane components. T3S ATPases, YscN orthologs, promote effector protein unfolding and secretion by dissociating their cognate chaperones [12]. We have previously shown that CdsN is the ATPase of the *C. pneumoniae* T3SS and binds several effectors and chaperones, and the proposed C-ring protein CdsQ [25].

Thus, the interaction between Cpn0803 and CdsN is expected if Cpn0803 is secreted through the injectisome. Spaeth *et al.* have recently presented data that supports a role for CdsQ in *C. trachomatis* as a platform that organizes effector/chaperone complexes at the basal body of the T3S apparatus [14]. Thus, the interaction of Cpn0803 with CdsQ is also consistent with a possible role as a T3S effector or chaperone protein. The interaction of Cpn0803 with the needle filament protein, CdsF, suggests that Cpn0803 may function at the tip of the injectisome and also supports its role in T3S. Taken together, these observations suggest that Cpn0803 may function as an effector or chaperone protein in *Chlamydia* T3S.

Cpn0803 crystallized in the hexagonal space group $P6_3$, with two molecules in the asymmetric unit. A DALI search with the structure of Cpn0803 yielded no significant hits to any proteins in the current structural databases. Since CT584 (Cpn0803 ortholog) was predicted to be the needle-tip protein in *C. trachomatis* based on biophysical comparisons, we evaluated whether the structure of Cpn0803 had any similarity to needle-tip orthologs. Cpn0803 shares very little amino acid orthology, secondary or tertiary structure similarity with LcrV or IpaD. The only shared characteristic between these three proteins is a 4-helix bundle at the N-terminus. However, the central coiled-coil motif, which is conserved in all needle-tip families, is absent from Cpn0803 [15]. Based on both PISA analysis of the crystal structure and size-exclusion chromatography data of the recombinant protein, Cpn0803 appears to exist in a dimer/hexamer equilibrium in solution. Based on the crystal structure, the Cpn0803 hexamer is globular and approximately 9.5 nm in diameter in its longest dimension. However, the subunits

are tightly packed and do not form a pore. To function as an LcrV ortholog, the oligomeric state of the needle-tip must permit passage of effector proteins through the T3S apparatus [26]. Thus, the oligomeric state and crystal structure of Cpn0803 does not support its role as the needle-tip protein. However, it is possible that alternative oligomeric forms exist which contain a pore, possibly after translocation through the needle-complex.

We have shown that Cpn0803 interacts with both PA and PI. The volume of the hydrophobic pocket within the dimerization interface of the crystal structure of Cpn0803 is approximately 211.3 \AA^3 , making this hydrophobic pocket large enough to bind a small molecule. PA and PI are approximately 415 and 196 \AA^3 , respectively, indicating that PI, but not PA, could bind in the pocket. Conformational changes in the structure of Cpn0803 induced by oligomerization could lead to changes in the size of the hydrophobic pocket and facilitate binding of other small molecules. It is possible that Cpn0803 undergoes conformational changes upon binding PA or PI, and that this change is required for Chlamydial infection of host cells and effector translocation. *Chlamydia* is known to recruit proteins involved in phosphatidylinositol-4-phosphate (PI4) metabolism to regulate the PI composition of the inclusion membrane, which is necessary for optimal chlamydial development [27]. It is possible that Cpn0803 also plays a role in regulating PI levels in the inclusion. Also, phosphatidylinositol-3,4,5- P_3 is synthesized at sites of chlamydial entry upon host cell infection and may be important for actin recruitment and activation of specific guanine nucleotide exchange factors (GEFs) [28]. Cpn0803 may play a role in regulating these GEFs within the host cell upon infection through its

association with PI. Thus, the Cpn0803 interaction with PI supports a possible role as a T3S effector protein.

We employed Pepscan epitope mapping to determine the Cpn0803 binding surfaces involved in the interaction with CdsN, CdsQ, and CdsF [22, 23]. We found that Cpn0803 possesses specific surfaces mediating these interactions. The binding surface for CdsN corresponded to residues 22 - 36 on the N-terminal domain of Cpn0803. Based on the crystal structure, this surface would be buried within the hexameric state of Cpn0803. Therefore, cytoplasmic Cpn0803 likely interacts with CdsN as a dimer. Partial unfolding of the dimer would further permit secretion through the needle. CdsQ binding was mapped to a surface on Cpn0803 corresponds to residues 153 - 161 located at the C-terminus. The separation between the N-terminal CdsN and the C-terminal CdsQ binding surfaces may be important in the “hand-off” or transfer of Cpn0803 from the cargo transporter protein CdsQ to the ATPase CdsN. The CdsF binding surface on Cpn0803 corresponds to residues 109-129. This CdsF binding surface is partially inaccessible in the hexameric Cpn0803 state, but exposed in the dimer, suggesting that the Cpn0803 exists as a dimer upon interaction with CdsF. The observation that the interactions between Cpn0803 and CdsN / CdsF only occur with dimeric Cpn0803 suggests that the hexameric form may represent a stable cytoplasmic Cpn0803 structure, prior to inner membrane recruitment and subsequent secretion. The oligomerization may also be required for effector function in the host cell.

In the absence of a genetically tractable system for *Chlamydia*, and the inability to knockout Cpn0803, the definitive role of Cpn0803 cannot be determined. The epitope

mapping of binding surfaces for key T3S proteins, such as the needle-filament protein CdsF and the ATPase CdsN, supports the role of Cpn0803 in type III secretion and possibly as an effector protein. However, the crystal structure of Cpn0803 has very little similarity to LcrV or IpaD orthologs and does not support its role as the needle-tip protein. Whether Cpn0803 represents a novel class of needle-tip proteins, or plays an alternative role in T3SS such as that of an effector protein, requires further investigation.

METHODS

Expression Plasmids

C. pneumoniae CWL029 (VR1310:ATCC) (GenBank accession # AE001363) was used to isolate genomic DNA for cloning and protein expression. Full length *cdsN*, *cdsQ*, *cdsF*, and *cpn0803* were amplified from CWL029 using AttB-containing primers (Gateway; Invitrogen). Amplified products were cloned into pDONR₂₀₁ (Gateway; Invitrogen) to generate pENT vectors which were then used in LR reactions (Gateway; Invitrogen) to produce pEX vectors containing genes of interest. Either pEX₁₇ (N terminal His-tag) or pEX₁₅ (N terminal GST-tag) vectors were used for protein expression. All constructs were confirmed by DNA sequencing.

Purification of Recombinant Proteins

E. coli pellets containing over-expressed His- or GST-tagged proteins were thawed on ice and sonicated using a Fischer Scientific Sonic Dismembrator Model 100, followed by centrifugation at 20,000 x g for 40 minutes to remove insoluble material. Supernatants containing His-tagged protein for use in GST pull-down assays were stored at 4°C. GST tagged protein for use in GST pull-down assays were bound to 300 µL of glutathione beads overnight at 4°C, then blocked overnight in Tris Buffered Saline with 0.1% Tween-20 and 4% BSA and stored at 4°C until use. Purity was assessed using SDS-PAGE and Coomassie blue staining. For His-tagged proteins, columns were

washed with increasing imidazole concentrations and proteins were eluted with 300 mM imidazole then dialyzed extensively against activity buffer.

Glutathione plate assays

The glutathione-plate assay was performed using 96-well Pierce Glutathione Coated Plates. Briefly, 200 μ L of a lysate over-expressing a GST fusion protein was added to each well and incubated at 4°C for 2 hours. Next, the lysate was removed and the plate was washed with 200 μ L of PBS five times. The plate was blocked using 4% BSA in TBST for 2 hours at 4°C, and then washed five times with 200 μ L of PBS. Bacterial lysate (300 μ L) over-expressing a poly-histidine fused protein was added to each well and incubated at 4°C for 2 hours. To disrupt non-specific interactions, the plate was washed eight times with 500 mM NaCl, 0.1% Triton X-100, 50 mM TRIS-HCl pH 7.5. After the wash, the wells were blocked with a 4% BSA solution in TBST for 45 minutes at room temperature. Mouse-anti-6xHis monoclonal antibody (1 : 1000 dilution in PBST) was incubated for 45 minutes at room temperature. Bound antibody was detected using a goat-anti-mouse horseradish peroxidase conjugate (1 : 1000 dilution in PBST) and incubated at room temperature for 45 minutes, followed by 100 μ L of 5 mg/mL OPD (o-Phenylenediamine) (Pierce) added to each well and incubated at room temperature for 30 minutes before reading the absorbance at 450 nm using a Bio-Tek ELx800 plate reader. An interaction was considered positive if it was two standard deviations above the negative control (GST alone).

GST pull-downs

To examine the interaction of Cpn0803 with CdsN, CdsF, and CdsQ, GST pull-down assays were performed as described previously by Johnson et al, 2008, with the following modifications [29]. Briefly, glutathione-agarose beads (30 μ L) bound to 50 ng of GST-tagged protein was used in the assay. The beads were incubated overnight at 4°C with the *E. coli* lysate expressing the His-tagged proteins. Beads were collected by centrifugation and washed with 0.1% Triton X-100 and increasing concentrations of NaCl to eliminate spurious protein interactions. The presence of GST- and His-tagged proteins was confirmed by both Coomassie blue and Western blot. GST alone bound to glutathione beads was used as a negative control for the pull-down.

Production and affinity purification of rabbit polyclonal antibody to Cpn0803

Hyper-immune rabbit antisera was raised against Cpn0803. Briefly, His-Cpn0803 was expressed in *E. coli* BL21 and purified on Ni nitrilotriacetic acid (NTA) agarose (Qiagen) according to established procedures, and 500 μ g was delivered to Cocalico Biologicals, Inc. (Reamstown, PA), as a Coomassie-stained sodium dodecyl sulfate-polyacrylamide gel electrophoresis (SDS-PAGE) gel slice. Three rounds of immunizations with the adjuvant Titermax were employed. Immunoglobulin G (IgG) molecules were precipitated from the hyper-immune antisera with 50% saturated ammonium sulfate solution, resuspended in cold phosphate-buffered saline (PBS), and dialyzed into PBS. Activated CH-Sepharose beads (Sigma) were coupled with 30 mg of His-Cpn0803 and used to affinity purify the rabbit anti-Cpn0803 IgG. Briefly, antibody

was incubated with the His-Cpn0803-conjugated beads overnight at 4°C with rocking and washed with ice-cold PBS until the A_{280} was less than 0.02. Glycine (100 mM, pH 3.0) was used to elute the rabbit anti-Cpn0803 IgG molecules in 1 ml fractions into Eppendorf tubes containing 10 μ l of 1.5 M Tris, pH 8.8. Fractions were analyzed by probing Western blots containing chlamydial EB lysate and an *E. coli* lysate containing overexpressed His-Cpn0803.

Co-purification assays

Co-purification assays were performed essentially as described previously to investigate the interaction of Cpn0803 from EB with GST-tagged T3S proteins [30]. Briefly, 72 hr postinfection, EB were purified on a discontinuous gradient and lysed in PBS containing 1% Triton X-100 for 1 hr. EB lysates were precleared by microcentrifugation at 16,000 \times *g* for 30 min and then incubated with GST-tagged proteins in PBS for 6 h. Twenty microliters of glutathione agarose beads were then added to each tube overnight. Beads were collected by brief centrifugation, washed four times with binding buffer containing 20 mM imidazole, and boiled in 2x SDS-PAGE loading buffer. Co-purified Cpn0803 was detected by Western blotting and ECL using hyper-immune guinea pig anti-Cpn0803 antiserum.

Crystal structure of Cpn0803

All Cpn0803 crystals were grown at 18°C using the hanging-drop vapour diffusion method. Equal volumes of Cpn0803 (3.0 mg/mL) in storage buffer (0.12 M

potassium chloride, 0.2 M Tris pH 7.0) were mixed with crystallization solution (0.2 M potassium nitrate, 20% w/v PEG 3350) and dehydrated against 500 μ L of 1.5 M ammonium sulfate. Cpn0803-SeMet crystals were grown in the same manner by streak seeding with native crystals and gradually increasing the concentration of ammonium sulfate in the well solution to 2.0 M.

Native and SAD (SeMet) data sets were collected at 1.1 and 0.979 \AA wavelengths on beamlines X29 and X25 respectively of the National Synchrotron Light Source at Brookhaven National Laboratory. Data sets were processed and scaled with HKL2000 to 2.0 and 2.3 \AA , respectively [30]. Of the 12 SeMet sites expected based on primary sequence, 11 were located by AutoSol in the anomalous data set. The Phenix software package was used to calculate initial phase information to generate an experimental map [31]. A preliminary model was built which was then used for Molecular Replacement into the higher resolution, native data set of Cpn0803 using AutoMR. Model building and structure refinement of Cpn0803 was carried out through multiple iterations of Phenix-Refine and manual manipulation in COOT until the values of R and R_{free} converged and geometry statistics reached acceptable ranges [32, 33]. Surface area calculations were performed with the PDBe PISA server and volume calculations were performed using Chimera and the CASTp server [20, 21]. All structural illustrations were generated with PyMol [34]. Crystal structure similarity predictions were obtained using the DALI server [35].

Size-exclusion chromatography

Purified Cpn0803 (250 μ l) in gel filtration buffer (20 mM Tris pH 7, 100 mM KCl, 5 mg/mL protein concentration) was injected into a Superdex S200 10/300 GL gel filtration column (Amersham Biosciences, Piscataway, New Jersey) at 0.1 mL/min. The column was standardized using the LMW and HMW gel filtration standard kit (GE Life Sciences). Elution fractions (1 mL) were collected at a flow rate of 1 mL/min. Peak fractions were examined by anti-His Western blot.

Membrane lipid strip assay

Membrane lipid strips were purchased from Echelon and protein binding assays were performed according to the manufacturer's protocol. Briefly, lipid strips were blocked overnight in blocking buffer (PBS, 0.1% Tween, 5% BSA) at 4°C. Next, His-Cpn0803 or His-CdsL (negative control) were added to the lipid strips at a concentration of 0.5 μ g/mL and incubated at room temperature for 1 h. The protein solution was discarded and the lipid strips were washed 5 times with PBS-T for 5 min. The lipid strips were then probed for bound His-tagged protein using anti-His antibody (1:10000 dilution) and visualized with ECL reagent.

ACKNOWLEDGEMENTS

We acknowledge Brian Coombes PhD and Raphael Valdivia PhD for their critical reviews of the manuscript. This work was supported in part by Canadian Institutes of Health Research Grants to MSJ (MOP 89903) and JBM. CBS received a doctoral scholarship from the Father Sean O'Sullivan Research Center, St. Joseph's Healthcare, Hamilton.

REFERENCES

1. Hoare A, Timms P, Bavoil P, Wilson D (2008) Spatial constraints within the chlamydial host cell inclusion predict interrupted development and persistence. *BMC Microbiol* 8: 5.
2. Scidmore M, Hackstadt T (2008) Mammalian 14-3-3beta associates with the *Chlamydia trachomatis* inclusion via its interaction with IncG. *Mol Microbiol* 39: 1638-1650.
3. Wylie J, Hatch G, McClarty G (1997) Host cell phospholipids are trafficked to and then modified by *Chlamydia trachomatis*. *J Bacteriol* 179: 7233-7242
4. Hybiske K, Stephens R (2007) Mechanisms of host cell exit by the intracellular bacterium *Chlamydia*. *Proc Natl Acad Sci U. S. A* 104:11430-11435.
5. Galan J, Collmer A (1999) Type III secretion machines: bacterial devices for protein delivery into host cells. *Science* 284: 1322-1328.
6. Galan J, Wolf-Watz H (2006) Protein delivery into eukaryotic cells by type III secretion machines. *Nature* 444: 567-573.
7. Hayes C, Aoki S, Low D (2010) Bacterial contact-dependent delivery systems. *Annu. Rev. Genet.* 44: 71-90.
8. Hayward R, Cain R, McGhie E, Phillips N, Garner M, et al (2005) Cholesterol binding by the bacterial type III translocon is essential for virulence effector delivery into mammalian cells. *Mol Microbiol* 56: 590-603.

9. van der Goot F, Tran van Nhieu G, Allaoui A, Sansonetti P, Lafont F (2004) Rafts can trigger contact-mediated secretion of bacterial effectors via a lipid-based mechanism. *J Biol Chem* 279: 47792-47798.
10. Lafont F, Tran Van Nhieu G, Hanada K, Sansonetti P, van der Goot F (2002) Initial steps of *Shigella* infection depend on the cholesterol/sphingolipid raft-mediated CD44-IpaB interaction. *EMBO J* 21: 4449-57.
11. Marenne M, Journet L, Mota L, Corenlis G (2003) Genetic analysis of the formation of the Ysc-Yop translocation pore in macrophages by *Yersinia enterocolitica*: role of LcrV, YscF and YopN. *Microb Pathog* 35: 243-58.
12. Akeda Y, Galan J (2005) Chaperone release and unfolding of substrates in type III secretion. *Nature* 437: 911-915.
13. Lara-Tejero M, Kato J, Wagner S, Liu X, Galan J (2011) A sorting platform determines the order of protein secretion in bacterial type III systems. *Science*. 331: 1188-1191.
14. Spaeth K, Chen Y, Valdivia R (2009) The chlamydial type III secretion system c-ring engages chaperone-effector protein complexes. *PLoS Pathog* 5.
15. Mueller C, Dittmann S, Grimminger V, Walter S, Heesemann J (2005) The V-antigen of *Yersinia* forms a distinct structure at the tip of injectosome needles. *Science* 310: 674-676.
16. Roehrich A, Argudo I, Johnson S, Blocker A, Veenendaal A (2010) The extreme C terminus of *Shigella flexeri* IpaB is required for regulation of type III secretion, needle tip composition, and binding. *Infect and Immune* 78: 1682-1691.

17. Shen D, Saurya S, Wagner C, Nishioka H, Blocker A (2010) Domains of the *Shigella flexeri* type III secretion system IpaB protein involved in secretion regulation. *Infect Immun* 78:4999-5010.
18. Derewenda U, Mateja A, Devedjiev Y, Routzahn K, Evdokimov A, et al (2004) The structure of *Yersinia pestis* V-antigen, an essential virulence factor and mediator of immunity against plague. *Structure* 12: 301-306.
19. Markham A, Jaafar Z, Kemege K, Middaugh C, Hefty S (2009) Biophysical characterization of the *Chlamydia trachomatis* CT584 supports its potential role as a type III secretion needle tip protein. *Biochemistry* 48: 10353-10361.
20. Pettersen EF, Goddard TD, Huang CC, Couch GS, Greenblatt DM, Meng EC, Ferrin TE (2004) *J Comput Chem.* 25: 1605-1612.
21. Dundas J, Ouyang Z, Tseng J, Binkowski A, Turpaz Y, Liang J (2006) CASTp: computed atlas of surface topography of proteins with structural and topographical mapping of functionally annotated residues. *Nucleic Acid Research* 34:W116-W118.
22. Timmerman P, Puijk W, Meloen R (2007) Functional reconstruction and synthetic mimicry of a conformational epitope using CLIPS technology. *J Mol Recognit* 20: 283-99.
23. Stone C, Bulir D, Emdin C, Pirie R, Profilio E, et al. (2011) *Chlamydia pneumoniae* CdsL regulates CdsN ATPase activity, and disruption with a peptide mimetic prevents bacterial invasion. *Front. Microbio.* 2: 21.

24. Hefty P, Stephens R (2007) Chlamydia type III secretion system is encoded on ten operons preceded by sigma 70-like promoter elements. *J. Bacteriol.* 189: 198-206.
25. Stone C, Johnson D, Bulir D, Gilchrist J, Mahony J (2008) Characterization of the putative type III secretion ATPase CdsN (Cpn0707) of *Chlamydomphila pneumoniae*. *J Bacteriol* 190: 6580-8.
26. Caroline G, Faudry E, Yu-Sing T, Sylvie E, Attree I (2008) Oligomerization of PcrV and LcrV, protective antigens of *Pseudomonas aeruginosa* and *Yersinia pestis*. *J Biol Chem* 283: 23940-23949.
27. Moorhead A, Jung J, Smirnov A, Kaufer S, Scidmore M (2010) Multiple host proteins that function in phosphatidylinositol-4-phosphate metabolism are recruited to the Chlamydial inclusion. *Infect. Immun.* 78: 1990-2007.
28. Lane B, Mutchler C, Al Khodor S, Grieshaber S, Carabeo R (2008) Chlamydial entry involves TARP binding of guanine nucleotide exchange factors. *PLoS Pathog.* 4.
29. Johnson D, Stone C, Mahony J (2008) Interactions between CdsD, CdsQ and CdsL, three putative *Chlamydomphila pneumoniae* type III secretion proteins. *J Bacteriol* 190: 2972-2980.
30. Otwinowski Z, Minor W (1997) Processing of X-ray diffraction data collected in oscillation mode. In Carter CWJ, Sweet RM (eds.), *Methods in Enzymology: Macromolecular Crystallography, Part A*. Academic Press, New York, Vol. 276: 307-326.

31. Adams PD, Grosse-Kunstleve RW, Hung LW, Ioerger TR, McCoy AJ, Moriarty NW, Read RJ, Sacchettini JC, Sauter NK and Terwilliger TC (2002) PHENIX: Building new software for automated crystallographic structure determination. *Acta Crystallogr. D Biol. Crystallogr.* 58: 1948-1954.
32. Emsley P, Cowtan K (2004) Coot: Model-building tools for molecular graphics. *Acta Crystallogr. D Biol. Crystallogr.* 60: 2126-2132.
33. Krissinel E, Henrick K (2007) Inference of macromolecular assemblies from crystalline state. *J. Mol. Biol.* 372: 774-797.
34. The PyMOL Molecular Graphics System, Version 1.2r3pre, Schrödinger, LLC.
35. Holm L, Rosenström P (2010) Dali server: conservation mapping in 3D. *Nucleic Acids Research* 38: W545-549.

Table 5.1 – Data Collection and Model Refinement Statistics

	SeMet	Native
Data collection		
Space group	P6 ₃	P6 ₃
Cell parameters		
a,b,c (Å)	85.28, 85.28, 97.83	86.39, 86.39, 99.59
α, β, γ (°)	90, 90, 120	90, 90, 120
Molecules in ASU	2	2
Resolution (Å) ^a	50.0 – 2.30	50 – 2.00
Unique reflections	35, 361	28, 547
Redundancy ^a	4.4 (4.5)	9.7 (9.2)
Completeness (%) ^a	100.0(100.0)	100.0 (100.0)
I/ σ (I) ^a	10.75 (2.15)	23.06 (4.10)
Rmerge (%) ^a	12.1 (72.8)	9.1 (66.9)
Wilson B	-	26.19
Model refinement		
Resolution (Å) ^a		43.196 – 2.00
R _{work} /R _{free} (%)		17.74/20.85
Reflections _{observed}		27, 704
Reflections _{Rfree}		1, 416
No. atoms		
Protein		2, 953
Ligand/ion		0
Water		245
R.m.s.d. bond		
Lengths (Å)		0.009
Angles (°)		1.233
Average B Factor (Å ²)		36.79

PDB Accession Code

3Q9D

^a Statistics for the highest resolution shell are shown in parentheses.

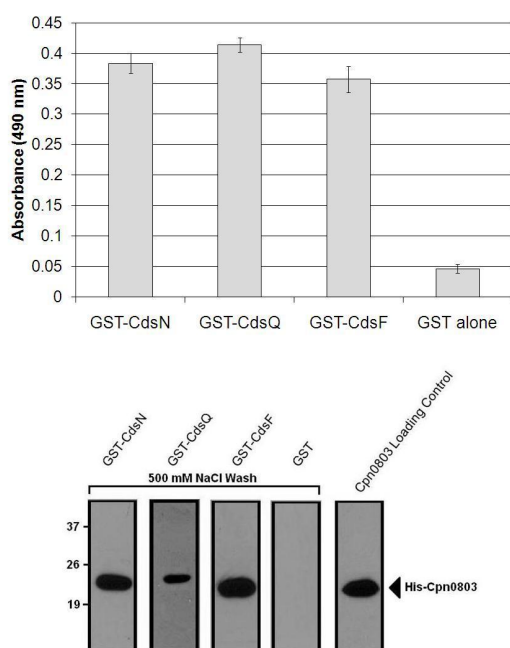


Figure 5.1. Cpn0803 interacts with type III secretion components *in vitro*. **A.** A glutathione plate assay was applied to screen for interactions of Cpn0803 between either CdsN, CdsQ or CdsF. His-Cpn0803 was applied to GST-CdsN, -CdsQ and -CdsF immobilized on glutathione plates, washed three times with PBS, and monitored using a colorimetric assay. Data is represented on the graph as the mean \pm standard deviation for each interaction. A significant interaction was considered to be two standard deviations above the negative control (GST alone against Cpn0803). As a positive control, we screened GST-Cpn0803 against Cpn0803. Cpn0803 interacted significantly with CdsN, CdsQ, CdsF, and Cpn0803 while it did not interact with GST alone. **B.** We applied GST pull-down assays to corroborate the interactions found with the glutathione plate assay. GST-CdsN, -CdsQ, -CdsF or GST alone immobilized on glutathione beads were

incubated with an *E. coli* lysate over-expressing His-Cpn0803 and washed with 500 mM NaCl. GST-CdsN, -CdsQ, and CdsF co-purified with Cpn0803 under 500 mM NaCl conditions while GST alone did not

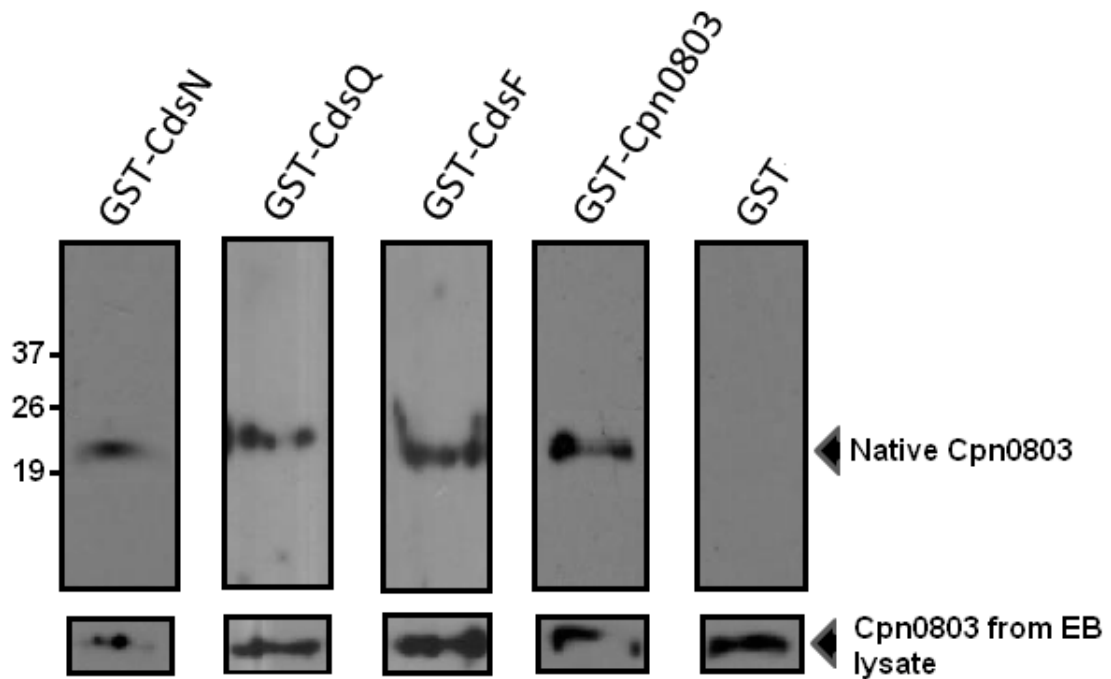


Figure 5.2. Cpn0803 interacts with type III secretion components *in vivo*. *C. pneumoniae* EB lysates were incubated with recombinant GST-CdsN, -CdsF, -CdsQ or -Cpn0803. Glutathione agarose beads were incubated with the lysates overnight, collected, and washed with 500 mM NaCl. The protein on the beads was analyzed by SDS PAGE and Western blot with anti-Cpn0803 antibody. Native Cpn0803 co-purified with GST-CdsN, -CdsF, and -CdsQ. As a positive control, Cpn0803 also copurified with GST-Cpn0803, but not with GST alone.

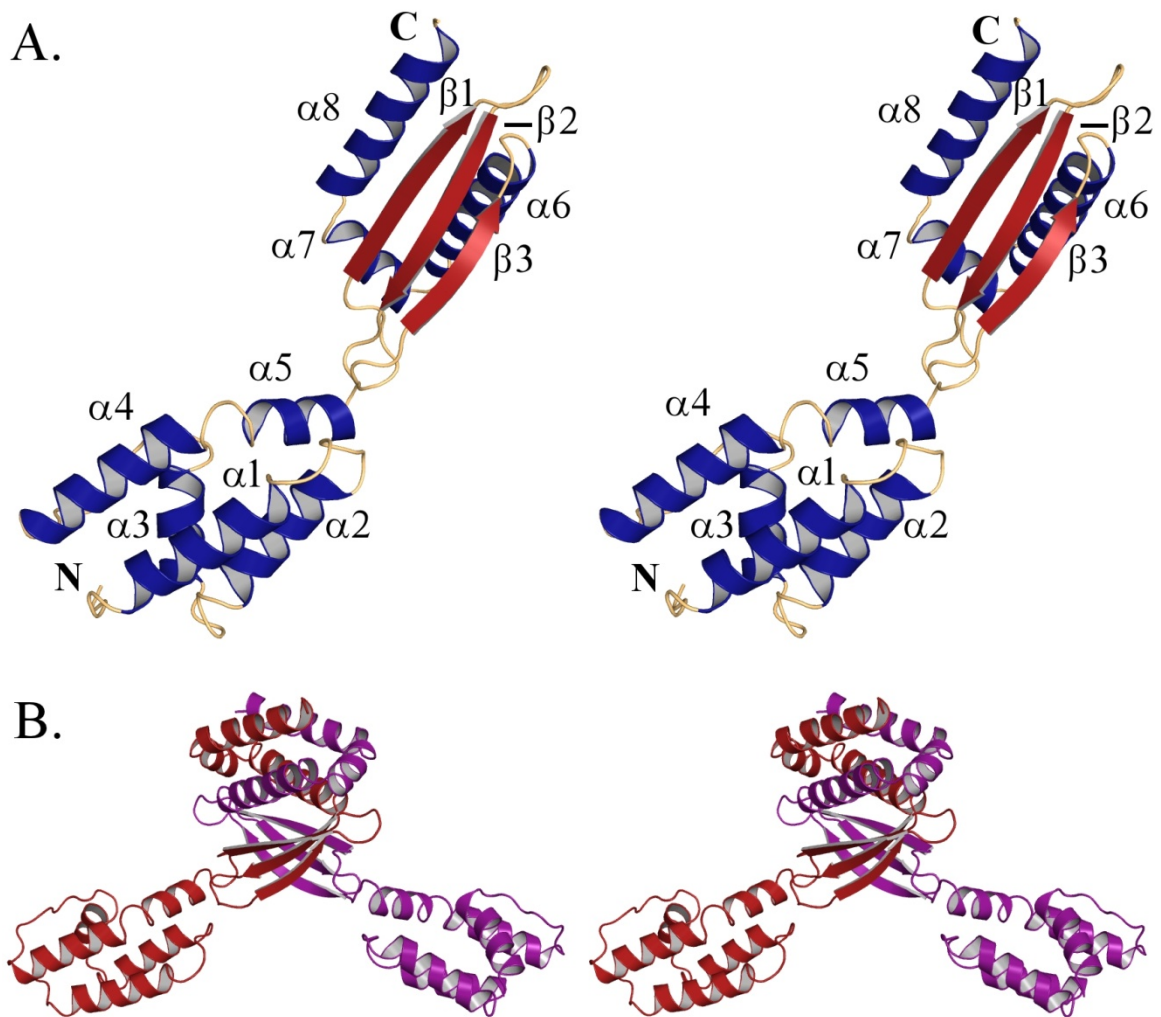


Figure 5.3. Stereo image of Cpn0803 monomer and dimer. The structure of full-length Cpn0803 was determined by SAD phasing of an anomalous data set collected from crystals of SeMet derivatized protein. The overall structure of Cpn0803 has a unique fold compared to LcrV from *Yersinia* or IpaD from *Shigella*, but contains the conserved N-terminal 4-helix bundle. **A.** Cartoon representation of the Cpn0803 monomer. Secondary structure elements are colored as follows, α -helices in blue and β -strands in red. **B.** Cartoon representation of the Cpn0803 dimer colored by chain.

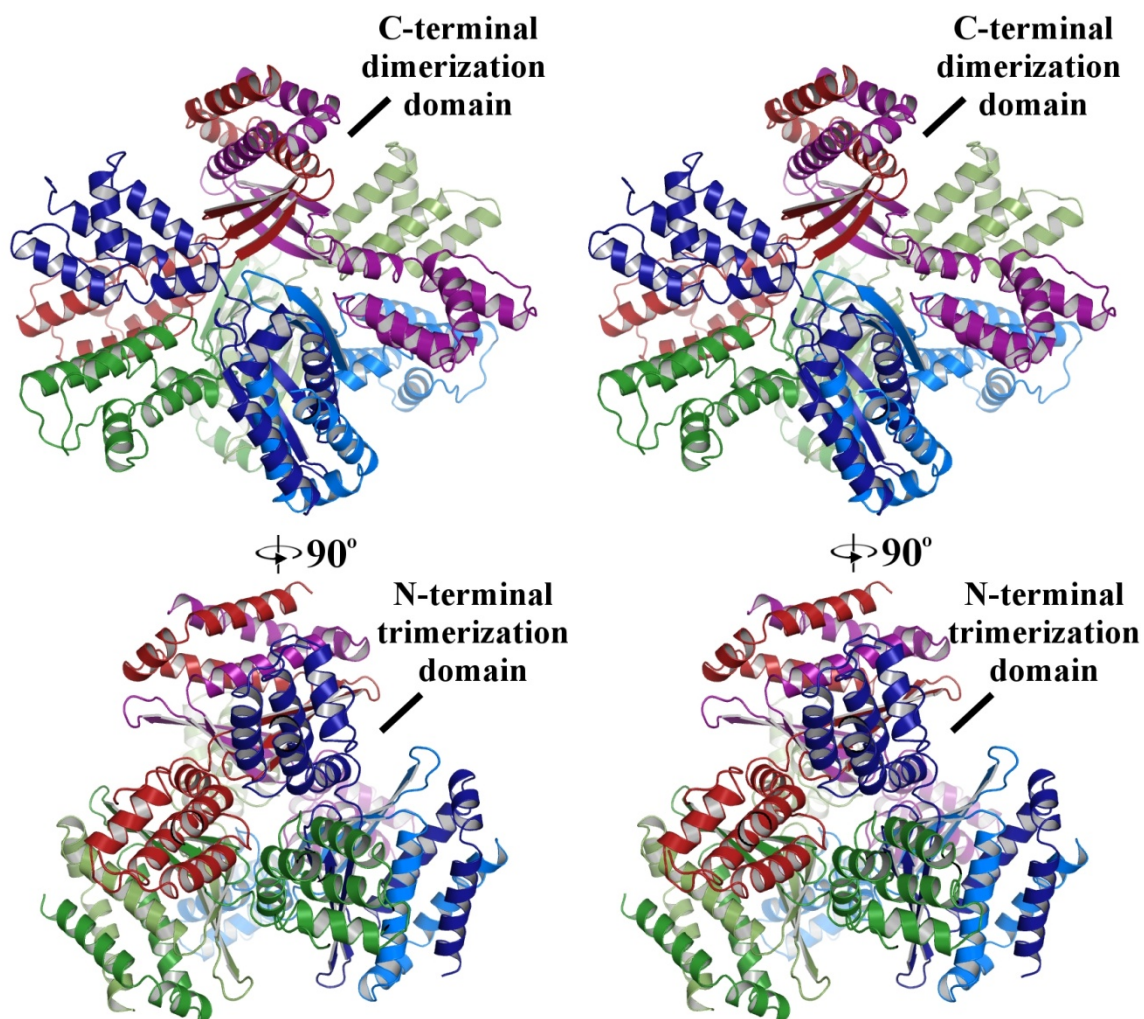


Figure 5.4. Stereo image of a predicted Cpn0803 hexamer colored by chain. We evaluated Cpn0803 for its ability to form multimers by analysis with the PISA server. Based on crystal contacts and buried surface area, the biologically active unit of Cpn0803 was predicted to be a hexamer formed by a trimer of dimers. The individual monomeric units are shown in different colours.

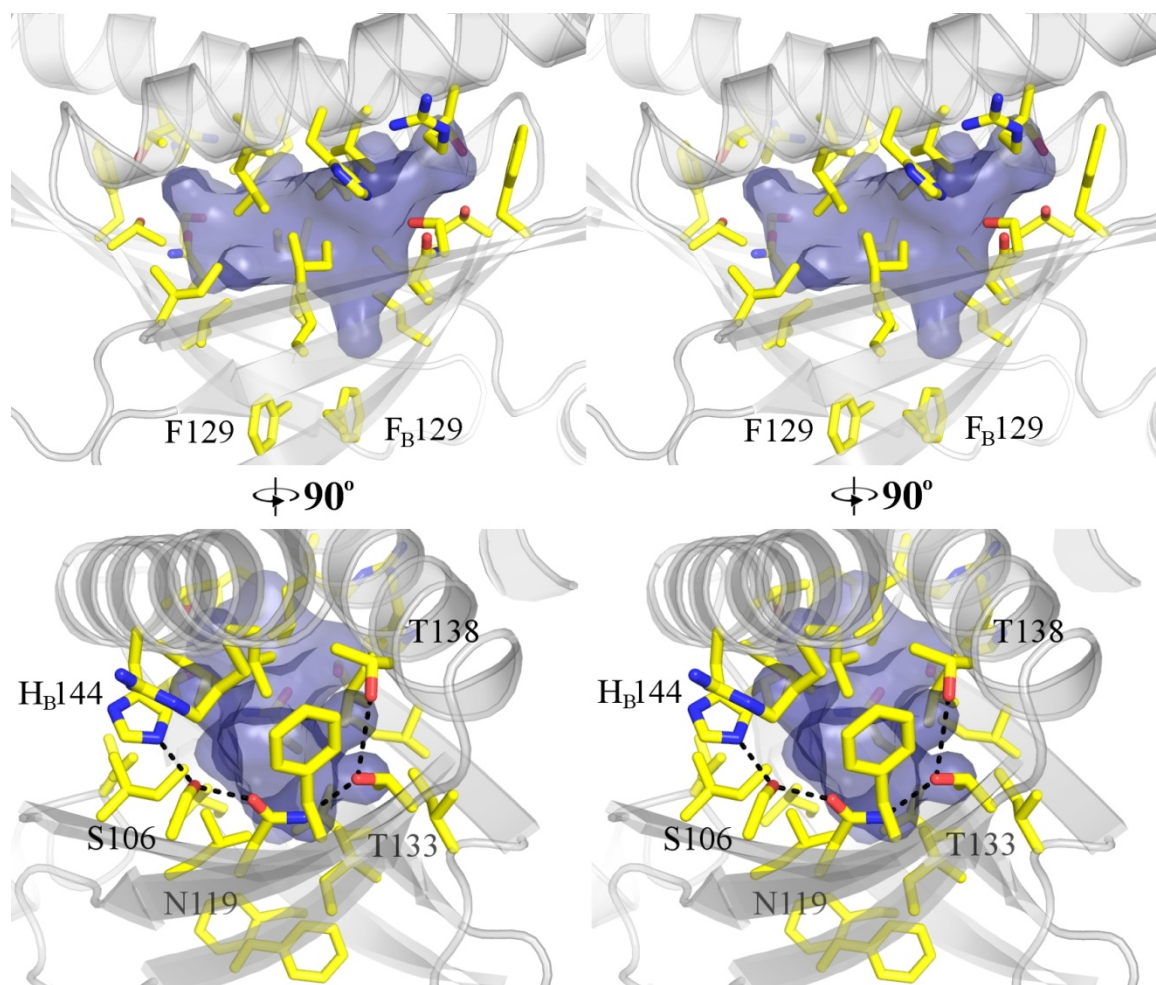


Figure 5.5. Stereo image of the hydrophobic pocket in Cpn0803. Dimerization of Cpn0803 results in the formation of a cone-shaped hydrophobic pocket between the two 3-stranded β -sheets, closed off at the 'top' by α -6 from both chains A and B, and stoppered at the 'bottom' by F129. The amino acid residues lining the interior of the pocket are represented in stick form.

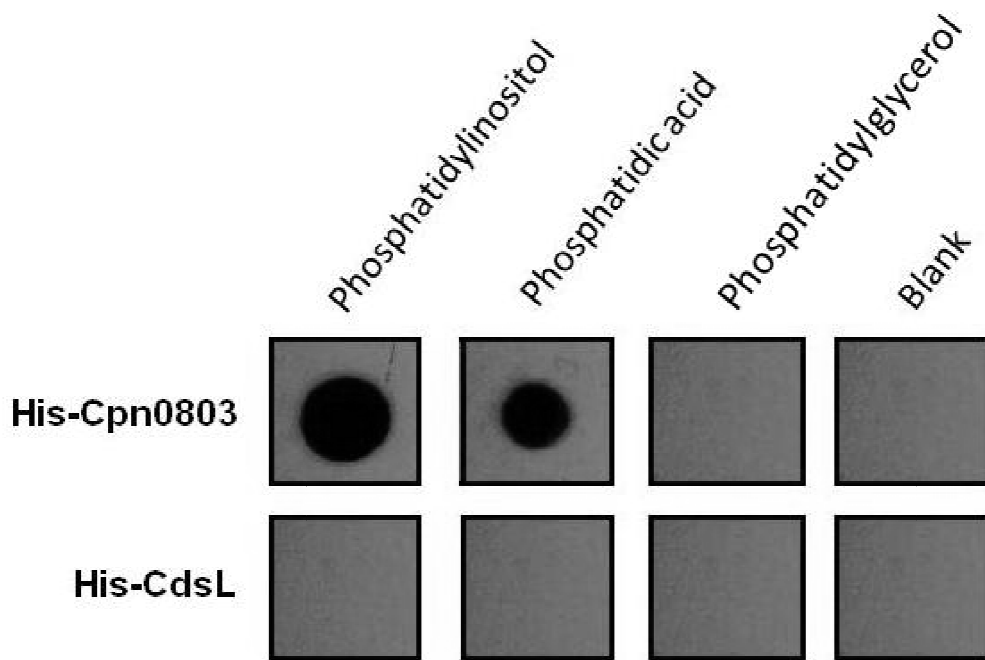


Figure 5.6. Cpn0803 interacts with phosphatidylinositol and phosphatidic acid. His-Cpn0803 was incubated with membrane lipid strips containing purified eukaryotic membrane components and visualized by anti-his antibody and ECL reagents. Cpn0803 interacted with phosphatidylinositol and phosphatidic acid, but none of the other molecules evaluated. His-CdsL, as a negative control, did not interact with any lipid components.

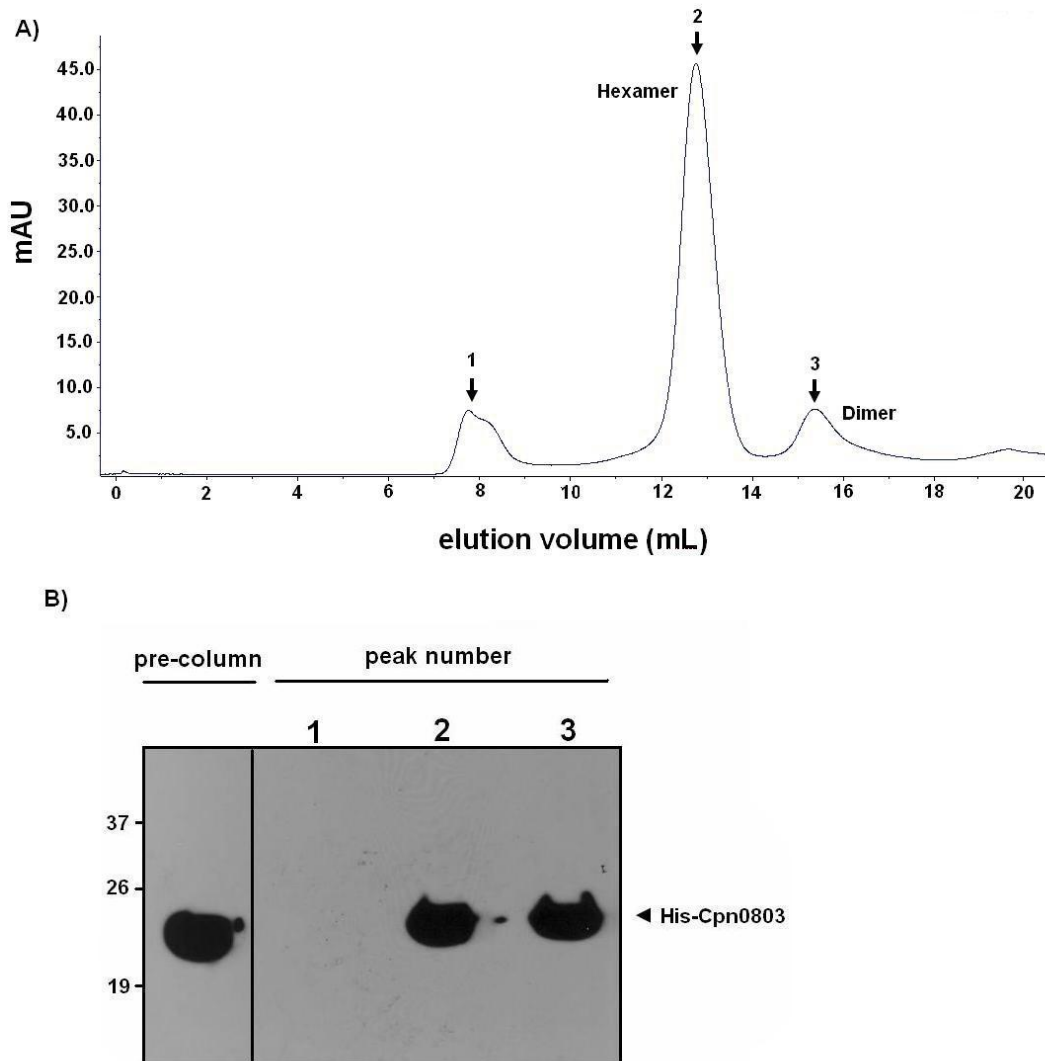
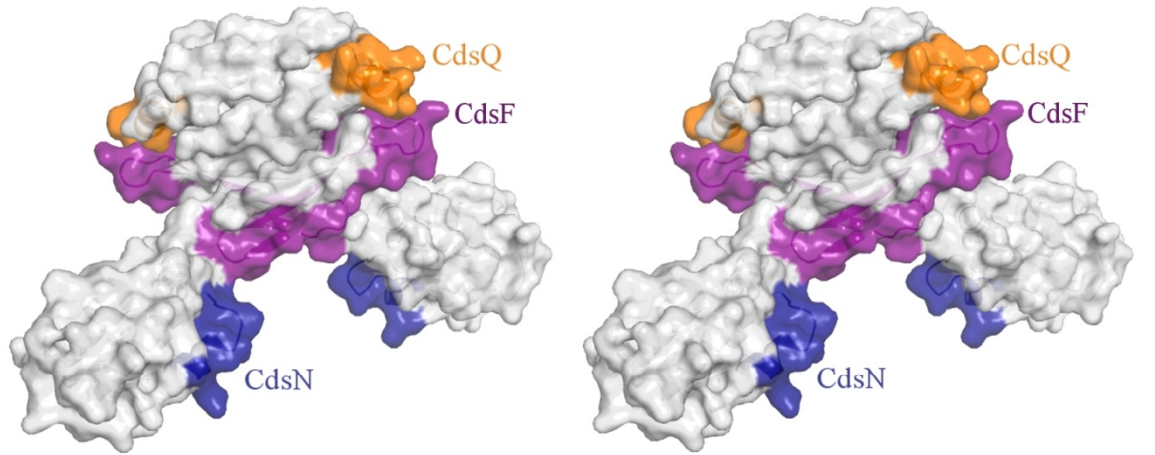


Figure 5.7. Cpn0803 exists in a hexameric and dimeric state in solution. A. Gel filtration chromatography was used to analyze purified His-Cpn0803. We found two dominant peaks, one corresponding to a hexamer and one corresponding to a dimer. **B.** Peak fractions in the elution volumes were collected and analyzed by anti-His Western blot. Cpn0803 was present in the peak fractions.

A.



┌ CdsN ─┐
 MAAKTKTLELEDNVFLLLEGNLKRIFATPIGYTTFRREFQNVVFNCAANGQQEIAN
 FFEMLINGKLTQELAPQQKQAAHSLIAEFMMPIRVAKDIHERGEFINFITSDMLT
└ CdsF ─┘
┌ CdsQ ─┐
 QQERCIFLNRLARVDGQEFLLMTDVQNTCHLIRHLLARLLEAQKNPVGEKNLQ
 EIQQEITSLKNHFDELTKALQ

B.

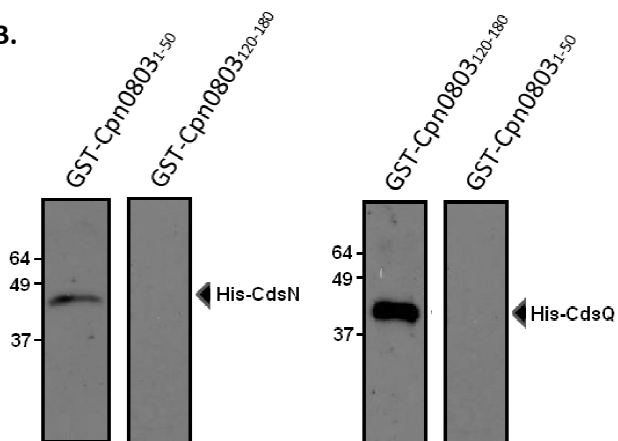


Figure 5.8. Pepscan mapping of the Cpn0803 binding regions shown in stereo. A. Pepscan epitope mapping against a Cpn0803 peptide library was performed to determine the residues of Cpn0803 responsible for mediating its interactions with CdsN, CdsF and CdsQ. Recombinant CdsN, CdsF and CdsQ was reacted against the Cpn0803 peptide library and monitored for the corresponding interacting regions. The corresponding surfaces are color-coded as follows: CdsN in blue (residues 22-26), CdsF in purple (residues 109-128), and CdsQ in orange (residues 153-161). **B.** To corroborate the Pepscan results, we expressed 50 amino acid fragments of Cpn0803 encompassing the CdsN and CdsQ binding domains and performed GST pull-down assays against recombinant CdsN or CdsQ. GST-Cpn0803₁₂₀₋₁₇₀, containing the CdsQ binding domain, copurified with His-CdsQ under high salt conditions. GST-Cpn0803₁₋₅₀, which does not contain the CdsQ binding domains, did not copurify with CdsQ. GST-Cpn0803₁₂₀₋₁₈₀, which does not contain the CdsN binding domain, did not copurify with CdsN.

CHAPTER SIX

DISCUSSION

The type III secretion system has been referred to as ‘irreducibly complex’, and used as evidence against the theory of evolution (Dawkins 2006). The extreme evolutionary cost of developing such a complex machine must be offset by equally large evolutionary benefits. Gram-negative bacteria rely on a combination of stealth and active suppression of the immune system to replicate within host cells. The T3SS secretes immune-dampening effector proteins at specific points throughout the life cycle. Orchestrating the correct chronological sequence of events (such as effector secretion) is equally important as constructing a functional injectisome, and adds to the levels of complexity required for successful bacterial infection. Effector proteins often have opposing functions, and simultaneous or mistimed secretion could negate the aggressive actions of the bacteria.

Although our understanding of the T3S mechanism has expanded in the last decade, *Chlamydia* lags behind other bacterial fields due to the genetic intractability and difficult culturing process of the bacteria. Merely five years ago, the most basic components of the *Chlamydia* T3SS remained as hypothetical, annotated proteins. Although evidence existed that *Chlamydia* possessed a complete repertoire of T3S genes, a thorough biochemical characterization of the system had not yet been performed. Even today, gaps exist in our knowledge; the exact role of T3S at the different *Chlamydia* developmental stages remains unclear, and identification of other basic T3S components, such as the complete effector set and the needle-tip sensor protein, is yet to be completed.

My initial goal was to demonstrate that *Chlamydia pneumoniae* possessed an enzymatically active T3S ATPase, a central component of the injectisome. From this initial enzymatic characterization, I expanded my work to the CdsN paralog FliI, demonstrating that there are more putative T3S components than initially identified. This observation adds to the complexity of the *Chlamydia* life-cycle. Next, I identified and characterized an effector protein that associated with CdsN and is secreted into the host-cell (Cpn0803). This concept of an effector associating with the ATPase, traversing the bacterial membranes via the injectisome channel, and ultimately reaching the host-cell cytoplasm is undoubtedly the core of the T3S pathway.

In this chapter, I discuss potential interrelationships between the data described in chapters 2 through 5. In the last five years, the T3S field has significantly expanded, and I have drawn on recent advancements from the Chlamydial and T3S literature to identify the implications of my work.

CHLAMYDIA TYPE III SECRETION GENETIC REDUNDANCY- POSSIBLE ROLES

Chlamydia are non-motile bacteria that lack a flagellum, yet contain a conserved set of flagellar genes. In this section, I discuss the possibility that the flagellar proteins are involved in T3S, allowing *Chlamydia* to secrete a different set of effectors from the RB and EB stage by integrating into the basal structure at specific time points. This information is largely hypothetical and based primarily on the observations that the flagellar genes are expressed at different times than the corresponding T3S genes, and

that the flagellar genes associate with T3S structural components (CdsN, CdsL) and effectors (CopN, Cpn0803).

CdsN and FliI: the two type III secretion ATPases

The mysterious ‘flagellar’ genes present in all Chlamydiae characterized to date have long posed many unanswered questions: what is their function in the chlamydial life cycle? Are they remnants of an ancient flagellar architecture, or do they play a more important role? The small size of the *Chlamydia* genome suggests that if these genes no longer served a purpose, they likely would have been eliminated. FliI is paralogous to CdsN, the T3S ATPase, with significant sequence similarity (Stone 2010). Also, the predicted three-dimensional structure of FliI and CdsN (using a homology modeling approach) shows very few differences. This would suggest that CdsN and FliI play similar roles in the life-cycle. Here, we discuss the possibility that CdsN and FliI are both involved in T3S, but function at different stages of the developmental cycle.

Accumulating evidence suggests that *Chlamydia* use T3S at both the EB and RB stage, facilitating invasion of host cells (secretion of TARP) and immune evasion (secretion of inclusion proteins) (Brinkworth 2011; Dehoux 2011; Fields 2003). The EB secretes effector proteins across the host-cell membrane, while the RB secretes effectors through the inclusion membrane. This is similar to the SPI-1 and SPI-2 genetic pathogenicity island system of *Salmonella*, which are used for invasion and intracellular survival, respectively (Galan 2001). SPI-1 secretes effectors that trigger significant cytoskeletal rearrangements during invasion, while SPI-2 secretes effectors that modulate

intracellular trafficking and enable the bacteria to replicate within a *Salmonella* containing vacuole (Galan 2001). However, *Salmonella* genetically compartmentalizes the genes encoding SPI-1 and SPI-2 proteins on distinct pathogenicity islands, while the *Chlamydia* type III secretion genes are scattered throughout the genome in several operons (Hefty 2007). Also, SPI-1 and SPI-2 encode separate T3S injectisomes, while *Chlamydia* appears to encode genes sufficient to form only one fully-functional apparatus (Kalman 1999). Based on this observation, we hypothesized that the flagellar genes function as T3S components at different stages of the life cycle and allow *Chlamydia* to construct semi-unique injectisomes in the EBs and RBs.

Initially, we wanted to determine if CdsN and FliI have similar protein-interaction profiles. We found that FliI has a similar protein-interaction profile as CdsN, interacting with CdsL (tethering protein, Stone 2009, Stone 2010), CopN (plug protein and negative regulator, Stone 2009, 2010), and CdsD (inner membrane T3S component, Stone 2009), which supports the role of FliI in T3S.

CdsN is expressed mid to late-cycle, during the late stages of RB replication and close to the transformation through IBs back to EBs (Slepenkin 2003). This expression profile could allow for accumulation and pre-loading of CdsN in EBs. Supporting this hypothesis, CdsN is abundant in EBs but absent in early-stage RBs, suggesting that CdsN plays a role in EB T3S, but not RB (Saka 2011). FliI expression has not been evaluated in detail, but is expressed before CdsN (mid cycle) (Belland 2003). Thus, it is possible that FliI functions in RBs (Saka 2011, Betts-Hampikian 2010).

T3S ATPases are known to act as inner-membrane recognition gates, organizing effector proteins at the base of the injectisome and selecting them for secretion (Akeda 2005). The varying requirements of *Chlamydia* during the life cycle suggests that the EB and RB require a different set of effector proteins; EBs induce actin recruitment to the site of attachment and other activities facilitating bacterial internalization and inclusion establishment (Jewett 2006; Moore 2008). RBs require effectors with immune-dampening activities and those that facilitate nutrient acquisition (Hatch 1975). It is possible that CdsN and FliI function in the EB and RB, respectively, and result in a different set of effectors being secreted at the different developmental stages. This would suggest that CdsN and FliI have similar binding profiles for structural or membrane components of the injectisome, but that some effector proteins will bind specifically to either CdsN or FliI. A recent study by Martinez-Argudo and Blocker demonstrated that there are different classes of effectors; namely early, middle and late depending on when they function in the T3S process (Martinez-Argudo 2010). It is likely that FliI and CdsN will bind similar early effector proteins (such as CopN) since these effectors are important for regulating T3S and would function at both the EB and RB stage. Differences will arise between CdsN and FliI binding of middle and late effectors (TARP, Cpn0585). The conserved interaction between the ATPases and early effectors is supported by *in vitro* binding experiments between CdsN, FliI and CopN. One alternative explanation for the presence of two ATPases is that they function as a hybrid oligomer with enhanced enzymatic activity. Oligomerization of YscN (the *Yersinia* T3S ATPase) is known to synergistically increase enzymatic activity by creating a positively charged

pocket to bind the negatively charged ATP (Zarivach 2007). It was possible that CdsN and FliI function together at both stages of infection, but *in vitro* binding experiments did not support this since CdsN and FliI did not interact. Also, CdsN is absent from early stage RBs (Saka 2011).

The major limitations of these studies are the lack of *in vivo* corroboration of the protein binding experiments and of a genetic model to evaluate the function of the flagellar proteins. Many of the interactions we demonstrated have been previously characterized in other Gram-negative bacteria and were not surprising. Thus, *in vivo* corroboration of these interactions did not seem necessary. However, in the future if differences in the FliI and CdsN protein interactomes are found, *in vivo* protein interaction studies will be important. Until recently, no genetic model existed for *Chlamydia*. With the development of a plasmid-based transformation system for *Chlamydia*, the role of the flagellar ATPase may be confirmed (Wang 2011). Also, it remains possible that FliI plays an entirely different role in the *Chlamydia* life-cycle unrelated to T3S and that these protein interactions are artifacts of the structural similarity to CdsN. Overall, these observations support the hypothesis that the flagellar ATPase (FliI) is associated with T3S and suggests that FliI may function in RBs while CdsN functions in EBs.

FlhA and FliF: possible role for duplication of inner-membrane components

Besides FliI, two other flagellar genes are present in all sequenced *Chlamydia* strains to date. FlhA is the paralog of CdsV, an inner membrane component which

coordinates assembly of the export apparatus (Diepold 2011). FliF is the paralog of CdsJ, another integral membrane protein involved in stabilizing the injectisome at the inner membrane (Cornelis 2002). These two genes, combined with FliI, are not sufficient to form a fully functional T3S or flagellar apparatus, but they can form a rudimentary basal structure (Kubori 1992). FliF in flagellar systems forms the MS-ring and can spontaneously self-insert into the inner membrane, forming the initial platform for flagellar construction (Bigot 2005). FlhA is known to play an important role in keeping the export gate closed in the absence of the ATPase and regulator protein (Moore 2010). This rudimentary structure consisting of FlhA and FliF may be used as a platform for further assembly of the T3S injectisome. In *Chlamydia*, binding studies have demonstrated that FlhA and FliF associate with T3S components, as well as form a complex with each other (Stone 2010). This information supports that concept that FlhA and FliF are incorporated into the T3S injectisome at a specific time in the *Chlamydia* life-cycle.

FlhA and FliF are expressed during the mid *Chlamydia* cycle (Belland 2003). This would suggest that they are used during the RB stage, similar to FliI. Based on this hypothesis, one injectisome (in the EB) would use CdsV, CdsJ and CdsN as basal body components, selecting for effector proteins such as the TARP upon host-cell contact and subsequent invasion. The second injectisome (in the RB) would contain the basal components FlhA, FliF and FliI, and select for effectors such as the inclusion proteins. Likely, in the RBs, FliF would initially insert into the membrane, forming a platform on which FlhA can bind and regulate secretion events. FliI and its regulator (CdsL,

discussed below) can then bind to this ‘hybrid’ injectisome consisting of the putative flagellar proteins and T3S proteins. In this scenario, *Chlamydia* is able to select for an entirely different set of effector proteins by only exchanging two basal body T3S components and the ATPase. This swapping mechanism is an efficient approach to create a unique injectisome at different developmental stages without duplicating every T3S structural gene. One other important protein involved in the selection of effectors, the C-ring protein (YscQ orthologs), would likely also be required to efficiently select and organize a different set of effector proteins in the EB versus the RB (Spaeth 2009; Lara-Tejero 2011). Interestingly, CdsQ is absent in RBs but abundant in EBs, suggesting that a CdsQ paralog may exist in RBs that has yet to be identified (Saka 2011). Alternatively, CdsQ may function at both stages and coordinate different effectors for the ATPase FliI.

Other examples of genetic redundancy in *Chlamydia*

The flagellar genes are not the only examples of gene duplication in the chlamydial T3S repertoire. For example, the putative translocator proteins, which form a pore in the host-cell membrane, are present in two copies. CopB/B2 and CopD/D2 have a high sequence similarity but are encoded in two different operons (Chellas-Gery 2011). The corresponding translocator chaperones, Lcrh-1 and Lcrh-2, are also present in two copies (Fields 2005). One set of translocators may function in the RB stage, associating with FliI prior to secretion, and form a pore in the inclusion membrane. The other set may function in the EB stage, associating with CdsN, and form a pore in the host-cell membrane. It is possible there are slight differences required for pore formation in the

host-membrane versus the inclusion membrane, but this requires further investigation. It is also possible that the translocators have effector functions in the host cell after effector translocation is complete.

POSSIBLE ROLE OF THE *CHLAMYDIA* TYPE III SECRETION ATPASES

This section proposes a function for the two T3S ATPases in effector-chaperone release (based on protein binding assays) and effector secretion at the inner membrane. It also discusses the co-regulation of CdsN and FliI by a single T3S protein and the implications of this observation.

Coordination of effector – chaperone complexes at the inner membrane

Translocation of a fully-folded protein through the injectisome channel is spatially prohibitive, thus requiring partial or complete unfolding of an effector protein prior to secretion. In a landmark 2005 study by Akeda and Galan, it was shown that the *Salmonella* T3S ATPase InvC catalyzes dissociation of effector – chaperone complexes, followed by effector secretion through the needle (Akeda 2005). Effector chaperones are believed to play a role in maintaining their cognate effector proteins in a ‘secretion incompetent’ state in the bacterial cytosol (Thomas 2004). Upon dissociation from the chaperone, the effector can progress into the host cell. In this section, we discuss the possibility that CdsN and FliI may also function in this capacity based on their interaction with T3S effectors and chaperones.

Initially, we examined whether CdsN associates with known effector or chaperone proteins. We found that CdsN, the *C. pneumoniae* T3S ATPase, interacts with CopN (a T3S effector) and Cpn0803 (putative needle-tip or effector protein). Our lab has also shown that CdsN interacts with Lcrh-2 (CopN and CopB/B2 chaperone) and Cpn0827 (T3S effector) (Toor 2011). The fact that CdsN associates with chaperones and effectors suggests that it functions at the inner membrane in a similar fashion as InvC; dissociating effector – chaperone complexes. We have also shown that FliI associates with CopN and Cpn0803, suggesting that FliI also coordinates chaperone-effector complexes, but possibly at a different developmental stage (Supplementary Figure 6.1.7). Until recently, very few chaperone – effector complexes had been characterized in *Chlamydia*. However, Brinkworth et al. recently identified the TARP-specific chaperone (Slc1) which would require dissociation upon *Chlamydia* entry into host cells (Brinkworth 2011). Based on the fact that TARP is involved in entry, the TARP-Slc1 complex may associate with CdsN, which we hypothesize functions during the EB stage. The translocator proteins, CopB/B2 and CopD/D2, also have specific chaperones (Lcrh-1 and Lcrh-2, respectively) (Chellas-Gery 2011; Fields 2005). Our lab is in the process of characterizing these interactions (Bulir et al., unpublished data). With the identification of several new effector-chaperone pairs, chaperone release assays could be performed to confirm that CdsN functions as an inner-membrane recognition gate, priming effector proteins for secretion. Also, differential effector / chaperone release between CdsN and FliI could be used to determine if the two ATPases catalyze the release of different substrates.

After identifying numerous interactions between CdsN and other T3S structural/effector components, we explored the CdsN domains mediating these interactions. Our lab has identified binding domains in CdsN that mediate these interactions using PepScan epitope mapping and GST pull-downs using CdsN fragments (Toor 2011; Stone 2011; Stone 2008) In total, 14 T3S-associated proteins were screened against the CdsN PepScan library to identify the binding domains, including (in collaboration with Dr. Radhey Gupta at McMaster University) 5 cytoplasmic *C. trachomatis* proteins. The exact role of these 5 cytoplasmic proteins is unknown, but they could function as effector or chaperone proteins. By combining the information from PepScan mapping and GST pull-downs of structural and cytoplasmic components, we identified two distinct domains in CdsN mediating specific protein interactions (Supplementary Figure 6.1.6). One large CdsN domain mediates interactions with soluble T3S components (Lcrh-2, CopN, Cpn0803, Cpn0827), while another interacts with structural and membrane-associated components (CdsL, CdsD, CdsU). Thus, CdsN may compartmentalize its protein interactions, allowing it to maintain numerous associations at one time. CdsN will likely only bind one effector-chaperone pair at a time as it prepares the effector for secretion, but the interactions with structural T3S components may be more permanent. As an example, we mapped the Cpn0803 interaction onto the CdsN hexamer based on the predicted CdsN crystal structure (modeled from EscN) (Supplementary Figure 6.1.3). Cpn0803 binds around the N-terminal hexamer pore entrance. Based on this information, it is likely the N-terminal face of the CdsN hexamer orients towards the bacterial cytoplasm, while the C-terminal face orients towards the

bacterial inner membrane. This effector protein binding location would allow for chaperone release followed by immediate translocation through the needle. This binding location is also compatible with CdsN functioning as an inner membrane unfolds of effectors, similar to the AAA+ family of unfoldases (Martin 2008). These unfoldases function by pulling an exposed polypeptide tag of the target protein through an electronegative pore (Martin 2008). It is tempting to speculate that in the T3SS chaperones play a role in maintaining and presenting the unfolded polypeptide tag to the ATPase for subsequent unfolding.

The major limitations of these studies are that chaperone-release assays have not been performed with chlamydial ATPases. We have preliminary evidence suggesting that CdsN can catalyze the release of CopN from its chaperone Lcrh-2, but further experiments are required (data not shown). Also, the hydrophobic nature of some T3S components could result in false-positive PepScan mapping results. However, we have confirmed the PepScan mapping results for the CdsN – CdsL and CdsN – CdsQ interactions using site-directed mutagenesis and found them to be accurate. Overall, we have found that CdsN associates with effector and chaperone proteins, and that FliI associates with at least two effectors (CopN and Cpn0803). This suggests that the T3S ATPases are involved with regulating T3S, possibly releasing cognate chaperones from their effectors.

Co-regulation of the type III secretion ATPases

The ability to activate and inhibit the T3SS is paramount to a successful bacterial infection as a constitutively active T3S could be detrimental to the infection process. A mechanism to inhibit the ATPase, which is central to the secretion process, would be an efficient approach to regulate the T3SS. In *Yersinia*, YscL is known to both tether the ATPase to the membrane and down-regulate enzymatic activity (Blaylock 2006). Initially, we found that CdsL associates with CdsN *in vitro* (Stone 2008). In the next study, we found that CdsL also associated with FliI, the second T3S ATPase (Stone 2010). As discussed above, this supports the concept that FliI is associated with T3S.

In flagellar systems, FliH orthologs typically down-regulate the enzymatic activity of FliI (Minamino 2003). However, no FliH ortholog (CdsL paralog) has been identified in *Chlamydia*. Using a genomic approach, we sought to identify a possible FliH ortholog that may regulate FliI enzymatic activity. Our initial search identified Cpn0859 (encoded directly upstream of FliI), which was shown to interact with FliI, but had no effect on its enzymatic activity (Stone 2010). Thus, Cpn0859 remains a T3S protein of unknown function, but based on its size, solubility and association with FliI, may be an effector or chaperone.

CdsL is expressed throughout the entire *C. pneumoniae* life cycle (Slepenkin 2003). This led us to hypothesize that CdsL functions at both stages of development (*i.e.* the EB and RB). Based on this hypothesis, and the fact that the two ATPases may function at the different stages, we evaluated whether CdsL down-regulated both CdsN and FliI enzymatic activity. We found that CdsL inhibited CdsN enzymatic activity,

which has been shown for orthologs of other Gram-negative bacteria and is not surprising (Stone 2011). However, CdsL also down-regulated FliI enzymatic activity, demonstrating that CdsN and FliI are regulated by the same T3S protein (Supplementary Figure 6.1.7). Using PepScan domain mapping, we found that CdsN has two binding domains for CdsL, one of which is close to the ATPase P-loop that coordinates the binding of ATP for hydrolysis (Stone 2008). Based solely on PepScan mapping and *in vitro* binding assays of the CdsN-CdsL binding site, we proposed a potential mechanism of CdsL down-regulation of CdsN based on sterically hindering ATP access to the P-loop (Stone 2011). The existence of a second CdsN binding domain for CdsL potentially supports the two roles of CdsL (tethering and enzymatic down-regulation) (Pallen 2006). The corresponding amino acid segments on FliI have between 60 and 100% similarity and 20 to 30% identity to the domains on CdsN. Thus, it is possible that CdsL functions by the same mechanism on FliI, sterically hindering access of ATP to the P-loop. However, the exact binding domain on FliI for CdsL is currently unknown. We considered that CdsL may be a non-specific ATPase down-regulator, but exposure of GspE (the *C. pneumoniae* T2S ATPase) to CdsL did not affect enzymatic activity (Stone 2011). These observations provide further evidence that FliI and the flagellar proteins are incorporated into the T3S injectisome. Also, CdsL may regulate T3S via the ATPases during the entire *Chlamydia* life-cycle.

CPN0803: FUNCTION UNKNOWN

This section discusses the effector protein Cpn0803, which was identified and found to associate with both CdsN and FliI. We discuss the possibility that Cpn0803 is secreted from both the EB and the RB based on its association with both T3S ATPases. Also, since the *C. trachomatis* ortholog of Cpn0803 (CT584) has been proposed as the T3S needle-tip protein, we discuss evidence which both supports and refutes this hypothesis.

Cpn0803 may be secreted by both EBs and RBs

We have discussed the potential role of FliI and CdsN in coordinating effector-chaperone complexes at the inner membrane and priming effectors for secretion. Next, we wanted to identify a specific effector protein and determine whether it associated with either CdsN or FliI. Recently, the *C. trachomatis* protein CT584 was proposed as the needle-tip protein, an early effector protein in T3S (Markham 2009). Needle-tip proteins are thought to have many roles; for example, they are present on the injectisome tip and act as a chaperone for the translocator proteins during insertion into the membrane (Caroline 2008). Also, they may have functions within the host cell after their chaperoning role is complete (Sodhi 2005). Thus, we further evaluated the interaction between CdsN, FliI, and Cpn0803.

We first wanted to determine if Cpn0803 is secreted into host cells, as has been seen with some LcrV orthologs, since secreted effectors should interact with T3S ATPases (Akeda 2005; Gauthier 2003). We found that Cpn0803 is present in HeLa cells

2 hours after *Chlamydia* infection, suggesting that it is secreted from EBs upon invasion (Supplementary Figure 6.1.1). We did not evaluate if Cpn0803 is present in HeLa cells at later time-points in the infection cycle.

Based on this observation, we assumed that Cpn0803 would interact with CdsN (the putative EB T3S ATPase). Using GST pull-down assays, we found that Cpn0803 associates with both CdsN (Stone 2011) and FliI (Supplementary Figure 6.1.7). Based on our hypothesis, this suggests that Cpn0803 plays a role during both stages of infection (EB and RB). Also, this interaction is consistent with the role of CdsN/FliI in dissociating effector substrates from their cognate chaperones prior to secretion. However, the Cpn0803 chaperone is currently unknown. Cpn0803 also bound within the effector binding domain on CdsN identified by PepScan epitope mapping, consistent with its role as an effector (Supplementary Figure 6.1.6). However, whether Cpn0803 plays the role of the needle-tip protein of *C. pneumoniae* remains unknown. Since Cpn0803 associates with the two ATPases (CdsN and FliI), it may be secreted from both EBs and RBs and have effector functions. For example, Sodhi et al. showed that recombinant LcrV inhibited activation of murine peritoneal macrophages (Sodhi 2011). Our lab has preliminary data suggesting that Cpn0803 associates with β -actin, which may be involved in its effector function. However, we were not able to show any changes in actin polymerization / depolymerization in the presence of Cpn0803 alone (data not shown). However, the fact that Cpn0803 associates with the ATPases and is secreted into the host cell suggests it has specific effector functions.

Evidence supporting the role of Cpn0803 as the needle-tip protein

Lacking a genetic system for Chlamydiae, it is difficult to assign specific roles to T3S proteins. Many roles are inferred based on genetic similarity or protein interactions, but needle-tip proteins are notoriously unique between bacteria, excluding some specific tertiary structural similarities. CT584 of *C. trachomatis* (Cpn0803 ortholog) was assigned as the needle-tip protein based primarily on biochemical characterization and comparison to other LcrV orthologs. They explored CT584 biochemical characteristics such as Far-UV circular dichroism, Fourier transform infrared spectroscopy, UV absorbance spectroscopy, ANS extrinsic fluorescence, turbidity, right angle static light scattering, and analytical ultracentrifugation (Markham 2009). Based on these attributes, CT584 was very similar to LcrV orthologs.

We have found some evidence that supports the role of Cpn0803 as the needle-tip protein (LcrV ortholog). First, its interaction with both CdsN and FliI support its role as an effector protein, and thus the needle-tip protein. Also, Cpn0803 has a specific interaction with CdsF, the needle-filament protein. This interaction is rare in the T3SS and few other soluble proteins (besides the needle-tip) would require such an association (Marenne 2003). Size-exclusion chromatography supports the formation of larger-ordered Cpn0803 structures, as has been seen in *Pseudomonas* (Caroline 2008). LcrV orthologs are thought to form tetrameric or pentameric structures on the tip of the injectisome in a ring-like form, allowing the passage of translocator proteins through their pore. It is possible that upon unfolding/refolding through the injectisome needle, the oligomeric state of LcrV changes to accommodate requirements at the needle-tip

(Caroline 2008). Since our data suggests that Cpn0803 exists primarily as a dimer/hexamer equilibrium in the bacterial cytoplasm, a similar phenomenon may occur in *Chlamydia*.

Based on the fact that LcrV orthologs form ring-like structures, using electron microscopy (EM) we evaluated whether Cpn0803 formed ring-like structures in solution in collaboration with Dr. Joaquin Ortega. We saw that Cpn0803 formed approximately 100 Å ring-like structures with a 20-30 Å pore, consistent with what has been seen in *Pseudomonas* (Caroline 2008) (Supplementary Figure 6.1.2). Based on this observation, and combined with PepScan analysis, we used the Rosetta docking server to model a tetrameric Cpn0803 structure with dimensions consistent with those observed by EM. The Rosetta docking server supported the ring-shaped tetramer model of Cpn0803 and found that it was energetically favourable (Supplementary Figure 6.1.5). The larger-ordered structure we observed in gel filtration was initially thought to be a hexamer, but the large stokes radius of tetrameric Cpn0803 could result in elution at lower volumes than a predicted tetramer on the column. Thus, this quaternary structure of Cpn0803 supports its role as the needle-tip protein.

Also, we found that Cpn0803 associates with lipid components such as phosphatidic acid and phosphatidylinositol. Supporting this interaction, Cpn0803 possessed a hydrophobic binding pocket large enough to accommodate a small-molecule. In *Shigella*, the needle-tip protein (IpaD) is known to bind deoxycholate in the middle of the coiled-coil region, which induces structural changes in the protein (Dickenson 2011). These structural changes in IpaD play a role in recruiting the translocator proteins to the

injectisome tip for translocon pore formation. It is possible that these membrane components that bind Cpn0803 could function in triggering T3S upon host cell contact and recruiting CopB/B2 or CopD/D2 to the needle-tip.

Evidence refuting the role of Cpn0803 as the needle-tip protein

Generally, needle-tip proteins are identified by crystallographic analysis. There are three classes of needle-tip proteins (Ysc, Inv-Mxi-Spa, and Esc families), all of which contain a characteristic long central alpha-helix that generally form a coiled-coil motif (Caroline 2008). This motif is important for the structural integrity of the protein and its association with the needle-filament protein for docking at the needle-tip. This domain also plays a role in translocator insertion into the host cell membrane and pore formation. The Inv-Mxi-Spa class also contains an N-terminal motif with structural similarity to common chaperones, suggesting a self-chaperoning function of the domain (Johnson 2007).

Crystallographic analysis of Cpn0803 did not reveal this long, central coiled-coil motif or the N-terminal chaperone-like domain. Instead, Cpn0803 crystallized as a dimer with a small coiled-coil formed at the dimerization interface. The monomer consisted primarily of short alpha-helices with an N-terminal 4-helix bundle. Thus, the crystal structure of Cpn0803 does not support its role as the needle-tip protein. It is possible that Cpn0803 represents a novel, unique needle-tip class, separate from Ysc, Mxi-Spa-Inv, and Esc, but this requires further investigation. It is also possible that a second

component functions in concert with Cpn0803 at the needle-tip in host cell sensing, but this component has not been identified.

MAKING SENSE OF THE INNER MEMBRANE COMPLEX

The inner membrane protein complex of the T3SS is well studied in many Gram-negative bacteria, but the *Chlamydia* injectisome remains relatively uncharacterized. In this section, I discuss known protein interactions in the *Chlamydia* inner membrane export apparatus based on current literature, and incorporate novel findings from our lab. Based on this information, I discuss the structure of the inner membrane of the *C. pneumoniae* T3S injectisome.

The export apparatus of *C. pneumoniae*

The export apparatus of Gram-negative bacteria consists of inner membrane components which help coordinate effector proteins through the injectisome. This export apparatus is well studied in Gram-negative bacteria such as *Yersinia* and *Salmonella*, but the *Chlamydia* inner membrane proteins remain largely uncharacterized. Our lab has previously shown that CdsQ, CdsL and CdsD form a complex at the inner membrane (Johnson 2008). We extended these observations to show that CdsN and FliI also associate with this complex.

CdsQ is found in both the soluble and insoluble fractions of a *Chlamydia* lysate and is believed to act as a platform for the recognition and engagement of chaperones complexed to secretory cargo (Spaeth 2009). CdsQ forms the C-ring of the injectisome at

the inner-membrane, and may coordinate docking of a msc in *C. trachomatis* (Spaeth 2009). In *Salmonella*, the CdsQ ortholog (SpaO), in combination with OrgA and OrgB, have been shown to control the hierarchy of effector secretion by forming a sorting-platform at the inner membrane (Lara-Tejero 2011). In agreement with these studies, we have shown that CdsQ associates with effectors (Cpn0827, CopN) and chaperones (Lcrh-2, Cpn0706) (Toor 2011). The interaction we observed between CdsN and CdsQ could suggest that CdsQ facilitates transfer of chaperone-effector complexes to the ATPase for dissociation. Also, using PepScan epitope mapping, we found that the CdsQ binding domain on Cpn0803 was distant from the CdsN binding domain, possibly facilitating this transfer or ‘hand-off’ of Cpn0803 from CdsQ to the ATPase.

Upon delivery of chaperone-effector cargo, the ATPase must be activated to initiate secretion. The interaction between CdsQ and CdsL suggests that CdsQ may play a role in releasing the CdsL repression of CdsN upon effector-chaperone delivery. It is possible that CdsQ sequesters CdsL away from the ATPase upon hand-off of the effector-chaperone cargo, activating the ATPase activity and subsequent effector secretion. The hand-off of effector/chaperone cargo from CdsQ to CdsN may expose the CdsQ binding domain for CdsL. Interestingly, CdsQ is abundant in EBs but absent in RBs, suggesting that *Chlamydia* may encode an unidentified CdsQ paralog to function during the RB stage with FliI, FlhA, and FliF.

CdsD is a unique protein containing two FHA-2 domains which are known to become phosphorylated by protein kinase D (PknD) (Johnson 2008). The purpose of this phosphorylation event is unknown, but it could be involved in signal transduction from

the needle-tip to the inner-membrane upon host-cell contact. Since CdsD associated with CdsN, it could play a role in initiating early T3S events upon host-cell contact, possibly also by relieving the CdsL repression on CdsN. This would be required since CopN plugs the injectisome pore prior to host-cell contact, and CdsD activation of CdsN would catalyze secretion of CopN and activation of T3S. Also, CdsD is abundant in both EBs and RBs, suggesting that it functions at both stages (Saka 2011).

CopN, the T3S plug protein, is believed to prevent premature activation of T3S by partially inserting itself into the injectisome and effectively plugging the pore from the inner membrane (Silva-Herzog 2011). The CopN cognate chaperones prevent secretion of CopN until they are removed by CdsN (Silva-Herzog 2011). Initiation of T3S occurs when a signal is transduced from the outer membrane which triggers removal of the CopN chaperone and unplugging of the injectisome. The CopN interactions with both CdsN and FliI suggest that the T3S ATPases likely facilitate CopN chaperone removal in both the EB and RB. Thus, CopN is one of the first effectors at both stages of development (Fields 2000).

SECRETION PATHWAY OF CPN0803- POSSIBLE MECHANISM

Based on the information discussed in the above sections, I have proposed two secretion mechanisms. One is regarding Cpn0803 secretion from the EB and the other from the RB. This section is highly theoretical and based largely on protein binding data, the crystal structure and EM of Cpn0803, and relevant literature.

EB secretion pathway

There are two potential EB secretion mechanisms depending on the function of Cpn0803. First, we discuss the secretion pathway if Cpn0803 represents a new class of needle-tip proteins. In the EB, Cpn0803 is secreted after dissociation from its cognate chaperone (currently unknown) by CdsN where it forms a tetrameric complex at the tip of the injectisome. Cpn0803 likely traverses the injectisome as an unfolded monomer and forms a ring-like tetrameric complex at the needle-tip. CdsL dissociation from CdsN is required to activate ATPase activity and allow for Cpn0803 secretion. CdsQ may play a role in the dissociation of CdsN and CdsL upon delivery of the Cpn0803 cargo to the ATPase. After Cpn0803 is secreted, injectisome construction is complete and CdsL again represses CdsN enzymatic activity until host-cell contact occurs. CopN (the putative plug protein) is in place at the base of the needle, preventing premature secretion of effectors. The CopN specific chaperones prevent secretion until interacting with CdsN. Once situated at the needle-tip, host-cell contact exposes Cpn0803 to relevant small molecules (possibly phosphatidic acid or phosphatidylinositol), which may induce a conformational change in Cpn0803. This hydrophobic binding pocket in Cpn0803 is supported by a network of hydrogen bonding which, if disrupted by small-molecule binding, could significantly alter the conformation of the protein. Needle-tip proteins are known to undergo conformational changes at the injectisome tip upon small molecule binding (Dickenson 2011). Once this conformational change occurs, a signal is transduced to the inner membrane (possibly via CdsD phosphorylation) where CdsL is released from CdsN, activating the ATPase and subsequent secretion of CopN. The translocator

proteins now traverse the injectisome and form a pore in the host-cell membrane in concert with Cpn0803. Either CopB/B2 or CopD/D2 function at this stage. Once the translocator pore is complete, the remainder of the bacterial effector proteins are secreted and actin is recruited to the site of attachment to facilitate bacterial internalization and inclusion formation. TARP and CPAF are primary EB effector proteins and would be secreted at this time. Cpn0803 is then secreted into the host cell either from a bacterial cytoplasmic pool or by an alternative T3S mechanism that occurs from outside the cell (Akopyan 2011). At this time, Cpn0803 performs its own effector functions within the cell, possibly associating with β -actin or recruiting phosphatidylinositol to the inclusion membrane.

Alternatively, if Cpn0803 is not the needle-tip protein, it is simply secreted upon host-cell contact into the eukaryotic cell to perform its effector function. Cpn0803 will not be localized to the tip of the injectisome and will be secreted from the bacterial cytoplasm.

RB secretion pathway

Secretion of Cpn0803 from the RB is similar to secretion from the EB, with a few important differences. First, Cpn0803 may be dissociated from its chaperone by FliI, not CdsN, since FliI likely functions in the RB. Also, Cpn0803 chaperones the translocator proteins into the inclusion membrane to form a pore by which the *Chlamydia* can communicate with the host-cell and direct nutrients and lipids to the inclusion. The

primary effector proteins at this stage are the inclusion proteins (Cpn0585, IncA, IncB), which would associate with FliI prior to secretion.

RBs are metabolically active and replicate within the inclusion. If each new RB constructs a *de novo* injectisome, it is possible that the exponential increase in effector secretion during RB replication could harm the host cell and disrupt the life-cycle. The observation that the flagellar genes are expressed in early-stage RBs suggests that as the RBs divide the T3S components are not replenished (Saka 2011). This would ensure that effector secretion is consistent throughout RB replication and does not increase to a detrimental level due to an exponential increase in the number of RBs.

FUTURE EXPERIMENTS AND SUGGESTIONS

The *Chlamydia* field is advancing at an enormous rate, and recent findings have presented the opportunity for more in depth studies. In this section, I discuss some applications of the recent advances in genetics as well as progress towards a cell-free *Chlamydia* system.

Applying *Chlamydia* genetics

The opportunity to genetically manipulate the *Chlamydia* genome presents an unprecedented advancement in the *Chlamydia* field. Numerous questions regarding the *Chlamydia* life-cycle can now be addressed and answered. The most complex of questions, such as confirming the role of the flagellar proteins in the life-cycle, or identifying which set of translocator proteins function in the EB versus the RB, can now

be simply addressed. The only disadvantage of these systems is that plasmid-based transformation is limited to *C. trachomatis* since *C. pneumoniae* lacks a plasmid. *C. pneumoniae* transformation requires the arduous task of creating point mutations in the genome without the ability to complement the system (Kari 2011). With regards to this thesis, application of the genetic system to knock out the specific flagellar genes and monitor phenotypic changes would be very revealing. Based on the hypothesis that FliI functions in the RB, knocking out the FliI gene would still allow for *C. pneumoniae* invasion but prevent proper assembly of the RB injectisome. Thus, a genetic system can be used to explore the exact role of the flagellar proteins. Also, by applying a genetic system, the exact role of Cpn0803 could be explored. If Cpn0803 plays the role of an effector, and not the needle-tip protein, knocking out the Cpn0803 gene would not prevent secretion of other effectors such as TARP, and *vice versa*.

Towards a cell-free system

The lack of a cell-free culture system for *Chlamydia* poses another major challenge. However, recent progress in developing cell-free systems for other obligate intracellular bacteria may be applicable to *Chlamydia*. For example, *Coxiella burnetii* is an obligate, intracellular bacteria that is genetically intractable. However, Omsland et al. recently developed a cell free media for *Coxiella* by monitoring the organism's transcriptome during metabolism and identifying nutritional requirements (Omsland 2009). Based on this information, they designed a media that supports *Coxiella* growth. A similar approach to be applied to *Chlamydia*; if the nutritional requirements during

growth are identified, it is possible that a media can be supplemented with these requirements.

CLOSING REMARKS

Studying *Chlamydia* is not for the faint-of-heart as it poses many challenges that other bacteriologists need not address. The lack of a genetic system and rigorous culturing techniques stimulates creativity and the application of novel techniques. This study has characterized the *C. pneumoniae* T3SS, demonstrating that there are two functional ATPases which both associate with T3S components. Also, a specific effector protein also associates with these ATPases and is secreted into the host cell. Although these studies are simple in other organisms, in *Chlamydia* the role of the T3S ATPases remains unclear. Future studies applying the recently developed genetic system and other cutting-edge techniques will certainly address many of the fundamental questions that have long existed in the *Chlamydia* field.

REFERENCES

Aizawa S (2001) Bacterial flagella and type III secretion systems. FEMS Microbiol. Lett. 202: 157-164.

Akeda Y, Galan J (2004) Genetic analysis of the Salmonella enterica type III secretion-associated ATPase InvC defines discrete functional domains. J. Bacteriol. 186: 2402-2412.

Akeda Y, Galan J (2005) Chaperone release and unfolding of substrates in type III secretion. Nature 437:911-915

Akopyan K, Edgren T, Wang-Edgren H, Rosqvist R, Fahlgren A, Wolf-Watz H, et al (2011) Translocation of surface-localized effectors in type III secretion. Proc. Natl. Acad. Sci. U.S.A. 108: 1639-44.

Alksne L, Projan S (2000) Bacterial virulence as a target for antimicrobial therapy. Curr. Opin. Biotech. 11: 625-626.

Amer A, Ahlund M, Broms J, Forsberg A, Francis M (2011) Impact of the N-terminal secretor domain on YopD translocator function in *Yersinia pseudotuberculosis* type III secretion. J. Bacteriol. 193: 6683-700.

Anderson D, Schneewind O (1998) A mRNA signal for the type III secretion of Yop proteins by *Yersinia pseudotuberculosis*. *Science* 278: 1140-1143.

Archuleta D, Du Y, English C, Lory S, Lesser C, Ohi M, Spiller B (2011) The Chlamydial effector Chlamydial outer protein N (CopN) sequesters tubulin and prevents microtubule assembly. *J. Biol. Chem.* 286: 33992-8.

Arnold R, Jehl A, Rattei T (2010) Targeting effectors: the molecular recognition of type III secreted proteins. *Microbes. Infect.* 12: 346-358.

Ayers M, Howell P, Burrows L (2010) Architecture of the type II secretion and type IV pilus machineries. *Future Microbiol.* 5: 1203-18.

Baron C (2010) Antivirulence drugs to target bacterial secretion systems. *Curr. Opin. Micro.* 13: 100-105.

Bartra S, Cherepanov P, Forsberg A, Schesser K (2001) The *Yersinia* YopE and YopH type III effector proteins enhance bacterial proliferation following contact with eukaryotic cells. *BMC Microbiol.* 1: 22.

Beatty W, Morrison R, Byrne G (1994) Persistent chlamydiae: from cell culture to a paradigm for chlamydia pathogenesis. *Microbiol. Rev.* 58, 686-699.

Belland R (2003) Transcriptome analysis of chlamydial growth during IFN- γ -mediated persistence and reactivation. *Proc. Nat. Acad. Sci. U. S. A.* 100: 15971-15976.

Berger L, Volp K, Matthews S, Speare R, Timms P (1999) *Chlamydia pneumoniae* in a free-ranging giant barred frog (*Mixophyes iterarus*) from Australia. *J. Clin. Microbiol.* 37: 2378-2380.

Betts H, Twiggs L, Sal M, Wyrick P, Fields K (2008) Bioinformatic and biochemical evidence for the identification of the type III secretion system needle protein of *Chlamydia Trachomatis*. *J. Bacteriol.* 190: 1680-1690.

Betts-Hampikian H, Fields K (2010) The Chlamydia type III secretion mechanism: Revealing cracks in a tough nut. *Front. Microbiol.* 1:114.

Betts-Hampikian H, Fields K (2011) Disulfide bonding within components of the *Chlamydia* type III secretion apparatus correlates with development. *J. Bacteriol.* 193: 6950-9.

Bigot A, Pagniez H, Botton E, Frehel C, Dubail I, Jacquet C, Charbit A, Raynaud C (2005) Role of FliF and FliI of *Listeria monocytogenes* in flagellar assembly and pathogenicity. *Infect. Immun.* 75: 5530-9.

Binet R, Maurelli T (2009) Transformation and isolation of allelic exchange mutants of *Chlamydia psittaci* using recombinant DNA introduced through electroporation. Proc. Natl. Acad. Sci. U. S. A. 106: 292-7.

Bingle L, Bailey C, Pallen M (2008) Type VI secretion: a beginner's guide. Curr. Opin. Microbiol. 11: 3-8.

Birtalan S, Ghosh P (2001) Structure of the *Yersinia* type III secretion system chaperone SycE. Nat. Struc. Bio. 8: 974-978.

Blaylock B, Riordan K, Missiakas D, Schneewind O (2006) Characterization of the *Yersinia enterocolitica* type III secretion ATPase YscN and its regulator, YscL. J. Bacteriol. 188:3525-3534.

Boyd A, Lambermont I, Cornelis G (2000) Competition between the Yops of *Yersinia enterocolitica* for delivery into eukaryotic cells: role of the SycE chaperone binding domain on YopE. J. Bacteriol. 182: 4811-4821.

Brinkworth A, Malcolm D, Pedrosa A, Roguska K, Shahbazian S, Graham J, Hayward R, Carabeo R (2011) *Chlamydia trachomatis* Slc1 is a type III secretion chaperone that enhances the translocation of its invasion effector substrate TARP. Mol. Micro. 82: 131-144.

Broms J, Forslund A, Forsberg A, Francis M (2003) Dissection of homologous translocon operons reveal a distinct role for YopD in type III secretion by *Yersinia pseudotuberculosis*. *Microbiology*. 149: 2615-26.

Broz P, Mueller C, Muller S, Phillippsen A, Sorg I, Engel A, Cornelis G (2007) Function and molecular architecture of the *Yersinia injectisome* tip complex. *Mol. Micro*. 65: 1311-1320.

Burghout P, Boxtel R, Gelder P, Ringler P, Muller S, et al (2004) Structure and electrophysiological properties of the YscC secretin from the type III secretion system of *Yersinia enterocolitica*. *J. Bacteriol*. 186: 4645-4654.

Caroline G, Faudry E, Yu-Sing T, Sylvie E, Attree I (2008) Oligomerization of PcrV and LcrV, protective antigens of *Pseudomonas aeruginosa* and *Yersinia pestis*. *J Biol. Chem*. 283: 23940-23949.

Chatterjee S, Zhong D, Nordhues B, Battaile K, Lovell S, et al (2011) The crystal structures of the *Salmonella* type III secretion system tip protein SipD in complex with deoxycholate and chenodeoxycholate. *Prot. Sci*. 20: 75-86.

Cheng L, Schneewind O (1999) *Yersinia enterocolitica* type III secretion on the role of SycE in targeting YopE into HeLa cells. *J. Biol. Chem.* 274: 22102-22108.

Chellas-Gery B, Wolf K, Tisoncik J, Hackstadt T, Fields K (2011) Biochemical and localization analyses of putative type III secretion translocator proteins CopB and CopB2 of *Chlamydia trachomatis* reveal significant distinctions. *Infect and Immun.* 79: 3036-3045.

Christian J, Heymann J, Paschen S, Vier J, Schauenburg L, Rupp J, Meyer T, Hacker G, Heuer D (2011) Targeting of a *Chlamydia* protease impedes intracellular bacterial growth. *PLoS Pathog.* 7.

Clifton D, Fields K, Grieshaber S, Dooley C, Fischer E, Mead D, Carabeo R, Hackstadt T (2004) A chlamydial type III translocated protein is tyrosine-phosphorylated at the site of entry and associated with actin recruitment. *Proc. Nat. Acad. Sci. U.S.A.* 101: 10166-10171.

Coles A, Reynolds D, Harper A, Devitt A, Pearce J (1993) Low-nutrient induction of abnormal chlamydia development: a novel component of chlamydial pathogenesis? *FEMS Microbiol. Lett.* 106: 193-200.

Cornelis G (2002) The *Yersinia* Ysc-Yop 'type III' weaponry. *Nat. Rev. Mol. Cell. Bio.* 3: 742-52.

Cornelis G (2006) The type III secretion injectisome. *Nature reviews.* 4: 811-825.

Cornelis G (2010) The type III secretion injectisome, a complex nanomachine for intracellular 'toxin' delivery. *Biol. Chem.* 391: 645-751.

Corsara D, Venditti D (2006) Diversity of the parachlamydiae in the environment. *Crit. Rev. Microbiol.* 32: 185-199.

Dahlgren M, Kauppi A, Olsson I, Linusson A, Elofsson M (2007) Design, synthesis and multivariate quantitative structure-activity relationship of salicylanides- potent inhibitors of type III secretion in *Yersinia*. *J. Med. Chem.* 50: 6177-6188.

Dawkins R (2006) *The God Delusion*. United Kingdom: Bantam Books.

Dehoux P, Flores R, Dauga C, Zhong G, Subtil A (2011) Multi-genome identification and characterization of chlamydiae-specific type III secretion substrates: the Inc proteins. *BMC genomics.* 12: 109.

Delepelaire P (2004) Type I secretion in Gram-negative bacteria. *Biochim. Biophys. Acta.* 1694: 149-161.

Dickenson N, Zhang L, Epler C, Adam P, Picking W, et al. (2011) Conformational changes in IpaD from *Shigella flexneri* upon binding bile salts provide insights into the second step of type III secretion. *Biochemistry* 50: 172-180.

Diepold A, Amstutz M, Abel S, Jenal U, Cornelis G (2010) Deciphering the assembly of the *Yersinia* type III secretion injectisome. *EMBO.* 29: 1928-1940.

Diepold A, Wiesand U, Cornelis G (2011) The assembly of the export apparatus (YscR, S, T, U, V) of the *Yersinia* type III secretion apparatus occurs independently of other structural components and involves the formation of an YscV oligomer. *Mol. Microbiol.* 82: 502-14.

Dress-Werringloer U, Bhuiyan M, Zhao Y, Gerard H, Whittum-Hudson J, Hudson A (2009). Initial characterization of *Chlamydomonas reinhardtii* cultured from the late-onset Alzheimer brain. *International Journal of Medical Microbiology.* 299: 187-201.

Enninga J, Rosenshine I (2009) Imaging the assembly, structure and activity of type III secretion systems. *Cell. Micro.* 11: 1462-1470.

Edqvist P, Alil M, Liu J, Francis M (2007) Minimal YopB and YopD translocator secretion by *Yersinia* is sufficient for Yop-effector delivery into target cells. *Microbes Infect.* 9: 224-33.

Everett K, Bush R, Anderson A (1999) Emended description of the order Chlamydiales, proposal of Parachlamydiaceae fam. nov. and Simkaniaceae fam. nov., each containing one monotypic genus, revised taxonomy of the family Chlamydiaceae, including a new genus and five new species, and standards for identification of organisms.

Essig A, Heinemann M, Simnacher U, Marre R (1997) Infection of *Acanthamoeba castellanii* by *Chlamydia pneumoniae*. *Appl. Environ. Microbiol.* 63: 1396-1399.

Felise H, Nguyen H, Pfuetzner R, Barry K, Jackson S, Blanc M, Bronstein P, Kline T, Miller S (2008) An inhibitor of Gram-negative bacterial virulence protein secretion. *Cell Host & Microbe.* 4: 325-336.

Fields K, Hackstadt T (2000) Evidence for the secretion of *Chlamydia trachomatis* CopN by a type III secretion mechanism. *Mol. Microbiol.* 38:1048-1060.

Fields K, Mead D, Dooley C, Hackstadt T (2003) *Chlamydia trachomatis* type III secretion: evidence for a functional apparatus during early cycle development. *Mol. Micro.* 48: 671-683.

Fields K, Fischer E, Mead D, Hackstadt T (2005) Analysis of putative *Chlamydia trachomatis* chaperones Scc2 and Scc3 and their use in identification of type III secretion substrates. *J. Bacteriol.* 187: 6466-78.

Fields K, Straley S (1999) LcrV of *Yersinia pestis* enters infected eukaryotic cells by a virulence plasmid-independent mechanism. *Infect. Immun.* 67: 4801-4813.

Filloux A (2004) The underlying mechanisms of type II protein secretion. *Biochim. Biophys. Acta.* 1694: 163-179.

Galan J, Collmer A (1999) Type III secretion machines: bacterial devices for protein delivery into host cells. *Science* 284: 1322-1328.

Galan J (2001) Salmonella interactions with host cells: type III secretion at work. *Annu. Rev. Cell Dev.* 17: 53-86.

Galan J, Wolf-Watz H (2006) Protein delivery into eukaryotic cells by type III secretion machines. *Nature* 444: 567-573.

Gauthier, A., Finlay, B (2003). Translocated intimin receptor and its chaperone interact with ATPase of the type III Secretion apparatus of Enteropathogenic *Escherichia coli*. J. Bacteriol. 185:6747-6755.

Gauthier A, Robertson M, Lowden M, Ibarra J, Puente J, Finlay B (2005) Transcriptional inhibitor of virulence factors in enteropathogenic *E. coli*. Anti. Agents and Chemo. 49: 4101-09.

Gerard-Vincent M, Robert V, Ball G, Bleves S, Michel G, Lazdunski A, Filloux A (2002) Identification of XcpP domains that confer functionality and specificity to the *Pseudomonas aeruginosa* type II secretion apparatus. Mol. Microbiol. 44: 1651-65.

Gieffers J, Rupp J, Gebert A, Solbach W, Klinger M (2004) First-choice antibiotics at subinhibitory concentrations induce persistence of *Chlamydia pneumoniae*. Anti. Agents. Chem. 48: 1402-1405.

Grayston J (1989) *Chlamydia pneumoniae*, strain TWAR. CHEST. 95: 664-669.

Goure J, Broz P, Attree O, Cornelis G, Attree I (2005) Protective anti-V antibodies inhibit *Pseudomonas* and *Yersinia* translocon assembly within host membranes. J. Infect. Dis. 15: 218-225.

Grayston J (2005) *Chlamydia pneumoniae* and atherosclerosis. *Clinical Infectious Disease*. 40: 1131-1132.

Hoare A, Timms P, Bavoil P, Wilson D (2008) Spatial constraints within the Chlamydial host cell inclusion predict interrupted development and persistence. *BMC Microbiol*. 8:5.

Hackstadt T (1999) Cell Biology. In: Stephens, R., *Chlamydia: Intracellular Biology, Pathogenesis, and Immunity*. Washington: American Society for Microbiology, 101-137.

Hakansson S, Persson K, Galyov C, Rosqvist R, Homble F, Wolf-Watz H (1996) The YopB protein of *Yersinia pseudotuberculosis* is essential for the translocation of Yop effector proteins across the target cell plasma membrane and displays contact-dependent membrane disrupting activity. *EMBO*. 15: 5812-23.

Hammerschlag M, Golden N, Oh M, Gelling M, Sturdevant M, Brown P, Aras Z, Neuheff S, Dumornay W, Roblin P (1993) Single dose of azithromycin for the treatment of genital Chlamydial infections in adolescents. *J. Pediatr*. 122: 961-5.

Hatch T (1975) Utilization of L-cell nucleoside triphosphates by *Chlamydia psittaci* for ribonucleic acid synthesis. *J. Bacteriol*. 122: 393-400.

Hefty P, Stephens R (2007) Chlamydial type III secretion system is encoded on ten operons preceded by sigma 70-like promoter elements. *J. Bacteriol.* 189:198-206.

Henderson-Begg S, Livermore D, Hall L (2006) Effect of subinhibitory concentrations on mutation frequency in *Streptococcus pneumoniae*. *J. Anti. Chemo.* 57: 849-854.

Henderson I, Navarro-Garcia F, Desvaux M, Fernandez R, Ala Aldeen D (2004) Type V secretion pathway: the autotransporter story. *Microbiol. Mol. Biol. Rev.* 68: 692-744.

Herrmann M, Schuhmacher A, Muhldorfer I, Melchers K, Prothmann C, Dammeier S (2006) Identification and characterization of secreted effector proteins of *Chlamydomytila pneumoniae* TW183. *Res. Microbiol.* 157:513-524.

Heuer D, Rejman Lipinski A, Machuy N, Karlas A, Wehrens A, Siedler F, Brinkmann V, Meyer T (2009) *Chlamydia* causes fragmentation of the golgi compartment to ensure reproduction. *Nature* 457: 731-5.

Hiroyuki M, Young G (2009) Translocated effectors of *Yersinia*. *Curr. Opin. Micro.* 12: 94-100.

Hodgkinson J, Horsley A, Stabat D, Simon M, Johnson S, et al (2009) Three-dimensional reconstruction of the *Shigella* T3SS transmembrane regions reveal 12-fold symmetry and novel features throughout. *Nat. Struct. Mol. Biol.* 16: 477-485.

Hsia R, Pannekoek Y, Ingerowski E, Bavoil P (1997). Type III secretion genes identify a putative virulence locus of *Chlamydia*. *Mol. Microbiol.* 25: 351-9.

Hu X, Lee M, Wallqvist A (2009) Interaction of the disordered *Yersinia* effector protein YopE with its cognate chaperone SycE. *Biochemistry* 48: 11158-11160.

Huang J, Lesser C, Lory S (2008) The essential role of CopN protein in *Chlamydia pneumoniae* intracellular growth. *Nature* 456: 112-115.

Hueck C (1998) Type III secretion systems in bacterial pathogens of animals and plants. *Microbiol. Mol. Biol. Rev.* 62: 379-433.

Hybiske K, Stephens R (2007) Mechanisms of host cell exit by the intracellular bacterium *Chlamydia*. *Proc. Natl. Acad. Sci. U. S. A.* 104: 11430-5.

Imada K, Minamino T, Tahara A, Namba K (2007) Structural similarity between the flagellar type III ATPase FliI and the F1-ATPase subunits. *Proc. Natl. Acad. Sci. U. S. A.* 104: 485-490.

Jewett T, Fischer E, Mead D, Hackstadt T (2006) Chlamydial TARP is a nucleator of actin. *Proc. Nat. Acad. Sci. U.S.A.* 103: 15509-15604.

Johnson S, Roversi P, Espina M, Olive A, Deane J, Birket S, Field T, Picking W, Blocker A, Galyov E, Picking W, Lea S (2007) Self-chaperoning of the type III secretion system needle-tip protein IpaD and BipD. *J. Biol. Chem.* 282: 4035-4044.

Johnson D, Stone C, Mahony J (2008) Interactions between CdsD, CdsQ, and CdsL, three putative *Chlamydomphila pneumoniae* type III secretion proteins. *J. Bacteriol.* 190: 2972-80

Johnson D, Stone C, Bulir D, Coombes B, Mahony J (2009) A novel inhibitor of *Chlamydomphila pneumoniae* protein kinase (PknD) inhibits phosphorylation of CdsD and suppresses bacterial replication. *BMC Microbiol.* 14: 218.

Journet L, Agrain C, Broz P, Cornelis G (2003) The needle length of bacterial injectisomes is determined by a molecular ruler. *Science* 302: 1757-60.

Kalman S, Michell W, Marathe R, Lammel C, Fan J, Hyman R, Olinger L, Grimwood J, Davis R, Stephens R (1999) Comparative genomes of *Chlamydia pneumoniae* and *C. trachomatis*. *Nat. Genet.* 21: 385-389.

Kari L, Goheen M, Randall L, Taylor L, Carlson J, Whitmire W, Virok D, Rajaram K, Endresz V, McClarty G, Nelson D, Caldwell H (2011) Generation of targeted *Chlamydia trachomatis* null mutants. Proc. Natl. Acad. Sci. U. S. A. 108: 189-93.

Kauppi A, Andersson D, Norberg H, Sundin C, Linusson A (2007) Inhibitors of type III secretion in *Yersinia*: design, synthesis and multivariate QSAR of 2-arylsulfonylamino-benzanilides. Bio. Med. Chem. 15: 6994-7011.

Kauppi A, Nordfelth R, Uvell H, Wolf-Watz H, Elofsson M (2003) Targeting bacterial virulence: inhibitors of type III secretion in *Yersinia*. Chemistry & Biology. 10: 241-249.

Kerschen E, Cohen D, Kaplan A, Straley S (2004) The plague virulence protein YopM targets the innate immune response by causing a global depletion of NK cells. Infect Immun. 72: 4589-4602.

Keyser P, Elofsson M, Rosell S, Wolf-Watz, H (2008) Virulence blockers as alternatives to antibiotics: type III secretion inhibitors against Gram-negative bacteria. J. Int. Med. 264: 17-29.

Kihara M, Minamino T, Yamaguchi S, Macnab R (2001) Intergenic suppression between the flagellar MS ring protein FliF of *Salmonella* and FlhA, a membrane component of its export apparatus. J. Bacteriol. 183: 1655-1662.

Kleba B, Stephens R (2008) *Chlamydia* effector proteins localized to the host cell cytoplasmic compartment. *Infect. Immun.* 76: 4842-4850.

Kubori T, Shimamoto N, Yamaguchi A, Namba K, Aizawa S (1992) Morphological pathway of flagellar assembly in *Salmonella typhimurium*. *J. Mol. Biol.* 226: 433-446.

Kuo C, Jackson L, Campbell A, Grayson J (1995) *Chlamydia pneumoniae* (TWAR). *Clin. Microbiol. Rev.* 8: 451-461.

Kuo C, Wang S, Grayston J (1972) Differentiation of TRIC and LGV organisms based on enhancement of infectivity by DEAE-dextran in cell culture. *J. Infect. Dis.* 125: 313-317.

Kuo C, Wang S, Grayston J (1973) Effect of polycations, polyanions, and neuraminidase on the infectivity of trachoma-inclusion conjunctivitis and lymphogranuloma venereum organisms in HeLa cells: sialic acid residues as possible receptors for trachoma-inclusion conjunctivitis. *Infect. Immun.* 8: 74-79.

Lee Y, Almqvist F, Hultgren S (2003) Targeting virulence for antimicrobial therapy. *Curr. Opin. Pharmacol.* 3: 513-519.

Lara-Tejero M, Kato J, Wagner S, Liu X, Galan J (2011) A sorting platform determines the order of protein secretion in bacterial type III systems. *Science* 331: 1188-1191.

Lorenzini E, Singer A, Singh B, Lam R, Skarina T, Chirgadze N, Savchenko A, Gupta R (2010) Structure and protein-protein interaction studies on *Chlamydia trachomatis* protein CT670 (YscO homolog). *J. Bacteriol.* 192: 2746-2756.

Lunelli M, Hurwitz R, Lambers J, Kolbe M (2011) Crystal structure of PrgI-SipD: Insight into a secretion competent state of the type three secretion system needle tip and its interaction with host ligands. *PLoS Pathog.* 7.

Lyskov S, Gray J (2008) The RosettaDock server for local protein-protein docking. *Nucleic Acids Research* 36: 233-238.

Marenne M, Journet L, Mota L, Corenlis G (2003) Genetic analysis of the formation of the Ysc-Yop translocation pore in macrophages by *Yersinia enterocolitica*: role of LcrV, YscF and YopN. *Microb. Pathog.* 35: 243-58.

Markham A, Jaafar Z, Kernege K, Middaugh C, Hefty P (2009) Biophysical characterization of *Chlamydia trachomatis* CT584 supports its potential role as the type III secretion needle tip protein. *Biochemistry* 48(43): 10353-61.

Martin A, Baker T, Sauer R (2008) Pore loops of the AAA+ ClpX machine grip substrates to drive translocation and unfolding. *Nat. Struct. Mol. Biol.* 15: 1147-51.

Marrie T, Peeling R, Reid T, De C (2003) Chlamydia species as a cause of community-acquired pneumonias in Canada. *Eur. Respir. J.* 21: 779-784

Martinez-Argudo I, Blocker A (2010) The *Shigella* T3SS needle transmits a signal for MxiC release, which controls secretion of effectors. *Mol. Micro.* 78: 1365-1378.

Matsumoto A (1982) Surface projections of *Chlamydia psittaci* elementary bodies as revealed by freeze-deep-etching. *J. Bacteriol.* 151: 1040-2

Matsumoto H, Young G (2009) Translocated effectors of *Yersinia*. *Curr. Opin. Micro.* 12: 94-100.

McMurry J, Arnam J, Kihara M, Macnab R (2004) Analysis of the cytoplasmic domains of *Salmonella* FlhA and interactions with component flagellar export machinery. *J. Bacteriol.* 186: 7586-7592.

Meijer A, Roholl P, Ossewaarde J, Jones B, Nowak B (2006) Molecular evidence for association of chlamydiales bacteria with epitheliocystis in leafy seadragon (*Phycodrus*

eques), silver perch (*Bidyanus bidyanus*), and barramundi (*Lates calcarier*). *Appl. Environ. Microbiol.* 72: 284-290.

Minamino T, Morimoto Y, Hara N, Namba K (2011) An energy transduction mechanism used in bacterial flagellar type III protein export. *Nat. Commun.* 2: 475.

Minamino T, Gonzalez-Pedrajo B, Kihara M, Namba K, Macnab R (2003) The ATPase FliI can interact with the type III flagellar protein export apparatus in the absence of its regulator, FliH. *J. Bacteriol.* 185: 3983-8.

Misyurina O, Chipitsyna E, Finashutina Y, Lazarev V, Akopian T, Savicheva A, Govorun V (2004) Mutations in a 23S rRNA Gene of *Chlamydia trachomatis* Associated with Resistance to Macrolides. *Anti. Agents. Chem.* 48: 1347-1349.

Mittal R, Peak-Chew S, McMahon H (2006) Acetylation of MEK2 and I kappa B kinase (IKK) activation loop residues by YopJ inhibits signaling. *Proc. Nat. Acad. Sci. U.S.A.* 103: 18574-18579.

Montagner C, Arguint C, Cornelis G (2011) Translocators YopB and YopD from *Yersinia* form a multimeric integral membrane complex in eukaryotic cell membranes. *J. Bacteriol.* 193:6923-8.

Moore E, Fischer E, Mead D, Hackstadt T (2008) The Chlamydial inclusion preferentially intercepts basolaterally directed sphingomyelin-containing exocytic vacuoles. *Traffic* 9: 2130-2140.

Moore S, Jia Y (2010) Structure of the cytoplasmic domain of the flagellar secretion apparatus component FlhA from *Helicobacter pylori*. *J. Biol. Chem.* 285: 21060-21069.

Moraes T, Spreter T, Strynadka N (2008) Piecing together the type III injectisome of bacterial pathogens. *Curr. Opin. Struc. Bio.* 18: 258-266.

Moulder J (1965) Metabolic capabilities and deficiencies of rickettsiae and psittacosis group. *Int. J. Lepr.* 33: Suppl-504.

Moulder J (1966) The relation of the psittacosis group (chlamydiae) to bacteria and viruses. *Annu. Rev. Microbiol.* 20: 107-130.

Mounier J, Popoff M, Enninga J, Frame M, Sansonetti P, Nhieu G (2009) The IpaC carboxyterminal effector domain mediates Src-dependent actin polymerization during *Shigella* invasion of epithelial cells. *PLoS Pathog.* 5: 1-15.

Mueller C, Broz P, Muller S, Ringler P, Erne-Brand F, et al (2005) The V-antigen of *Yersinia* forms a distinct structure at the tip of injectisome needles. *Science* 310: 674-676

Nordfelth R, Kauppi A, Norberg H, Wolf-Watz H, Elofsson M (2005) Small-molecule inhibitors specifically targeting type III secretion. *Infect. Immun.* 73: 3104-3114.

Omsland A, Cockrell D, Howe D, Fischer E, Virtaneva K, Sturdevant D, Porcella S, Heinzen R (2009) Host cell-free growth of the Q fever bacterium *Coxiella burnetii*. *Proc. Nat. Acad. Sci. U. S. A.* 106: 4430-4434

Orth K (2002) Function of *Yersinia* effector YopJ. *Curr Opin Microbiol.* 5: 38-43.

Paldanius M, Bloigu A, Alho M, Leinonen M, Saikku P (2005) Prevalence and persistence of *Chlamydia pneumoniae* antibodies in healthy laboratory personnel in Finland. *Clin. Diagn. Lab Immunol.* 12: 654-659.

Pallen M, Bailey C, Beatson S (2006) Evolutionary links between FliH/YscL-like proteins from bacterial type III secretion systems and second-stalk components of the F₀F₁ and vacuolar ATPases. *Protein Sci.* 15:935-940.

Pan N, Brady M, Leong J, Goguen J (2009) Targeting type III secretion in *Yersinia pestis*. *Anti Agents.* 53: 385-392

Pandey A, Sodhi A (2011) Recombinant YopJ induces apoptotic cell death in macrophages through TLR2. *Mol. Immunol.* 48: 392-8.

Pedersen P, Amzel L (1993) Structure, reaction center, mechanism, and regulation of one of nature's most unique machines. *J. Biol. Chem.* 268: 9937-9940.

Peters J, Wilson D, Myers G, Timms P, Bavoil P (2007) Type III secretion a la *Chlamydia*. *Trends Microbiol.* 15: 241-51.

Pettersson J, Holmstrom A, Hill J, Leary S, Frithz-Lindsten E et al (1999) The V-antigen of *Yersinia* is surface exposed before target cell contact and involved in virulence protein translocation. *Mol. Micro.* 32: 961-76.

Pilar A, Coombes B (2011) A fresh look at the type III secretion system: two-step model of effector translocation in pathogenic bacteria. *Front. Microbiol.* 2: 1-3

Pozidis C, Chalkiadaki A, Gomez-Serrano A, Stahlberg H, Brown I, Tampakaki A, et al (2003) Type III protein translocase: HrcN is a peripheral ATPase that is activated by oligomerization. *J. Biol. Chem.* 278: 25816-25824.

Prehna G, Ivanov M, Bliska J, Stebbins C (2006) *Yersinia* virulence depends on mimicry of host Rho-family nucleotide dissociation inhibitors. *Cell* 126: 869-880.

Pukatzki S, Ma A, Sturtevant D, Krastins B, Sarracino D, Nelson W, Heidelberg J, Mekalanos J (2006) Identification of a conserved bacterial protein secretion system in *Vibrio cholera* using the Dictyostelium host model system. Proc. Natl. Acad. Sci. U. S. A. 103: 1528-33.

Rathinavelan T, Tang C, De Guzman R (2011) Characterization of the interaction between the *Salmonella* type III secretion tip protein SipD and the needle protein PrgI by paramagnetic relaxation enhancement. J. Biol. Chem. 286: 4922-4930.

Riordan K, Schneewind O (2008) YscU cleavage and the assembly of *Yersinia* type III secretion machine components. Mol. Micro. 68: 1485-501.

Rodgers L, Gamez A, Riek R, Ghosh P (2008) The type III secretion chaperone SycE promotes a localized disorder-to-order transition in the natively unfolded effector YopE. J. Biol. Chem. 283: 20857-20863.

Rodgers L, Mukerjea R, Birtalan S, Friedberg D, Ghosh P (2010) A solvent exposed patch in chaperone-bound YopE is required for translocation by the type III secretion system. J. Bacteriol. 192: 3114-3122.

Roehrich A, Argudo I, Johnson S, Blocker A, Veenendaal A (2010) The extreme C terminus of *Shigella flexeri* IpaB is required for regulation of type III secretion, needle tip composition, and binding. *Infect and Immun.* 78: 1682-1691.

Saka H, Thompson J, Chen Y, Kumar Y, Dubois L, Moseley A, Valdivia R (2011) Quantitative proteomics reveals metabolic and pathogenic properties of *Chlamydia trachomatis* developmental forms. *Mol. Microbiol.* 82:1185-203.

Sandkvist M (2001) Type II secretion and pathogenesis. *Infect. Immun.* 69: 3523-3535.

Sato H, Frank D (2011) Multi-functional characteristics of the *Pseudomonas aeruginosa* type III needle-tip protein, PcrV; comparison to orthologs in other Gram-negative bacteria. *Front. Microbiol.* 2.

Sato H, Hunt M, Weiner J, Hansen A, Frank D (2011) Modified needle-tip PcrV proteins reveal distinct phenotypes relevant to the control of type III secretion and intoxication by *Pseudomonas aeruginosa*. *PLoS One.* 29.

Schachter J, Caldwell H (1980) Chlamydiae. *Annu. Rec. Microbiol.* 34: 285-309.

Scidmore M, Hackstadt T (2008) Mammalian 14-3-3beta associates with the *Chlamydia trachomatis*. *Mol. Microbiol.* 39: 1638-1650.

Slepenkin A, Motin V, de la Maza L, Peterson E (2003) Temporal expression of type III secretion genes of *Chlamydia pneumoniae*. *Infect. Immun.* 71: 2555-62.

Sorg I, Wagner S, Amstutz M, Muller S, Broz P, et al (2007) YscU recognizes translocators as substrates of the *Yersinia injectisome*. *EMBO.* 26: 3015-3024.

Spaeth K, Chen Y, Valdivia R (2009) The chlamydia type III secretion system c-ring engages chaperone-effector protein complexes. *PLoS Pathog.* 5

Stratton C, Wheldon D (2006) Multiple sclerosis: an infectious syndrome involving *Chlamydia pneumoniae*. *TRENDS in Microbiology.* 14: 474-479.

Shao F (2008) Biochemical functions of *Yersinia* type III effectors. *J. Biol. Chem.* 283: 20857-20863.

Shen D, Saurya S, Wagner C, Nishioka H, Blocker A (2010) Domains of the *Shigella flexeri* type III secretion system IpaB protein involved in secretion regulation. *Infect. Immun.* 78: 4999-5010.

Silva-Herzog E, Ferracci F, Jackson M, Joseph S, Plano G (2008) Membrane localization and topology of the *Yersinia pestis* YscJ lipoprotein. *Microbiology.* 154: 593-607.

Silva-Herzog E, Joseph S, Avery A, Coba J, Wolf K, Fields K, Plano G (2011) Scc1 (CP0432) and Scc4 (CP0033) function as a type III secretion chaperone for CopN of *Chlamydia pneumoniae*. *J. Bacteriol.* 193: 3490-3496.

Sodhi A, Sharma R, Batra H (2005) *Yersinia* rLcrV and rYopB inhibits the activation of murine peritoneal macrophages in vitro. *Immunol. Lett.* 15: 146-52.

Soscia C, Hachani A, Bernadac A, Filloux A, Bleves S (2007) Cross-talk between type III secretion and flagellar assembly systems in *Pseudomonas aeruginosa*. *J. Bacteriol.* 189: 3124-3132.

Spreter T, Yop C, Sanowar S, Andre I, Kimbrough K, et al (2009) A conserved structural motif mediates formation of the periplasmic rings in the type III secretion system. *Nat. Struc.* 16: 468-476.

Stone C, Bulir D, Emdin C, Pirie R, Porfilio E, Slootstra J, Mahony J (2011) *Chlamydia pneumoniae* CdsL regulates CdsN ATPase activity, and disruption with a peptide mimetic prevents bacterial invasion. *Front. Micro.* Epub 2011.

Stone C, Bulir D, Gilchrist J, Toor R (2010) Interactions between flagellar and type III secretion proteins in *Chlamydia pneumoniae*. *BMC Microbiol.* 22: 18.

Stone C, Johnson D, Bulir D, Gilchrist J, Mahony J (2008) Characterization of the putative type III secretion ATPase CdsN (Cpn0707) of *Chlamydomophila pneumoniae*. J Bacteriol. 190: 6580-8.

Stuart E, Webley W, Norkin L (2003) Lipid rafts, caveolae, caveolin-1, and entry by Chlamydiae into host cells. Exp. Cell. Res. 287: 67-78.

Sun P, Tropea J, Austin B, Cherry S, Waugh D (2008) Structural characterization of the *Yersinia pestis* type III secretion needle protein YscF in complex with its heterodimeric chaperone YscE/YscG. J. Mol. Bio. 377: 819-830.

Thomas J, Stafford G, Hughes C (2004) Docking of cytosolic chaperone-substrate complexes at the membrane ATPase during flagellar type III protein export. Proc. Natl. Acad. Sci. U. S. A. 101:3945-3950.

Timmerman P, Puijk WC, and Melen RH (2007). Functional reconstruction and synthetic mimicry of a conformational epitope using CLIPSTTM technology. J.Mol. Recognit. 20: 283-299.

Toor R, Stone C, Mahony J (2011) CdsQ of *Chlamydia pneumoniae* delivers chaperone-effector complexes to the inner membrane ATPase CdsN. Trans. Biomed. In press.

Vanrompay D, Butaye P, Van A, Ducatelle R, Haesebrouck F (1997) The prevalence of *Chlamydia psittaci* infections in Belgian commercial turkey poults. *Vet. Microbiol.* 54: 85-93.

Viboud G, Meija E, Biska J (2006) Comparison of YopE and YopT activities in counteracting host signaling responses to *Yersinia pseudotuberculosis* infection. *Cell Microbiol.* 8: 1504-1515.

Villareal C, Whittum-Hudson J, Hudson A (2002) *Arthritis Research.* 4: 5-9.

Wang Y, Kahane S, Cutcliffe L, Skilton R, Lambden P, Clarke I (2011) Development of a transformation system for *Chlamydia trachomatis*: restoration of glycogen biosynthesis by acquisition of a plasmid shuttle vector. *PLoS Pathog.* Epub 2011.

Wang Y, Nordhues B, Zhong D, De Guzman R (2010) NMR characterization of the interaction of the *Salmonella* type III secretion system protein SipD and bile salts. *Biochemistry* 49: 4220-4226.

Wallden K, Rivera-Caldaza A, Waksman G (2010) Type IV secretion systems: versatility and diversity in function. *Cellular Microbiology* 12: 1203-1219.

Weeks S, Hill J, Friedlander A, Welkos S (2002) Anti-V antigen antibody protects macrophages from *Yersinia pestis*-induced cell death and promotes phagocytosis. *Microb. Pathog.* 32: 227-37.

Wiesand U, Sorg I, Amstutz M, Wagner S, Wan Den Heuvel J, et al (2009) Structure of the type III secretion recognition protein YscU from *Yersinia enterocolitica*. *J. Mol. Bio.* 385: 854-66.

Woestyn S, Allaoui A, Wattiau P, Cornelis G (1994) YscN, the putative energizer of the *Yersinia* Yop secretion machinery. *J. Bacteriol.* 176: 1561-9

Wilharm G, Lehmann V, Neumayer W, Trcek J, Heesemann J (2004) *Yersinia enterocolitica* type III secretion: evidence for the ability to transport folded proteins that are folded prior to secretion. *BMC Micro.* 4: 27.

Wylie J, Hatch G, McClarty G (1997) Host cell phospholipids are trafficked to and then modified by *Chlamydia trachomatis*. *J. Bacteriol.* 179: 7233-7242

Wyrick P, Choong J, Davis C, Knight S, Royal M, Maslow A, Bagnell C (1989). Entry of genital *Chlamydia trachomatis* into polarized human epithelial cell. *Infect. Immun.* 57: 2378-2389.

Zarivach R, Vuckovic M, Deng W, Finlay B, Strynadka N (2007) Structural analysis of a prototypical ATPase from the type III secretion system. *Nat. Struct. Mol. Biol.* 14:131-137.

Zhang J, Stephens R (1992) Mechanism of *C. trachomatis* attachment to eukaryotic host cells. *Cell* 69: 861-869.

Zhong G (2009) Killing me softly: chlamydial use of proteolysis for evading host defenses. *Trends Microbiol.* 17: 467-474.

APPENDICES

6.1 Supplemental Figures

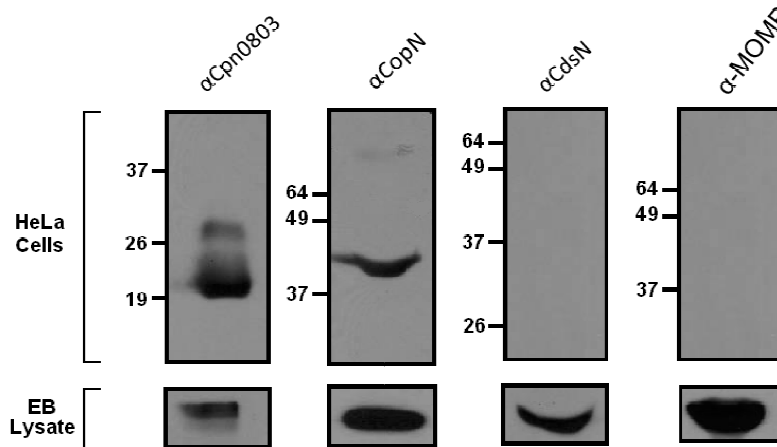


Figure 6.1.1 Secretion of Cpn0803 into HeLa cells. HeLa cells were infected with *C. pneumoniae* and analyzed for the presence of Cpn0803, CdsN/MOMP (negative controls), and CopN (positive control) using specific antibodies. Cpn0803 was secreted into HeLa cells while CdsN and MOMP were not detected. CopN was also detected in HeLa cells upon infection.

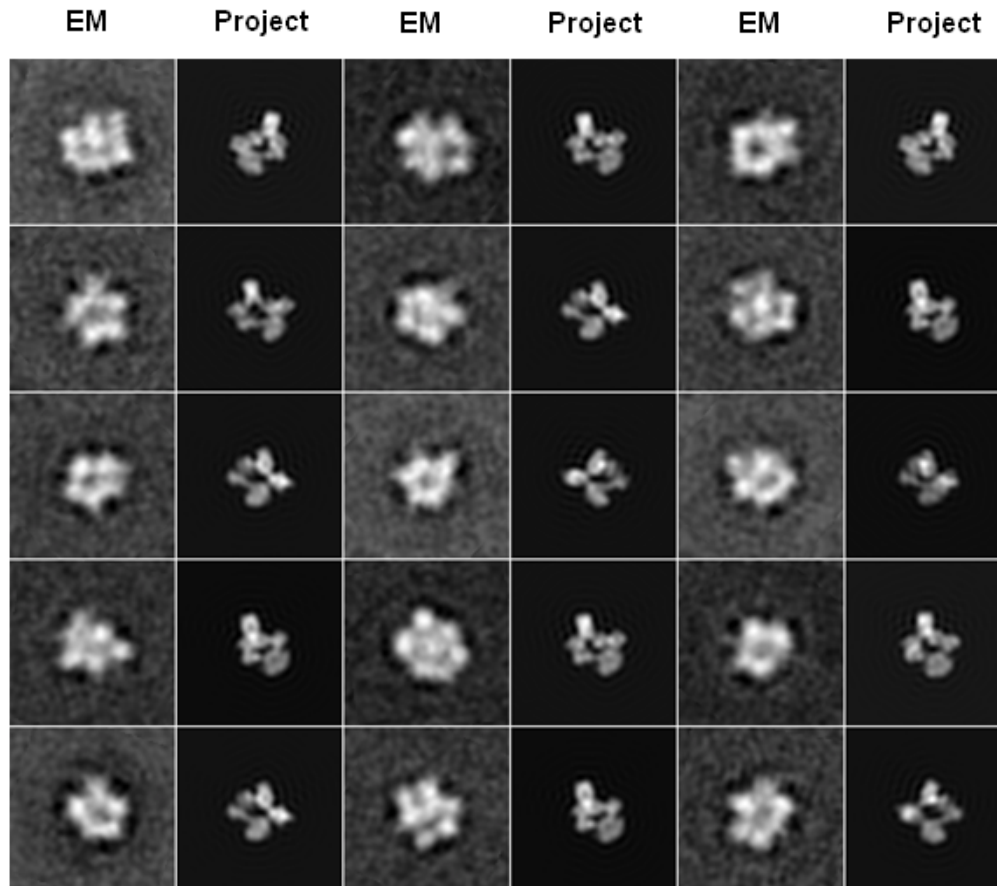


Figure 6.1.2 Ring-like structure of Cpn0803 in solution. Cpn0803 was immobilized on carbon grids at a concentration of 50 $\mu\text{g/ml}$ and visualized using transmission electron microscopy. The observed structures using electron microscopy (EM) were compared to the projections of the tetramer model (project). Cpn0803 in solution has a clear pore with similarities to the tetramer model.

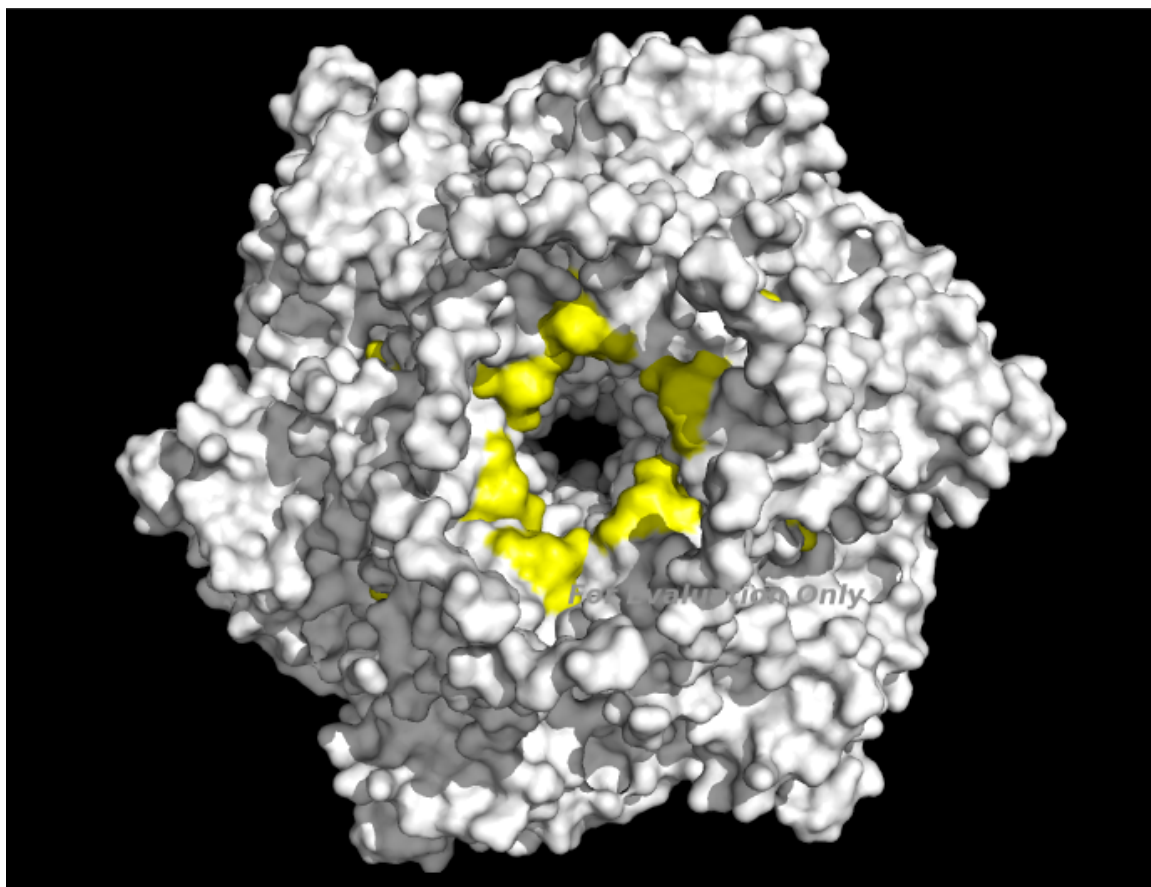


Figure 6.1.3 CdsN binding domain for Cpn0803. PepScan analysis identified a discrete domain on CdsN mediating the interaction with Cpn0803. Grey shows the CdsN predicted hexamer and yellow depicts the Cpn0803 binding domain.

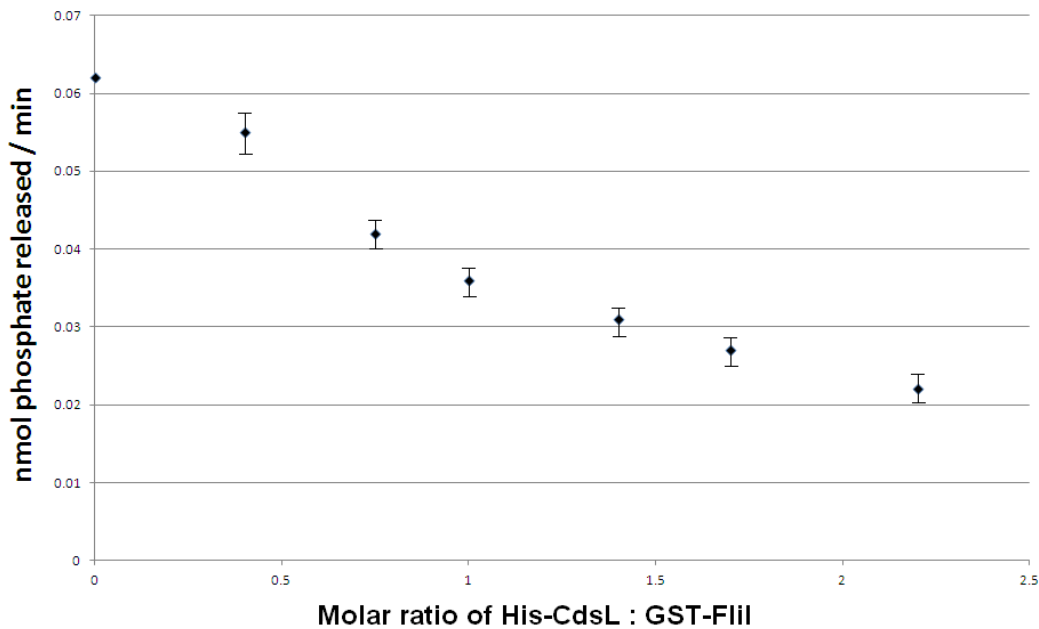


Figure 6.1.4 CdsL down-regulates the flagellar ATPase FliI. Aliquots (100 ng) of GST-FliI were assayed for enzymatic activity using the malachite green assay to detect released inorganic phosphate from ATP. His-CdsL was added to the reaction mixture at molar ratios between 0.4 and 2.2, and ATPase activity of FliI was monitored. Increasing amounts of CdsL resulted in a decrease in FliI enzymatic activity. The maximum reduction of activity was seen at a 2.2 CdsL : 1 FliI molar ratio (65% reduction in CdsN enzymatic activity). All experiments were performed in triplicate and data is presented as the mean with error bars representing 1 SD of the mean.

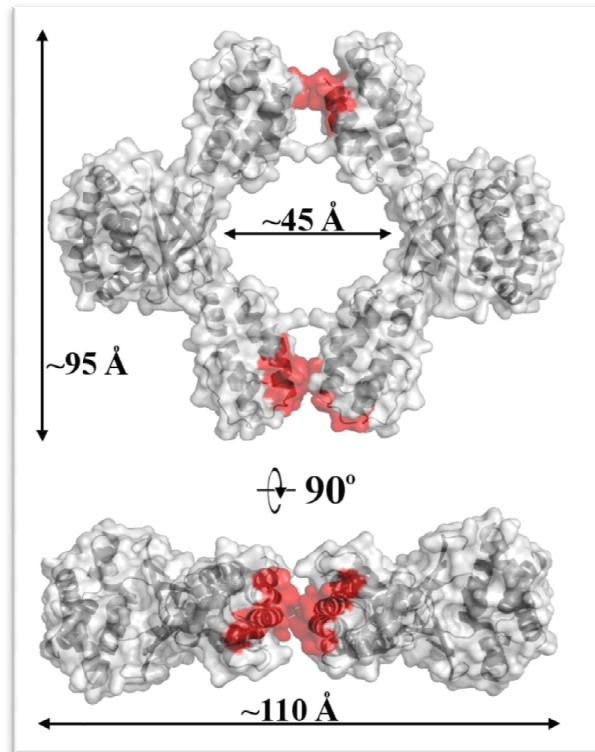


Figure 6.1.5 Cpn0803 tetramer based on RosettaDock and PepScan mapping.

PepScan mapping identified novel residues in the N-terminal region mediating oligomerization (residues 5 to 20). Based on this data, we generated a tetrameric model of Cpn0803 which was submitted and verified using the RosettaDock server. The resulting tetrameric structure had a maximum internal pore diameter of 34.37 Å and a maximum external diameter of 109.07 Å. The Cpn0803 oligomerization domains identified by Pepscan analysis are shown in red.

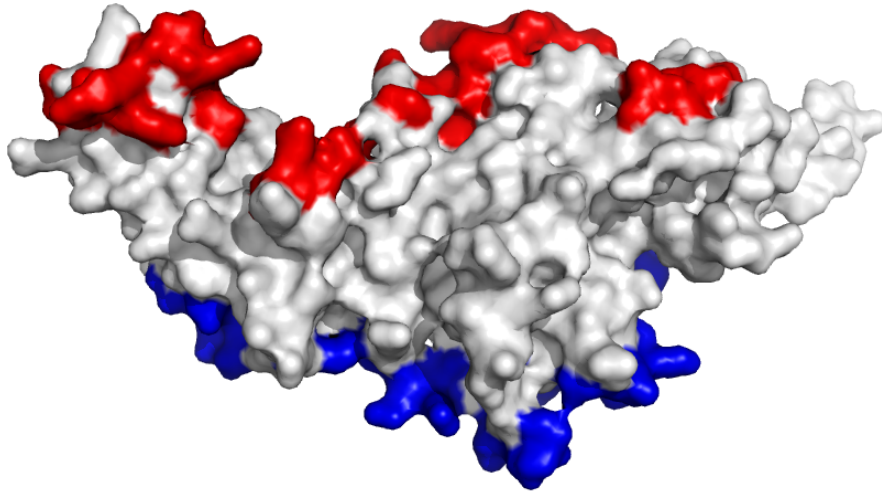


Figure 6.1.6 CdsN has two distinct binding domains for effectors and structural components. Using PepScan epitope mapping, we screened 5 structural proteins and 9 effector/chaperone proteins against the CdsN library. In red is the binding domain for structural components, and in blue is the binding domains for effector proteins. CdsN has two distinct binding domains on different faces of the protein for soluble and structural components of the T3SS.

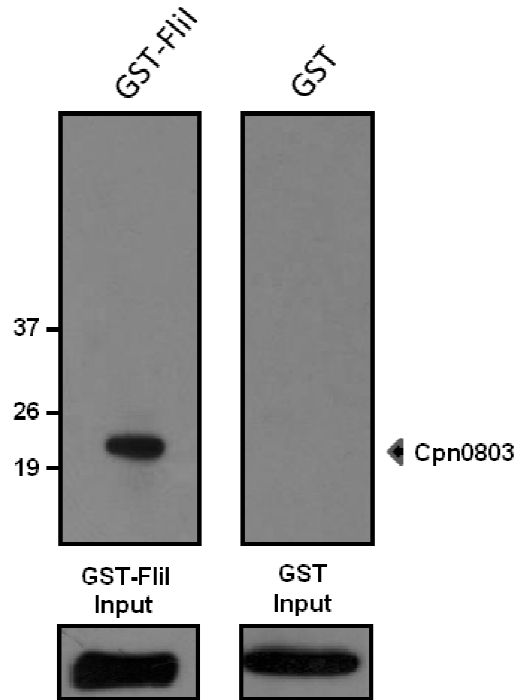


Figure 6.1.7 His-Cpn0803 copurifies with GST-FliI. GST-FliI was immobilized on glutathione beads and incubated with an *E. coli* lysates overexpressing His-Cpn0803. GST-FliI associated with Cpn0803 in the presence of 500 mM NaCl, while GST alone did not.

6.2. Supplementary Materials and Methods

6.2.1 Cpn0803 secretion into host cells

HeLa cells were infected with *C. pneumoniae* at an MOI of 3. HeLa cells were harvested and bead lysed, centrifuged at 3000 x g for 10 min to clear HeLa cell debris, and ultracentrifuged at 18000 rpm for 45 min to clear any EBs from the lysate. The lysate was then filtered three times at 0.2 μ m to ensure that all chlamydial EBs were removed from the lysate. The entire HeLa cell lysate was then TCA precipitated with 10% TCA overnight at 4°C. The precipitated protein was electrophoresed on an 11% polyacrylamide gel, and secreted Cpn0803 was visualized using anti-Cpn0803 polyclonal antibody. As a control, chlamydial α -CdsN and α -MOMP were not present in the HeLa cell lysate, suggesting that cell-lysis did not result in the presence of Cpn0803. CopN, which is known to be secreted, was used as a positive control.

6.2.2 EM visualization of Cpn0803 in solution

Cpn0803 was purified on a Ni-NTA column and diluted to a final concentration of 50 μ g/ml in 20 mM Tris-pH 7, 100 mM KCl. Cpn0803 was then immobilized on carbon grids and visualized by a Jeol 1200 electron microscope at 80 kV, and pictures were captured with an AMT digital camera. xMIP was used to generate class averages and EM projections of the tetramer model.

6.2.3 RosettaDock server analysis of Cpn0803

The coordinates of Cpn0803 from *C. pneumoniae* were used as an initial structure for the docking analyses. The initial tetrameric structure was identified by PepScan mapping, and the RosettaDock server was used to energetically optimize this structure. Extensive structural perturbations with RosettaDock identified the lowest energy models.